# The computational power of many-body systems

by

Zak Webb

A thesis
presented to the University of Waterloo
in fulfillment of the
thesis requirement for the degree of
Doctor of Philosophy
in
Physics and Astronomy (Quantum Information)

Waterloo, Ontario, Canada, 2016

## Author's Declaration

I hereby declare that I am the sole author of this thesis. This is a true copy of the thesis, including any required final revisions, as accepted by my examiners.

I understand that my thesis may be made electronically available to the public.

**Abstract**

Many-body systems are well known throughout physics to be hard problems to exactly solve, but much of this is folklore resulting from the lack of an analytic solution to these systems. This thesis attempts to classify the complexity inherent in many of these systems, and give quantitative results for why the problems are hard. In particular, we analyze the many-particle system corresponding to a multi-particle quantum walk, showing that the time evolution of such systems on a polynomial sized graph is universal for quantum computation, and thus determining how a particular state evolves is as hard as an arbitrary quantum computation. We then analyze the ground energy properties of related systems, showing that for bosons, bounding the ground energy of the same Hamiltonian with a fixed number of particles is QMA-complete. Similar techniques also show that the single-particle case has related computational power. Finally, a nice relation between spin systems and hard-core bosons can be used to show that bounding the smallest eigenvalue of the XY-model is QMA-complete.

**Acknowledgements**

I would like to thank my advisor, Andrew Childs, for his great help and support during my graduate studies at the University of Waterloo. His research guidance and support during hard times was very helpful, and this thesis would not be written without his support.

I would also like to thank David Gosset, who acted as a sounding board, and guided much of my research. He was a fountain of useful ideas, with an ability to conceive of complex solutions to difficult problems. His work ethic made many of the results in this thesis possible.

I'd like to thank Norbert Lütkenhaus, who helped get me back on my feet during troubled times, as well as Chris Pugh, who got me started and kept me going. To all of my friends at the Institute for Quantum Computing, from the optics groups of my early years to the eclectic bunch now eating cookies at 4, thank you.

## Dedication

This is dedicated to the ones I love, my family and friends.

# Table of Contents

# List of Figures

# Chapter 1

# Introduction

The first thing I would like to mention is that this thesis is not complete. I ran out of time and was unable to complete the thesis. I had to submit something to the graduate office, and this is it. I do apologize, and I expect to have major revisions required. At this point, I do not believe that any one chapter is actually completed, and in fact many of the state results have not been completely written up. Basically, I recognize that this thesis is defensible as is, and am planning major revisions.

When examining the physics literature, the three-body problem is extremely well known, as is its usual impossibility to solve. In these cases, people generally mean that there does not exist a closed form solution in general, but can we quantify exactly how hard the problem is?

In particular, if one is working with some particular many body system, how hard is it to compute various attributes about the system. I'd really like to know the answer.

While such questions have not generally been asked in physics, classifying the computation power of a problem in terms of the necessary resources in order to solve it is a foundational idea in computer science. The entire field of computational complexity arose in the attempt to classify these problems. This thesis will attempt to use tools founded in this field and apply them to the various physical systems.

## 1.1 Quantum walk

Over the years, randomness proved itself as a useful tool, allowing access to physical systems that are too large to accurately simulate. By assuming the dynamics of such systems can be modelled as independent events, Markov chains provide insight to the structure of the dynamics. These ideas can then be cast into the framework of random walk, where the generating Markov matrix describes the weighted, directed graph on which the walk takes place.

Using the principle of "put quantum in front," one can then analyze what happens when the random dynamics are replaced by unitary dynamics. This actually poses a little difficulty, as there is no obvious way to make a random walk have unitary dynamics. In particular, there are many ways that the particle can arrive at one particular vertex in the underlying graph, and thus after arriving at the vertex there is no way to reverse the dynamics.

There are (at least) two ways to get around this. One continues with the discrete-time structure of a random walk, and keeps track of a ”direction” in addition to the position of the particle. Each step of the walk is then a movement in the chosen direction followed by a unitary update to the direction register. These Szegedy walks are extremely common in the literature, and go by the name of ”discrete-time quantum walk.”

Another way to get around the reversibility problem is to generalize the continuous-time model of random walks. In particular, assuming that the underlying graph is symmetric, we look at the unitary generated by taking the adjacency matrix of the graph as a Hamiltonian. This is a one-parameter family of unitaries, and thus easily reversible. The “continuous-time quantum walk” model is the one we'll be focussing on in this thesis.

## 1.2 Many-body systems

Everything in nature has many particles, and the reason that physicists are so interested in smaller dynamics is the relatively understandable fact that many-body systems are extremely complicated. The entire branch of statistical physics was created in an attempt to make a coherent understanding of these large systems, since writing down the dynamics of every particle is impossible in general.

Along these lines, many models of simple interactions between particles exist in the literature. As an example, on can consider a lattice of occupation sites, where bosons can sit at any point in the lattice. Without interactions between the particles, the dynamics are easily understood as decoupled plane waves. However, by including even a simple energy penalty when multiple particles occupy the same location (i.e. particles don't like to bunch), we no longer have a closed form solution and are required to look at things such as the Bethe ansatz.

## 1.3 Computational complexity

While this is a physics thesis, much of my work is focused on understanding the computational power of these physical systems, and as such an understanding of the classification framework is in order. I should explain some of the motivation behind this area of research, giving a bit of background for the physicist.

These classifications are generally described by languages, or subsets of all possible 0-1 strings. In particular, given some string $x$, the requisite power in order to determine whether the string belongs to a language or not describes the complexity of the language.

## 1.4 Layout of thesis

With all of this background in mind, we'd like to give a basic understanding of what this thesis is going to entail. The underlying theme of this thesis is to understand the computational power of quantum walk, when restricted to various questions. As such, we will look both at the single and multi-particle cases. Note that most of this thesis is based on the papers [?], [?], [?], and [?]. While I am an author on all four papers, Andrew Childs and David Gosset are co-authors on all four papers, while Daniel Nagaj and Mouktik Raha are co-authors on [?].

However, in Chapter 2, we will at first define various terms related to computational complexity that will be of use to us, as well as some lemmas that might be of independent interest.

In Chapter **??** we will describe single-particle scattering on graphs. In particular, we will give some simple motivations and understanding of what is going on in a simple case. This chapter will also describe some basic algorithmic uses for the single particle case. This paper will include some review of previous papers [**TO DO:** *Cite quantum walk papers*] that I have not written, as well as a broad overview of techniques used in [?] and [?].

At this point, we will transition into understanding the computational power of time evolving according to single- and multi-particle quantum walks. In particular, Chapter **??** will include a novel proof that quantum walk of a single particle on an exponentially sized graph for polynomial time is universal quantum computing, using techniques slightly different than that of [?][**TO DO:** *Find correct citation*] . While this proof has not been submitted as a paper in any journal, it makes use of many of the techniques of [?]. In Chapter **??**, we extend this result to show that a multi-particle quantum walk with almost any finite-range interaction is universal for quantum computing, the main result of [?].

With the computational power of time evolved quantum walk, we will want to understand the ground energy problem of the quantum walk. In particular, Chapter **??** shows that determining whether the ground energy of a sparse, row-computable graph is above or below some threshold is QMA-complete, which is work is found in an appendix of the [?] paper. As this corresponds exactly to the ground energy problem of a single particle quantum walk on an exponentially large, but specifiable, graph, this shows that the ground energy problem for single-particle quantum walk is QMA-complete. Chapter **??** then expands on this result, and shows that the ground energy problem for multi-particle quantum walk with bosons on simple graphs is QMAcomplete. While this result follows the proof techniques of [?] and [?], the extension to arbitrary finite-range interactions for bosons is novel.

With the quantum walk interactions out of the way, Chapter 8 makes use of these results on the multi-particle ground energy problem to study the ground energy problem of various spin systems.

Finally, Chapter **??** concludes with some discussion of these results, along with some avenues for future research.

# Chapter 2

# Mathematical Preliminaries

Several topics in this thesis require a background that not all researcher will have experience in. Especially as this thesis is multi-disciplinary, I would like to include at least some basic introduction to various physical and computer science topics. Additionally, several lemmas used in this manuscript might be of independent interest, as their applicability is not restricted to the various models studied in this thesis.

## 2.1 Mathematical notation

Perhaps the most simple point that I would like to raise before the thesis begins in ernest is the notation that I will use throughout the paper. Much of the paper uses notation not necessarily standard in every area of physics or computer science, and I want to make sure that no confusion occurs. I will assume that various notations that are common do not need to be described, such at $\mathcal{H}$ describing a Hilbert space, or that $\mathbb{I}$ describes a the identity operator on a particular Hilbert space.

The first such notation will be for the shorthand definition of sets of particular size. Namely,

$$[k] := \{0, 1, \cdots, k-1\}. \tag{2.1}$$

This is a set of size $k$, with the elements ordered and labeled by the integers from 0 to $k-1$. We will often think of these as elements from $\mathbb{Z}_k$, with addition and multiplication defined over the integers modulo $k$.

Often this paper will want to investigate systems with many particles, and we will want an operator to only act nontrivially on one particle. In particular, if we have a Hilbert space $\mathcal{H}_{\text{total}} = \mathcal{H}_{\text{single}}^{\otimes N}$ that consists of $N$ copies of some single Hilbert space, and if we have an operator $M$ that acts on $\mathcal{H}_{\text{single}}$, we can define an operator $M^{(w)}$ that acts nontrivially only on the $w$-th copy of $\mathcal{H}_{\text{single}}$, namely

$$M^{(w)} = \mathbb{I}^{\otimes w-1} \otimes M \otimes \mathbb{I}^{N-w}. \tag{2.2}$$

In this manner, only the $w$-th copy of $\mathcal{H}_{\text{single}}$ is effected.

As we will also be working with graphs, we will want to note that the letter $G$ usually denotes a particular graph. Further, $A(G)$ describes the adjacency matrix of the graph $G$.

$V(G)$ then describes the vertex set of $G$, and $E(G)$ describes the edge set of $G$. Note that this thesis will always deal with undirected graphs, with at most a single edge between vertices. As such, the adjacency matrix $A(G)$ will be a symmetric 0-1 matrix. We will at times want to work with a simple graph, in which self-loops do not occur, but unless otherwise specified a graph $G$ might contain self-loops.

Much of the work in this thesis, especially when describing the ground energy of particular Hamiltonian, deals only with positive semi-definite operators. As such, if $A$ is a positive semi-definite matrix, then $\gamma(A)$ is the smallest non-zero eigenvalue. Note that if $A$ has a 0-eigenvalue, then this corresponds to the energy gap between the ground state and the first excited state, but if $A$ does not have a 0-eigenvalue then this is simply the smallest eigenvalue of $A$.

Finally, let us assume that $A$ acts on a Hilbert space $\mathcal{H}$, and that $\mathcal{S}$ is a subspace of $\mathcal{H}$. We will then write the restriction of $A$ to the subspace $\mathcal{S}$ as $A\big|_{\mathcal{S}}$.

## 2.2 Indistinguishable particles

I have a lot of things about indistinguishable particles. I should really only talk about it in one place. I think this would be a great place.

## 2.3 Complexity Theory

While this thesis is for the physics department, many of the results require some basic quantum complexity theory. In particular, the computer science idea for classification of computational problems in terms of the requisite resources gives a particularly nice interpretation of why certain physical systems don't equilibrate, and give a simple explanation on why certain systems do not have a known closed form solution.

This is a simple introduction, with a focus designed to make the rest of this thesis comprehensible to those without a background in complexity theory. For a more formal introduction to Complexity Theory, I would recommend [**?**], with a more in depth review found in [**?**]. For a focus on complexity as found in quantum information, I would recommend [**?**].

### 2.3.1 Languages and promise problems

The main foundation of computational complexity is in the classification of languages based on the requisite number of resources to determine whether some string is in a language. Unfortunately, this requires the definition of many of these terms.

In particular, what exactly is a string? Any person who has taken a basic programming class knows that a string is simply a word, but the mathematical definition is slightly more complicated. In particular, we first need to define an alphabet, and then define a string over a particular alphabet.

**Definition 1** (Alphabet)**.** An alphabet is a finite collection of symbols.

Usually, an arbitrary alphabet is denoted by $\Gamma$, while the binary alphabet is denoted by $\Sigma = \{0, 1\}$. Usually, the particular alphabet has no impact on a particular complexity result, as any finite alphabet can be represented via the binary alphabet with overhead that is logarithmic in the size of the alphabet (basically, just use a binary encoding of the new alphabet).

With this definition of an alphabet, a string is simply a finite sequence of elements from the alphabet. In particular, we define $\Gamma^n$ to be all length $n$ sequences of elements from $\Gamma$, and then define

$$\Gamma^* = \bigcup_{n=0}^{\infty} \Gamma^n. \tag{2.3}$$

With this $\Gamma^*$ is the set of all strings over $\Gamma$.

With this, computational complexity then deals with understanding subsets of these strings. In particular, let $\Pi_{\text{yes}}$ be a subset of $\Gamma^*$. The language problem related to $\Pi_{\text{yes}}$ is then to understand what resources are necessary to determine whether a given $x \in \Gamma^*$ is also contained in $\Pi_{\text{yes}}$. This can be trivial, such as for the case of $\Pi_{\text{yes}} = \Gamma^*$, or it can be impossible, such as in the case of the famous Halting Problem.

[**TO DO:** *Find halting problem stuff*]

Related to these language problems are promise problems, in which there are two subsets of $\Gamma^*$, namely $\Pi_{\text{yes}}$ and $\Pi_{\text{no}}$, such that $\Pi_{\text{yes}} \cap \Pi_{\text{no}} = \emptyset$. We are then *promised* that the $x \in \Gamma^*$ that we need to sort is contained either $\Pi_{\text{yes}} \cup \Pi_{\text{no}}$. This generally opens up some more interesting problems, as without this restriction certain complexity classes do not make sense.

### 2.3.2 Turing machines

Up to this point, we have only discussed various classifications of strings, and stated that we will want to understand the various resources required to sort a given string into one of two different strings, but we have not explained how these resources are defined. There are various ways to do this, depending on the various computational model one is interested in, but at the highest level, we really only need to define a Turing machine.

These are a mathematical construction, that allow for the explicit definition of algorithms. In particular, they consist of a "finite-state machine" and an infinite tape. The finite-state machine is essentially just a small number of internal states, and the infinite state represents the ability to write down and then read an unbounded amount of information. The intuitive idea behind this construction is that the finite-state machine encodes some finite algorithm (which does not depend on the input to the algorithm), while the infinite tape holds the input to the problem, along with a workspace so that the Turing machine can keep track of various pieces of information.

More concretely,

[**TO DO:** *Get turing Machine stuff*]

#### 2.3.2.1 Reductions

Note that up to this point, we have not noticed any relations between different languages.

### 2.3.3 Useful complexity classes

Once we have an understanding of what defines a relation, and how these are related, we can attempt to classify those languages that require different resources in order to solve.

#### 2.3.3.1 Classical complexity classes

Perhaps the most well known question in computational complexity is the Pvs NPproblem. However, what exactly are these classes. At a most basic level, one can think of Pas those classification problems that have an efficient classical solution, while NPare those that can be checked in an efficient manner.

**Definition 2** (P)**.** A promise problem ...

**Definition 3** (NP)**.** A promise problem ...

#### 2.3.3.2 Bounded-Error Quantum Polynomial Time

Intuitively, the idea behind Bounded-Error Quantum Polynomial Time (BQP) consists of those problems that can be solved by a quantum computer efficiently.

**Definition 4** (BQP)**.** A promise problem $\Pi = (\Pi_{\text{yes}}, \Pi_{\text{no}})$ if there exist polynomials

#### 2.3.3.3 Quantum Merlin-Arthur

In addition to having an understanding of when a quantum computer can solve a particular problem, we will also want an understanding of those problems that most likely cannot be

**Definition 5** (QMA)**.** A promise problem $\Pi = (\Pi_{\text{yes}}, \Pi_{\text{no}})$ if there ..

## 2.4 Various Mathematical Lemmas

In addition to these various complexity results, it will also be useful to have a list of certain mathematical lemmas that will be used several times in the thesis. These lemmas might also be of independent interest.

### 2.4.1 Truncation Lemma

Perhaps the first such lemma we called the truncation lemma. The idea behind this lemma is to approximate the evolution of a state under some particular Hamiltonian with another, where the differences between the two Hamiltonians only occur far from the support of the given state. One would expect that since the state must evolve "far" in order to reach the differs between the two Hamiltonians, the evolution between the two will be close. This lemma makes this intuition precise.

**Lemma 1** (Truncation Lemma)**.** *Let $H$ be a Hamiltonian acting on a Hilbertspace $\mathcal{H}$ and let $|\Phi\rangle \in \mathcal{H}$ be a normalized state. Let $\mathcal{K}$ be a subspace of $\mathcal{H}$, let $P$ be the projector onto $\mathcal{K}$, and let $\tilde{H} = PHP$ be the Hamiltonian within this subspace. Suppose that, for some $T > 0$, $W \in \{H, \tilde{H}\}$, $N_0 \in \natural$, and $\delta > 0$, we have, for all $0 \le t \le T$,*

$$e^{-iWt}|\Phi\rangle = |\gamma(t)\rangle + |\epsilon(t)\rangle \textit{ with } \||\epsilon(t)\rangle\| \le \delta$$

*and*

$$(1-P)H^r|\gamma(t)\rangle = 0 \textit{ for all } r \in \{0,1,\ldots,N_0-1\}.$$

*Then, for all $0 \le t \le T$,*

$$\left\|\left(e^{-iHt} - e^{-i\tilde{H}t}\right)|\Phi\rangle\right\| \le \left(\frac{4e\|H\|t}{N_0} + 2\right)\left(\delta + 2^{-N_0}(1+\delta)\right).$$

This lemma actually combines two different methods. The first assumes that the

**Proposition 1.** *Let $H$ be a Hamiltonian acting on a Hilbert space $\mathcal{H}$, and let $|\Phi\rangle \in \mathcal{H}$ be a normalized state. Let $\mathcal{K}$ be a subspace of $\mathcal{H}$ such that there exists an $N_0 \in \natural$ so that for all $|\alpha\rangle \in \mathcal{K}^\perp$ and for all $n \in \{0,1,2,\ldots,N_0-1\}$, $\langle\alpha|H^n|\Phi\rangle = 0$. Let $P$ be the projector onto $\mathcal{K}$ and let $\tilde{H} = PHP$ be the Hamiltonian within this subspace. Then*

$$\|e^{-it\tilde{H}}|\Phi\rangle - e^{-itH}|\Phi\rangle\| \le 2\left(\frac{e\|H\|t}{N_0}\right)^{N_0}.$$

*Proof.* Define $|\Phi(t)\rangle$ and $|\tilde{\Phi}(t)\rangle$ as

$$|\Phi(t)\rangle = e^{-itH}|\Phi\rangle = \sum_{k=0}^{\infty}\frac{(-it)^k}{k!}H^k|\Phi\rangle \qquad |\tilde{\Phi}(t)\rangle = e^{-it\tilde{H}}|\Phi\rangle = \sum_{k=0}^{\infty}\frac{(-it)^k}{k!}\tilde{H}^k|\Phi\rangle.$$

Note that by assumption, $\tilde{H}^k|\Phi\rangle = H^k|\Phi\rangle$ for all $k < N_0$, and thus the first $N_0$ terms in the two above sums are equal. Looking at the difference between these two states, we have

$$\begin{aligned}
\||\Phi(t)\rangle - |\tilde{\Phi}(t)\rangle\| &= \left\|\sum_{k=0}^{\infty}\frac{(-it)^k}{k!}\left(H^k - \tilde{H}^k\right)|\Phi\rangle\right\| \\
&= \left\|\sum_{k=0}^{N_0-1}\frac{(-it)^k}{k!}\left(H^k - \tilde{H}^k\right)|\Phi\rangle - \sum_{k=N_0}^{\infty}\frac{(-it)^k}{k!}\left(H^k - \tilde{H}^k\right)|\Phi\rangle\right\| \\
&\le \sum_{k=N_0}^{\infty}\frac{t^k}{k!}\left(\|H\|^k + \|\tilde{H}\|^k\right) \\
&\le 2\sum_{k=N_0}^{\infty}\frac{t^k}{k!}\|H\|^k
\end{aligned}$$

where the last step uses the fact that $\|\tilde{H}\| \leq \|P\|\|H\|\|P\| = \|H\|$. Thus for any $c \geq 1$, we have

$$\begin{aligned}
\||\,\Phi(t)\,\rangle - |\,\tilde{\Phi}(t)\,\rangle\| &\leq \frac{2}{c^{N_0}} \sum_{k=N_0}^{\infty} \frac{(ct)^k}{k!} \|H\|^k \\
&\leq \frac{2}{c^{N_0}} \exp(ct\|H\|).
\end{aligned}$$

We obtain the best bound by choosing $c = N_0/\|Ht\|$, which gives

$$\||\,\Phi(t)\,\rangle - |\,\tilde{\Phi}(t)\,\rangle\| \leq 2\left(\frac{e\|H\|t}{N_0}\right)^{N_0}$$

as claimed. (If $c < 1$ then the bound is trivial.) $\square$

**Proposition 2.** *Let $U_1, \ldots, U_n$ and $V_1, \ldots, V_n$ be unitary operators. Then for any $|\,\psi\,\rangle$,*

$$\left\|\left(\prod_{i=n}^{1} U_i - \prod_{i=n}^{1} V_i\right)|\,\psi\,\rangle\right\| \leq \sum_{j=1}^{n} \left\|(U_j - V_j)\prod_{i=j-1}^{1} U_i|\,\psi\,\rangle\right\|. \tag{2.4}$$

*Proof.* The proof is by induction on $n$. The case $n = 1$ is obvious. For the induction step, we have

$$\begin{aligned}
\left\|\left(\prod_{i=n}^{1} U_i - \prod_{i=n}^{1} V_i\right)|\,\psi\,\rangle\right\| &= \left\|\left(\prod_{i=n}^{1} U_i - V_n\prod_{i=n-1}^{1} U_i + V_n\prod_{i=n-1}^{1} U_i - \prod_{i=n}^{1} V_i\right)|\,\psi\,\rangle\right\| && (2.5)\\
&\leq \left\|(U_n - V_n)\prod_{i=n-1}^{1} U_i|\,\psi\,\rangle\right\| + \left\|\left(\prod_{i=n-1}^{1} U_i - \prod_{i=n-1}^{1} V_i\right)|\,\psi\,\rangle\right\| && (2.6)\\
&\leq \sum_{j=1}^{n} \left\|(U_j - V_j)\prod_{i=j-1}^{1} U_i|\,\psi\,\rangle\right\| && (2.7)
\end{aligned}$$

where the last step uses the induction hypothesis. $\square$

*Proof of Lemma 1.* For $M \in \natural$ write

$$\begin{aligned}
\|(e^{-iHt} - e^{-i\tilde{H}t})|\,\Phi\,\rangle\| &= \left\|\left(\left(e^{-iH\frac{t}{M}}\right)^M - \left(e^{-i\tilde{H}\frac{t}{M}}\right)^M\right)|\,\Phi\,\rangle\right\| \\
&\leq \sum_{j=1}^{M} \left\|\left(e^{-iH\frac{t}{M}} - e^{-i\tilde{H}\frac{t}{M}}\right)e^{-iW(j-1)\frac{t}{M}}|\,\Phi\,\rangle\right\| \\
&\leq \sum_{j=1}^{M} \left\|\left(e^{-iH\frac{t}{M}} - e^{-i\tilde{H}\frac{t}{M}}\right)\left(|\,\gamma(\tfrac{(j-1)t}{M})\,\rangle + |\,\epsilon(\tfrac{(j-1)t}{M})\,\rangle\right)\right\| \\
&\leq 2M\delta + \sum_{j=1}^{M} \left\|\left(e^{-iH\frac{t}{M}} - e^{-i\tilde{H}\frac{t}{M}}\right)\frac{|\,\gamma(\frac{(j-1)t}{M})\,\rangle}{\left\||\,\gamma(\frac{(j-1)t}{M})\,\rangle\right\|}\right\| \left\||\,\gamma(\tfrac{(j-1)t}{M})\,\rangle\right\| \\
&\leq 2M\delta + 2M\left(\frac{e\|H\|t}{MN_0}\right)^{N_0}(1+\delta)
\end{aligned}$$

where in the second line we have used Proposition **??** and in the last step we have used Proposition **??** and the fact that $\||\gamma(t)\rangle\| \leq 1+\delta$. Now, for some $\eta > 1$, choose

$$M = \left\lceil \frac{\eta e \|H\| t}{N_0} \right\rceil$$

for $0 < t \leq T$ to get

$$\begin{aligned}\|(e^{-iHt} - e^{-i\tilde{H}t})|\Phi\rangle\| &\leq 2M\left(\delta + \eta^{-N_0}(1+\delta)\right) \\ &\leq 2\left(\frac{\eta e\|H\|t}{N_0} + 1\right)\left(\delta + \eta^{-N_0}(1+\delta)\right).\end{aligned}$$

The choice $\eta = 2$ gives the stated conclusion. □

Note that it would be slightly better to take a smaller value of $\eta$. However, this does not significantly improve the final result; the above bound is simpler and sufficient for our purposes.

### 2.4.2 Nullspace Projection Lemma

When we discuss the ground spaces and ground energies of various Hamiltonians, we will often want to know what happens to the ground spaces and ground energies when two such Hamiltonians are added together (such as adding penalties enforcing particular initial states). As such, the Nullspace Projection Lemma exactly discusses how such systems add together. As far as I am aware this lemma was initially used (implicitly) by Mizel et. al. [**TO DO:** *find correct reference*] We then used this in our proof of the QMA-completeness for the Bose-Hubbard model. We then found an additional place that used a similar lemma, with slightly better bounds. While the improvement is minor, here is a proof of the improved bound (and note that the improvement was left as a proof for the reader in the newer result).

**Lemma 2** (Nullspace Projection Lemma)**.** *Let $H_A$ and $H_B$ be positive semi-definite matrices. Suppose that the nullspace, $S$, of $H_A$ is nonempty, and that*

$$\gamma\big(H_B|_S\big) \geq c > 0 \qquad \textit{and} \qquad \gamma(H_A) \geq d > 0. \tag{2.8}$$

*Then,*

$$\gamma(H_A + H_B) \geq \frac{cd}{d + \|H_B\|}. \tag{2.9}$$

*Proof.* Let $|\psi\rangle$ be a normalized state satisfying

$$\langle\psi|H_A + H_B|\psi\rangle = \gamma(H_A + H_B). \tag{2.10}$$

Let $\Pi_S$ be the projector onto the nullspace of $H_A$. First suppose that $\Pi_S|\psi\rangle = 0$, in which case

$$\langle\psi|H_A + H_B|\psi\rangle \geq \langle\psi|H_A|\psi\rangle \geq \gamma(H_A) \tag{2.11}$$

and the result follows. On the other hand, if $\Pi_S|\psi\rangle \neq 0$ then we can write

$$|\psi\rangle = \alpha|a\rangle + \beta|a^\perp\rangle \tag{2.12}$$

with $|\alpha|^2 + |\beta|^2 = 1$, $\alpha \neq 0$, and two normalized states $|a\rangle$ and $|a^\perp\rangle$ such that $|a\rangle \in S$ and $|a^\perp\rangle \in S^\perp$. (If $\beta = 0$ then we may choose $|a^\perp\rangle$ to be an arbitrary state in $S^\perp$ but in the following we fix one specific choice for concreteness.) Note that any state $|\phi\rangle$ in the nullspace of $H_A + H_B$ satisfies $H_A|\phi\rangle = 0$ and hence $\langle\phi|a^\perp\rangle = 0$. Since $\langle\phi|\psi\rangle = 0$ and $\alpha \neq 0$ we also see that $\langle\phi|a\rangle = 0$. Hence any state

$$|f(q,r)\rangle = q|a\rangle + r|a^\perp\rangle \tag{2.13}$$

is orthogonal to the nullspace of $H_A + H_B$, and

$$\gamma(H_A + H_B) = \min_{|q|^2+|r|^2=1} \langle f(q,r)|H_A + H_B|f(q,r)\rangle. \tag{2.14}$$

Within the subspace $Q$ spanned by $|\,a\,\rangle$ and $|\,a^\perp\,\rangle$, note that

$$H_A|_Q = \begin{pmatrix} w & v^* \\ v & z \end{pmatrix} \qquad H_B|_Q = \begin{pmatrix} 0 & 0 \\ 0 & y \end{pmatrix} \tag{2.15}$$

where $w = \langle a|H_B|a\rangle$, $v = \langle a^\perp|H_B|a\rangle$, $y = \langle a^\perp|H_A|a^\perp\rangle$, and $z = \langle a^\perp|H_B|a^\perp\rangle$, and that we are interested in the smaller eigenvalue of

$$M = H_A|_Q + H_B|_Q = \begin{pmatrix} w & v^* \\ v & y+z \end{pmatrix}. \tag{2.16}$$

Letting $\epsilon_+$ and $\epsilon_-$ be the two eigenvalues of $M$ with $\epsilon_+ \geq \epsilon_-$, note that

$$\epsilon_+ = \|M\| \leq \|H_A|_Q\| + \|H_B|_Q\| \leq y + \|H_B|_Q\| \leq y + \|H_B\|, \tag{2.17}$$

where we have used the Cauchy interlacing theorem to note that $\|H_B|_Q\| \leq \|H_B\|$. Additionally, we have that

$$\epsilon_+\epsilon_- = \det(M) = w(y+z) - |v|^2 \geq wy \tag{2.18}$$

where we used the fact that $H_B|_Q$ is positive-semidefinite. Putting this together, we have that

$$\gamma(H_A + H_B) = \min_{|q|^2+|r|^2=1} \langle f(q,r)|H_A + H_B|f(q,r)\rangle = \epsilon_- \geq \frac{wy}{y + \|H_B\|}. \tag{2.19}$$

As the right hand side increased monotonically with both $w$ and $y$, and as $w \geq \gamma(H_B|_S) \geq c$ and $y \geq \gamma(H_A) \geq d$, we have

$$\gamma(H_A + H_B) \geq \frac{cd}{d + \|H_B\|} \tag{2.20}$$

as required. $\square$

# Chapter 3

# Scattering on graphs

Scattering has a long history of study in the physics literature. Ranging from the classical study of colliding objects to the analysis of high energy collisions of protons, studying the interactions of particles can be very interesting.

## 3.1 Motivation

Let us first take motivation from one of the most simple quantum systems: a free particle in one dimension. Without any potential or interactions, we have that the time independent Schrödinger equation reads

$$\frac{\partial^2}{\partial x^2}\psi(x) = -\frac{2m}{\hbar^2}E\psi(x) = -k^2\psi(x), \tag{3.1}$$

which requires the (unnormalizable) solutions,

$$\psi(x) = \exp(-ikx) \tag{3.2}$$

for real $k$. These *momentum states* correspond to particles travelling with momentum $k$ along the real line, and form a basis for the possible states of the system.

If we now also include some finite-range potential, or a potential $V$ that is non-zero only for $|x| < d$ for some range $d$, then outside this range the eigenstates remain unchanged. The only difference is that we will deal with a superposition of states for each energy instead of the pure momentum states. In particular, the scattering eigenbasis for this system will become

$$\psi(x) = \begin{cases} \exp(-ikx) + R(k)\exp(ikx) & x \leq -d \\ T(k)\exp(-ikx) & x \geq d \\ \phi(x,k) & |x| \leq d \end{cases} \tag{3.3}$$

for some functions $R(k)$, $T(k)$, and $\phi(x,k)$.

In addition to these scattering states, it is possible for bound states to exist. These states are only nonzero for $|x| < d$, as the potential allows for the particles to simply sit at a particular location. One of the canonical examples is a finite well in one dimension, in which depending on the depth of the well, any number of bound states can exist.

### 3.1.1 Infinite path

With this motivation in mind, let us now look at the discretized system corresponding to a graph. In particular, instead of a continuum of positions states in one dimension, we restrict the position states to integer values, with transport only between neighboring integers. Explicitly, the position basis for this Hilbert space can be labeled by $n \in \mathbb{N}$. In this basis, the discretized second derivative takes the form

$$\Delta^2 = \sum_{x=-\infty}^{\infty} (|\,x+1\,\rangle - 2|\,x\,\rangle + |\,x-1\,\rangle)\langle\,x\,| = \sum_{x=-\infty}^{\infty} \big(|\,x+1\,\rangle\langle\,x\,| + |\,x-1\,\rangle\langle\,x\,|\big) - 2\mathbb{I}. \tag{3.4}$$

If we then rescale the energy levels, we have that the identity term in the right hand side of (3.4) can be removed, so that $\Delta^2$ on this discretized one-dimensional system is proportional to the adjacency matrix of an infinite path.

With this representation of the second derivative operator, we can then see that the time-independent Schrödinger equation then becomes

$$\Delta^2|\,\psi\,\rangle = \Big(\sum_{x=-\infty}^{\infty} \big(|\,x+1\,\rangle\langle\,x\,| + |\,x-1\,\rangle\langle\,x\,|\big) - 2\mathbb{I}\Big)|\,\psi\,\rangle = E'_\psi|\,\psi\,\rangle. \tag{3.5}$$

If we rescale the energy term, and then break the vector equation into its components, we find that

$$\langle\,x+1\,|\,\psi\,\rangle + \langle\,x-1\,|\,\psi\,\rangle = E_\psi\langle\,x\,|\,\psi\,\rangle \tag{3.6}$$

for all $x \in \mathbb{Z}$. If we then make the ansatz that $\langle\,x\,|\,\psi\,\rangle = e^{ikx}$ for some $k$, we find that

$$\langle\,x+1\,|\,\psi\,\rangle + \langle\,x-1\,|\,\psi\,\rangle = e^{ik}e^{ikx} + e^{-ik}e^{ikx} = E_\psi e^{ikx} = E_\psi\langle\,x\,|\,\psi\,\rangle \qquad \Rightarrow \tag{3.7}$$

$$E_\psi = e^{ik} + e^{-ik} = 2\cos(k). \tag{3.8}$$

If we then use the fact that $E_\psi$ must be real, and that the amplitudes should not diverge to infinity as $x \to \pm\infty$, we find that the only possible values of $k$ are between $[-\pi, \pi)$. Hence, in analogy with the continuous case, the eigenbasis of the Hamiltonian corresponds to momentum states, but where the possible momenta only range over $[-\pi, \pi)$. We represent this momentum state with momenta $k$ as $|\,\tilde{k}\,\rangle$.

We can then talk about the "speed" of these states, which is given by

$$s = \left|\frac{dE_k}{dk}\right| = 2\sin(|k|). \tag{3.9}$$

Note that in the case of small $k$, we recover the linear relationship between speed and momentum. In this way, as the distance between the vertices grows smaller, we recover the continuum case.

One slight problem with this, however, is that these momentum states are not normalizable, and thus technically are not states in the Hilbert space. Additionally, there are an uncountable number of states, while the position basis contains only a countable number of basis states. It turns out that these basis elements are $\delta$-function orthogonal, in that

$$\langle\,\tilde{k}\,|\,\tilde{p}\,\rangle = \sum_{x=-\infty}^{\infty} e^{-ikx}e^{ikp} = \sum_{x=-\infty}^{\infty} e^{i(p-k)x} = 2\pi\delta(p-k), \tag{3.10}$$

so that we can decompose the identity on this space as

$$\mathbb{I} = \sum_{x=-\infty}^{\infty} |\, x\,\rangle\langle\, x\,| = \frac{1}{2\pi}\int_{-\pi}^{\pi} dk |\, \tilde{k}\,\rangle\langle\, \tilde{k}\,|. \tag{3.11}$$

## 3.2 Scattering off of a graph

Now that we understand the eigenstates of a discretized, one-dimensional, free particle, we should attempt to understand what happens when we include a finite potential. One method to do this is to add a potential function, with explicit potential energies at various vertices of the infinite path. However, if we wish to examine scattering only on unweighted graphs, we need to be a little more clever. As such, we will connect graphs in such a way that far from our changes the graph will look identical to that of an infinite path. In particular, we will eventually connect semi-infinite (i.e., infinite in only one direction) paths to a finite graph.

With this construction, the eigenvalue equation must still be satisfied along the semi-infinite paths, and thus the form of the eigenstates along the paths must still be of the form $e^{ikx}$ for some $k$ and $x$. However, we can no longer assume that $k$ is real, as the fact that the attached semi-infinite paths are only infinite in one direction allow for an exponentially decaying amplitudes along the paths. Additionally, we can have nontrivial correlations between the amplitudes among the different paths.

Note that much of this discussion can be found in [**?**].

### 3.2.1 Infinite path and a Graph

In the most simple example, let us attached a graph $\widetilde{G}$ to an infinite path. In particular, we assume that $\widetilde{G}$ is attached to a single vertex of the infinite path, and that the graph is attached by adding an edge from each vertex in $S \subset V(\widetilde{G})$ to one specific vertex of the infinite path, which we label 0. Calling this new graph $G$, the adjacency matrix of $G$ is then

$$A(G) = A(\widetilde{G}) + \sum_{v\in S\subset V(\widetilde{G})} |\, v\,\rangle\langle\, 0\,| + |\, 0\,\rangle\langle\, v\,| + \sum_{x=-\infty}^{\infty} |\, x\,\rangle\langle\, x+1\,| + |\, x+1\,\rangle\langle\, x\,|. \tag{3.12}$$

If we then want to inspect the eigenvectors of this Hamiltonian, we find that the eigenvalue equation on the infinite path is identical to that of an infinite path without the graph attached. Hence, we can see that any eigenstate of the Hamiltonian must take the form $A_k e^{ikx} + B_{-k}e^{-ikx}$ for some $k$ along the infinite paths.

With this assumption, we can see that there are three distinct cases for the form of the eigenstates. In particular, the eigenstate could have no amplitude along the infinite paths, being confined to the finite graph $\widehat{G}$. It could also be a normalizable state not confined to the finite graph $\widehat{G}$, in that the amplitude along the infinite paths decays exponentially. Finally, the eigenstate could be an unnormalizable state, in which case we will call the state a scattering state.

Let us assume that the state is a scattering state. Note that the eigenvalue of the state must be between $[-2, 2]$, and that the form of the eigenstate along the paths must be scalar multiples of $e^{ikx}$ and $e^{-ikx}$. Explicitly, the state must be of the form

$$\langle x | \psi \rangle = \begin{cases} A_k e^{ikx} + B_k e^{ikx} & x \leq 0 \\ C_k e^{ikx} + D_k e^{ikx} & x \geq 0 \end{cases} \tag{3.13}$$

where we note that the amplitude can change at $x = 0$ since we have attached the graph $\widetilde{G}$. However, we do have that $A_k + B_k = C_k + D_k$, since the amplitude at 0 is single valued. Additionally, we have that the eigenvalue of this state is given by $2\cos(k)$. Note that we have not yet determined the form of the eigenstate inside the graph $\widetilde{G}$, but if we define $|\phi\rangle$ to be the restriction of $|\psi\rangle$ to the finite graph $\widetilde{G}$, then $|\phi\rangle$ must satisfy the equation

$$A(G)|\phi\rangle + (A_k + B_k)\sum_{v\in S} |v\rangle\langle v|\phi\rangle = 2\cos(k)|\phi\rangle, \tag{3.14}$$

where the additional term arises from the fact that the vertices in $S$ are connected to the vertex 0. Finally, we have that

$$2\cos(k)\langle 0|\psi\rangle = Ae^{-ik} + B_k e^{ik} + C_k e^{ik} + D_k e^{-ik} + \sum_{v\in S}\langle v|\phi\rangle, \tag{3.15}$$

since the eigenvalue equation must be satisfied at 0.

While all of this seems rather complicated, we can focus on the case where $A_k = 1$ and $D_k = 0$ and the case where $A_k = 0$ and $D_k = 1$ individually, so that along one of the semi-infinite paths (corresponding to $x > 0$ or $x < 0$), the amplitude is given by $e^{ikx}$ or $e^{-ikx}$. These two states correspond to the eigenstates of the infinite path with the amplitudes given by $e^{-ikx}$ and $e^{ikx}$, with changes representing how adding the graph $\widetilde{G}$ affect the eigenstates.

With this assumption, let us first look at the case where $A_k = 1$ and $D_k = 0$. We then have that the eigenstates take the form

$$\langle x | \psi \rangle = \begin{cases} e^{-ikx} + B_k e^{ikx} & x \leq 0 \\ C_k e^{-ikx} & x \geq 0 \end{cases} \tag{3.16}$$

so that $1 + B_k = C_k$. Note that this is reminiscent of a scattering state, with reflection amplitude $B_k$ and transmission amplitude $C_k$, so that we take this intuition.

### 3.2.2 General graphs

More generally, let $\widehat{G}$ be any finite graph, with $n+m$ vertices and an adjacency matrix given by the block matrix

$$A(\widehat{G}) = \begin{pmatrix} A & B^\dagger \\ B & D \end{pmatrix}, \tag{3.17}$$

where $A$ is an $N \times N$ matrix, $B$ is an $m \times N$ matrix, and $D$ is an $m \times m$ matrix. When examining graph scattering, we will be interested in the graph $G$ given by the graph-join of $\widehat{G}$ and $N$ semi-infinite paths, with an additional edge between each of the first $N$ vertices of $\widehat{G}$ and the first vertex of one semi-infinite path.

We shall label label the first $N$ vertices of the graph $\widehat{G}$ as $(1, i)$, where $i \in [N]$, as these correspond to the first vertex in each semi-infinite path, and we will call these the *terminal vertices*. We refer to the other $m$ vertices of $\widehat{G}$ as the *internal vertices* of $\widehat{G}$, and label them as $w \in [m]$, and we refer to the vertices on the $N$ semi-infinite paths as $(x, i)$, where $i \in [N]$ labels which infinite path the vertex is located on (corresponding to which vertex $(1, i)$ the path is attatched to), while $x \in \mathbb{N}$ and $x \geq 2$ labels the distance along the semi-infinite path the vertex is located. With this labeling of the vertices of $G$, the adjacency matrix of $G$ is then given by

$$A(G) = A(\widehat{G}) + \sum_{j=1}^{N} \sum_{x=1}^{\infty} \big( |\, x, j\,\rangle\langle x+1, j\,| + |\, x+1, j\,\rangle\langle x, j\,| \big). \tag{3.18}$$

At this point, we want to examine the possible eigenstates of the matrix $A(G)$. It turns out that there are 3 different kinds of eigenstates, corresponding to the different qualitative properties of the eigenstate along the semi-infinite paths.

While we will mostly be interested in the third such type, it is important to understand the other kinds of eigenstates.

#### 3.2.2.1 Confined bound states

The easiest states to analyze are the confined bound states, which are eigenstates in which the only nonzero amplitudes are on vertices inside the finite graph $\widehat{G}$. If any vertex on the semi-infinite paths has nonzero amplitude for some eigenstate of the Hamiltonian, then the form of the Hamiltonian forces all vertices on that path to have nonzero amplitude, and thus these confined bound states are exactly those states that have finite support in the basis of vertex states.

To find these confined bound states, we restrict our Hilbert space to the space spanned by the internal vertices of $\widehat{G}$. The states of interest then correspond to the eigenstates of $D$ (the induced adjacency matrix of $A(G)$ when restricted to the internal vertices of $\widehat{G}$) with the additional restriction that the state lies in the nullspace of $B^\dagger$, so that we can extend this state to the full Hilbert space by simply assuming all other amplitudes are zero.

As we originally assumed that there are only $m$ internal vertices of $\widehat{G}$, there are at most $m$ such confined bound states. Additionally, note that there are no restrictions on the eigenvalues of these states, other than those that are inherited from any restrictions placed on it by $D$ (such as the energy being bounded by the maximum degree of $\widehat{D}$).

#### 3.2.2.2 Unconfined bound states

The next possible type of eigenstates are those that are not confined to the finite graph $\widehat{G}$ but are still normalizable. Since these states still have amplitude along the semi-infinite paths, we know that they must be of the form $Ae^(ikx)$, for some $A$ and $k$. However, when $k$ is not real (corresponding to a decaying amplitude along the paths), we have that

$$2\cos(k) = 2\cos(k_r + ik_i) = 2\cos(k_r)\cosh(k_i) - i\sin(k_r)\sinh(k_i). \tag{3.19}$$

Hence, if we assume that the state is normalizable, then $k_i \neq 0$, and as the adjacency matrix is Hermitian, we must have that the eigenvalue is real, forcing $k_r = \pi n$ for some $n \in \mathbb{N}$. Note that this then implies that $e^{ik} = z$, for some $z \in (-1, 1) \setminus \{0\}$ (where 0 corresponds to the confined bound states).

[**TO DO:** *Finish this section, and determine whether this is finite or infinite.*]

#### 3.2.2.3 Half-bound states

The half-bound states are the limit of the states as $\kappa \to 0$. In particular, they are those states where the amplitude along the infinite paths take the form $(\pm 1)^x$. These states aren't quite bound, in that they are not normalizable, but they are also not quite scattering states, as they correspond to non-moving scattering states. They won't play much of a role in this paper, but I did want to mention them.

#### 3.2.2.4 Scattering states

We finally reach the point of scattering states, or those states we can use for computational tasks. We first assume that we are orthogonal to all bound states, and in particular that we are othogonal to all confined bound states. This allows us to uniquely construct the scattering states (without this assumption, if there existed a confined bound state at the appropriate energy, then we could simply add any multiple of the confined bound state to get a different scattering state).

Taking some intuition from the classical case, we will construct a set of states that correspond to sending a particle in towards the graph $\widehat{G}$ along one of the semi-infinite paths and understanding how it scatters off of the graph. Namely, for each $i \in [N]$ we will assume that there exists a state with amplitude along the $i$-th path of the form $e^{ikx} + S_{i,i}(k)e^{-ikx}$ for $k \in (-\pi, 0)$, and that the rest of the paths have amplitudes given by $S_{i,q}(k)e^{ikx}$. More concretely, we assume that the form of the states is given on the infinite paths by

$$\langle x, q \,|\, \mathrm{sc}_j(k) \rangle = \delta_{j,q} e^{-ikx} + S_{qj} e^{ikx}. \tag{3.20}$$

We then need to see whether such an eigenstate exists. In this case, note that $S_{qj}$ corresponds to the transmitted amplitude along the $q$-th path if the particle was incident along the $j$-th path.

If we continue to make the assumption that these states exist, we can also write the amplitudes of the $m$ interval vertices as a column vector, as $\vec{\psi}_i(k)$, in which $\vec{\psi}_{i(k)}$ is the projection of $|\mathrm{sc}_j(k)\rangle$ onto the internal vertices of $\widehat{G}$. We can then collect these vectors into an $N \times m$ matrix, namely

$$\Psi(k) := \begin{pmatrix} \vec{\psi}_1(k) & \vec{\psi}_2(k) & \cdots & \vec{\psi}_N(k) \end{pmatrix} \tag{3.21}$$

[**TO DO:** *check if this is correct $N \times m$ or $m \times N$*]

Noting that the amplitudes for $\vec{\mathrm{sc}_j(k)}$ on the terminal vertices is given by $e^{-ik}|1, j\rangle + S_j(k)e^{ik}$ (thinking of $S_j(k)$ as a vector), we can then collect all of the eigenvalue equations for the vertices in $\widehat{G}$ (both internal and termal) as

$$\begin{pmatrix} A & B^\dagger \\ B & D \end{pmatrix} \begin{pmatrix} e^{-ik}\mathbb{I} + S(k)e^{ik} \\ \Psi(k) \end{pmatrix} + \begin{pmatrix} e^{-2ik}\mathbb{I} + e^{2ik}S(k) \\ 0 \end{pmatrix} = 2\cos(k) \begin{pmatrix} e^{-ik}\mathbb{I} + S(k)e^{ik} \\ \Psi(k) \end{pmatrix}. \tag{3.22}$$

By examining the lower half of this matrix equation, we can see that

$$\Psi(z) = \frac{1}{2\cos(k)\mathbb{I} - D}\big(e^{-ik}B + e^{ik}BS(z)\big), \tag{3.23}$$

which gives the amplitudes of the internal vertices in terms of the scattering matrix.

If we then examine the upper half of the matrix equation, we find that

$$A\big(e^{-ik}\mathbb{I} + e^{ik}S(k)\big) + B^\dagger\Psi(k) + \big(e^{-2ik}\mathbb{I} + e^{2ik}S(z)\big) = 2\cos(k)\big(e^{-ik}\mathbb{I} + e^{ik}S(k)\big) \qquad \Rightarrow \tag{3.24}$$

$$-\left(\mathbb{I} - e^{ik}\left(A + B^\dagger\frac{1}{2\cos(k) - D}B\right)\right)S(k) = \mathbb{I} - e^{-ik}\left(A + B^\dagger\frac{1}{2\cos(k) - D}B\right). \tag{3.25}$$

Hence, if we define

$$Q(k) = \mathbb{I} - e^{ik}\left(A + B^\dagger\frac{1}{2\cos(k) - D}B\right), \tag{3.26}$$

we find that

$$S(k) = -Q(k)^{-1}Q(-k). \tag{3.27}$$

Putting this all together, we then have that the states $|\mathrm{sc}_j(k)\rangle$ exist for all $k$ in which the matrix operations defining $S(k)$ are well defined. In particular, we take the inverse of $2\cos(k)\mathbb{I} - D$, and the inverse of $Q(k)$. These only possibly have problems when

#### 3.2.2.5 Easier calculation of $S$-matrix

[**TO DO:** *come up with a better name of this cycle*]

While the above is useful for most values of $k \in (-pi, 0)$, unfortunately there are specific values of $k$ (such as those for which $D$ has eigenvalue $2\cos(k)$) in which the above analysis doesn't hold do to the singularity of some particular matrices. If we want to show that these scattering states exist for all $k \in (-\pi, 0)$, we need to somehow show that these singularities are just a problem of the analysis and are not intrinsic barriers to existence.

Along these lines, let us extend our analysis to complex $z$, instead of only focusing on the real line. As such, let us define the matrix

$$\gamma(z) := \begin{pmatrix} zA - \mathbb{I} & zB^\dagger \\ zB & zD - (1+z^2)\mathbb{I} \end{pmatrix}. \tag{3.28}$$

Note that

$$\begin{pmatrix} \mathbb{I} & zB^\dagger \\ 0 & zD - (1+z^2)\mathbb{I} \end{pmatrix} \begin{pmatrix} -Q(z) & 0 \\ \frac{z}{zD-(1+z^2)\mathbb{I}}B & \mathbb{I} \end{pmatrix} = \begin{pmatrix} -Q(z) + zB^\dagger\frac{1}{D-(z+z^{-1})}B & zB^\dagger \\ zB & zD - (1+z^2)\mathbb{I} \end{pmatrix} \tag{3.29}$$

$$= \gamma(z) \tag{3.30}$$

Additionally, if we note that the inverse of a block diagonal matrix can be written as

$$\begin{pmatrix} X & Y \\ Z & W \end{pmatrix}^{-1} = \begin{pmatrix} \left(X - YW^{-1}Z\right)^{-1} & -X^{-1}Y\left(W - ZX^{-1}Y\right)^{-1} \\ -W^{-1}Z\left(X - YW^{-1}Z\right)^{-1} & \left(W - ZX^{-1}Y\right)^{-1} \end{pmatrix}, \tag{3.31}$$

then we can see that

$$\gamma(z)^{-1} = \begin{pmatrix} -Q(z) & 0 \\ \frac{z}{zD-(1+z^2)\mathbb{I}}B & \mathbb{I} \end{pmatrix}^{-1} \begin{pmatrix} \mathbb{I} & zB^\dagger \\ 0 & zD - (1+z^2)\mathbb{I} \end{pmatrix}^{-1} \tag{3.32}$$

$$= \begin{pmatrix} -Q(z)^{-1} & 0 \\ \frac{z}{zD-(1+z^2)\mathbb{I}}BQ(z)^{-1} & \mathbb{I} \end{pmatrix} \begin{pmatrix} \mathbb{I} & -B^\dagger \frac{z}{zD-(1+z^2)\mathbb{I}} \\ 0 & \frac{1}{zD-(1+z^2)\mathbb{I}} \end{pmatrix}. \tag{3.33}$$

We can then use this to see that

$$\gamma(z)^{-1}\gamma(z^{-1}) = \begin{pmatrix} -Q(z)^{-1} & 0 \\ \frac{z}{zD-(1+z^2)\mathbb{I}}BQ(z)^{-1} & \mathbb{I} \end{pmatrix} \begin{pmatrix} \mathbb{I} & -B^\dagger \frac{z}{zD-(1+z^2)\mathbb{I}} \\ 0 & \frac{1}{zD-(1+z^2)\mathbb{I}} \end{pmatrix} \begin{pmatrix} \mathbb{I} & z^{-1}B^\dagger \\ 0 & z^{-1}D - (1+z^{-2})\mathbb{I} \end{pmatrix} \begin{pmatrix} -Q(z^{-1}) \\ \frac{z^{-1}}{z^{-1}D-(1+z^{-2})\mathbb{I}}B \end{pmatrix} \tag{3.34}$$

$$= \begin{pmatrix} -Q(z)^{-1} & 0 \\ \frac{z}{zD-(1+z^2)\mathbb{I}}BQ(z)^{-1} & \mathbb{I} \end{pmatrix} \begin{pmatrix} \mathbb{I} & 0 \\ 0 & z^{-2}\mathbb{I} \end{pmatrix} \begin{pmatrix} -Q(z^{-1}) & 0 \\ \frac{z^{-1}}{z^{-1}D-(1+z^{-2})\mathbb{I}}B & \mathbb{I} \end{pmatrix} \tag{3.35}$$

$$= \begin{pmatrix} -Q(z)^{-1} & 0 \\ \frac{z}{zD-(1+z^2)\mathbb{I}}BQ(z)^{-1} & z^{-2}\mathbb{I} \end{pmatrix} \begin{pmatrix} -Q(z^{-1}) & 0 \\ \frac{z^{-1}}{z^{-1}D-(1+z^{-2})\mathbb{I}}B & \mathbb{I} \end{pmatrix} \tag{3.36}$$

$$= \begin{pmatrix} Q(z)^{-1}Q(z^{-1}) & 0 \\ \frac{1}{D-(z+z^{-1})\mathbb{I}}B\left(z^{-2}\mathbb{I} - Q(z)^{-1}Q(z^{-1})\right) & z^{-2}\mathbb{I} \end{pmatrix} \tag{3.37}$$

$$= -\begin{pmatrix} S(z) & 0 \\ z^{-1}\Psi(s) & -z^{-2}\mathbb{I} \end{pmatrix} \tag{3.38}$$

As such, we can write we have a nice representation of the scattering matrix and the interior amplitudes in terms of the matrix $\gamma$. If we then note that

$$\gamma(z)^{-1} = \frac{1}{\det \gamma(z)} \operatorname{adj} \gamma(z) \tag{3.39}$$

where $\operatorname{adj}\gamma(z)$ is the adjugate matrix of $\gamma(z)$, then by (3.38) we can then see that the entries of $S(z)$ are rational functions of $z$.

[**TO DO:** *this still doesn't explain why we can define the S-matrix this way when things aren't invertable explanation*]

### 3.2.3 Scattering matrix properties

While the use of the $\gamma$ matrix gives an explicit construction of the form of the eigenstates on the internal vertices, it is also useful to note that the scattering matrix at a particular momentum $k$ can be expressed as

$$S(k) = -Q(z)^{-1}Q(z^{-1}), \tag{3.40}$$

where $z = e^{ik}$, and the matrices $Q(z)$ are given by

$$Q(z) = \mathbb{I} - z\Big(A + B^\dagger \frac{1}{\frac{1}{z} + z - D} B\Big). \tag{3.41}$$

Note that $Q(z)$ and $Q(z^{-1})$ commute for all $z \in \mathbb{C}$, as they can both be written as $\mathbb{I} + zH(z + z^{-1})$.

Using this expression for the scattering matrix, it is easy to see that $S(k)$ is a unitary matrix, as

$$S(k)^\dagger = -Q(z^{-1})^\dagger (Q(z)^{-1})^\dagger \tag{3.42}$$

and that

$$Q(z)^\dagger = \mathbb{I}^\dagger - z^\dagger \Big(A^\dagger + B^\dagger \Big(\frac{1}{\frac{1}{z} + z - D}\Big)^\dagger (B^\dagger)^\dagger\Big) = \mathbb{I} - z^\dagger \Big(A + B^\dagger \frac{1}{\frac{1}{z^\dagger} + z^\dagger - D} B\Big) = Q(z^\dagger) \tag{3.43}$$

and thus

$$S(k)^\dagger = -Q(z^{-1})^\dagger (Q(z)^{-1})^\dagger = -Q(z) Q(z^{-1})^{-1} = Q(z^{-1})^{-1} Q(z) = S(k)^{-1} \tag{3.44}$$

where we used the fact that $z = e^{ik}$ so that $z^\dagger = z^{-1}$, and the fact that $Q(z)$ and $Q(z^{-1})$ commute.

Additionally, we can make use of the fact that $S$ is derived from an unweighted graph to show that the scattering matrices are symmetric. In particular, note that $Q(z)$ is symmetric for all $z$, since $D$ is symmetric, symmetric matrices are closed under inversion, $A$ is symmetric and $B$ is a 0-1 matrix. As such, we have that

$$S(k)^T = -\big(Q(z)^{-1} Q(z^{-1})\big)^T = -Q(z^{-1})^T (Q(z)^{-1})^T \tag{3.45}$$

$$= -Q(z^{-1}) Q(z)^{-1} = -Q(z)^{-1} Q(z^{-1}) = S(k) \tag{3.46}$$

where we used the fact that $Q(z)$ and $Q(z^{-1})$ commute.

Putting this together, we have that $S(k)$ is a symmetric, unitary matrix for all $k$.

### 3.2.4 Orthonormality of the scattering states

[**TO DO:** *go over this section more*]

We now establish the delta-function normalization of the scattering states. Let

$$\Pi_1 = \sum_{x=1}^{\infty} \sum_{q=1}^{N} |x, q\rangle\langle x, q|$$

$$\Pi_2 = \mathbb{I} - \sum_{x=2}^{\infty} \sum_{q=1}^{N} |x, q\rangle\langle x, q|$$

$$\Pi_3 = \sum_{q=1}^{N} |1, q\rangle\langle 1, q|.$$

We show that, for $k \in (-\pi, 0)$, $p \in (-\pi, 0)$, and $i, j \in \{1, \dots, N\}$,

$$\langle \mathrm{sc}_i(p)|\mathrm{sc}_j(k)\rangle = \langle \mathrm{sc}_i(p)|\Pi_1 + \Pi_2 - \Pi_3|\mathrm{sc}_j(k)\rangle = 2\pi\delta_{ij}\delta(k-p). \tag{3.47}$$

First write

$$\begin{aligned}
\langle \mathrm{sc}_i(p)|\Pi_1|\mathrm{sc}_j(k)\rangle &= \sum_{x=1}^{\infty}\sum_{q=1}^{N}(\delta_{iq}e^{ipx} + S^*_{qi}(p)e^{-ipx})(\delta_{jq}e^{-ikx} + S_{qj}(k)e^{ikx}) \\
&= \frac{1}{2}\left(\delta_{ij} + \sum_{q=1}^{N} S^*_{qi}(p)S_{qj}(k)\right)\left(\sum_{x=1}^{\infty} e^{i(p-k)x} + \sum_{x=1}^{\infty} e^{-i(p-k)x}\right) \\
&\quad + \frac{1}{2}\left(\delta_{ij} - \sum_{q=1}^{N} S^*_{qi}(p)S_{qj}(k)\right)\left(\sum_{x=1}^{\infty} e^{i(p-k)x} - \sum_{x=1}^{\infty} e^{-i(p-k)x}\right) \\
&\quad + \frac{1}{2}(S^*_{ji}(p) + S_{ij}(k))\left(\sum_{x=1}^{\infty} e^{-i(p+k)x} + \sum_{x=1}^{\infty} e^{i(p+k)x}\right) \\
&\quad + \frac{1}{2}(S^*_{ji}(p) - S_{ij}(k))\left(\sum_{x=1}^{\infty} e^{-i(p+k)x} - \sum_{x=1}^{\infty} e^{i(p+k)x}\right).
\end{aligned}$$

We use the following identities for $p, k \in (-\pi, 0)$:

$$\begin{aligned}
\sum_{x=1}^{\infty} e^{i(p-k)x} + \sum_{x=1}^{\infty} e^{-i(p-k)x} &= 2\pi\delta(p-k) - 1 \\
\sum_{x=1}^{\infty} e^{i(p+k)x} + \sum_{x=1}^{\infty} e^{-i(p+k)x} &= -1 \\
\sum_{x=1}^{\infty} e^{i(p-k)x} - \sum_{x=1}^{\infty} e^{-i(p-k)x} &= i\cot\left(\frac{p-k}{2}\right) \\
\sum_{x=1}^{\infty} e^{i(p+k)x} - \sum_{x=1}^{\infty} e^{-i(p+k)x} &= i\cot\left(\frac{p+k}{2}\right).
\end{aligned}$$

These identities hold when both sides are integrated against a smooth function of $p$ and $k$. Substituting, we get

$$\begin{aligned}
\langle \mathrm{sc}_i(p)|\Pi_1|\mathrm{sc}_j(k)\rangle = 2\pi\delta_{ij}\delta(p-k) &+ \delta_{ij}\left(\frac{i}{2}\cot\left(\frac{p-k}{2}\right) - \frac{1}{2}\right) \\
&+ \sum_{q=1}^{N} S^*_{qi}(p)S_{qj}(k)\left(-\frac{i}{2}\cot\left(\frac{p-k}{2}\right) - \frac{1}{2}\right) \\
&+ S^*_{ji}(p)\left(-\frac{1}{2} - \frac{i}{2}\cot\left(\frac{p+k}{2}\right)\right) \\
&+ S_{ij}(k)\left(-\frac{1}{2} + \frac{i}{2}\cot\left(\frac{p+k}{2}\right)\right)
\end{aligned} \tag{3.48}$$

where we used unitarity of the $S$-matrix to simplify the first term. Now turning to $\Pi_2$ we have

$$\langle \mathrm{sc}_i(p)|H\Pi_2|\mathrm{sc}_j(k)\rangle = 2\cos(p)\langle \mathrm{sc}_i(p)|\Pi_2|\mathrm{sc}_j(k)\rangle$$

and

$$\begin{aligned}\langle \mathrm{sc}_i(p)|H\Pi_2|\mathrm{sc}_j(k)\rangle = \langle \mathrm{sc}_i(p)|\Bigg(&2\cos(k)\Pi_2|\mathrm{sc}_j(k)\rangle + \sum_{q=1}^{N}(e^{-ik}\delta_{qj} + S_{qj}(k)e^{ik})|2,q\rangle \\ &- \sum_{q=1}^{N}(e^{-2ik}\delta_{qj} + S_{qj}(k)e^{2ik})|1,q\rangle\Bigg).\end{aligned}$$

Using these two equations we get

$$\begin{aligned}(2\cos(p) - 2\cos(k))\langle \mathrm{sc}_i(p)|\Pi_2|\mathrm{sc}_j(k)\rangle = {}&\delta_{ij}(e^{2ip-ik} - e^{-2ik+ip}) + S^*_{ji}(p)(e^{-2ip-ik} - e^{-2ik-ip}) \\ &+ S_{ij}(k)(e^{2ip+ik} - e^{2ik+ip}) \\ &+ \sum_{q=1}^{N} S^*_{qi}(p)S_{qj}(k)(e^{-2ip+ik} - e^{2ik-ip}).\end{aligned}$$

Noting that

$$\langle \mathrm{sc}_i(p)|\Pi_3|\mathrm{sc}_j(k)\rangle = \sum_{q=1}^{N}(\delta_{iq}e^{ip} + S^*_{qi}(p)e^{-ip})(\delta_{jq}e^{-ik} + S_{qj}(k)e^{ik}),$$

we have

$$\begin{aligned}\langle \mathrm{sc}_i(p)|\Pi_2 - \Pi_3|\mathrm{sc}_j(k)\rangle = {}&\delta_{ij}\left(\frac{e^{2ip-ik} - e^{-2ik+ip}}{2\cos(p) - 2\cos(k)} - e^{ip-ik}\right) \\ &+ S^*_{ji}(p)\left(\frac{e^{-2ip-ik} - e^{-2ik-ip}}{2\cos(p) - 2\cos(k)} - e^{-ip-ik}\right) \\ &+ S_{ij}(k)\left(\frac{e^{2ip+ik} - e^{2ik+ip}}{2\cos(p) - 2\cos(k)} - e^{ip+ik}\right) \\ &+ \sum_{q=1}^{N} S^*_{qi}(p)S_{qj}(k)\left(\frac{e^{-2ip+ik} - e^{2ik-ip}}{2\cos(p) - 2\cos(k)} - e^{-ip+ik}\right) \\ = {}&\delta_{ij}\left(\frac{1}{2} - \frac{i}{2}\cot\left(\frac{p-k}{2}\right)\right) + S^*_{ji}(p)\left(\frac{1}{2} + \frac{i}{2}\cot\left(\frac{p+k}{2}\right)\right) \\ &+ S_{ij}(k)\left(\frac{1}{2} - \frac{i}{2}\cot\left(\frac{p+k}{2}\right)\right) \\ &+ \sum_{q=1}^{N} S^*_{qi}(p)S_{qj}(k)\left(\frac{1}{2} + \frac{i}{2}\cot\left(\frac{p-k}{2}\right)\right).\end{aligned} \tag{3.49}$$

Adding equation (3.48) to equation (3.49) gives equation (3.47).

[**TO DO:** *These form an orthonormal basis if you also include the bound states, but this is Theorem 1 from Andrew and David's Levison's Theorem II paper. I'm not sure if I should include it.*]

## 3.3 Applications of graph scattering

### 3.3.1 NAND Trees

The motivating idea for understanding graph scattering was an explicit algorithm that computes the value of a NAND tree with $N$ leaves in $\mathcal{O}(\sqrt{N})$ time. In particular, a NAND tree is a complete binary tree of depth $\log N$, where each leaf has a particular binary value. Each node of the tree is then assigned a binary value by evaluating the NAND of its children, and the value of the entire tree is the value of the root node. Classically, any randomized algorithm requires $\mathcal{O}(N^{0.753})$ queries to the roots in order to evaluate the value of the tree, and thus this gives an example of a quantum speedup.

The reason that we are interested in this is that the original algorithm uses graph scattering as the actual algorithm. In particular, a binary tree is attached to an infinite path at the root, and then additional vertices are attached to the leaves depending on whether the binary value is 0 or 1. It turns out that at energy 0 (i.e., momentum $-\pi/2$), such a tree has perfect transmission from one path to the other if the tree evaluates to 1, and perfect reflection if the tree evaluates to 0. Hence, if a wave packet with momentum centered around $-\pi/2$ is scattered off of such a graph, then if we determine the location of the particle after it has scattered we evaluate the tree.

In this case, the requisite size of the wavepacket turns out to be $\mathcal{O}(\sqrt{N})$, and thus this amount of time is required in order for the scattering to occur. This is closely related to the number of queries to the values of the input variables in order to compute the value of the tree, and thus this is a quantum algorithm that has a provable speedup over classical computing.

### 3.3.2 Momentum dependent actions

While the NAND trees gives a good example of how the process works, in that the scattering evaluates a binary function, we can use similar ideas in order to have nontrivial scattering behavior. In particular, the NAND tree algorithm utilizes the fact that some graph either completely reflects or transmits at one particular momenta in order to evaluate the function, but we can also create graphs that have different behaviors at different momenta, or that perfectly transmits to some subset of the attached paths (i.e., generalizations to multiple semi-infinite paths).

#### 3.3.2.1 R/T gadgets

The easiest thing we could hope for are exactly similar to the NAND trees experiment, in that if there are only two attached semi-infite paths, then at some fixed momenta it either completely transmits, or it completely reflects. However, in contrast to the NAND tree, we will only work with a single graph, and use it to filter out some momenta.

Basically, the idea behind R/T gadgets is to perfectly transmit at some momenta, while perfectly reflecting at other momenta. This will then allow us to filter out certain unwanted wavepackets, and allow us to only deal with the momenta of interest. Further, these simple gadgets can be used as a simple building block in the construction of other graphs, allowing us to have more complicated graphs.

#### 3.3.2.2 Momentum Switches

In addition to a simple graph that only reflects or transmits certain momenta, we can generalize the idea to a kind of routing behavior. In particular, we can attempt to construct a graph with three attached semi-infinite paths, in which when a wavepacket is incident on one particular path, it either perfectly transmits to the second path, or it perfectly transmits to the third path, depending on the incident momenta. In this way, we construct something like a momentum dependent railroad switch, sending different wavepackets to different locations.

In the grand scheme of things, this is extremely useful, as it allows for more general momentum dependent actions.

### 3.3.3 Encoded unitary

Finally, we can also encode unitary actions using these graphs, in that by necessity these scattering matrices must be unitary. In particular, let us examine what happens to a graph with four attached semi-infinite paths, when at some chosen momentum a wavepacket from either of the first two paths gets perfectly transmits to the last two paths. In this case, the S-matrix becomes a block matrix, with the two $2 \times 2$ blocks in the diagonal both zero matrices. As such, the off diagonal matrices must also be unitary, and if we think of the two input paths as an encoded qubit (with a wavepacket along one path corresponding to an encoded $|0\rangle$ state and a wavepacket along the other path correpsonding to an encoded $|1\rangle$ state) then this scattering procedure performs some encoded unitary transformation on the qubit.

## 3.4 Construction of graphs with particular scattering behavior

While we have shown that the scattering behavior of some given graph is easy to compute, finding a graph with a given scattering behavior is much more difficult. We don't even know whether such an operation is decidable, and thus constructing an efficient algorithm for finding a graph with a given scattering behavior seems unlikely. However, there are specific behaviors at particular momenta in which constructions are known, and some small sized graphs that have been found via exhaustive searches.

### 3.4.1 R/T gadgets

[**TO DO:** *Go over this section, and revise*]

Perhaps the most simple behavior will be two-terminal gadgets that either perfectly reflect at some particular momenta, or perfectly transmit. While this is still a rather complicated problem when the terminals can be any vertices of the graph, things become tractable when we want to only attach a graph to a single vertex of an infinite path. In this case, everything works out as expected.

We refer to the graph shown in Figure **??** as $\hat{G}$, and we write $G$ for the full graph obtained by attaching two semi-infinite paths to terminals $(1,1)$ and $(1,2)$. As shown in the Figure, the graph $\hat{G}$ for a type 1 gadget is determined by a finite graph $G_0$ and a subset $P = \{p_1, \ldots, p_n\} \subseteq V(G_0)$ of its vertices, called the *periphery*. Each vertex in the periphery is connected to a vertex denoted $a$, and $a$ is also connected to two terminals $(1,1)$ and $(1,2)$. A type 1 R/T gadget with $n = 1$ has only one edge between $G_0$ and $a$; in this special case we also call it a *type 2 R/T gadget* (see Figure **??**).

Looking at the eigenvalue equation for the scattering state $|{}_1(k)\rangle$ at vertices $(1,1)$ and $(1,2)$, we see that the amplitude at vertex $a$ satisfies

$$\langle a|{}_1(k)\rangle = 1 + R(k) = T(k).$$

Thus perfect reflection at momentum $k$ occurs if and only if $R(k) = -1$ and $\langle a|{}_1(k)\rangle = 0$, while perfect transmission occurs if and only if $T(k) = 1$ and $\langle a|{}_1(k)\rangle = 1$. Using this fact, we now derive conditions on the graph $G_0$ that determine when perfect transmission and reflection occur.

For type 1 gadgets, we give a necessary and sufficient condition for perfect reflection: $G_0$ should have an eigenvector for which the sum of amplitudes on the periphery is nonzero.

**Lemma 3.** *Let $\hat{G}$ be a type 1 R/T gadget. A momentum $k \in (-\pi, 0)$ is in the reflection set $\mathcal{R}$ if and only if $G_0$ has an eigenvector $|\chi_k\rangle$ with eigenvalue $2\cos(k)$ satisfying*

$$\sum_{i=1}^{n} \langle p_i|\chi_k\rangle \neq 0. \tag{3.50}$$

*Proof.* First suppose that $\hat{G}$ has perfect reflection at momentum $k$, i.e., $R(k) = -1$ and $\langle a|{}_1(k)\rangle = 0$. Since $\langle (1,1)|{}_1(k)\rangle = e^{-ik} - e^{ik} \neq 0$ and $\langle (1,2)|{}_1(k)\rangle = 0$, to satisfy the eigenvalue equation at vertex $a$, we have

$$\sum_{j=1}^{n} \langle p_j|{}_1(k)\rangle = e^{ik} - e^{-ik} \neq 0.$$

Further, since $G_0$ only connects to vertex $a$ and the amplitude at this vertex is zero, the restriction of $|{}_1(k)\rangle$ to $G_0$ must be an eigenvector of $G_0$ with eigenvalue $2\cos(k)$. Hence the condition is necessary for perfect reflection.

Next suppose that $G_0$ has an eigenvector $|\chi_k\rangle$ with eigenvalue $2\cos(k)$ satisfying (3.50), with the sum equal to some nonzero constant $c$. Define a scattering state $|\psi_k\rangle$ on the Hilbert space of the full graph $G$ with amplitudes

$$\langle v|\psi_k\rangle = \frac{e^{ik} - e^{-ik}}{c} \langle v|\chi_k\rangle$$

for all $v \in V(G_0)$, $\langle a|\psi_k\rangle = 0$, and

$$\langle (x,j)|\psi_k\rangle = \begin{cases} e^{-ikx} - e^{ikx} & j = 1 \\ 0 & j = 2 \end{cases}$$

for all $x \in \mathbb{Z}^+$.

We claim that $|\psi_k\rangle$ is an eigenvector of $G$ with eigenvalue $2\cos(k)$. The state clearly satisfies the eigenvalue equation on the semi-infinite paths since it is a linear combination of states with momentum $\pm k$. At vertices of $G_0$, the state is proportional to an eigenvector of $G_0$, and since the state as no amplitude at $a$, the eigenvalue equation is also satisfied at these vertices. It remains to see that the eigenvalue equation is satisfied at $a$, but this follows immediately by a simple calculation.

Since $|\psi_k\rangle$ has the form of a scattering state with perfect reflection, we see that $R(k) = -1$ and $T(k) = 0$ as claimed. □

The following Lemma gives a sufficient condition for perfect transmission (which is also necessary for type 2 gadgets). Let $g_0$ denote the induced subgraph on $V(G_0) \setminus P$ where $P = \{p_i : i \in [n]\}$ is the periphery.

**Lemma 4.** *Let $\hat{G}$ be a type 1 R/T gadget and let $k \in (-\pi, 0)$. Suppose $|\xi_k\rangle$ is an eigenvector of $g_0$ with eigenvalue $2\cos k$ and with the additional property that, for all $i \in [n]$,*

$$\sum_{\substack{v \in V(g_0): \\ (v,p_i) \in E(G_0)}} \langle v|\xi_k\rangle = c \neq 0 \tag{3.51}$$

*for some constant $c$ that does not depend on $i$. Then $k$ is in the transmission set $\mathcal{T}$. If $\hat{G}$ is a type 2 R/T gadget, then this condition is also necessary.*

*Proof.* If $g_0$ has a suitable eigenvector $|\xi_k\rangle$ satisfying (3.51), define a scattering state $|\psi_k\rangle$ on the full graph $G$, with amplitudes $\langle a|\psi_k\rangle = 1$,

$$\langle v|\psi_k\rangle = \begin{cases} -\frac{1}{c}\langle v|\xi_k\rangle & v \in V(g_0) \\ 0 & v \in P \end{cases} \tag{3.52}$$

in the graph $G_0$, and

$$\langle (x,j)|\psi_k\rangle = \begin{cases} e^{-ikx} & j = 1 \\ e^{ikx} & j = 2 \end{cases}$$

for $x \in \mathbb{Z}^+$. As in the proof of Lemma 3, the state $|\psi_k\rangle$ is clearly satisfies the eigenvalue equation (with eigenvalue $2\cos(k)$) at vertices on the semi-infinite paths and vertices of $g_0$. The factor of $-\frac{1}{c}$ in (3.52) is chosen so that the eigenvalue condition is satisfied at vertices in $P$. It is easy to see that the eigenvalue condition is also satisfied at $a$.

Since $|\psi_k\rangle$ is a scattering eigenvector of $G$ with eigenvalue $2\cos(k)$ and perfect transmission, we have $T(k) = 1$.

Now suppose $\hat{G}$ is a type 2 R/T gadget (as shown in Figure **??**), with $P = \{p\}$. Perfect transmission along with the eigenvalue equation at vertex $a$ implies

$$\langle p|{}_1(k)\rangle = 0,$$

so the restriction of $|{}_1(k)\rangle$ to $g_0$ must be an eigenvector (since $p$ is the only vertex connected to $g_0$). The eigenvalue equation at $p$ gives

$$\langle a|{}_1(k)\rangle + \sum_{w\colon (w,p)\in E(G_0)} \langle w|{}_1(k)\rangle = 0 \quad \Longrightarrow \quad \sum_{w\colon (w,p)\in E(G_0)} \langle w|{}_1(k)\rangle = -1.$$

Hence the restriction of $|_1(k)\rangle$ to $V(g_0)$ is an eigenvector of the induced subgraph, with the additional property that the sum of the amplitudes at vertices connected to $p$ is nonzero. $\square$

#### 3.4.1.1 Explicit constructions

While the above gives a nice abstract explanation for the construction of R/T gadgets, it doesn't provide us with a concrete example without the graphs that satisfy the assumptions of the lemmas. As such, let us look at two simple graphs.

As a first example, suppose $G_0$ is a finite path of length $l_1 + l_2 - 2$ connected to $a$ at the $l_1$th vertex, as shown in Figure **??**. We determine the reflection and transmission sets as a function of $l_1$ and $l_2$.

Using Lemma 3, we see that perfect reflection occurs at momentum $k \in (-\pi, 0)$ if and only if the path has an eigenvector with eigenvalue $2\cos(k)$ with non-zero amplitude on vertex $l_1$. Recall that the path of length $L$ (where the length of a path is its number of edges) has eigenvectors $|\psi_j\rangle$ for $j \in [L+1]$ given by

$$\langle x|\psi_j\rangle = \sin\left(\frac{\pi j x}{L+2}\right) \tag{3.53}$$

with eigenvalues $\lambda_j = 2\cos(\pi j/(L+2))$. Hence

$$\mathcal{R}_{\text{path}} = \left\{-\frac{\pi j}{l_1+l_2} : j \in [l_1+l_2-1] \text{ and } \frac{j l_1}{l_1+l_2} \notin \mathbb{Z}\right\}.$$

To characterize the momenta at which perfect transmission occurs, consider the induced subgraph obtained by removing the $l_1$th vertex from the path of length $l_1 + l_2 - 2$ (a path of length $l_1 - 2$ and a path of length $l_2 - 2$). We can choose bases for the eigenspaces of this induced subgraph so that each eigenvector has all of its support on one of the two paths, and has nonzero amplitude on one of the vertices $l_1 - 1$ or $l_1 + 1$. Thus Lemma 4 implies that $\hat{G}$ perfectly transmits for all momenta in the set

$$\mathcal{T}_{\text{path}} = \left\{-\frac{\pi j}{l_1} : j \in [l_1-1]\right\} \cup \left\{-\frac{\pi j}{l_2} : j \in [l_2-1]\right\}.$$

For example, setting $l_1 = l_2 = 2$, we get $\mathcal{T}_{\text{path}} = \{-\frac{\pi}{2}\}$ and $\mathcal{R}_{\text{path}} = \{-\frac{\pi}{4}, -\frac{3\pi}{4}\}$.

Now let us suppose $G_0$ is a cycle of length $r$. Labeling the vertices by $x \in [r]$, where $x = r$ is the vertex attached to the path (as shown in Figure **??**), the eigenvectors of the $r$-cycle are

$$\langle x|\phi_m\rangle = e^{2\pi i x m/r}$$

with eigenvalue $2\cos(2\pi m/r)$, where $m \in [r]$. For each momentum $k = -2\pi m/r \in (-\pi, 0)$, there is an eigenvector with nonzero amplitude on the vertex $r$ (i.e., $\langle r|\phi_m\rangle \neq 0$), so Lemma 3 implies that perfect reflection occurs at each momentum in the set

$$\mathcal{R}_{\text{cycle}} = \left\{-\frac{\pi j}{r} : j \text{ is even and } j \in [r-1]\right\}.$$

To see which momenta perfectly transmit, we use Lemma 4. Consider the induced subgraph obtained by removing vertex $r$. This subgraph is a path of length $r - 2$ and has eigenvalues $2\cos(\pi m/r)$ for $m \in [r-1]$ as discussed in the previous section. Using the expression (3.53) for the eigenvectors, we see that the sum of the amplitudes on the two ends is nonzero for odd values of $m$. Perfect transmission occurs for each of the corresponding momenta:

$$\mathcal{T}_{\text{cycle}} = \left\{-\frac{\pi j}{r} : j \text{ is odd and } j \in [r-1]\right\}.$$

For example, the 4-cycle (i.e., square) has $\mathcal{T}_{\text{cycle}} = \{-\frac{\pi}{4}, -\frac{3\pi}{4}\}$ and $\mathcal{R}_{\text{cycle}} = \{-\frac{\pi}{2}\}$.

### 3.4.2 Momentum switches

[**TO DO:** *Go over this section, and revise/make it fit*]

To construct momentum switches between pairs of momentum, it will be worthwhile to first construct two R/T gadgets between the two momenta, with the two gadgets having swapped reflection and transmission sets. We will then construct something like a railroad switch, by placing the two gadgets immediately after a 3-claw; this construction will then be that the wavepacket will only see one of the two outgoing paths, and function exactly how we want it to.

We now construct a momentum switch between the reflection and transmission sets $\mathcal{R}$ and $\mathcal{T}$ of a type 2 R/T gadget. We attach the gadget and its reversal (defined in Section **??**) to the leaves of a claw, as shown in Figure **??**. Specifically, given a type 2 R/T gadget $\hat{G}$, the corresponding momentum switch $\hat{G}^{\prec}$ consists of a copy of $G_0$, a copy of $G_0^{\leftrightarrow}$, and a claw. The three leaves of the claw are the terminals. Vertex $p$ of $G_0$ is connected to leaf 2 of the claw, and vertices $w_1^{(1)}, \ldots, w_r^{(1)}$ of $G_0^{\leftrightarrow}$ are each connected to leaf 3 of the claw.

The high-level idea of the switch construction is as follows. For momenta in the transmission set, the gadget perfectly transmits while its reversal perfectly reflects, so the claw is effectively a path connecting terminals 1 and 2. For momenta in the reflection set, the roles of transmission and reflection are reversed, so the claw is effectively a path connecting terminals 1 and 3.

**Lemma 5.** *Let $\hat{G}$ be a type 2 R/T gadget with reflection set $\mathcal{R}$ and transmission set $\mathcal{T}$. The gadget $\hat{G}^{\prec}$ described above is a momentum switch between $\mathcal{R}$ and $\mathcal{T}$.*

*Proof.* We construct a scattering eigenstate for each momentum $k \in \mathcal{T}$ with perfect transmission from path 1 to path 2, and similarly construct a scattering eigenstate for each momentum $k' \in \mathcal{R}$ with perfect transmission from 1 to 3. These eigenstates show that $S_{2,1}(k) = 1$ and $S_{3,1}(k') = 1$. Since the S-matrix is symmetric and unitary, this gives the complete form of the S-matrix for all momenta in $\mathcal{R} \cup \mathcal{T}$. In particular, this shows that $\hat{G}^{\prec}$ is a momentum switch between $\mathcal{R}$ and $\mathcal{T}$.

We first construct the scattering states for momenta $k \in \mathcal{T}$. Lemma 4 shows that the graph $g_0$ has a $2\cos(k)$-eigenvector $|\xi_k\rangle$ satisfying equation (3.51) with some nonzero constant $c$. We define a state $|\mu_k\rangle$ on $G^{\prec}$ and we show that it is a scattering eigenstate with perfect transmission between paths 1 and 2. The amplitudes of $|\mu_k\rangle$ on the semi-infinite paths and the claw are

$$\langle (x,1)|\mu_k\rangle = e^{-ikx} \qquad \langle 0|\mu_k\rangle = 1 \qquad \langle (x,2)|\mu_k\rangle = e^{ikx} \qquad \langle (x,3)|\mu_k\rangle = 0.$$

The rest of the graph consists of the three copies of the subgraph $g_0$ and the vertices $p$ and $u_{\leftrightarrow}$. The corresponding amplitudes are

$$\langle v|\mu_k\rangle = \begin{cases} -\frac{1}{c}\langle v|\xi_k\rangle & v \in V(g_0^{(1)}) \\ \frac{1}{c}\langle v|\xi_k\rangle & v \in V(g_0^{(2)}) \\ -\frac{e^{ik}}{c}\langle v|\xi_k\rangle & v \in V(g_0^{(3)}) \\ 0 & v = p \text{ or } v = u_{\leftrightarrow}. \end{cases}$$

We claim that $|\mu_k\rangle$ is an eigenstate of the Hamiltonian with eigenvalue $2\cos(k)$. As in previous proofs, the state clearly satisfies the eigenvalue condition on the semi-infinite paths and at the vertices of $G_0$ and $G_0^{\leftrightarrow}$, and the factors of $\frac{1}{c}$ in the above equation are chosen so that it also satisfies the eigenvalue condition at vertices $p$ and $u_{\leftrightarrow}$. Since $|\mu_k\rangle$ is a scattering state with perfect transmission from path 1 to path 2, we see that $S_{2,1}(k) = 1$.

Finally, we construct an eigenstate $|\nu_{k'}\rangle$ with perfect transmission from path 1 to path 3 for each momentum $k' \in \mathcal{R}$. This state has the form

$$\langle (x,1)|\nu_{k'}\rangle = e^{-ik'x} \qquad \langle 0|\nu_{k'}\rangle = 1 \qquad \langle (x,2)|\nu_{k'}\rangle = 0 \qquad \langle (x,3)|\nu_{k'}\rangle = e^{ik'x}$$

on the semi-infinite paths and the claw. Lemma 3 shows that $G_0$ has a $2\cos(k')$-eigenstate $|\chi_{k'}\rangle$ with $\langle p|\chi_{k'}\rangle \neq 0$, which determines the form of $|\nu_{k'}\rangle$ on the remaining vertices:

$$\langle v|\nu_{k'}\rangle = \begin{cases} -\frac{1}{\langle p|\chi_{k'}\rangle}\langle v|\chi_{k'}\rangle & v \in V(G_0) \\ -\frac{e^{ik'}}{\langle p|\chi_{k'}\rangle}\langle v|\chi_{k'}\rangle & v \in V(g_0^{(2)}) \\ -e^{ik'} & v = u^{\leftrightarrow} \\ 0 & \text{otherwise.} \end{cases}$$

As before, it is easy to check that this a momentum-$k'$ scattering state with perfect transmission from path 1 to path 3, so $S_{3,1}(k') = 1$.

Thus the gadget from Figure **??** is a momentum switch between $\mathcal{R}$ and $\mathcal{T}$. $\square$

#### 3.4.2.1 Explicit examples

[**TO DO:** *work this section*]

### 3.4.3 Encoded unitaries

While there is no efficient method to find graphs that apply some fixed encoded unitary, it is possible to search over all small graphs that have some particular implementation.

[**CITE:** *Find this small graphs thing*]

Essentially, the main idea behind this method is that since we can easily compute the scattering matrix for a particular graph at a particular momentum, if we want to find a graph that has some prescribed scattering behavior at a prescribed momenta we simply assume that such a graph exists with a particular number of internal vertices, and then search over all graphs of that size. While this exhaustive search is not guaranteed to find such a graph, a surprising number of systems can be found with this structure.

In particular, if we restrict ourselves to simple momenta, in which the energy $2\cos(k)$ is in some simple extension of the rationals, then most simple scattering behaviors can be found.

Graphs that end up being of particular use are those that allow for encoded unitary transformations. As such, we want to find graphs in which the attached paths can be partitioned into two sets, corresponding to input paths and output paths. We then want the scattering matrices at some particular momenta to be block matrices, with the diagonal blocks being zero matrices.

While this puts a large restriction on the graphs, many such graphs have been found. In particular [**CITE:** *small graphs scattering stuff*] has run an exhaustive search for such matrices up to size [**TO DO:** *find size*] . Some graphs that will be of particular interest to us are those that serve as a universal set of gates at two particular momenta. In particular, we will find uses for graphs that at momenta $-\frac{\pi}{4}$ implement a phase gate and implement a basis changing gate, and graphs that at momenta $-\frac{\pi}{2}$ implement a Hadamard gate.

These graphs are as follows: [**TO DO:** *show these graphs*]

## 3.5 Various facts about scattering

While we have the previous constructions that yield graphs with particular behavior, we will also want to understand some simple relations between graphs and their respective scattering matrices. In particular, understanding what properties are necessary in order to have a given scattering matrix, and understanding the relation between various the scattering matrices of various momenta.

### 3.5.1 Degree-3 graphs are sufficient

One of the most simple assumptions that could be made is that certain scattering behaviors require high degree graphs. In particular, the idea that having many connections might allow for some additional correlations between the outputs on larger graphs.

If we restrict our attention to only a finite number of rational momenta, however, this does not turn out to be the case. We can show that any graph can be replaced by a degree three graph with an identical scattering behavior at some fixed momenta. In particular, we show that a single vertex can be replaced by a finite path while still satisfying the eigenvalue equation at some fixed momenta, which determine the length of the path.

As a degree two graphs are the graph joins of cycles and paths, degree three graphs are the smallest graphs to have nontrivial scattering behaviors. This lemma shows that, in a certain sense, they are also all that are required.

**Lemma 6.** *Let $\widehat{G}$ be a finite graph, and let $M$ be a finite set of rational multiples of $\pi$. If $v \in V(G)$ is a degree $d$ vertex, there exists a graph $H$ that extends $G$ with the vertex $v$ being replaced by a degree-($\lceil \frac{d}{2} \rceil + 1$) subgraph such that the scattering matrices at the momenta $k \in M$ are preserved.*

*Proof.* The main idea behind this proof is to partition the vertices adjacent to $v$ into two sets, and then replace $v$ by a finite path, with the two sets connected to opposites ends of the finite path. By choosing the length of the path correctly, we can show that the amplitudes at either end of the path can be taken as the same amplitude of $v$ at each momenta in $M$, so that the eigenvalue equation remains satisfied with the same amplitudes on every vertex other than $v$, keeping the scattering matrices the same.

In particular, let $v$ be the degree $d$ vertex in $G$, and let $S = \{w \in V(G) : w \sim v\}$. Additionally, let us arbitrarily partition $S$ into two sets, $S_1$ and $S_2$, such that $\big||S_1|-|S_2|\big| \leq 1$.

As each $k \in M$ is a finite set of rational multiples of $\pi$, there exists some $m' \in \mathbb{N}$ such that for each $k \in M$, $mk = 2\pi j$ for some $j \in \mathbb{N}$. Let us then examine the graph $H$ where $v$ is replaced by a path of length $m+1$ and $S_1$ is attached to one end of the path while $S_2$ is attached to the other end. Explicitly:

$$
\begin{aligned}
V(H) &= V(G) \setminus \{v\} \cup \{(v,j) : j \in [m+1]\} && (3.54)\\
E(H) &= \big\{e \in E(G) : v \notin e\big\} \cup \big\{\{(v,j),(v,j+1)\} : j \in [m]\big\} \cup \\
&\qquad \big\{\{s,(v,0)\} : s \in S_1\big\} \cup \big\{\{s,(v,m)\} : s \in S_2\big\}. && (3.55)
\end{aligned}
$$

Now, for any $k \in M$, let $|\,\phi\,\rangle$ be an eigenstate of $A(G)$ with eigenvalue $2\cos(k)$. We will show that there exists an eigenstate $|\,\psi\,\rangle$ of $A(H)$ with energy $2\cos(k)$ such that for any $w \in V(G) \setminus \{v\}$, $\langle\, w\,|\,\phi\,\rangle = \langle\, w\,|\,\psi\,\rangle$. Concretely, for any vertex other than $v$, let us define $|\,\psi\,\rangle$ in this manner, and note that $|\,\psi\,\rangle$ satisfies the eigenvalue equation with energy $2\cos(k)$ for all vertices other than those in $S$ or those replacing $v$ by assumption. Additionally, let

$$
\alpha = \sum_{w \in S_1} \langle\, w\,|\,\phi\,\rangle \qquad \beta = \langle\, v\,|\,\phi\,\rangle \qquad \gamma = \sum_{w \in S_2} \langle\, w\,|\,\phi\,\rangle. \tag{3.56}
$$

We will then defined the amplitude along the path replacing the vertex $v$ as

$$
\langle\,(v,j)\,|\,\psi\,\rangle = \beta\cos(kj) + \frac{\gamma - \beta\cos(k)}{\sin(k)}\sin(kj). \tag{3.57}
$$

Note that $\langle\,(v,0)\,|\,\psi\,\rangle = \langle\,(v,m)\,|\,\psi\,\rangle = \beta = \langle\, v\,|\,\phi\,\rangle$, and thus the eigenvalue equation is satisfied at all vertices in $S$ with energy $2\cos(k)$. As the eigenstates along a path with energy $2\cos(k)$ are scalar multiples of $\sin(kx)$ and $\cos(kj)$, we can also see that the eigenvalue equation is necessarily satisfied for all $(v,j)$ with $j \neq 0$ and $j \neq m$.

If we then examine the eigenvalue equation at $(v,0)$, we can see that

$$
\begin{aligned}
\sum_{s \in S_1} \langle\, s\,|\,\psi\,\rangle + \langle\,(v,1)\,|\,\psi\,\rangle &= \alpha + \beta\cos(k) + \frac{\gamma - \beta\cos(k)}{\sin(k)}\sin(k) && (3.58)\\
&= \alpha + \gamma && (3.59)\\
&= 2\cos(k)\beta = 2\cos(k)\langle\,(v,0)\,|\,\psi\,\rangle && (3.60)
\end{aligned}
$$

where the third equality follows from the fact that $|\,\phi\,\rangle$ satisfies the eigenvalue equation at $v$ with eigenvalue $2\cos(k)$.

Let us finally examine the eigenvalue equation at $(v,m)$, noting that

$$
\begin{aligned}
\sum_{s \in S_2} \langle\, s\,|\,\psi\,\rangle + \langle\,(v,m-1)\,|\,\psi\,\rangle &= \gamma + \beta\cos(k(m-1)) + \frac{\gamma - \beta\cos(k)}{\sin(k)}\sin(k(m-1)) && (3.61)\\
&= \gamma + \beta\cos(k) - \big(\gamma - \beta\cos(k)\big) && (3.62)\\
&= 2\cos(k)\beta = 2\cos(k)\langle\,(v,0)\,|\,\psi\,\rangle && (3.63)
\end{aligned}
$$

where the second equality follows from some trigonometric identities. We can then see that $|\psi\rangle$ satisfies the eigenvalue equation at $(v, m)$ with energy $2\cos(k)$.

Putting this together, we have that $|\psi\rangle$ is an eigenvector of $A(H)$ with energy $2\cos(k)$ such that $|\psi\rangle$ and $|\phi\rangle$ are identical on those vertices contained in both $G$ and $H$. As this result holds for any energy $2\cos(k)$ eigenvector of $A(G)$, and as the two graphs are identical along the semi-inifinite paths, we have that the scattering matrices for these two graphs are identical, and thus the scattering matrices are preserved under this degree reduction procedure. □

By repeated use of this lemma, we can then see that if we are only interested in the scattering behavior of a graph at particular momenta, then we need only examine degree three graphs.

### 3.5.2 Not all momenta can be split

In addition, it might be useful to see when particular scattering behavior is possible or not. As such ,we will show that no momentum switch can exist between the pairs of momenta $-\frac{\pi}{4}$ and $-\frac{3\pi}{4}$. The proof will actually show that no R/T gadget exists between these two momenta, but as any momentum switch can be turned into an R/T gadget, this will be sufficient.

[**TO DO:** *Go over this section, and revise*]

#### 3.5.2.1 Basis vectors with entries in $\mathbb{Q}(\sqrt{2})$

Recall the general setup shown in Figure **??**: $N$ semi-infinite paths are attached to a finite graph $\hat{G}$. Consider an eigenvector $|\tau_k\rangle$ of the adjacency matrix of $G$ with eigenvalue $2\cos(k)$ for $k \in (-\pi, 0)$. In general this eigenspace is spanned by incoming scattering states with momentum $k$ and confined bound states [**?**] (which have zero amplitude on the semi-infinite paths). We can thus write the amplitudes of $|\tau_k\rangle$ on the semi-infinite paths as

$$\langle (x,j) | \tau_k \rangle = \kappa_j \cos(k(x-1)) + \sigma_j \sin(k(x-1))$$

for $x \in \mathbb{Z}^+$, $j \in [N]$, and $\kappa_j, \sigma_j \in \mathbb{C}$, and the amplitudes on the internal vertices as

$$\langle w | \tau_k \rangle = \iota_w$$

for $\iota_w \in \mathbb{C}$, where $w$ indexes the internal vertices. We write the adjacency matrix of $\hat{G}$ as a block matrix as in (**??**). Since the state $|\tau_k\rangle$ satisfies the eigenvalue equation on the semi-infinite paths, it remains to satisfy the conditions specified by the block matrix equation

$$\begin{pmatrix} A & B^\dagger \\ B & D \end{pmatrix} \begin{pmatrix} \kappa \\ \iota \end{pmatrix} + \cos(k) \begin{pmatrix} \kappa \\ 0 \end{pmatrix} + \sin(k) \begin{pmatrix} \sigma \\ 0 \end{pmatrix} = 2\cos(k) \begin{pmatrix} \kappa \\ \iota \end{pmatrix}.$$

Hence, the nullspace of the matrix

$$M = \begin{pmatrix} A - \cos(k)\mathbb{I} & \sin(k)\mathbb{I} & B^\dagger \\ 0 & 0 & 0 \\ B & 0 & D - 2\cos(k)\mathbb{I} \end{pmatrix}$$

is in one-to-one correspondence with the $2\cos(k)$-eigenspace of the infinite matrix (here the first block corresponds to $\kappa$, the second to $\sigma$, and the third to $\iota$). Further, $M$ only has entries in $\mathbb{Q}(\cos(k), \sin(k))$, so its nullspace has a basis with amplitudes in $\mathbb{Q}(\cos(k), \sin(k))$, as can be seen using Gaussian elimination.

We are interested in the specific cases $2\cos(k) = \pm\sqrt{2}$ corresponding to $k = -\frac{\pi}{4}$ or $k = -\frac{3\pi}{4}$. In these cases $\mathbb{Q}(\cos(k), \sin(k)) = \mathbb{Q}(\sqrt{2})$, and we may choose a basis for the nullspace of $M$ with amplitudes from $\mathbb{Q}(\sqrt{2})$. Furthermore, $\cos(kx), \sin(kx) \in \mathbb{Q}(\sqrt{2})$ for all $x \in \mathbb{Z}^+$, so with such a choice of basis, each amplitude of $|\,\tau_k\,\rangle$ is also an element of $\mathbb{Q}(\sqrt{2})$.

As noted above, the spectrum of $G$ may include confined bound states [**?**] with eigenvalue $\pm\sqrt{2}$. However, any such states are eigenstates of the adjacency matrix of $\hat{G}$ subject to the additional (rational) constraints that the amplitudes on the terminals are zero. As such, the confined bound states have a basis over $\mathbb{Q}(\sqrt{2})$. We can use this basis to restrict attention to those states orthogonal to confined bound states using only constraints over $\mathbb{Q}(\sqrt{2})$, so there exists a basis over $\mathbb{Q}(\sqrt{2})$ for the $N$-dimensional subspace of scattering states with energy $\pm\sqrt{2}$ that are orthogonal to the confined bound states. Finally, since $\mathbb{Q}(\sqrt{2})$ can be seen as a two-dimensional vector space over $\mathbb{Q}$, note that for any member of this basis $|\,\tau_k\,\rangle$ there exist rational vectors $|\,u_k\,\rangle, |\,w_k\,\rangle$ such that $|\,\tau_k\,\rangle = |\,u_k\,\rangle + \sqrt{2}|\,w_k\,\rangle$. Since $H^2|\,\tau_k\,\rangle = 2|\,\tau_k\,\rangle$, we have $H|\,u_k\,\rangle = \pm 2|\,w_k\,\rangle$ and $H|\,w_k\,\rangle = \pm|\,u_k\,\rangle$, so

$$|\,\tau_k\,\rangle = (H \pm \sqrt{2}\mathbb{I})|\,w_k\,\rangle. \tag{3.64}$$

#### 3.5.2.2 No R/T gadget and hence no momentum switch

Recall from Section **??** that a momentum switch between two momenta $k$ and $p$ can always be converted into an R/T gadget between $k$ and $p$. Here we show that if an R/T gadget perfectly reflects at momentum $-\frac{\pi}{4}$, then it must also perfectly reflect at momentum $-\frac{3\pi}{4}$. This implies that no R/T gadget exists between these two momenta, and thus no momentum switch exists.

We use the following basic fact about two-terminal gadgets several times:

**Fact 1.** *If a two-terminal gadget has a momentum-$k$ scattering state $|\,\phi\,\rangle$ with zero amplitude along path 2, then the gadget perfectly reflects at momentum $k$.*

*Proof.* Without loss of generality, we may assume that $|\,\phi\,\rangle$ is orthogonal to all confined bound states. If $|\,\phi\,\rangle$ has zero amplitude along path 2, then there exist some $\mu, \nu \in \mathbb{C}$ such that

$$\langle\,(x,2)\,|\,\phi\,\rangle = \mu\langle\,(x,2)\,|\,{}_2(k)\,\rangle + \nu\langle\,(x,2)\,|\,{}_1(k)\,\rangle = \mu e^{-ikx} + \mu R e^{ikx} + \nu T e^{ikx} = 0$$

for all $x \in \mathbb{Z}^+$. Since this holds for all $x$, we have $\mu = \mu R + \nu T = 0$. Since $\mu$ and $\nu$ cannot both be zero, we have $T = 0$. $\square$

For an R/T gadget, the scattering states (at some fixed momentum) that are orthogonal to the confined bound states span a two-dimensional space. As shown in Section 3.5.2.1, we can expand each scattering eigenstate at momentum $k = -\frac{\pi}{4}$ in a basis with entries in $\mathbb{Q}(\sqrt{2})$, where each basis vector takes the form (3.64). This gives

$$|\,{}_1(-\tfrac{\pi}{4})\,\rangle = (H + \sqrt{2}\mathbb{I})(\alpha|\,Ↄ\,\rangle + \beta|\,\,\rangle)$$

where $\alpha, \beta \in \mathbb{C}$, $\alpha \neq 0$, and $|\, a\,\rangle$ and $|\, b\,\rangle$ are rational 2-eigenvectors of $H^2$.

If $T(-\frac{\pi}{4}) = 0$, then for all $x \geq 0$,

$$\langle x, 2|{}_1(-\tfrac{\pi}{4})\rangle = 0 = \langle x, 2|(H + \sqrt{2}\mathbb{I})(\alpha|\supset\rangle + \beta|\ \rangle).$$

Dividing through by $\alpha$ and rearranging, we get that for all $x \geq 0$,

$$\frac{\beta}{\alpha}(\langle x, 2|H|\, b\,\rangle + \sqrt{2}\langle x, 2|\, b\,\rangle) = -\langle x, 2|H|\, a\,\rangle - \sqrt{2}\langle x, 2|\, a\,\rangle.$$

If the left-hand side is not zero, then $\beta/\alpha \in \mathbb{Q}(\sqrt{2})$ since $H$, $|\, a\,\rangle$, and $|\, b\,\rangle$ are rational. If the left-hand side is zero, then $(H + \sqrt{2}\mathbb{I})|\, a\,\rangle$ is an eigenstate at energy $2\cos(k)$ with no amplitude along path 2, so $\beta = 0$ (using Fact 1), and again $\beta/\alpha \in \mathbb{Q}(\sqrt{2})$.

Now write $\beta/\alpha = r + s\sqrt{2}$ with $r, s \in \mathbb{Q}$, and consider the rational 2-eigenvector of $H^2$

$$|\, c\,\rangle := |\, a\,\rangle + (r + sH)|\, b\,\rangle.$$

Note that

$$\alpha(H + \sqrt{2}\mathbb{I})|\, c\,\rangle = \alpha(H + \sqrt{2}\mathbb{I})|\, a\,\rangle + \alpha(rH + r\sqrt{2} + sH^2 + sH\sqrt{2})|\, b\,\rangle.$$

Since $|\, b\,\rangle$ is a 2-eigenvector of $H^2$ and $\beta/\alpha = r + s\sqrt{2}$, this simplifies to

$$\alpha(H + \sqrt{2}\mathbb{I})|\, c\,\rangle = \alpha(H + \sqrt{2}\mathbb{I})|\, a\,\rangle + \beta(H + \sqrt{2}\mathbb{I})|\, b\,\rangle = |{}_1(-\tfrac{\pi}{4})\rangle, \tag{3.65}$$

so $|{}_1(-\frac{\pi}{4})\rangle$ can be written as $\alpha(H + \sqrt{2}\mathbb{I})$ times a rational 2-eigenvector of $H^2$.

Since $\langle x, 2|{}_1(-\frac{\pi}{4})\rangle = 0$ for all $x \geq 1$ (and $\alpha \neq 0$), we have

$$\langle x, 2|(H + \sqrt{2}\mathbb{I})|\, c\,\rangle = \langle x, 2|H|\, c\,\rangle + \sqrt{2}\langle x, 2|\, c\,\rangle = 0.$$

As $H$ is a rational matrix and $|\, c\,\rangle$ is a rational vector, the rational and irrational components must both be zero, implying $\langle x, 2|\, c\,\rangle = \langle x, 2|H|\, c\,\rangle = 0$ for all $x \geq 1$. Furthermore, since $|{}_1(-\frac{\pi}{4})\rangle$ is a scattering state with zero amplitude on path 2, it must have some nonzero amplitude on path 1 and thus there is some $x_0 \in \mathbb{Z}^+$ for which $\langle x_0, 1|\, c\,\rangle \neq 0$ or $\langle x_0, 1|H|\, c\,\rangle \neq 0$.

Now consider the state obtained by replacing $\sqrt{2}$ with $-\sqrt{2}$:

$$|{}_1(-\tfrac{\pi}{4})\rangle := \alpha(H - \sqrt{2}\mathbb{I})|\, c\,\rangle.$$

This is a $-\sqrt{2}$-eigenvector of $H$, which can be confirmed using the fact that $|\, c\,\rangle$ is a 2-eigenvector of $H^2$. As $\langle x, 2|H|c\rangle = \langle x, 2|c\rangle = 0$ for all $x \geq 1$, $\langle x, 2|{}_1(-\frac{\pi}{4})\rangle = 0$ for all $x \geq 1$. Furthermore the amplitude at vertex $(x_0, 1)$ is nonzero, i.e., $\langle x_0, 1|{}_1(-\frac{\pi}{4})\rangle \neq 0$, and hence $|{}_1(-\frac{\pi}{4})\rangle$ has a component orthogonal to the space of confined bound states (which have zero amplitude on both semi-infinite paths). Hence, there exists a scattering state with eigenvalue $-\sqrt{2}$ with no amplitude on path 2. By Fact 1, the gadget perfectly reflects at momentum $-\frac{3\pi}{4}$. It follows that no perfect R/T gadget (and hence no perfect momentum switch) exists between these momenta.

This proof technique can also establish non-existence of momentum switches between other pairs of momenta $k$ and $p$. For example, a slight modification of the above proof shows that no momentum switch exists between $k = -\frac{\pi}{6}$ and $p = -\frac{5\pi}{6}$.

### 3.5.3 Laplacians vs adjacency matrix

[**TO DO:** *If I have time, write this section*]

## 3.6 Finite truncation

## 3.7 Finite truncation

While the intuition all deals with infinite paths and wavepackets with some exact momenta, we will unfortunately have to deal with finite approximations to these ideals. While the Lemma **??** deals with the finite sized graphs, the restriction to finite sized wavepackets will unfortunately be slightly more complicated.

Unfortunately, much of this complication arises from the simple fact that the time evolved wavepackets do not have a nice form, and thus our approximations to these wavepackets are somewhat cumbersome. However, if we assume that the initial wavepacket was a a square window on the momenta of interest some distance from the finite sized graph, the time evolved state essentially has the same state moved forward in time.

**Theorem 1.** *Let $\widehat{G}$ be an $(N+m)$-vertex graph. Let $G$ be the graph obtained from $\widetilde{G}$ by attaching semi-infinite paths to the first $N$ of its vertices, and let $S$ be the corresponding $S$-matrix. Let $H_G$ be the quantum walk Hamiltonian of equation* ***[CITE:*** *correct equation]* . *Let $k \in (-\pi, 0)$, $M, L \in \mathbb{N}$, $j \in [N]$, and*

$$|\,\psi^j(0)\,\rangle = \frac{1}{\sqrt{L}} \sum_{x=M+1}^{M4L} e^{-ikx} |\,x, j\,\rangle. \tag{3.66}$$

*Let $c_0$ be a constant independent of $L$. Then, for all $0 \le t \le c_0 L$,*

$$\left\| e^{-iH_G t} |\,\psi^j(0)\,\rangle - |\,\alpha^j(t)\,\rangle \right\| = \mathcal{O}(L^{-1/4}) \tag{3.67}$$

*where*

$$|\,\alpha^j(t)\,\rangle = \frac{1}{\sqrt{L}} e^{-2it\cos k} \sum_{x=1}^{\infty} \sum_{q=1}^{N} (\delta_{qj} e^{-ikx} R(x - \lfloor 2t \sin k \rfloor) + S_{qj}(k) e^{ikx} R(-x - \lfloor 2t \sin k \rfloor)) |\,x, q\rangle \tag{3.68}$$

*with*

$$R(l) = \begin{cases} 1 & \textit{if } l - M \in [L] \\ 0 & \textit{otherwise.} \end{cases} \tag{3.69}$$

n this section we prove Theorem **??**. The proof is based on (and follows closely) the calculation from the appendix of reference [**?**].

Recall from (**??**) that the scattering eigenstates of $H_G^{(1)}$ have the form

$$\langle x, q | \mathrm{sc}_j(k) \rangle = e^{-ikx} \delta_{qj} + e^{ikx} S_{qj}(k)$$

for each $k \in (-\pi, 0)$.

Before delving into the proof, we first establish that the state $|\alpha^j(t)\rangle$ is approximately normalized. This state is not normalized at all times $t$. However, $\langle\alpha^j(t)|\alpha^j(t)\rangle = 1+\mathcal{O}(L^{-1})$, as we now show:

$$\begin{aligned}
\langle\alpha^j(t)|\alpha^j(t)\rangle &= \frac{1}{L}\sum_{x=1}^{\infty}\left|e^{-ikx}R(x-\lfloor 2t\sin k\rfloor) + S_{jj}(k)e^{ikx}R(-x-\lfloor 2t\sin k\rfloor)\right|^2 \\
&\quad + \frac{1}{L}\sum_{q\neq j}\sum_{x=1}^{\infty}|S_{qj}(k)|^2 R(-x-\lfloor 2t\sin k\rfloor) \\
&= \frac{1}{L}\sum_{x=1}^{\infty}\left[R(x-\lfloor 2t\sin k\rfloor) + R(-x-\lfloor 2t\sin k\rfloor)\right] \\
&\quad + \frac{1}{L}\sum_{x=1}^{\infty}\left(e^{-2ikx}S_{jj}^*(k) + e^{2ikx}S_{jj}(k)\right)R(x-\lfloor 2t\sin k\rfloor)R(-x-\lfloor 2t\sin k\rfloor) \\
&= 1+\frac{1}{L}\sum_{x=1}^{\infty}\left(e^{-2ikx}S_{jj}^*(k)+e^{2ikx}S_{jj}(k)\right)R(x-\lfloor 2t\sin k\rfloor)R(-x-\lfloor 2t\sin k\rfloor)+\mathcal{O}(L^{-1})
\end{aligned}$$

where we have used unitarity of $S$ in the second step. When it is nonzero, the second term can be written as

$$\frac{1}{L}\sum_{x=1}^{b}\left(e^{-2ikx}S_{jj}^*(k) + e^{2ikx}S_{jj}(k)\right)$$

where $b$ is the maximum positive integer such that $\{-b, b\} \subset \{M+1+\lfloor 2t\sin k\rfloor, \ldots, M+L+\lfloor 2t\sin k\rfloor\}$. Performing the sums, we get

$$\begin{aligned}
\left|\frac{1}{L}\sum_{x=1}^{b}\left(e^{-2ikx}S_{jj}^*(k) + e^{2ikx}S_{jj}(k)\right)\right| &= \frac{1}{L}\left|S_{jj}^*(k)e^{-2ik}\frac{e^{-2ikb}-1}{e^{-2ik}-1} + S_{jj}(k)e^{2ik}\frac{e^{2ikb}-1}{e^{2ik}-1}\right| \\
&\leq \frac{2}{L|\sin k|}.
\end{aligned}$$

Thus we have $\langle\alpha^j(t)|\alpha^j(t)\rangle = 1+\mathcal{O}(L^{-1})$.

*Proof of Theorem* **??**. Define

$$|\psi^j(t)\rangle = e^{-iH_G^{(1)}t}|\psi^j(0)\rangle$$

and write

$$|\psi^j(t)\rangle = |w^j(t)\rangle + |v^j(t)\rangle$$

where

$$|w^j(t)\rangle = \int_{-\epsilon}^{\epsilon}\frac{d\phi}{2\pi}e^{-2it\cos(k+\phi)}\sum_{q=1}^{N}|\mathrm{sc}_q(k+\phi)\rangle\langle\mathrm{sc}_q(k+\phi)|\psi^j(0)\rangle$$

and $\langle w^j(t)|v^j(t)\rangle = 0$. We take $\epsilon = \frac{|\sin k|}{2\sqrt{L}}$. Now

$$\langle\mathrm{sc}_q(k+\phi)|\psi^j(0)\rangle = \frac{1}{\sqrt{L}}\sum_{x=M+1}^{M+L}\left(e^{i\phi x}\delta_{qj} + e^{-i(2k+\phi)x}S_{qj}^*(k+\phi)\right),$$

so

$$|w^j(t)\rangle = |w_A^j(t)\rangle + \sum_{q=1}^{N} |w_B^{q,j}(t)\rangle$$

where

$$\begin{aligned}
|w_A^j(t)\rangle &= \int_{-\epsilon}^{\epsilon} \frac{d\phi}{2\pi} e^{-2it\cos(k+\phi)} f(\phi) |\mathrm{sc}_j(k+\phi)\rangle \\
|w_B^{q,j}(t)\rangle &= \int_{-\epsilon}^{\epsilon} \frac{d\phi}{2\pi} e^{-2it\cos(k+\phi)} g_{qj}(\phi) |\mathrm{sc}_q(k+\phi)\rangle
\end{aligned}$$

with

$$\begin{aligned}
f(\phi) &= \frac{1}{\sqrt{L}} \sum_{x=M+1}^{M+L} e^{i\phi x} \\
g_{qj}(\phi) &= \frac{1}{\sqrt{L}} \sum_{x=M+1}^{M+L} e^{-i(2k+\phi)x} S_{qj}^*(k+\phi).
\end{aligned}$$

We will see that $|\,\psi^j(t)\,\rangle \approx |\,w^j(t)\,\rangle \approx |\,w_A^j(t)\,\rangle \approx |\,\alpha^j(t)\,\rangle$.

Now

$$\langle w_A^j(t)|w_A^j(t)\rangle = \int_{-\epsilon}^{\epsilon} \frac{d\phi}{2\pi} \left|f(\phi)\right|^2 = \frac{1}{L}\int_{-\epsilon}^{\epsilon} \frac{d\phi}{2\pi} \frac{\sin^2(\frac{1}{2}L\phi)}{\sin^2(\frac{1}{2}\phi)}$$

but

$$\frac{1}{L}\int_{-\pi}^{\pi} \frac{d\phi}{2\pi} \frac{\sin^2(\frac{1}{2}L\phi)}{\sin^2(\frac{1}{2}\phi)} = 1$$

and

$$\begin{aligned}
\frac{1}{L}\left(\int_{\epsilon}^{\pi} + \int_{-\pi}^{-\epsilon}\right) \frac{d\phi}{2\pi} \frac{\sin^2(\frac{1}{2}L\phi)}{\sin^2(\frac{1}{2}\phi)} &= \frac{2}{L}\int_{\epsilon}^{\pi} \frac{d\phi}{2\pi} \frac{\sin^2(\frac{1}{2}L\phi)}{\sin^2(\frac{1}{2}\phi)} \\
&\leq \frac{2}{L}\int_{\epsilon}^{\pi} \frac{d\phi}{2\pi} \frac{\pi^2}{\phi^2} \\
&\leq \frac{\pi}{L\epsilon}.
\end{aligned} \tag{3.70}$$

Therefore

$$1 \geq \langle w_A^j(t)|w_A^j(t)\rangle \geq 1 - \frac{\pi}{L\epsilon}.$$

Similarly,

$$\langle w_B^{qj}(t)|w_B^{qj}(t)\rangle = \int_{-\epsilon}^{\epsilon} \frac{d\phi}{2\pi} \frac{\left|S_{qj}(k+\phi)\right|^2}{L} \frac{\sin^2(\frac{1}{2}L(2k+\phi))}{\sin^2(\frac{1}{2}(2k+\phi))},$$

and, using the unitarity of $S$,

$$\begin{aligned}
\sum_{q=1}^{N} \langle w_B^{qj}(t)|w_B^{qj}(t)\rangle &= \frac{1}{L}\int_{-\epsilon}^{\epsilon} \frac{d\phi}{2\pi} \frac{\sin^2(\frac{1}{2}L(2k+\phi))}{\sin^2(\frac{1}{2}(2k+\phi))} \\
&\leq \frac{1}{L}\int_{-\epsilon}^{\epsilon} \frac{d\phi}{2\pi} \frac{1}{\sin^2(\frac{1}{2}(2k+\phi))}.
\end{aligned}$$

Now $|\sin(k+\phi/2)-\sin k|\le|\phi|/2$ (by the mean value theorem). So

$$\sin^2\left(k+\frac{\phi}{2}\right)\ge\left(|\sin k|-\left|\frac{\phi}{2}\right|\right)^2.$$

Since $\epsilon=\frac{|\sin k|}{2\sqrt{L}}<|\sin k|$ we then have

$$\begin{aligned}\sum_{q=1}^{N}\langle w_B^{qj}(t)|w_B^{qj}(t)\rangle &\le \frac{1}{L}\int_{-\epsilon}^{\epsilon}\frac{d\phi}{2\pi}\frac{4}{\sin^2 k}\\ &=\frac{4\epsilon}{\pi L\sin^2 k}.\end{aligned}$$

Hence

$$\begin{aligned}\langle w^j(t)|w^j(t)\rangle &\ge \langle w_A^j(t)|w_A^j(t)\rangle-2\left|\sum_{q=1}^{N}\langle w_A^j(t)|w_B^{qj}(t)\rangle\right|\\ &\ge 1-\frac{\pi}{L\epsilon}-2\left\|\sum_{q=1}^{n}|w_B^{qj}(t)\rangle\right\|\\ &\ge 1-\frac{\pi}{L\epsilon}-2\sum_{q=1}^{n}\left\||w_B^{qj}(t)\rangle\right\|\\ &\ge 1-\frac{\pi}{L\epsilon}-4\sqrt{\frac{\epsilon N}{\pi L\sin^2 k}},\end{aligned}$$

so

$$\langle v^j(t)|v^j(t)\rangle\le\frac{\pi}{L\epsilon}+4\sqrt{\frac{\epsilon N}{\pi L\sin^2 k}}$$

since $\langle v^j(t)|v^j(t)\rangle+\langle w^j(t)|w^j(t)\rangle=1$. Thus

$$\begin{aligned}\left\||\psi^j(t)\rangle-|w_A^j(t)\rangle\right\| &=\left\||v^j(t)\rangle+\sum_{q=1}^{N}|w_B^{qj}(t)\rangle\right\|\\ &\le\left(\frac{\pi}{L\epsilon}+4\sqrt{\frac{\epsilon N}{\pi L\sin^2 k}}\right)^{\frac{1}{2}}+2\sqrt{\frac{\epsilon N}{\pi L\sin^2 k}}.\end{aligned}$$

With our choice $\epsilon=\frac{|\sin k|}{2\sqrt{L}}$, we have $\||\psi^j(t)\rangle-|w_A^j(t)\rangle\|=\emptyset(L^{-1/4})$.

We now show that

$$\left\||w_A^j(t)\rangle-|\alpha^j(t)\rangle\right\|=\emptyset(L^{-1/8}). \tag{3.71}$$

Letting

$$P=\sum_{q=1}^{N}\sum_{x=1}^{\infty}|x,q\rangle\langle x,q|$$

be the projector onto the semi-infinite paths, to show equation (3.71) it is sufficient to show that

$$\left\| P|w_A^j(t)\rangle - |\alpha^j(t)\rangle \right\| = \emptyset(L^{-1/4}) \tag{3.72}$$

since this implies that

$$\begin{aligned}\left\| P|w_A^j(t)\rangle \right\| &= \left\| |\alpha^j(t)\rangle \right\| + \emptyset(L^{-1/4}) \\ &= 1 + \emptyset(L^{-1/4})\end{aligned}$$

and hence

$$\begin{aligned}\left\| (1-P)\, |w_A^j(t)\rangle \right\|^2 &= \left\| |w_A^j(t)\rangle \right\|^2 - \left\| P|w_A^j(t)\rangle \right\|^2 \\ &\leq 1 - \left(1 + \emptyset(L^{-1/4})\right) \\ &= \emptyset(L^{-1/4}).\end{aligned} \tag{3.73}$$

From the above formula we now see that inequality (3.72) implies (3.71).

Noting that

$$\frac{1}{\sqrt{L}} R(l) = \int_{-\pi}^{\pi} \frac{d\phi}{2\pi} e^{-i\phi l} f(\phi),$$

we write

$$\begin{aligned}\langle x, q|\alpha^j(t)\rangle = e^{-2it\cos k} \Bigg( &\delta_{qj} e^{-ikx} \int_{-\pi}^{\pi} \frac{d\phi}{2\pi} e^{-i\phi(x - \lfloor 2t\sin k \rfloor)} f(\phi) \\ &+ S_{qj}(k) e^{ikx} \int_{-\pi}^{\pi} \frac{d\phi}{2\pi} e^{-i\phi(-x - \lfloor 2t\sin k \rfloor)} f(\phi) \Bigg).\end{aligned} \tag{3.74}$$

On the other hand,

$$\langle x, q|w_A^j(t)\rangle = \int_{-\epsilon}^{\epsilon} \frac{d\phi}{2\pi} e^{-2it\cos(k+\phi)} f(\phi) \left( e^{-i(k+\phi)x} \delta_{qj} + e^{i(k+\phi)x} S_{qj}(k+\phi) \right). \tag{3.75}$$

Using equations (3.74) and (3.75) we can write

$$P|w_A^j(t)\rangle = |\alpha^j(t)\rangle + \sum_{i=1}^{7} |c_i^j(t)\rangle$$

where $P|c_i^j(t)\rangle = |c_i^j(t)\rangle$ and

$$\begin{aligned}
\langle x,q|c_1^j(t)\rangle &= \delta_{qj}e^{-2it\cos k}e^{-ikx}\int_{-\pi}^{\pi}\frac{d\phi}{2\pi}e^{-i\phi x}f(\phi)\left(e^{2it\phi\sin k}-e^{i\phi\lfloor 2t\sin k\rfloor}\right)\\
\langle x,q|c_2^j(t)\rangle &= S_{qj}(k)e^{-2it\cos k}e^{ikx}\int_{-\pi}^{\pi}\frac{d\phi}{2\pi}e^{i\phi x}f(\phi)\left(e^{2it\phi\sin k}-e^{i\phi\lfloor 2t\sin k\rfloor}\right)\\
\langle x,q|c_3^j(t)\rangle &= -\delta_{qj}e^{-2it\cos k}e^{-ikx}\left(\int_{\epsilon}^{\pi}+\int_{-\pi}^{-\epsilon}\right)\frac{d\phi}{2\pi}e^{-i\phi x}f(\phi)e^{2it\phi\sin k}\\
\langle x,q|c_4^j(t)\rangle &= -S_{qj}(k)e^{-2it\cos k}e^{ikx}\left(\int_{\epsilon}^{\pi}+\int_{-\pi}^{-\epsilon}\right)\frac{d\phi}{2\pi}e^{i\phi x}f(\phi)e^{2it\phi\sin k}\\
\langle x,q|c_5^j(t)\rangle &= \delta_{qj}e^{-ikx}\int_{-\epsilon}^{\epsilon}\frac{d\phi}{2\pi}e^{-i\phi x}f(\phi)\left(e^{-2it\cos(k+\phi)}-e^{-2it\cos k+2it\phi\sin k}\right)\\
\langle x,q|c_6^j(t)\rangle &= S_{qj}(k)e^{ikx}\int_{-\epsilon}^{\epsilon}\frac{d\phi}{2\pi}e^{i\phi x}f(\phi)\left(e^{-2it\cos(k+\phi)}-e^{-2it\cos k+2it\phi\sin k}\right)\\
\langle x,q|c_7^j(t)\rangle &= e^{ikx}\int_{-\epsilon}^{\epsilon}\frac{d\phi}{2\pi}e^{i\phi x}e^{-2it\cos(k+\phi)}f(\phi)\left(S_{qj}(k+\phi)-S_{qj}(k)\right).
\end{aligned}$$

We now bound the norm of each of these states:

$$\begin{aligned}
\langle c_1^j(t)|c_1^j(t)\rangle &= \sum_{q=1}^{N}\sum_{x=1}^{\infty}\left|\delta_{qj}e^{-2it\cos k}e^{-ikx}\int_{-\pi}^{\pi}\frac{d\phi}{2\pi}e^{-i\phi x}f(\phi)\left(e^{2it\phi\sin k}-e^{i\phi\lfloor 2t\sin k\rfloor}\right)\right|^2\\
&\le \sum_{q=1}^{N}\sum_{x=-\infty}^{\infty}\left|\delta_{qj}e^{-2it\cos k}e^{-ikx}\int_{-\pi}^{\pi}\frac{d\phi}{2\pi}e^{-i\phi x}f(\phi)\left(e^{2it\phi\sin k}-e^{i\phi\lfloor 2t\sin k\rfloor}\right)\right|^2\\
&= \int_{-\pi}^{\pi}\frac{d\phi}{2\pi}\left|f(\phi)\right|^2\left|e^{2it\phi\sin k}-e^{i\phi\lfloor 2t\sin k\rfloor}\right|^2\\
&\le \int_{-\pi}^{\pi}\frac{d\phi}{2\pi}\left|f(\phi)\right|^2\left(2t\phi\sin k-\lfloor 2t\sin k\rfloor\phi\right)^2\\
&\le \int_{-\pi}^{\pi}\frac{d\phi}{2\pi}\left|f(\phi)\right|^2\phi^2
\end{aligned}$$

where we have used the facts that $|e^{is}-1|^2\le s^2$ for $s\in\mathbb{R}$ and $|2t\sin k-\lfloor 2t\sin k\rfloor|<1$. In the above we performed the sum over $x$ using the identity

$$\sum_{x=-\infty}^{\infty}e^{i(\phi-\tilde{\phi})x}=2\pi\delta(\phi-\tilde{\phi})\text{ for }\phi,\tilde{\phi}\in(-\pi,\pi).$$

We use this fact repeatedly in the following calculations. Continuing, we get

$$\begin{aligned}
\langle c_1^j(t)|c_1^j(t)\rangle &\le \frac{1}{L}\int_{-\pi}^{\pi}\frac{d\phi}{2\pi}\frac{\sin^2(\frac{1}{2}L\phi)}{\sin^2(\frac{1}{2}\phi)}\phi^2\\
&\le \frac{1}{L}\int_{-\pi}^{\pi}\frac{d\phi}{2\pi}\frac{1}{\sin^2(\frac{1}{2}\phi)}\phi^2\\
&\le \frac{\pi^2}{L}
\end{aligned}$$

using the fact that $\sin^2(\phi/2) \geq \phi^2/\pi^2$ for $\phi \in [-\pi, \pi]$. Similarly we bound $\langle c_2^j(t)|c_2^j(t)\rangle \leq \pi^2/L$.

Using equation (3.70) we get

$$\begin{aligned}
\langle c_3^j(t)|c_3^j(t)\rangle &\leq \left(\int_{\epsilon}^{\pi} + \int_{-\pi}^{-\epsilon}\right)\frac{d\phi}{2\pi}\left|f(\phi)\right|^2 \\
&\leq \frac{\pi}{L\epsilon}
\end{aligned}$$

and similarly for $\langle c_4^j(t)|c_4^j(t)\rangle$. Next, we have

$$\begin{aligned}
\langle c_5^j(t)|c_5^j(t)\rangle &\leq \int_{-\epsilon}^{\epsilon}\frac{d\phi}{2\pi}\left|f(\phi)\right|^2\left|e^{-2it\cos(k+\phi)} - e^{-2it\cos k + 2it\phi\sin k}\right|^2 \\
&\leq \int_{-\epsilon}^{\epsilon}\frac{d\phi}{2\pi}\left|f(\phi)\right|^2\left(2t\cos\left(k+\phi\right) - 2t\cos k + 2t\phi\sin k\right)^2 \\
&= \int_{-\epsilon}^{\epsilon}\frac{d\phi}{2\pi}\left|f(\phi)\right|^2\left(2t\cos k\left(\cos\phi - 1\right) + 2t\sin k\left(\phi - \sin\phi\right)\right)^2 \\
&\leq \int_{-\epsilon}^{\epsilon}\frac{d\phi}{2\pi}\left|f(\phi)\right|^2 4t^2\phi^4 \\
&= \frac{4t^2}{L}\int_{-\epsilon}^{\epsilon}\frac{d\phi}{2\pi}\frac{\sin^2(\frac{1}{2}L\phi)}{\sin^2(\frac{1}{2}\phi)}\phi^4 \\
&\leq \frac{4t^2}{L}\int_{-\epsilon}^{\epsilon}\frac{d\phi}{2\pi}\pi^2\phi^2 \\
&= \frac{4\pi}{3L}t^2\epsilon^3
\end{aligned}$$

and we have the same bound for $|c_6^j(t)\rangle$. Finally,

$$\langle c_7^j(t)|c_7^j(t)\rangle \leq \int_{-\epsilon}^{\epsilon}\frac{d\phi}{2\pi}\left|f(\phi)\right|^2\sum_{q=1}^{N}\left|S_{qj}(k+\phi) - S_{qj}(k)\right|^2.$$

Now, for each $q \in \{1, \ldots, N\}$,

$$|S_{qj}(k+\phi) - S_{qj}(k)| \leq \Gamma|\phi|$$

where the Lipschitz constant

$$\Gamma = \max_{q,j\in\{1,\ldots,N\}}\max_{k'\in[-\pi,\pi]}\left|\frac{d}{dk'}S_{qj}(k')\right|$$

is well defined since each matrix element $S_{qj}(k')$ is a bounded rational function of $e^{ik'}$, as can be seen from equation (**??**). Hence

$$
\begin{aligned}
\langle c_7^j(t)|c_7^j(t)\rangle &\leq \int_{-\epsilon}^{\epsilon} \frac{d\phi}{2\pi} \left|f(\phi)\right|^2 N\Gamma^2\phi^2 \\
&= \frac{N\Gamma^2}{L}\int_{-\epsilon}^{\epsilon} \frac{d\phi}{2\pi}\frac{\sin^2(\frac{1}{2}L\phi)}{\sin^2(\frac{1}{2}\phi)}\phi^2 \\
&\leq \frac{N\Gamma^2}{L}\int_{-\epsilon}^{\epsilon} \frac{d\phi}{2\pi}\pi^2 \\
&= N\Gamma^2\frac{\pi\epsilon}{L}.
\end{aligned}
$$

Now using the bounds on the norms of each of these states we get

$$
\begin{aligned}
\left\|P|w_A^j(t)\rangle - |\alpha^j(t)\rangle\right\| &\leq 2\frac{\pi}{\sqrt{L}} + 2\sqrt{\frac{\pi}{L\epsilon}} + 2\sqrt{\frac{4\pi}{3L}t^2\epsilon^3} + \sqrt{N\Gamma^2\frac{\pi\epsilon}{L}} \\
&= \emptyset(L^{-1/4})
\end{aligned}
$$

using the choice $\epsilon = \frac{|\sin p|}{2\sqrt{L}}$ and the fact that $t = \emptyset(L)$. □

Note that this analysis assumes that $N = \emptyset(1)$, which is the case in our applications of Theorem **??**.

## 3.8 Conclusions and open problems

I need to say something here.

Find more gates.

Determine necessary conditions for momentum switches to occur.

Basically just do more research.

# Chapter 4

# Universality of single-particle scattering

With the basic understanding of scattering on graphs, we should be able to combine several graphs so as to show that single-particle quantum walks are universal. While this has already been shown by Andrew Childs [**?**], this is a slightly different graph and analysis, which will help with the understanding of the multi-particle case. In particular, the method for encoding a computation will be to have a long (but finite) path for each computational basis state of the circuit. We will use several graphs from the previous section so that each gate is implemented with a scattering event.

While the overall graph will be exponential in size, each individual scattering event will only involve either two or four semi-infinite paths, as our choice of universal gate set only mixes at most two computational basis states per gate. As such, we will be able to analyze the evolution of a sufficiently large wavepacket, and show that the evolution of such a wavepacket follows the expected evolution for a single gate. By then combining the graphs in such a manner, we will then be able to show that the final location of the wavepacket can be used to evaluate whether the simulated circuit accepts.

## 4.1 Single-gate blocks

Before we encode an entire computation into the evolution of a quantum walker, we first need to be able to encode a single gate. To do this, we will use the results of Chapter **??**, as we have already shown how to simulate the evolution of a universal gate set. Unfortunately, the results of that section do require that each of the input and output paths to be semi-infinite, which will be problematic for combining these evolutions in series.

However, if we examine Lemma **??**, we can see that for all times of interest, most of the amplitude remains close to the graph. Intuitively, we would thus expect the evolution for these times to remain mostly unchanged if we then remove those vertices far from the graph. This is actually the bulk of the Lemma **??**, which we will use to great effect in our proof.

Before we analyze the actual evolution, however, we will want to construct these small graphs themselves. As such, let us assume that we are working with $n$ qubits, and let us assume that we are applying the unitary $U$, where $U \in \{H, T, \mathrm{CNOT}\}$. With this

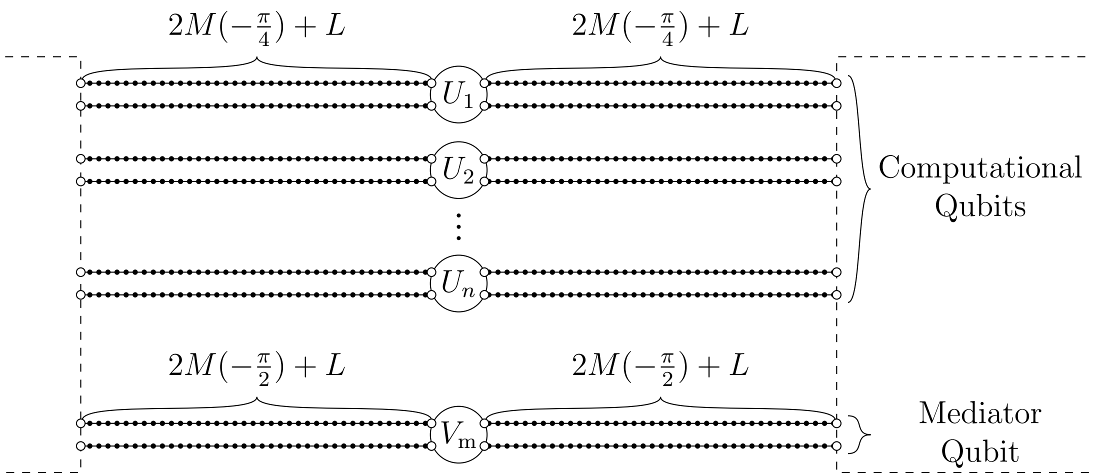


Figure 4.1: The intuitive idea for a single-particle block.

assumption, the graph corresponding to a single gate will then consist of $2^{n+1}$ paths of length $2M + L$, where $M$ and $L$ are integers to be determined, along with a scattering graph $G_U$ that implements the appropriate unitary evolution. Half of the long paths will correspond to the input paths, while the other half will correspond to the output paths. We will then connect these paths to the input and output vertices of $G_U$. In particular, the graph will look like Figure 4.1.

[**TO DO:** *fix figure*]

Additionally, as the scattering behavior of graphs is intrinsically related to the momentum of the wavepackets, we will need to decide on this before we finish the construction. In anticipation of Chapter **??**, as well as the simplicity of certain graphs, our construction will utilize $k = -\dfrac{\pi}{4}$.

### 4.1.1 Construction of $G_U$

With these choices, the graphs for $G_U$ will be relatively simple. For all graphs except for the amplitude mixing gate, the subgraphs will simply consist of paths, so that the evolution will essentially just be the same as on a long path, possibly with an encoded change of phase. For the amplitude mixing gate, things will be slightly di

If $U$ is a T-gate acting on qubit $j$, then the graph $G_U$ will consist of $2^{n-1}$ paths of length 2 connecting input $x_{\text{in}}$ to $x_{\text{out}}$, where $x_j = 0$, and $2^{n-1}$ paths of length 1 connecting input $x_{\text{in}}$ to output $x_{\text{out}}$ where $x_j = 1$. In this manner, the scattering amplitude will always have perfect transmision, and different momenta will only result in a different encoded gate (namely that this will be a $-\dfrac{k}{2}$-phase gate as opposed to a $\dfrac{\pi}{8}$-gate.

If $U$ is a CNOT-gate controlled by qubit $i$ and acting on qubit $j$, then this is even more simple than the T-gate. In particular, the graph $G_U$ will consist of $2^n$ paths of length 2, where input $x$ is connected to output $y$, where $x_k = y_k$ for all $k \neq j$, and $y_j = x_i + x_j - 2x_i x_j$.

Finally, if $U$ is the Basis-changing gate acting on qubit $j$, then things become slightly more complicated. In particular, $G_U$ then consists of $2^{n-1}$ copies of the graph Figure **??**, with inputs $x_{\text{input}}$ and $y_{\text{input}}$ with $x_i = y_i$ for all $i \neq j$, and $x_j = 1 - y_j$, and outputs $x_{\text{out}}$ and $y_{\text{out}}$.

These are represented pictoraly in Figure ??. Note that the paths corresponding to the basis states are ordered to make the figures coherent, and that the ordering depends on which qubits the gate acts.

[**TO DO:** *make figure*]

### 4.1.2 Evolution analysis

An important aspect to note about this graph is that while $G_U$ has exponentially many inputs and outputs, it actually consists of either $2^n$ or $2^{n-1}$ disconnected graphs, as our universal gate set only ever mixes at most two basis states. As such, each scattering event will only ever deal with finite sized graphs, and we will be able to use Lemma **??** without worry.

In particular, if we assume that the initial state is a superposition of square wavepackets that are all a distance $M$ from the

## 4.2 Combining blocks

With the understanding of exactly how a single graphs block is expected to simulate a single circuit, we will want to understand how to combine these blocks so as to be able to perform a simulation of an entire circuit.

## 4.3 Discussion and extensions

What else can go here?

# Chapter 5

# Universality of multi-particle scattering

I should really give a broad overview of the technique. Maybe not in any great detail, but I should really explain why things are going to go the way they are.

## 5.1 Multi-particle quantum walk

Now that we have analyzed the single particle quantum walk, we will want to understand how the multi-particle system works together. Unfortunately, this system is difficult in general to analyze, as the various interactions become intractable. In fact, we will eventually show that this is as hard as understanding the amplitudahedron, also known as universal quantum computation.

### 5.1.1 Two-particle scattering on an infinite path

While understanding the interactions of multi-particle interactions on an arbitrary graph is beyond our current understanding, we can simplify the model, and see what we can understand. Along those lines, we can restrict ourselves to the case where only two particles interact. Similarly, we can restrict ourselves to understanding their interaction on the most simple infinite graph; namely the infinite path.

As such, let us assume that there is some interaction with finite range between the particles, that depends only on the distance between the particles.

Here we derive scattering states of the two-particle quantum walk on an infinite path. We write the Hamiltonian in the basis $|x, y\rangle$, where $x$ denotes the location of the first particle and $y$ denotes the location of the second particle, with the understanding that bosonic states are symmetrized and fermionic states are antisymmetrized. The Hamiltonian (**??**) can be written as

$$H^{(2)} = H_x^{(1)} \otimes \mathbb{I}_y + \mathbb{I}_x \otimes H_y^{(1)} + \sum_{x,y\in\mathbb{Z}} \mathcal{V}(|x-y|)\,|x, y\rangle\langle x, y| \tag{5.1}$$

where $\mathcal{V}$ corresponds to the interaction term $\mathcal{U}$ and (with a slight abuse of notation) the subscript indicates which variable is acted on. Here

$$H^{(1)} = \sum_{x\in\mathbb{Z}} |\, x+1\,\rangle\langle\, x\,| + |\, x\,\rangle\langle\, x+1\,|$$

is the adjacency matrix of an infinite path. Our assumption that $\mathcal{U}$ has finite range $C$ means that $\mathcal{V}(r) = 0$ for $r > C$.

The scattering states we are interested in provide information about the dynamics of two particles initially prepared in spatially separated wave packets moving toward each other along the path with momenta $k_1 \in (-\pi, 0)$ and $k_2 \in (0, \pi)$.

We derive scattering eigenstates of this Hamiltonian by transforming to the new variables $s = x + y$ and $r = x - y$ and exploiting translation symmetry. Here the allowed values $(s, r)$ range over the pairs of integers where either both are even or both are odd. Writing states in this basis as $|s; r\rangle$, the Hamiltonian takes the form

$$H_s^{(1)} \otimes H_r^{(1)} + \mathbb{I}_s \otimes \sum_{r\in\mathbb{Z}} \mathcal{V}(|r|)\, |\, r\,\rangle\langle\, r\,|. \tag{5.2}$$

For each $p_1 \in (-\pi, \pi)$ and $p_2 \in (0, \pi)$ there is a scattering eigenstate $|\mathrm{sc}(p_1; p_2)\rangle$ of the form

$$\langle s; r|\mathrm{sc}(p_1; p_2)\rangle = e^{-ip_1 s/2}\langle r|\psi(p_1; p_2)\rangle,$$

where the state $|\psi(p_1; p_2)\rangle$ can be viewed as an effective single-particle scattering state of the Hamiltonian

$$2\cos\left(\frac{p_1}{2}\right) H_r^{(1)} + \sum_{r\in\mathbb{Z}} \mathcal{V}(|r|)\, |\, r\,\rangle\langle\, r\,| \tag{5.3}$$

with eigenvalue $4\cos(p_1/2)\cos(p_2)$. For a given $\mathcal{V}$, the state $|\psi(p_1; p_2)\rangle$ can be obtained explicitly by solving a set of linear equations (see for example [**?**]). It has the form

$$\langle r|\psi(p_1; p_2)\rangle = \begin{cases} e^{-ip_2 r} + R(p_1, p_2)e^{ip_2 r} & \text{if } r \le -C \\ f(p_1, p_2, r) & \text{if } |r| < C \\ T(p_1, p_2)e^{-ip_2 r} & \text{if } r \ge C \end{cases} \tag{5.4}$$

for $p_2 \in (0, \pi)$. Here the reflection and transmission coefficients $R$ and $T$ and the amplitudes of the scattering state for $|r| < C$ (described by the function $f$) depend on both momenta as well as the interaction $\mathcal{V}$. With $R$, $T$, and $f$ chosen appropriately, the state $|\mathrm{sc}(p_1; p_2)\rangle$ is an eigenstate of $H^{(2)}$ with eigenvalue $4\cos(p_1/2)\cos(p_2)$.

Since $\mathcal{V}(|r|)$ is an even function of $r$, we can also define scattering states for $p_2 \in (-\pi, 0)$ by

$$\langle s; r|\mathrm{sc}(p_1; p_2)\rangle = \langle s; -r|\mathrm{sc}(p_1; -p_2)\rangle.$$

These other states are obtained by swapping $x$ and $y$, corresponding to interchanging the two particles.

The states $\{|\mathrm{sc}(p_1;p_2)\rangle \colon p_1 \in (-\pi,\pi),\ p_2 \in (-\pi,0)\cup(0,\pi)\}$ are (delta-function) orthonormal:

$$\begin{aligned}
\langle \mathrm{sc}(p_1';p_2')|\mathrm{sc}(p_1;p_2)\rangle &= \langle \mathrm{sc}(p_1';p_2')|\left(\sum_{r,\,s \text{ even}} |r\rangle\langle r|\otimes|s\rangle\langle s|\right)|\mathrm{sc}(p_1;p_2)\rangle \\
&\quad + \langle \mathrm{sc}(p_1';p_2')|\left(\sum_{r,\,s \text{ odd}} |r\rangle\langle r|\otimes|s\rangle\langle s|\right)|\mathrm{sc}(p_1;p_2)\rangle \\
&= \sum_{s \text{ even}} e^{-i(p_1-p_1')s/2} \sum_{r \text{ even}} \langle\psi(p_1';p_2')|r\rangle\langle r|\psi(p_1;p_2)\rangle \\
&\quad + \sum_{s \text{ odd}} e^{-i(p_1-p_1')s/2} \sum_{r \text{ odd}} \langle\psi(p_1';p_2')|r\rangle\langle r|\psi(p_1;p_2)\rangle \\
&= 2\pi\delta(p_1-p_1') \sum_{r=-\infty}^{\infty} \langle\psi(p_1;p_2')|r\rangle\langle r|\psi(p_1;p_2)\rangle \\
&= 4\pi^2\delta(p_1-p_1')\delta(p_2-p_2')
\end{aligned}$$

where in the last step we used the fact that $\langle\psi(p_1;p_2')|\psi(p_1;p_2)\rangle = 2\pi\delta(p_2-p_2')$. To construct bosonic or fermionic scattering states, we symmetrize or antisymmetrize as follows. For $p_1 \in (-\pi,\pi)$ and $p_2 \in (0,\pi)$, we define

$$|\,\mathrm{sc}(p_1;p_2)\,\rangle_{\pm} = \frac{1}{\sqrt{2}}(|\,\mathrm{sc}(p_1;p_2)\,\rangle \pm |\,\mathrm{sc}(p_1;-p_2)\,\rangle).$$

Then

$$\langle\, s;r\,|\,\mathrm{sc}(p_1;p_2)\,\rangle_{\pm} = \frac{1}{\sqrt{2}} e^{-ip_1 s/2} \begin{cases} e^{-ip_2 r} \pm e^{i\theta_{\pm}(p_1,p_2)} e^{ip_2 r} & \text{if } r \le -C \\ f(p_1,p_2,r) \pm f(p_1,p_2,-r) & \text{if } |r| < C \\ e^{i\theta_{\pm}(p_1,p_2)} e^{-ip_2 r} \pm e^{ip_2 r} & \text{if } r \ge C \end{cases} \tag{5.5}$$

where $\theta_{\pm}(p_1,p_2)$ is a real function defined through

$$e^{i\theta_{\pm}(p_1,p_2)} = T(p_1,p_2) \pm R(p_1,p_2). \tag{5.6}$$

Note that $|T \pm R| = 1$; this follows from the potential $\mathcal{V}(|r|)$ being even in $r$ and from unitarity of the S-matrix. These eigenstates allow us to understand what happens when two particles with momenta $k_1 \in (-\pi,0)$ and $k_2 \in (0,\pi)$ move toward each other. Here $p_1 = -k_1 - k_2$ and $p_2 = (k_2 - k_1)/2$. Recall (from the main text of the paper) that we defined $e^{i\theta}$ to be the phase acquired by the two-particle wavefunction when $k_1 = -\pi/2$ and $k_2 = \pi/4$ ($\theta$ depends implicitly on the interaction $\mathcal{V}$ and the particle type), so $\theta = \theta_{\pm}(\pi/4, 3\pi/8)$ .

For $|r| \ge C$ the scattering state is a sum of two terms, one corresponding to the two particles moving toward each other and one corresponding to the two particles moving apart after scattering. The outgoing term has a phase of $T \pm R$ relative to the incoming term (as depicted in Figure **??**). This phase arises from the interaction between the two particles.

For example, consider the Bose-Hubbard model, where $\mathcal{V}(|r|) = U\delta_{r,0}$. Here $C = 0$ and $T = 1 + R$. In this case the scattering state $|\mathrm{sc}(p_1;p_2)\rangle_+$ is

$$\langle x,y|\mathrm{sc}(p_1;p_2)\rangle_+ = \frac{1}{\sqrt{2}} e^{-ip_1\left(\frac{x+y}{2}\right)} \left(e^{ip_2|x-y|} + e^{i\theta_+(p_1,p_2)} e^{-ip_2|x-y|}\right).$$

The first term describes the two particles moving toward each other and the second term describes them moving away from each other. To solve for the applied phase $e^{i\theta_+(p_1,p_2)}$ we look at the eigenvalue equation for $|\psi(p_1;p_2)\rangle$ at $r=0$. This gives

$$R(p_1,p_2) = -\frac{U}{U-4i\cos(p_1/2)\sin(p_2)}.$$

So for the Bose-Hubbard model,

$$e^{i\theta_+(p_1,p_2)} = T(p_1,p_2) + R(p_1,p_2) = -\frac{U+4i\cos(p_1/2)\sin(p_2)}{U-4i\cos(p_1/2)\sin(p_2)} = \frac{2\left(\sin(k_2)-\sin(k_1)\right)-iU}{2\left(\sin(k_2)-\sin(k_1)\right)+iU}.$$

For example, if $U = 2+\sqrt{2}$ then two particles with momenta $k_1 = -\pi/2$ and $k_2 = \pi/4$ acquire a phase of $e^{-i\pi/2} = -i$ after scattering.

For a multi-particle quantum walk with nearest-neighbor interactions, $\mathcal{V}(|r|) = U\delta_{|r|,1}$ and $C=1$. In this case the eigenvalue equations for $|\psi(p_1;p_2)\rangle$ at $r=-1$, $r=1$, and $r=0$ are

$$\begin{aligned}
4\cos\left(\frac{p_1}{2}\right)\cos(p_2)(e^{ip_2}+R(p_1,p_2)e^{-ip_2}) &= U(e^{ip_2}+R(p_1,p_2)e^{-ip_2}) \\
&\quad + 2\cos\left(\frac{p_1}{2}\right)\left(e^{2ip_2}+R(p_1,p_2)e^{-2ip_2}+f(p_1,p_2,0)\right) \\
4\cos\left(\frac{p_1}{2}\right)\cos(p_2)T(p_1,p_2)e^{-ip_2} &= UT(p_1,p_2)e^{-ip_2} \\
&\quad + 2\cos\left(\frac{p_1}{2}\right)\left(f(p_1,p_2,0)+T(p_1,p_2)e^{-2ip_2}\right) \\
2\cos(p_2)f(p_1,p_2,0) &= T(p_1,p_2)e^{-ip_2}+e^{ip_2}+R(p_1,p_2)e^{-ip_2},
\end{aligned}$$

respectively.

Solving these equations for $R$, $T$, and $f(p_1,p_2,0)$, we can construct the corresponding scattering states for bosons, fermions, or distinguishable particles (for more on the last case, see Section **??**). Unlike the case of the Bose-Hubbard model, we may not have $1+R=T$. For example, when $U=-2-\sqrt{2}$, $p_1=\pi/4$, and $p_2=3\pi/8$, we get $R=0$ and $T=i$ (see Section **??**).

### 5.1.2 Finite truncation

**Theorem 2.** *Let $H^{(2)}$ be a two-particle Hamiltonian of the form (5.1) with interaction range at most $C$, i.e., $\mathcal{V}(|r|)=0$ for all $|r|>C$. Let $\theta_\pm(p_1,p_2)$ be given by equation (5.6). Define $\theta=\theta_\pm(\pi/4,3\pi/8)$. Let $L\in\mathbb{N}^+$, let $M\in\{C+1,C+2,\ldots\}$, and define*

$$\begin{aligned}
|\chi_{z,k}\rangle &= \frac{1}{\sqrt{L}}\sum_{x=z-L}^{z-1} e^{ikx}|x\rangle \\
|\psi(0)\rangle &= \frac{1}{\sqrt{2}}\left(|\chi_{-M,-\frac{\pi}{2}}\rangle|\chi_{M+L+1,\frac{\pi}{4}}\rangle \pm |\chi_{M+L+1,\frac{\pi}{4}}\rangle|\chi_{-M,-\frac{\pi}{2}}\rangle\right).
\end{aligned}$$

*Let $c_0$ be a constant independent of $L$. Then, for all $0\le t\le c_0L$, we have*

$$\left\|e^{-iH^{(2)}t}|\psi(0)\rangle - |\alpha(t)\rangle\right\| = \mathcal{O}(L^{-1/8}),$$

*where*
$$|\alpha(t)\rangle = \sum_{x,y} a_{xy}(t)|x,y\rangle, \tag{5.7}$$
$a_{xy}(t) = \pm a_{yx}(t)$, *and, for* $x \leq y$,
$$a_{xy}(t) = \frac{1}{\sqrt{2}L} e^{-\sqrt{2}it} \left[e^{-i\pi x/2} e^{i\pi y/4} F(x,y,t) \pm e^{i\theta} e^{i\pi x/4} e^{-i\pi y/2} F(y,x,t)\right] \tag{5.8}$$
*where*
$$F(u,v,t) = \begin{cases} 1 & \text{if } u - 2\lfloor t \rfloor \in \{-M-L,\ldots,-M-1\} \text{ and } v + 2\left\lfloor \frac{t}{\sqrt{2}} \right\rfloor \in \{M+1,\ldots,M+L\} \\ 0 & \text{otherwise.} \end{cases}$$

In this section we prove Theorem 2. The main proof appears in Section **??**, relying on several technical lemmas proved in Section 5.1.2.1. The proof follows the method used in the single-particle case, which is based on the calculation from the appendix of reference [**?**].

Recall from (5.5) that for each $p_1 \in (-\pi,\pi)$ and $p_2 \in (0,\pi)$ there is an eigenstate $|\text{sc}(p_1;p_2)\rangle_\pm$ of $H^{(2)}$ of the form
$$\langle x,y|\text{sc}(p_1;p_2)\rangle_\pm = \frac{e^{-ip_1\left(\frac{x+y}{2}\right)}}{\sqrt{2}} \begin{cases} e^{-ip_2(x-y)} \pm e^{i\theta_\pm(p_1,p_2)} e^{ip_2(x-y)} & \text{if } x-y \leq -C \\ e^{-ip_2(x-y)} e^{i\theta_\pm(p_1,p_2)} \pm e^{ip_2(x-y)} & \text{if } x-y \geq C \\ f(p_1,p_2,x-y) \pm f(p_1,p_2,y-x) & \text{if } |x-y| < C \end{cases} \tag{5.9}$$
where
$$e^{i\theta_\pm(p_1,p_2)} = T(p_1,p_2) \pm R(p_1,p_2),$$
$C$ is the range of the interaction, $T$ and $R$ are the transmission and reflection coefficients of the interaction at the chosen momentum, $f$ describes the amplitudes of the scattering state within the interaction range, and the $\pm$ depends on the type of particle ($+$ for bosons, $-$ for fermions). The state $|\text{sc}(p_1;p_2)\rangle_\pm$ satisfies
$$H^{(2)}|\text{sc}(p_1;p_2)\rangle_\pm = 4\cos\frac{p_1}{2}\cos p_2 |\text{sc}(p_1;p_2)\rangle_\pm$$
and is delta-function normalized as
$${}_\pm\langle \text{sc}(p_1';p_2')|\text{sc}(p_1;p_2)\rangle_\pm = 4\pi^2 \delta(p_1 - p_1')\delta(p_2 - p_2'). \tag{5.10}$$
*Proof.* Expand $|\psi(0)\rangle$ in the basis of eigenstates of the Hamiltonian to get
$$|\psi(t)\rangle = e^{-iH^{(2)}t}|\psi(0)\rangle = |\psi_1(t)\rangle + |\psi_2(t)\rangle$$
where
$$|\psi_1(t)\rangle = \iint_{D_\epsilon} \frac{d\phi_1 d\phi_2}{4\pi^2} e^{-it4\cos\left(\frac{p_1}{2}+\frac{\phi_1}{2}\right)\cos(p_2+\phi_2)} |\text{sc}(p_1+\phi_1;p_2+\phi_2)\rangle_\pm \left({}_\pm\langle \text{sc}(p_1+\phi_1;p_2+\phi_2)|\psi(0)\rangle\right)$$

with $D_\epsilon = [-\epsilon, \epsilon] \times [-\epsilon, \epsilon]$, $p_1 = \pi/2 - \pi/4 = \pi/4$, $p_2 = (\pi/2 + \pi/4)/2 = 3\pi/8$, and with $|\psi_2(t)\rangle$ orthogonal to $|\psi_1(t)\rangle$. We take $\epsilon = a/\sqrt{L}$ for some constant $a$. Using equation (5.9) we get

$$|\,\psi_1(t)\,\rangle = |\psi_A(t)\rangle \pm |\psi_B(t)\rangle$$

where

$$\begin{aligned}
|\psi_A(t)\rangle &= \iint_{D_\epsilon} \frac{d\phi_1 d\phi_2}{4\pi^2} e^{-it4\cos(\frac{\pi}{8}+\frac{\phi_1}{2})\cos(\frac{3\pi}{8}+\phi_2)} A(\phi_1,\phi_2) |\mathrm{sc}(\tfrac{\pi}{4}+\phi_1; \tfrac{3\pi}{8}+\phi_2)\rangle_\pm && (5.11)\\
|\,\psi_B(t)\,\rangle &= \iint_{D_\epsilon} \frac{d\phi_1 d\phi_2}{4\pi^2} e^{-it4\cos(\frac{\pi}{8}+\frac{\phi_1}{2})\cos(\frac{3\pi}{8}+\phi_2)} e^{-i\theta_\pm(\frac{\pi}{4}+\phi_1,\frac{3\pi}{8}+\phi_2)} B(\phi_1,\phi_2,\tfrac{3\pi}{8}) |\mathrm{sc}(\tfrac{\pi}{4}+\phi_1; \tfrac{3\pi}{8}+\phi_2)\rangle_\pm
\end{aligned}$$

with

$$\begin{aligned}
A(\phi_1,\phi_2) &= \frac{1}{L} \sum_{x=-(M+L)}^{-(M+1)} \sum_{y=M+1}^{M+L} e^{i\phi_1\frac{x+y}{2}} e^{i\phi_2(x-y)} && (5.12)\\
B(\phi_1,\phi_2,k) &= \frac{1}{L} \sum_{x=-(M+L)}^{-(M+1)} \sum_{y=M+1}^{M+L} e^{i\phi_1\frac{x+y}{2}} e^{i(\phi_2+2k)(y-x)}.
\end{aligned}$$

Using the delta-function normalization of the scattering states (equation (5.10)) we get

$$\begin{aligned}
\langle\psi_B(t)|\psi_B(t)\rangle &= \iint_{D_\epsilon} \frac{d\phi_1 d\phi_2}{4\pi^2} \left|B(\phi_1,\phi_2,\tfrac{3\pi}{8})\right|^2\\
&\le \frac{16\pi^2}{L^2\epsilon^2}
\end{aligned}$$

by Lemma 9 (as long as $\epsilon < 3\pi/8$, which holds for $L$ sufficiently large). Similarly,

$$\begin{aligned}
1 &\ge \langle\psi_A(t)|\psi_A(t)\rangle\\
&= \iint_{D_\epsilon} \frac{d\phi_1 d\phi_2}{4\pi^2} \left|A(\phi_1,\phi_2)\right|^2\\
&\ge 1 - \frac{4\pi}{L\epsilon}
\end{aligned}$$

(from the first two facts in Lemma 9) and therefore

$$\begin{aligned}
\langle\psi_1(t)|\psi_1(t)\rangle &= \langle\psi_A(t)|\psi_A(t)\rangle + \langle\psi_B(t)|\psi_B(t)\rangle + \langle\psi_A(t)|\psi_B(t)\rangle + \langle\psi_B(t)|\psi_A(t)\rangle\\
&\ge 1 - \frac{4\pi}{L\epsilon} - 2\left|\langle\psi_A(t)|\psi_B(t)\rangle\right|\\
&\ge 1 - \frac{4\pi}{L\epsilon} - 2\left|\langle\psi_A(t)|\psi_A(t)\rangle\right|^{\frac{1}{2}} \left|\langle\psi_B(t)|\psi_B(t)\rangle\right|^{\frac{1}{2}}\\
&\ge 1 - \frac{12\pi}{L\epsilon}.
\end{aligned}$$

Hence

$$\langle\psi_2(t)|\psi_2(t)\rangle \le \frac{12\pi}{L\epsilon}$$

since

$$\langle\psi(t)|\psi(t)\rangle = \langle\psi_1(t)|\psi_1(t)\rangle + \langle\psi_2(t)|\psi_2(t)\rangle = 1.$$

Thus

$$\begin{aligned}\| \, |\psi(t)\rangle - |\psi_A(t)\rangle\| &= \| \, |\psi_B(t)\rangle + |\psi_2(t)\rangle\| \\ &\le \| \, |\psi_B(t)\rangle\| + \| \, |\psi_2(t)\rangle\| \\ &\le \frac{4\pi}{L\epsilon} + \sqrt{\frac{12\pi}{L\epsilon}}.\end{aligned}$$

Now

$$\begin{aligned}\| \, |\psi(t)\rangle - |\alpha(t)\rangle\| &\le \| \, |\psi(t)\rangle - |\psi_A(t)\rangle\| + \| \, |\psi_A(t)\rangle - |\alpha(t)\rangle\| \\ &\le \frac{4\pi}{L\epsilon} + \sqrt{\frac{12\pi}{L\epsilon}} + \| \, |\psi_A(t)\rangle - |\alpha(t)\rangle\| \\ &= \emptyset(L^{-1/4}) + \| \, |\psi_A(t)\rangle - |\alpha(t)\rangle\|\end{aligned}$$

using our choice $\epsilon = a/\sqrt{L}$. To complete the proof, we now show that the second term in this expression is bounded by $\emptyset(L^{-1/8})$.

**Lemma 7.** *With $|\psi_A(t)\rangle$ and $|\alpha(t)\rangle$ defined through equations (5.11) and (5.7), with $t \le c_0 L$ (for some constant $c_0$),*

$$\| \, |\psi_A(t)\rangle - |\alpha(t)\rangle\| = \emptyset(L^{-1/8}).$$

*Proof.* To simplify matters, note that both $|\psi_A(t)\rangle$ and $|\alpha(t)\rangle$ are either symmetric or anti-symmetric (i.e., $\langle x,y|\alpha(t)\rangle = \pm\langle y,x|\alpha(t)\rangle$ and $\langle x,y|\psi_A(t)\rangle = \pm\langle y,x|\psi_A(t)\rangle$). Taking $C$ to be the maximum range of the interaction in our Hamiltonian, we have

$$\| \, |\psi_A(t)\rangle - |\alpha(t)\rangle\| \le 2\left\|P_1|\psi_A(t)\rangle - P_1|\alpha(t)\rangle\right\| + \left\|P_2|\,\psi_A(t)\,\rangle\right\| + \left\|P_2|\,\alpha(t)\,\rangle\right\|,$$

where

$$P_1 = \sum_{y-x\ge C} |x,y\rangle\langle x,y| \qquad P_2 = \sum_{|x-y|<C} |\,x,y\,\rangle\langle\,x,y\,|.$$

Now, for $y - x \ge C$,

$$\begin{aligned}\langle x,y|\psi_A(t)\rangle &= \iint_{D_\epsilon} \frac{d\phi_1 d\phi_2}{4\pi^2} e^{-it4\cos(\frac{\pi}{8}+\frac{\phi_1}{2})\cos(\frac{3\pi}{8}+\phi_2)} A(\phi_1,\phi_2) \frac{e^{-i\left(\frac{\pi}{4}+\phi_1\right)\left(\frac{x+y}{2}\right)}}{\sqrt{2}} \\ &\qquad \left(e^{i\left(\frac{3\pi}{8}+\phi_2\right)(y-x)} \pm e^{-i\left(\frac{3\pi}{8}+\phi_2\right)(y-x)+i\theta_\pm(\frac{\pi}{4}+\phi_1,\frac{3\pi}{8}+\phi_2)}\right) \\ &= \iint_{D_\epsilon} \frac{d\phi_1 d\phi_2}{4\pi^2} \left[\frac{1}{\sqrt{2}} e^{-it4\cos(\frac{\pi}{8}+\frac{\phi_1}{2})\cos(\frac{3\pi}{8}+\phi_2)} A(\phi_1,\phi_2)\right. \\ &\qquad \left(e^{-i\pi x/2} e^{i\pi y/4} e^{-i\phi_1\left(\frac{x+y}{2}\right)} e^{i\phi_2(y-x)}\right. \\ &\qquad\quad \left.\left. \pm e^{i\pi x/4} e^{-i\pi y/2} e^{-i\phi_1\left(\frac{x+y}{2}\right)} e^{-i\phi_2(y-x)} e^{i\theta_\pm\left(\frac{\pi}{4}+\phi_1,\frac{3\pi}{8}+\phi_2\right)}\right)\right].\end{aligned}$$

From Lemma 10, for $x \le y$, the state $|\,\alpha(t)\,\rangle$ takes the form

$$\langle x, y|\alpha(t)\rangle = \frac{1}{\sqrt{2}} e^{-it\sqrt{2}} \Bigg[ e^{-i\pi x/2} e^{i\pi y/4} \Bigg( \iint_{D_\pi} \frac{d\phi_1 d\phi_2}{4\pi^2} A(\phi_1,\phi_2) e^{-i\phi_1\left(-\lfloor t\rfloor + \left\lfloor \frac{t}{\sqrt{2}}\right\rfloor + \frac{x+y}{2}\right)} e^{-2i\phi_2\left(-\lfloor t\rfloor - \left\lfloor \frac{t}{\sqrt{2}}\right\rfloor + \frac{x-y}{2}\right)} \Bigg) \pm e^{i\theta} e^{i\pi x/4} e^{-i\pi y/2} \Bigg( \iint_{D_\pi} \frac{d\phi_1 d\phi_2}{4\pi^2} A(\phi_1,\phi_2) e^{-i\phi_1\left(-\lfloor t\rfloor + \left\lfloor \frac{t}{\sqrt{2}}\right\rfloor + \frac{x+y}{2}\right)} e^{-2i\phi_2\left(-\lfloor t\rfloor - \left\lfloor \frac{t}{\sqrt{2}}\right\rfloor + \frac{y-x}{2}\right)} \Bigg) \Bigg],$$

where $D_\pi = [-\pi,\pi]\times[-\pi,\pi]$. Using these expressions for $|\,\psi_A(t)\,\rangle$ and $|\,\alpha(t)\,\rangle$, we now write

$$P_1|\psi_A(t)\rangle - P_1|\alpha(t)\rangle = \pm|e_1(t)\rangle + |e_2(t)\rangle \pm |f_1(t)\rangle + |f_2(t)\rangle \pm |g_1(t)\rangle + |g_2(t)\rangle \pm |h(t)\rangle$$

where each term in the above equation is supported only on states $|x,y\rangle$ such that $y-x \ge C$, and (for $y-x\ge C$)

$$\langle x, y|e_1(t)\rangle = \frac{e^{i\theta}}{\sqrt{2}} e^{-it\sqrt{2}} e^{i\pi x/4} e^{-i\pi y/2} \iint_{D_\pi} \frac{d\phi_1 d\phi_2}{4\pi^2} A(\phi_1,\phi_2) \Big[ e^{-i\phi_1\left(-t+\frac{t}{\sqrt{2}}+\frac{x+y}{2}\right)} e^{-2i\phi_2\left(-t-\frac{t}{\sqrt{2}}+\frac{y-x}{2}\right)} - e^{-i\phi_1\left(-\lfloor t\rfloor + \left\lfloor \frac{t}{\sqrt{2}}\right\rfloor + \frac{x+y}{2}\right)} e^{-2i\phi_2\left(-\lfloor t\rfloor - \left\lfloor \frac{t}{\sqrt{2}}\right\rfloor + \frac{y-x}{2}\right)} \Big]$$

$$\langle x, y|e_2(t)\rangle = \frac{1}{\sqrt{2}} e^{-it\sqrt{2}} e^{-i\pi x/2} e^{i\pi y/4} \iint_{D_\pi} \frac{d\phi_1 d\phi_2}{4\pi^2} A(\phi_1,\phi_2) \Big[ e^{-i\phi_1\left(-t+\frac{t}{\sqrt{2}}+\frac{x+y}{2}\right)} e^{-2i\phi_2\left(-t-\frac{t}{\sqrt{2}}+\frac{x-y}{2}\right)} - e^{-i\phi_1\left(-\lfloor t\rfloor + \left\lfloor \frac{t}{\sqrt{2}}\right\rfloor + \frac{x+y}{2}\right)} e^{-2i\phi_2\left(-\lfloor t\rfloor - \left\lfloor \frac{t}{\sqrt{2}}\right\rfloor + \frac{x-y}{2}\right)} \Big]$$

$$\langle x, y|f_1(t)\rangle = -\frac{e^{i\theta}}{\sqrt{2}} e^{-it\sqrt{2}} e^{i\pi x/4} e^{-i\pi y/2} \iint_{D_\pi\setminus D_\epsilon} \frac{d\phi_1 d\phi_2}{4\pi^2} A(\phi_1,\phi_2) e^{-i\phi_1\left(-t+\frac{t}{\sqrt{2}}+\frac{x+y}{2}\right)} e^{-2i\phi_2\left(-t-\frac{t}{\sqrt{2}}+\frac{y-x}{2}\right)}$$

$$\langle x, y|f_2(t)\rangle = -\frac{1}{\sqrt{2}} e^{-it\sqrt{2}} e^{-i\pi x/2} e^{i\pi y/4} \iint_{D_\pi\setminus D_\epsilon} \frac{d\phi_1 d\phi_2}{4\pi^2} A(\phi_1,\phi_2) e^{-i\phi_1\left(-t+\frac{t}{\sqrt{2}}+\frac{x+y}{2}\right)} e^{-2i\phi_2\left(-t-\frac{t}{\sqrt{2}}+\frac{x-y}{2}\right)}$$

$$\langle x, y|g_1(t)\rangle = \frac{e^{i\theta}}{\sqrt{2}} e^{i\pi x/4} e^{-i\pi y/2} \iint_{D_\epsilon} \frac{d\phi_1 d\phi_2}{4\pi^2} A(\phi_1,\phi_2) e^{-i\phi_1\left(\frac{x+y}{2}\right)} e^{-2i\phi_2\left(\frac{y-x}{2}\right)} \Big[ e^{-it4\cos\left(\frac{\pi}{8}+\frac{\phi_1}{2}\right)\cos\left(\frac{3\pi}{8}+\phi_2\right)} - e^{-it\left(\sqrt{2}+\sqrt{2}\left(\frac{\phi_1}{2}-\phi_2\right)-2\left(\frac{\phi_1}{2}+\phi_2\right)\right)} \Big]$$

$$\langle x, y|g_2(t)\rangle = \frac{1}{\sqrt{2}} e^{-i\pi x/2} e^{i\pi y/4} \iint_{D_\epsilon} \frac{d\phi_1 d\phi_2}{4\pi^2} A(\phi_1,\phi_2) e^{-i\phi_1\left(\frac{x+y}{2}\right)} e^{-2i\phi_2\left(\frac{x-y}{2}\right)} \Big[ e^{-it4\cos\left(\frac{\pi}{8}+\frac{\phi_1}{2}\right)\cos\left(\frac{3\pi}{8}+\phi_2\right)} - e^{-it\left(\sqrt{2}+\sqrt{2}\left(\frac{\phi_1}{2}-\phi_2\right)-2\left(\frac{\phi_1}{2}+\phi_2\right)\right)} \Big]$$

$$\langle x, y|h(t)\rangle = \frac{1}{\sqrt{2}} e^{i\pi x/4} e^{-i\pi y/2} \iint_{D_\epsilon} \frac{d\phi_1 d\phi_2}{4\pi^2} A(\phi_1,\phi_2) e^{-i\phi_1\left(\frac{x+y}{2}\right)} e^{-2i\phi_2\left(\frac{y-x}{2}\right)} e^{-it4\cos\left(\frac{\pi}{8}+\frac{\phi_1}{2}\right)\cos\left(\frac{3\pi}{8}+\phi_2\right)} \left( e^{i\theta_\pm\left(\frac{\pi}{4}+\phi_1, \frac{3\pi}{8}+\phi_2\right)} - e^{i\theta} \right).$$

We now proceed to bound the norm of each of these states. We repeatedly use the fact that, for $(\phi_1, \phi_2) \in D_\pi$,

$$\sum_{x,y=-\infty}^{\infty} e^{ix\left(\frac{1}{2}(\phi_1-\tilde{\phi}_1)-(\phi_2-\tilde{\phi}_2)\right)} e^{iy\left(\frac{1}{2}(\phi_1-\tilde{\phi}_1)+(\phi_2-\tilde{\phi}_2)\right)} = 4\pi^2\delta(\phi_1-\tilde{\phi}_1)\delta(\phi_2-\tilde{\phi}_2).$$

Using this formula we get

$$\begin{aligned}
\langle e_1(t)|e_1(t)\rangle &= \sum_{y-x\geq C} \langle e_1(t)|x,y\rangle\langle x,y|e_1(t)\rangle \\
&\leq \sum_{x=-\infty}^{\infty}\sum_{y=-\infty}^{\infty} \left|\frac{1}{\sqrt{2}}\iint_{D_\pi} \frac{d\phi_1 d\phi_2}{4\pi^2} A(\phi_1,\phi_2)\Big[e^{-i\phi_1\left(-t+\frac{t}{\sqrt{2}}+\frac{x+y}{2}\right)}\right. \\
&\qquad \left. e^{-2i\phi_2\left(-t-\frac{t}{\sqrt{2}}+\frac{y-x}{2}\right)} - e^{-i\phi_1\left(-\lfloor t\rfloor+\left\lfloor\frac{t}{\sqrt{2}}\right\rfloor+\frac{x+y}{2}\right)} e^{-2i\phi_2\left(-\lfloor t\rfloor-\left\lfloor\frac{t}{\sqrt{2}}\right\rfloor+\frac{y-x}{2}\right)}\Big]\right|^2 \\
&= \frac{1}{2}\iint_{D_\pi}\frac{d\phi_1 d\phi_2}{4\pi^2}\left|A(\phi_1,\phi_2)\right|^2 \left|e^{-i\phi_1\left(-t+\frac{t}{\sqrt{2}}\right)}e^{-2i\phi_2\left(-t-\frac{t}{\sqrt{2}}\right)}\right. \\
&\qquad \left. - e^{-i\phi_1\left(-\lfloor t\rfloor+\left\lfloor\frac{t}{\sqrt{2}}\right\rfloor\right)}e^{-2i\phi_2\left(-\lfloor t\rfloor-\left\lfloor\frac{t}{\sqrt{2}}\right\rfloor\right)}\right|^2.
\end{aligned}$$

Now use the fact that $\left|e^{-ic}-1\right|^2 \leq c^2$ for $c\in\mathbb{R}$ to get

$$\begin{aligned}
\langle e_1(t)|e_1(t)\rangle &\leq \frac{1}{2}\iint_{D_\pi}\left(\frac{d\phi_1 d\phi_2}{4\pi^2}\right)\left|A(\phi_1,\phi_2)\right|^2\Bigg(-\phi_1\left(-t+\frac{t}{\sqrt{2}}+\lfloor t\rfloor-\left\lfloor\frac{t}{\sqrt{2}}\right\rfloor\right) \\
&\qquad -2\phi_2\left(-t-\frac{t}{\sqrt{2}}+\lfloor t\rfloor+\left\lfloor\frac{t}{\sqrt{2}}\right\rfloor\right)\Bigg)^2 \\
&\leq 4\iint_{D_\pi}\frac{d\phi_1 d\phi_2}{4\pi^2}\left|A(\phi_1,\phi_2)\right|^2\left(\phi_1^2+4\phi_2^2\right)
\end{aligned}$$

using the Cauchy-Schwarz inequality and the fact that $\left|t-t/\sqrt{2}-\lfloor t\rfloor-\left\lfloor t/\sqrt{2}\right\rfloor\right|\leq 2$. So

$$\begin{aligned}
\langle e_1(t)|e_1(t)\rangle &\leq 4\left(\iint_{D_\pi\setminus D_\epsilon}\frac{d\phi_1 d\phi_2}{4\pi^2}+\iint_{D_\epsilon}\frac{d\phi_1 d\phi_2}{4\pi^2}\right)\left|A(\phi_1,\phi_2)\right|^2\left(\phi_1^2+4\phi_2^2\right) \\
&\leq 4\left(5\pi^2\right)\left(\frac{4\pi}{L\epsilon}\right)+20\epsilon^2 \\
&= \frac{80\pi^3}{L\epsilon}+20\epsilon^2
\end{aligned}$$

where we have used Lemma 9 and the fact that $\phi_1^2+4\phi_2^2\leq 5\epsilon^2$ on $D_\epsilon$. Similarly,

$$\langle e_2(t)|e_2(t)\rangle \leq \frac{80\pi^3}{L\epsilon}+20\epsilon^2.$$

Now

$$
\begin{aligned}
\langle f_1(t)|f_1(t)\rangle &\leq \frac{1}{2}\iint_{D_\pi \setminus D_\epsilon} \frac{d\phi_1 d\phi_2}{4\pi^2}\left|A(\phi_1,\phi_2)\right|^2 \\
&\leq \frac{2\pi}{L\epsilon}
\end{aligned}
$$

by Lemma 9, and similarly

$$
\langle f_2(t)|f_2(t)\rangle \leq \frac{2\pi}{L\epsilon}.
$$

Moving on to the next term,

$$
\begin{aligned}
\langle g_1(t)|g_1(t)\rangle &\leq \frac{1}{2}\iint_{D_\epsilon} \frac{d\phi_1 d\phi_2}{4\pi^2}\left|A(\phi_1,\phi_2)\right|^2 \Big| e^{-it4\cos\left(\frac{\pi}{8}+\frac{\phi_1}{2}\right)\cos\left(\frac{3\pi}{8}+\phi_2\right)} \\
&\qquad\qquad - e^{-it\left(\sqrt{2}+\sqrt{2}\left(\frac{\phi_1}{2}-\phi_2\right)-2\left(\frac{\phi_1}{2}+\phi_2\right)\right)}\Big|^2 \\
&\leq \frac{1}{2}\iint_{D_\epsilon} \frac{d\phi_1 d\phi_2}{4\pi^2}\Bigg[\left|A(\phi_1,\phi_2)\right|^2 t^2\left(4\cos\left(\frac{\pi}{8}+\frac{\phi_1}{2}\right)\cos\left(\frac{3\pi}{8}+\phi_2\right)\right. \\
&\qquad\qquad \left.-\sqrt{2}-\sqrt{2}\left(\frac{\phi_1}{2}-\phi_2\right)+2\left(\frac{\phi_1}{2}+\phi_2\right)\right)^2\Bigg] \qquad (5.13)
\end{aligned}
$$

using $\left|e^{-ic}-1\right|^2 \leq c^2$ for $c \in \mathbb{R}$. Now

$$
\begin{aligned}
4\cos\left(\frac{\pi}{8}+\frac{\phi_1}{2}\right)\cos\left(\frac{3\pi}{8}+\phi_2\right) &= 2\cos\left(\frac{\pi}{2}+\frac{\phi_1}{2}+\phi_2\right)+2\cos\left(-\frac{\pi}{4}+\frac{\phi_1}{2}-\phi_2\right) \\
&= -2\sin\left(\frac{\phi_1}{2}+\phi_2\right)+\sqrt{2}\cos\left(\frac{\phi_1}{2}-\phi_2\right)+\sqrt{2}\sin\left(\frac{\phi_1}{2}-\phi_2\right)
\end{aligned}
$$

so

$$
\begin{aligned}
&\left|4\cos\left(\frac{\pi}{8}+\frac{\phi_1}{2}\right)\cos\left(\frac{3\pi}{8}+\phi_2\right)-\sqrt{2}-\sqrt{2}\left(\frac{\phi_1}{2}-\phi_2\right)+2\left(\frac{\phi_1}{2}+\phi_2\right)\right| \\
&\quad\leq \left|\sqrt{2}\left(\cos\left(\frac{\phi_1}{2}-\phi_2\right)-1\right)\right|+\left|\sqrt{2}\left(\sin\left(\frac{\phi_1}{2}-\phi_2\right)-\left(\frac{\phi_1}{2}-\phi_2\right)\right)\right| \\
&\qquad+\left|2\left(\sin\left(\frac{\phi_1}{2}+\phi_2\right)-\left(\frac{\phi_1}{2}+\phi_2\right)\right)\right|. \\
&\quad\leq \sqrt{2}\left(\frac{\phi_1}{2}-\phi_2\right)^2+\sqrt{2}\left(\frac{\phi_1}{2}-\phi_2\right)^2+2\left(\frac{\phi_1}{2}+\phi_2\right)^2 \\
&\quad\leq 4\left(\left(\frac{\phi_1}{2}+\phi_2\right)^2+\left(\frac{\phi_1}{2}-\phi_2\right)^2\right),
\end{aligned}
$$

using $|\cos x - 1| \le x^2$ and $|\sin x - x| \le x^2$ for $x \in \mathbb{R}$. Plugging this into equation (5.13) we get

$$\begin{aligned}
\langle g_1(t)|g_1(t)\rangle &\le \frac{1}{2}\iint_{D_\epsilon} \frac{d\phi_1 d\phi_2}{4\pi^2} 16\,|A(\phi_1,\phi_2)|^2\, t^2 \left(\left(\frac{\phi_1}{2}+\phi_2\right)^2 + \left(\frac{\phi_1}{2}-\phi_2\right)^2\right)^2 \\
&\le 16t^2 \iint_{D_\epsilon} \frac{d\phi_1 d\phi_2}{4\pi^2}\,|A(\phi_1,\phi_2)|^2 \left(\left(\frac{\phi_1}{2}+\phi_2\right)^4 + \left(\frac{\phi_1}{2}-\phi_2\right)^4\right) \\
&\le \frac{16t^2}{L^2}\iint_{D_\epsilon} \frac{d\phi_1 d\phi_2}{4\pi^2} \frac{\sin^2(\frac{L}{2}[\frac{\phi_1}{2}+\phi_2])}{\sin^2(\frac{1}{2}[\frac{\phi_1}{2}+\phi_2])} \frac{\sin^2(\frac{L}{2}[-\frac{\phi_1}{2}+\phi_2])}{\sin^2(\frac{1}{2}[-\frac{\phi_1}{2}+\phi_2])} \\
&\qquad \left(\left(\frac{\phi_1}{2}+\phi_2\right)^4 + \left(\frac{\phi_1}{2}-\phi_2\right)^4\right)
\end{aligned}$$

where we used the Cauchy-Schwarz inequality in the second line and equation (5.17) in the last line. Changing coordinates to

$$\alpha_1 = \phi_1 + \frac{\phi_2}{2} \qquad \alpha_2 = \frac{\phi_1}{2} - \phi_2$$

and realizing that $|\alpha_1|, |\alpha_2| < 3\epsilon/2$ for $(\phi_1,\phi_2) \in D_\epsilon$, we see that

$$\begin{aligned}
\langle g_1(t)\,|g_1(t)\rangle &\le \frac{16t^2}{L^2}\int_{-3\epsilon/2}^{3\epsilon/2} \frac{d\alpha_1}{2\pi}\int_{-3\epsilon/2}^{3\epsilon/2} \frac{d\alpha_1}{2\pi} \frac{\sin^2(\frac{1}{2}L\alpha_1)}{\sin^2(\frac{1}{2}\alpha_1)} \frac{\sin^2(\frac{1}{2}L\alpha_2)}{\sin^2(\frac{1}{2}\alpha_2)} \left(\alpha_1^4+\alpha_2^4\right) \\
&= \frac{32t^2}{L^2}\int_{-3\epsilon/2}^{3\epsilon/2} \frac{d\alpha_1}{2\pi}\int_{-3\epsilon/2}^{3\epsilon/2} \frac{d\alpha_1}{2\pi} \frac{\sin^2(\frac{1}{2}L\alpha_1)}{\sin^2(\frac{1}{2}\alpha_1)} \frac{\sin^2(\frac{1}{2}L\alpha_2)}{\sin^2(\frac{1}{2}\alpha_2)} \alpha_1^4 \\
&\le \frac{32t^2}{L}\int_{-3\epsilon/2}^{3\epsilon/2} \frac{d\alpha_1}{2\pi} \frac{\sin^2(\frac{1}{2}L\alpha_1)}{\sin^2(\frac{1}{2}\alpha_1)} \alpha_1^4 \\
&\le \frac{32t^2}{L}\int_{-3\epsilon/2}^{3\epsilon/2} \frac{d\alpha_1}{2\pi} \frac{\pi^2}{\alpha_1^2} \alpha_1^4 \\
&= \frac{36\pi t^2 \epsilon^3}{L},
\end{aligned}$$

with a similar bound on $\langle g_2(t)|g_2(t)\rangle$.

Finally,

$$\langle h(t)|h(t)\rangle \le \frac{1}{2}\iint_{D_\epsilon} \frac{d\phi_1 d\phi_2}{4\pi^2}\,|A(\phi_1,\phi_2)|^2 \left| e^{i\theta_\pm(\frac{\pi}{4}+\phi_1, \frac{3\pi}{8}+\phi_2)} - e^{i\theta}\right|^2.$$

Recall that $e^{i\theta_\pm(p_1,p_2)} = T(p_1,p_2) \pm R(p_1,p_2)$ is obtained by solving for the effective single-particle S-matrix for the Hamiltonian (5.3). For $p_1$ near $\pi/4$ we divide this Hamiltonian by $2\cos(p_1/2)$ to put it in the form considered in [?], where the potential term is now $\mathcal{V}(|r|)/(2\cos(p_1/2))$. The entries $T(p_1,p_2)$ and $R(p_1,p_2)$ of this S-matrix are bounded rational functions of $z = e^{ip_2}$ and $(2\cos(p_1/2))^{-1}$ [?], so they are differentiable as a function of $p_1$ and

$p_2$ on some neighborhood $U$ of $(\pi/4, 3\pi/8)$ (and have bounded partial derivatives on this neighborhood).

For $\epsilon$ small enough that $D_\epsilon \subset U$ we get, using the mean value theorem and the fact that $\theta = \theta_\pm(\pi/4, 3\pi/8)$,

$$\begin{aligned}\left|e^{i\theta_\pm(\frac{\pi}{4}+\phi_1, \frac{3\pi}{8}+\phi_2)} - e^{i\theta}\right| &\leq \sqrt{\phi_1^2+\phi_2^2}\max_U\left|\vec{\nabla}e^{i\theta_\pm}\right| \quad \text{for } (\phi_1,\phi_2)\in D_\epsilon \\ &\leq \epsilon\Gamma\end{aligned}$$

for some constant $\Gamma$ (independent of $L$). Therefore

$$\begin{aligned}\langle h(t)|h(t)\rangle &\leq \frac{1}{2}\iint_{D_\epsilon}\frac{d\phi_1 d\phi_2}{4\pi^2}\left|A(\phi_1,\phi_2)\right|^2\epsilon^2\Gamma^2 \\ &\leq \frac{1}{2}\Gamma^2\epsilon^2.\end{aligned}$$

Putting these bounds together, we get

$$\begin{aligned}\|P_1|\psi_A(t)\rangle - P_1|\alpha(t)\rangle\| &\leq \||e_1(t)\rangle\| + \||e_2(t)\rangle\| + \||f_1(t)\rangle\| + \||f_2(t)\rangle\| \\ &\quad + \||g_1(t)\rangle\| + \||g_2(t)\rangle\| + \||h(t)\rangle\| \\ &\leq 2\left(\frac{80\pi^3}{L\epsilon}+20\epsilon^2\right)^{\frac{1}{2}} + 2\left(\frac{2\pi}{L\epsilon}\right)^{\frac{1}{2}} + 2\left(\frac{36\pi t^2\epsilon^3}{L}\right)^{\frac{1}{2}} + \frac{1}{\sqrt{2}}\Gamma\epsilon.\end{aligned}$$

Letting $\epsilon = a/\sqrt{L}$ and $t \leq c_0 L$ we get

$$\|\, P_1|\psi_A(t)\rangle - P_1|\alpha(t)\rangle\| = \emptyset(L^{-1/4}). \tag{5.14}$$

Since $P_2|\,\alpha(t)\,\rangle$ has support on at most $4CL$ basis states $|x,y\rangle$, and since $|\langle x,y|P_2|\alpha(t)\rangle|^2 = \emptyset(L^{-2})$, we get

$$\|P_2|\,\alpha(t)\,\rangle\| = \emptyset(L^{-1/2}). \tag{5.15}$$

We now use the bounds (5.14) and (5.15) and Lemma 8 to show that

$$\||\psi_A(t)\rangle - |\alpha(t)\rangle\| = \emptyset(L^{-1/8}). \tag{5.16}$$

First consider the case where the interaction range is $C = 0$ (as in the Bose-Hubbard model). In this case equation (5.16) follows directly from equation (5.14) and the facts that $\langle x,y|\alpha(t)\rangle = \pm\langle y,x|\alpha(t)\rangle$ and $\langle x,y|\psi_A(t)\rangle = \pm\langle y,x|\psi_A(t)\rangle$.

Now suppose $C \neq 0$. In this case

$$\begin{aligned}\left\|(1-P_2)\,|\psi_A(t)\rangle\right\|^2 &= 2\left\|P_1|\psi_A(t)\rangle\right\|^2 \\ &= 2\left(\|P_1|\alpha(t)\rangle\| + \emptyset(L^{-1/4})\right)^2 \\ &= 2\left(\frac{1}{2}\left\|(1-P_2)|\alpha(t)\rangle\right\|^2 + \emptyset(L^{-1/4})\right) \\ &= 1 + \emptyset(L^{-1}) - \langle\alpha(t)|P_2|\alpha(t)\rangle + \emptyset(L^{-1/4}) \\ &= 1 + \emptyset(L^{-1/4})\end{aligned}$$

where in the next-to-last line we have used Lemma 8. So

$$\begin{aligned}
\| |\psi_A(t)\rangle - |\alpha(t)\rangle\| &\le 2\,\|P_1|\psi_A(t)\rangle - P_1|\alpha(t)\rangle\| + \|P_2|\alpha(t)\rangle\| + \|P_2|\psi_A(t)\rangle\| \\
&= \emptyset(L^{-1/4}) + \emptyset(L^{-1/2}) + (1 - \|(1-P_2)\,|\psi_A(t)\rangle\|)^{\frac{1}{2}} \\
&= \emptyset(L^{-1/4}) + \emptyset(L^{-1/2}) + \emptyset(L^{-1/8}) \\
&= \emptyset(L^{-1/8})
\end{aligned}$$

which completes the proof. □

□

#### 5.1.2.1 Technical lemmas

In this section we prove three lemmas that are used in the proof of Theorem 2.

**Lemma 8.** *Let $|\alpha(t)\rangle$ be defined as in Theorem 2. Then*

$$\langle\alpha(t)|\alpha(t)\rangle = 1 + \emptyset(L^{-1}).$$

*Proof.* Define

$$\Pi = \sum_{x \le y} |x, y\rangle\langle x, y|.$$

Note that, since $\langle x, y|\alpha(t)\rangle = \pm\langle y, x|\alpha(t)\rangle$,

$$\begin{aligned}
\langle\alpha(t)|\alpha(t)\rangle &= 2\langle\alpha(t)|\Pi|\alpha(t)\rangle - \sum_{x=-\infty}^{\infty} \langle\alpha(t)|x, x\rangle\langle x, x|\alpha(t)\rangle \\
&= 2\langle\alpha(t)|\Pi|\alpha(t)\rangle + \emptyset(L^{-1})
\end{aligned}$$

where the last line follows since $|\langle x, x|\alpha(t)\rangle|^2$ is nonzero for at most $L$ values of $x$ and $|\langle x, x|\alpha(t)\rangle|^2 = \emptyset(L^{-2})$. We now show that

$$\langle\alpha(t)|\Pi|\alpha(t)\rangle = \frac{1}{2} + O(L^{-1}).$$

Note that

$$\begin{aligned}
\langle\alpha(t)|\Pi|\alpha(t)\rangle = \frac{1}{2L^2} \sum_{x \le y} \Bigg( & F(x, y, t) + F(y, x, t) \\
& \pm e^{i\theta} e^{\frac{3i\pi}{4}x} e^{-\frac{3i\pi}{4}y} F(x, y, t) F(y, x, t) \\
& \pm e^{-i\theta} e^{-\frac{3i\pi}{4}x} e^{\frac{3i\pi}{4}y} F(x, y, t) F(y, x, t) \Bigg).
\end{aligned}$$

Now $F(x, y, t) = 1$ if and only if $x \in \{-M - L + 2\lfloor t\rfloor, \ldots, -M - 1 + 2\lfloor t\rfloor\}$ and $y \in \{M + 1 - 2\lfloor t/\sqrt{2}\rfloor, \ldots, M + L - 2\lfloor t/\sqrt{2}\rfloor\}$. Similarly $F(y, x, t) = 1$ if and only if $x \in \{M+1-2\lfloor t/\sqrt{2}\rfloor, \ldots, M+L-2\lfloor t/\sqrt{2}\rfloor\}$ and $y \in \{-M-L+2\lfloor t\rfloor, \ldots, -M-1+2\lfloor t\rfloor\}$. So

$$\sum_{x \le y} F(y, x, t) = \sum_{y \le x} F(x, y, t)$$

and

$$\frac{1}{2L^2}\sum_{x\le y}\left[F(x,y,t)+F(y,x,t)\right]=\frac{1}{2L^2}\left(\sum_{x=-\infty}^{\infty}\sum_{y=-\infty}^{\infty}F(x,y,t)-\sum_{x=-\infty}^{\infty}F(x,x,t)\right)$$
$$=\frac{1}{2}+\emptyset(L^{-1}).$$

We now establish the bound

$$\left|\frac{1}{2L^2}\sum_{x\le y}e^{\frac{3i\pi}{4}x}e^{-\frac{3i\pi}{4}y}F(x,y,t)F(y,x,t)\right|=\emptyset(L^{-1})$$

to complete the proof. To get this bound, note that both $F(x,y,t)=1$ and $F(y,x,t)=1$ if and only if

$$x,y\in\{-M-L+2\lfloor t\rfloor,\dots,-M-1+2\lfloor t\rfloor\}$$
$$\text{and } x,y\in\left\{M+1-2\left\lfloor\frac{t}{\sqrt{2}}\right\rfloor,\dots,M+L-2\left\lfloor\frac{t}{\sqrt{2}}\right\rfloor\right\}.$$

Letting

$$B=\{-M-L+2\lfloor t\rfloor,\dots,-M-1+2\lfloor t\rfloor\}\cap\left\{M+1-2\left\lfloor\frac{t}{\sqrt{2}}\right\rfloor,\dots,M+L-2\left\lfloor\frac{t}{\sqrt{2}}\right\rfloor\right\},$$

we have

$$B=\{j,j+1,\dots,j+l\}$$

for some $j,l\in\mathbb{Z}$ with $l<L$. So

$$\begin{aligned}\frac{1}{2L^2}\left|\sum_{x\le y}e^{\frac{3i\pi}{4}x}e^{-\frac{3i\pi}{4}y}F(x,y,t)F(y,x,t)\right|&=\frac{1}{2L^2}\left|\sum_{x,y\in B,\,x\le y}e^{\frac{3i\pi}{4}x}e^{-\frac{3i\pi}{4}y}\right|\\&=\frac{1}{2L^2}\left|\sum_{y=j}^{j+l}\sum_{x=j}^{y}e^{\frac{3i\pi}{4}x}e^{-\frac{3i\pi}{4}y}\right|\\&=\frac{1}{2L^2}\left|\sum_{y=j}^{j+l}e^{-\frac{3i\pi}{4}y}e^{3i\frac{\pi}{4}j}\frac{e^{3i\frac{\pi}{4}(y+1-j)}-1}{e^{3i\frac{\pi}{4}}-1}\right|\\&\le\frac{(l+1)}{2L^2}\frac{2}{\left|e^{3i\frac{\pi}{4}}-1\right|}\\&=\emptyset(L^{-1})\end{aligned}$$

since $l<L$. □

**Lemma 9.** *Let $k\in(-\pi,0)\cup(0,\pi)$ and $0<\epsilon<\min\{\pi-|k|,|k|\}$. Let*

$$D_\epsilon=[-\epsilon,\epsilon]\times[-\epsilon,\epsilon]$$
$$D_\pi=[-\pi,\pi]\times[-\pi,\pi].$$

*Then*

$$\iint_{D_\pi} \frac{d\phi_1 d\phi_2}{4\pi^2}|A(\phi_1,\phi_2)|^2 = 1$$
$$\iint_{D_\pi \setminus D_\epsilon} \frac{d\phi_1 d\phi_2}{4\pi^2}|A(\phi_1,\phi_2)|^2 \le \frac{4\pi}{L\epsilon}$$
$$\iint_{D_\epsilon} \frac{d\phi_1 d\phi_2}{4\pi^2}|B(\phi_1,\phi_2,k)|^2 \le \frac{4\pi^2}{L^2\epsilon^2}.$$

*where* $A(\phi_1,\phi_2)$ *and* $B(\phi_1,\phi_2,k)$ *are given by equation (5.12).*

*Proof.* Using equation (5.12) we get

$$|A(\phi_1,\phi_2)|^2 = \frac{1}{L^2}\sum_{x,\tilde{x}=-(M+L)}^{-(M+1)}\sum_{y,\tilde{y}=M+1}^{M+L} e^{i\frac{\phi_1}{2}(x+y-(\tilde{x}+\tilde{y}))}e^{i\phi_2(x-y-(\tilde{x}-\tilde{y}))}.$$

Now

$$\int_{-\pi}^{\pi}\frac{d\phi_2}{2\pi}e^{i\phi_2(x-y-\tilde{x}+\tilde{y})} = \delta_{x-y,\tilde{x}-\tilde{y}},$$

so (suppressing the limits of summation for readability)

$$\begin{aligned}\iint_{D_\pi} \frac{d\phi_1 d\phi_2}{4\pi^2}|A(\phi_1,\phi_2)|^2 &= \frac{1}{L^2}\int_{-\pi}^{\pi}\frac{d\phi_1}{2\pi}\sum_{x,\tilde{x}}\sum_{y,\tilde{y}} e^{i\phi_1(y-\tilde{y})}\delta_{x-y,\tilde{x}-\tilde{y}} \\ &= \frac{1}{L^2}\sum_{x,\tilde{x}}\sum_{y,\tilde{y}}\delta_{y,\tilde{y}}\delta_{x-y,\tilde{x}-\tilde{y}} \\ &= 1\end{aligned}$$

which proves the first part.

By performing the sums in equation (5.12) we get

$$|A(\phi_1,\phi_2)|^2 = \frac{1}{L^2}\frac{\sin^2(\frac{1}{2}L[\frac{\phi_1}{2}+\phi_2])}{\sin^2(\frac{1}{2}[\frac{\phi_1}{2}+\phi_2])}\frac{\sin^2(\frac{1}{2}L[\frac{\phi_1}{2}-\phi_2])}{\sin^2(\frac{1}{2}[\frac{\phi_1}{2}-\phi_2])}. \tag{5.17}$$

Letting $\alpha_1 = \phi_1/2+\phi_2$ and $\alpha_2 = \phi_1/2-\phi_2$, we see that $|\alpha_1| \le 3\pi/2$, $|\alpha_2| \le 3\pi/2$, and $\alpha_1^2+\alpha_2^2 \ge 5\epsilon^2/2$ whenever $(\phi_1,\phi_2) \in D_\pi \setminus D_\epsilon$. Defining $D_{3\pi/2} = [-3\pi/2, 3\pi/2]^2$ we get

$(\alpha_1, \alpha_2) \in D_{3\pi/2} \setminus D_\epsilon$ whenever $(\phi_1, \phi_2) \in D_\pi \setminus D_\epsilon$. Hence

$$\begin{aligned}
\iint_{D_\pi \setminus D_\epsilon} \frac{d\phi_1 d\phi_2}{4\pi^2} |A(\phi_1, \phi_2)|^2 &\leq \frac{1}{L^2} \iint_{D_{3\pi/2} \setminus D_\epsilon} \frac{d\alpha_1 d\alpha_2}{4\pi^2} \frac{\sin^2(\frac{1}{2}L\alpha_1)}{\sin^2(\frac{1}{2}\alpha_1)} \frac{\sin^2(\frac{1}{2}L\alpha_2)}{\sin^2(\frac{1}{2}\alpha_2)} \\
&\leq \frac{4}{L} \left( \frac{1}{L} \int_{-\frac{3\pi}{2}}^{\frac{3\pi}{2}} \frac{d\alpha_1}{2\pi} \frac{\sin^2(\frac{1}{2}L\alpha_1)}{\sin^2(\frac{1}{2}\alpha_1)} \right) \left( \int_\epsilon^{3\pi/2} \frac{d\alpha_2}{2\pi} \frac{\sin^2(\frac{1}{2}L\alpha_2)}{\sin^2(\frac{1}{2}\alpha_2)} \right) \\
&\leq \frac{4}{L} \left( \int_{-2\pi}^{2\pi} \frac{d\alpha_1}{2\pi} \frac{1}{L} \frac{\sin^2(\frac{1}{2}L\alpha_1)}{\sin^2(\frac{1}{2}\alpha_1)} \right) \left( \int_\epsilon^{\frac{3\pi}{2}} \frac{d\alpha_2}{2\pi} \frac{1}{\sin^2(\frac{1}{2}\alpha_2)} \right) \\
&= \frac{8}{L} \left( \int_\epsilon^\pi \frac{d\alpha_2}{2\pi} \frac{1}{\sin^2(\frac{1}{2}\alpha_2)} + \int_\pi^{\frac{3\pi}{2}} \frac{d\alpha_2}{2\pi} \frac{1}{\sin^2(\frac{1}{2}\alpha_2)} \right) \\
&\leq \frac{8}{L} \left( \int_\epsilon^\pi \frac{d\alpha_2}{2\pi} \frac{\pi^2}{\alpha_2^2} + 2 \int_\pi^{\frac{3\pi}{2}} \frac{d\alpha_2}{2\pi} \right) \\
&= \frac{4\pi}{L\epsilon}
\end{aligned}$$

which proves the second inequality (in the next-to-last line we have used the fact that $\sin(x/2) > x/\pi$ for $x \in (0, \pi)$ and $\sin^2(x/2) > 1/2$ for $x \in (\pi, 3\pi/2)$).

Now

$$\begin{aligned}
|B(\phi_1, \phi_2, k)|^2 &= |A(\phi_1, -\phi_2 - 2k)|^2 \\
&\leq \frac{1}{L^2} \frac{1}{\sin^2\left(\frac{1}{2}\left[\frac{\phi_1}{2} + \phi_2 + 2k\right]\right)} \frac{1}{\sin^2\left(\frac{1}{2}\left[-\frac{\phi_1}{2} + \phi_2 + 2k\right]\right)}.
\end{aligned}$$

If $(\phi_1, \phi_2) \in D_\epsilon$ then $|k| - 3\epsilon/4 \leq |\pm\phi_1/4 + \phi_2/2 + k| \leq |k| + 3\epsilon/4$. Noting that $\epsilon$ is chosen such that $0 < \epsilon < \min\{\pi - |k|, |k|\}$, we get

$$\frac{\epsilon}{4} \leq \left| \pm \frac{\phi_1}{4} + \frac{\phi_2}{2} + k \right| \leq \pi - \frac{\epsilon}{4}$$

so

$$\begin{aligned}
|B(\phi_1, \phi_2, k)|^2 &\leq \frac{1}{L^2} \frac{1}{\sin^4(\frac{\epsilon}{4})} \\
&\leq \frac{16\pi^4}{L^2\epsilon^4}
\end{aligned}$$

and

$$\begin{aligned}
\iint_{D_\epsilon} \frac{d\phi_1 d\phi_2}{4\pi^2} |B(\phi_1, \phi_2, k)|^2 &\leq \frac{1}{4\pi^2} (2\epsilon)^2 \left( \frac{16\pi^4}{L^2\epsilon^4} \right) \\
&= \frac{16\pi^2}{L^2\epsilon^2}.
\end{aligned}$$

□

**Lemma 10.** *Let $a_{xy}(t)$ be as in Theorem 2. For $x \leq y$,*

$$a_{xy}(t) = \frac{1}{\sqrt{2}} e^{-it\sqrt{2}} \Bigg[ e^{-i\pi x/2} e^{i\pi y/4} \Bigg( \iint_{D_\pi} \frac{d\phi_1 d\phi_2}{4\pi^2} A(\phi_1, \phi_2) \\ e^{-i\phi_1\left(-\lfloor t\rfloor + \lfloor \frac{t}{\sqrt{2}} \rfloor + \frac{x+y}{2}\right)} e^{-2i\phi_2\left(-\lfloor t\rfloor - \lfloor \frac{t}{\sqrt{2}} \rfloor + \frac{x-y}{2}\right)} \Bigg) \\ \pm e^{i\theta} e^{i\pi x/4} e^{-i\pi y/2} \Bigg( \iint_{D_\pi} \frac{d\phi_1 d\phi_2}{4\pi^2} A(\phi_1, \phi_2) \\ e^{-i\phi_1\left(-\lfloor t\rfloor + \lfloor \frac{t}{\sqrt{2}} \rfloor + \frac{x+y}{2}\right)} e^{-2i\phi_2\left(-\lfloor t\rfloor - \lfloor \frac{t}{\sqrt{2}} \rfloor + \frac{y-x}{2}\right)} \Bigg) \Bigg].$$

*Proof.* The lemma follows from (5.8) and the fact that, for any two numbers $\gamma_1, \gamma_2$ such that $\gamma_1 + \gamma_2, \gamma_1 - \gamma_2 \in \mathbb{Z}$,

$$\iint_{D_\pi} \frac{d\phi_1 d\phi_2}{4\pi^2} A(\phi_1, \phi_2) e^{i\gamma_1\phi_1 + 2i\gamma_2\phi_2} = \begin{cases} \frac{1}{L} & \text{if } (-\gamma_1 - \gamma_2, -\gamma_1 + \gamma_2) \in S \\ 0 & \text{otherwise} \end{cases}$$

where $S = \{-M-L, \ldots, -M-1\} \times \{M+1, \ldots, M+L\}$. To establish this formula, observe that

$$\begin{aligned} \iint_{D_\pi} \frac{d\phi_1 d\phi_2}{4\pi^2} A(\phi_1, \phi_2) e^{i\gamma_1\phi_1 + 2i\gamma_2\phi_2} &= \frac{1}{L} \sum_{x=-M-L}^{-M-1} \sum_{y=M+1}^{M+L} \iint_{D_\pi} \frac{d\phi_1 d\phi_2}{4\pi^2} e^{i\phi_1\left(\gamma_1 + \frac{x+y}{2}\right)} e^{i\phi_2(x-y+2\gamma_2)} \\ &= \frac{1}{L} \sum_{x=-M-L}^{-M-1} \sum_{y=M+1}^{M+L} \int_{-\pi}^{\pi} \frac{d\phi_1}{2\pi} e^{i\phi_1\left(\gamma_1 + \frac{x-y}{2}\right)} \delta_{y,-x-2\gamma_2}. \end{aligned}$$

Here we have performed the integral over $\phi_2$ using the fact that $2\gamma_2$ is an integer. We then have

$$\begin{aligned} \iint_{D_\pi} \frac{d\phi_1 d\phi_2}{4\pi^2} A(\phi_1, \phi_2) e^{i\gamma_1\phi_1 + 2i\gamma_2\phi_2} &= \frac{1}{L} \sum_{x=-M-L}^{-M-1} \sum_{y=M+1}^{M+L} \int_{-\pi}^{\pi} \frac{d\phi_1}{2\pi} e^{i\phi_1(\gamma_1 + x + \gamma_2)} \delta_{y,-x-2\gamma_1} \\ &= \frac{1}{L} \sum_{x=-M-L}^{-M-1} \sum_{y=M+1}^{M+L} \delta_{x,-\gamma_1-\gamma_2} \delta_{y,\gamma_2-\gamma_1} \end{aligned}$$

as claimed. $\square$

## 5.2 Applying an encoded $C\theta$-gate

To implement the controlled phase gate between the mediator qubit and a computational qubit we use some facts about two-particle scattering on a long path. Recall that two indistinguishable particles of momentum $k_1$ and $k_2$ initially traveling toward each other will, after scattering, continue to travel as if no interaction occurred, except that the phase of the wave function is modified by the interaction. In general this phase depends on $k_1$ and $k_2$ (as well as the interaction $\mathcal{U}$ and the particle statistics). For us, $k_1 = -\pi/2$ and $k_2 = \pi/4$ (moving in opposite directions). We write $e^{i\theta}$ for the phase acquired at these momenta.

### 5.2.1 Momentum switch

In our scheme we design a subgraph that routes a computational particle and a mediator particle toward each other along a long path only when the two associated qubits are in state $|11\rangle$. This allows us to implement the two-qubit gate

$$\mathrm{C}\theta = \begin{pmatrix} 1 & 0 & 0 & 0 \\ 0 & 1 & 0 & 0 \\ 0 & 0 & 1 & 0 \\ 0 & 0 & 0 & e^{i\theta} \end{pmatrix}.$$

For some models $\mathrm{C}\theta = \mathrm{CP}$. We show in Section **??** that this holds in the Bose-Hubbard model (where the interaction term is $\mathcal{U}_{ij}(\hat{n}_i, \hat{n}_j) = (U/2)\delta_{i,j}\hat{n}_i(\hat{n}_i - 1)$) when the interaction strength is chosen to be $U = 2 + \sqrt{2}$, since in this case $e^{i\theta} = -i$. For nearest-neighbor interactions with fermions, with $\mathcal{U}_{ij}(\hat{n}_i, \hat{n}_j) = U\delta_{(i,j)\in E(G)}\hat{n}_i\hat{n}_j$, the choice $U = -2 - \sqrt{2}$ gives $e^{i\theta} = i$, so $\mathrm{CP} = (\mathrm{C}\theta)^3$. While tuning the interaction strength makes the CP gate easier to implement, almost any interaction between indistinguishable particles allows for universal computation. We can approximate the required CP gate by repeating the $\mathrm{C}\theta$ gate $a$ times, where $e^{ia\theta} \approx -i$ (which is possible for most values of $\theta$, assuming $\theta$ is known [**?**]).

Our strategy requires routing the particles onto a long path. This is done via a subgraph we call the *momentum switch*, as depicted in Figure **??**(a). The S-matrices for this graph at momenta $-\pi/4$ and $-\pi/2$ are

$$S_{\text{switch}}(-\pi/4) = \begin{pmatrix} 0 & 0 & e^{-i\pi/4} \\ 0 & -1 & 0 \\ e^{-i\pi/4} & 0 & 0 \end{pmatrix} \qquad S_{\text{switch}}(-\pi/2) = \begin{pmatrix} 1 & 0 & 0 \\ 0 & 0 & -1 \\ 0 & -1 & 0 \end{pmatrix}. \tag{5.18}$$

The momentum switch has perfect transmission between vertices 1 and 3 at momentum $-\pi/4$ and perfect transmission between vertices 2 and 3 at momentum $-\pi/2$. In other words, in the schematic shown in Figure **??**(a), the path a particle follows through the switch depends on its momentum. A particle with momentum $-\pi/2$ follows the double line, while a particle with momentum $-\pi/4$ follows the single line.

The graph used to implement the $\mathrm{C}\theta$ gate has the form shown in Figure **??**(b). We specify the number of vertices on each of the paths in Section **??**. To see why this graph implements a $\mathrm{C}\theta$ gate, consider the movement of two particles as they pass through the graph. If either particle begins in the state $|0_{\text{in}}\rangle$, then it travels along a path to the output without interacting with the second particle. When the computational particle (qubit $c$ in the figure) begins in the state $|1_{\text{in}}\rangle^c$, it is routed downward as it passes through the top momentum switch (following the single line). It travels down the vertical path and then is routed to the right (along the single line) as it passes through the bottom switch. Similarly, when the mediator particle begins in the state $|1_{\text{in}}\rangle^{\text{m}}$, it is routed upward (along the double line) through the vertical path at the bottom switch and then to the right (along the double line) at the top switch. If both particles begin in the state $|1_{\text{in}}\rangle$, then they interact on the vertical path. In this case, as the two particles move past each other, the wave function acquires a phase $e^{i\theta}$ arising from this interaction.

Note that timing is important: the wave packets of the two particles must be on the vertical path at the same time. We achieve this by choosing the number of vertices on each of the segments in the graph appropriately, taking into account the different propagation speeds of the two wave packets (see Section ?? for details).

The C$\theta$ gate is implemented using the graph shown in Figure ??. In this section we specify the logical input states, the logical output states, the distances $X$, $Z$, and $W$ appearing in the figure, and the total evolution time. With these choices, we show that a C$\theta$ gate is applied to the logical states at the end of the time evolution under the quantum walk Hamiltonian (up to error terms that are $\emptyset(L^{-1/4})$). The results of this section pertain to the two-particle Hamiltonian $H^{(2)}_{G'}$ for the graph $G'$ shown in Figure ??.

The logical input states are

$$|0_{\text{in}}\rangle^c = \frac{1}{\sqrt{L}} \sum_{x=M(-\frac{\pi}{4})+1}^{M(-\frac{\pi}{4})+L} e^{-i\frac{\pi}{4}x}|x,1\rangle \qquad |1_{\text{in}}\rangle^c = \frac{1}{\sqrt{L}} \sum_{x=M(-\frac{\pi}{4})+1}^{M(-\frac{\pi}{4})+L} e^{-i\frac{\pi}{4}x}|x,2\rangle$$

for the computational qubit and

$$|0_{\text{in}}\rangle^{\text{m}} = \frac{1}{\sqrt{L}} \sum_{y=M(-\frac{\pi}{2})+1}^{M(-\frac{\pi}{2})+L} e^{-i\frac{\pi}{2}y}|y,4\rangle \qquad |1_{\text{in}}\rangle^{\text{m}} = \frac{1}{\sqrt{L}} \sum_{y=M(-\frac{\pi}{2})+1}^{M(-\frac{\pi}{2})+L} e^{-i\frac{\pi}{2}y}|y,3\rangle$$

for the mediator qubit. We define symmetrized (or antisymmetrized) logical input states for $a, b \in \{0, 1\}$ as

$$\begin{aligned} |ab_{\text{in}}\rangle^{c,\text{m}} &= \text{Sym}(|a_{\text{in}}\rangle^c|b_{\text{in}}\rangle^{\text{m}}) \\ &= \frac{1}{\sqrt{2}}\left(|a_{\text{in}}\rangle^c|b_{\text{in}}\rangle^{\text{m}} \pm |b_{\text{in}}\rangle^{\text{m}}|a_{\text{in}}\rangle^c\right). \end{aligned}$$

We choose the distances $Z$, $X$, and $W$ from Figure ?? to be

$$Z = 4L \tag{5.19}$$

$$X = d_2 + L + M\left(-\frac{\pi}{2}\right) \tag{5.20}$$

$$W = d_1 + L + M\left(-\frac{\pi}{4}\right) \tag{5.21}$$

where

$$\begin{aligned} d_1 &= M\left(-\frac{\pi}{4}\right) \\ d_2 &= \left\lceil \frac{5L + 2d_1}{\sqrt{2}} - \frac{5}{2}L \right\rceil. \end{aligned}$$

With these choices, a wave packet moving with speed $\sqrt{2}$ travels a distance $Z + 2d_1 + L = 5L + 2d_1$ in approximately the same time that a wave packet moving with speed 2 takes to travel a distance $Z + 2d_2 + L = 5L + 2d_2$, since

$$t_{\text{II}} = \frac{5L + 2d_1}{\sqrt{2}} \approx \frac{5L + 2d_2}{2}.$$

We claim that the logical input states evolve into logical output states (defined below) with a phase of $e^{i\theta}$ applied in the case where both particles are in the logical state 1. Specifically,

$$\left\| e^{-iH_{G'}^{(2)} t_{\mathrm{II}}} |00_{\mathrm{in}}\rangle^{c,\mathrm{m}} - |00_{\mathrm{out}}\rangle^{c,\mathrm{m}} \right\| = \emptyset(L^{-1/4}) \tag{5.22}$$

$$\left\| e^{-iH_{G'}^{(2)} t_{\mathrm{II}}} |01_{\mathrm{in}}\rangle^{c,\mathrm{m}} - |01_{\mathrm{out}}\rangle^{c,\mathrm{m}} \right\| = \emptyset(L^{-1/4}) \tag{5.23}$$

$$\left\| e^{-iH_{G'}^{(2)} t_{\mathrm{II}}} |10_{\mathrm{in}}\rangle^{c,\mathrm{m}} - |10_{\mathrm{out}}\rangle^{c,\mathrm{m}} \right\| = \emptyset(L^{-1/4}) \tag{5.24}$$

$$\left\| e^{-iH_{G'}^{(2)} t_{\mathrm{II}}} |11_{\mathrm{in}}\rangle^{c,\mathrm{m}} - e^{i\theta}|11_{\mathrm{out}}\rangle^{c,\mathrm{m}} \right\| = \emptyset(L^{-1/4}) \tag{5.25}$$

where, letting $Q_1 = 2W + Z + 4 - M(-\pi/4) - L$ and $Q_2 = 2X + Z + 6 - M(-\pi/2) - L$,

$$|0_{\mathrm{out}}\rangle^c = \frac{e^{-it_{\mathrm{II}}\sqrt{2}}}{\sqrt{L}} \sum_{x=Q_1+1}^{Q_1+L} e^{-i\frac{\pi}{4}x}|x,1\rangle \qquad |1_{\mathrm{out}}\rangle^c = \frac{e^{-it_{\mathrm{II}}\sqrt{2}}}{\sqrt{L}} \sum_{x=Q_1+1}^{Q_1+L} e^{-i\frac{\pi}{4}x}|x,2\rangle$$

$$|0_{\mathrm{out}}\rangle^{\mathrm{m}} = \frac{1}{\sqrt{L}} \sum_{y=Q_2+1}^{Q_2+L} e^{-i\frac{\pi}{2}y}|y,4\rangle \qquad |1_{\mathrm{out}}\rangle^{\mathrm{m}} = \frac{1}{\sqrt{L}} \sum_{y=Q_2+1}^{Q_2+L} e^{-i\frac{\pi}{2}y}|y,3\rangle$$

and $|ab_{\mathrm{out}}\rangle^{c,\mathrm{m}} = \mathrm{Sym}\left(|a_{\mathrm{out}}\rangle^c |b_{\mathrm{out}}\rangle^{\mathrm{m}}\right)$.

Note that the input states are wave packets located a distance $M(k)$ from the ends of the input paths on the left-hand side of the graph in Figure **??**. Similarly, the output logical states are wave packets located a distance $M(k)$ from the ends of the output paths on the right-hand side.

The first three bounds (5.22), (5.23), and (5.24) are relatively easy to show, since in each case the two particles are supported on disconnected subgraphs and therefore do not interact. In each of these three cases we can simply analyze the propagation of the one-particle starting states through the graph. The symmetrized (or antisymmetrized) starting state then evolves into the symmetrized (or antisymmetrized) tensor product of the two output states.

For example, with input state $|00_{\mathrm{in}}\rangle^{c,\mathrm{m}}$, the evolution of the particle with momentum $-\pi/4$ occurs only on the top path and the evolution of the particle with momentum $-\pi/2$ occurs only on the bottom path. Starting from the initial state $|0_{\mathrm{in}}\rangle^c$ and evolving for time $t_{\mathrm{II}}$ with the single-particle Hamiltonian for the top path, we obtain the final state

$$|0_{\mathrm{out}}\rangle^c + \emptyset(L^{-1/4})$$

using the method of Section **??**. Similarly, starting from the initial state $|0_{\mathrm{in}}\rangle^{\mathrm{m}}$ and evolving for time $t_{\mathrm{II}}$ with the single-particle Hamiltonian for the bottom path of the graph we obtain the final state

$$|0_{\mathrm{out}}\rangle^{\mathrm{m}} + \emptyset(L^{-1/4}).$$

Putting these bounds together we get the bound (5.22).

In the case where the input state is $|10_{\mathrm{in}}\rangle^{c,\mathrm{m}}$ (or $|01_{\mathrm{in}}\rangle^{c,\mathrm{m}}$) the single-particle evolution for the particle with momentum $-\pi/4$ (or $-\pi/2$) is slightly more complicated, as in this case the particle moves through the momentum switches and the vertical path. The S-matrix of the momentum switch at the relevant momenta is given by equation (5.18). At momentum $-\pi/4$, the momentum switch has the same S-matrix as a path with 4 vertices (including the input and output vertices). At momentum $-\pi/2$, it has the same S-matrix as a path with 5 vertices (including input and output vertices). Note that our labeling of vertices on the output paths (in Figure **??**) takes this into account. The first vertices on the output paths connected to the momentum switches are labeled $(X + Z + 7, 3)$ and $(W + Z + 5, 2)$, respectively, reflecting the fact that a particle with momentum $-\pi/4$ has traveled $W$ vertices on the input path, $Z$ vertices through the middle segment, and has effectively traveled an additional 4 vertices inside the two switches. Similarly, a particle with momentum $-\pi/2$ effectively sees an additional 6 vertices from the two momentum switches.

To get the bound (5.24) we have to analyze the single-particle evolution for the computational particle initialized in the state $|1_{\text{in}}\rangle^c$. We claim that, after time $t_{\text{II}}$, the time-evolved state is

$$|1_{\text{out}}\rangle^c + \emptyset(L^{-1/4}).$$

It is easy to see why this should be the case in light of our discussion above: when scattering at momentum $-\pi/4$, the graph in Figure **??** is equivalent to one where each momentum switch is replaced by a path with 2 internal vertices connecting the relevant input/output vertices.

To make this precise, we use the method described in Section **??** for analyzing scattering through sequences of overlapping graphs using the truncation lemma. Here we should choose subgraphs $G_1$ and $G_2$ of the graph $G'$ in Figure **??** that overlap on the vertical path but where each subgraph contains only one of the momentum switches. A convenient choice is to take $G_1$ to be the subgraph containing the top switch and the paths connected to it (the vertices $(1, 2), \ldots, (W, 2)$, $(1, 5), \ldots, (Z, 5)$ and $(X+Z+7, 3), \ldots, (2X+Z+6, 3)$). Similarly, choose $G_2$ to be the bottom switch along with the three paths connected to it. The graphs $G_1$ and $G_2$ both contain the vertices $(1, 5), \ldots, (Z, 5)$ along the vertical path. Break up the total evolution time into two intervals $[0, t_\alpha]$ and $[t_\alpha, t_{\text{II}}]$. Choose $t_\alpha$ so that the wave packet, evolved for this time with $H^{(1)}_{G_1}$, travels through the top switch and ends up a distance $\Theta(L)$ from each switch, partway along the vertical path (up to terms bounded as $\emptyset(L^{-1/4})$, as in Section **??**). With this choice, the single-particle evolution with the Hamiltonian for the full graph is approximated by the evolution with $H^{(1)}_{G_1}$ on this time interval (see Section **??**). At time $t_\alpha$, the particle is outgoing with respect to scattering from the graph $G_1$, but incoming with respect to $G_2$. On the interval $[t_\alpha, t_{\text{II}}]$ the time evolution is approximated by evolving the state with $H^{(1)}_{G_2}$. During this time interval the particle travels through the bottom switch onto the final path, and at $t_{\text{II}}$ is a distance $M(-\pi/4)$ from the endpoint of the output path. Both switches have the same S-matrix (at momentum $-\pi/4$) as a path of length 4, so this analysis gives the output state $|10_{\text{out}}\rangle^{c,\text{m}}$ up to terms bounded as $\emptyset(L^{-1/4})$, establishing (5.24). For the bound (5.23), we apply a similar analysis to the trajectory of the mediator particle.

The case where the input state is $|11_{\text{in}}\rangle^{c,\text{m}}$ is more involved but proceeds similarly. In this case, to analyze the time evolution we divide the time interval $[0, t_{\text{II}}]$ into three segments $[0, t_A]$, $[t_A, t_B]$, and $[t_B, t_{\text{II}}]$. For each of these three time intervals we choose a subgraph $G_A$, $G_B$, $G_C$ of the graph $G'$ in Figure **??** and we approximate the time evolution by evolving with the Hamiltonian on the associated subgraph. We then use the truncation lemma to show that, on each time interval, the evolution generated by the Hamiltonian for the appropriate subgraph approximates the evolution generated by the full Hamiltonian, with error $\emptyset(L^{-1/4})$. Up to these error terms, at times $t = 0$, $t = t_A$, $t = t_B$, and $t = t_{\text{II}}$ the time-evolved state

$$e^{-iH^{(2)}_{G'}t}|11_{\text{in}}\rangle^{c,\text{m}}$$

has both particles in square wave packet states, each with support only on $L$ vertices of the graph, as depicted in Figure **??**.

We take $G_A$ to be the subgraph obtained from $G'$ by removing the vertices labeled $(\lceil 1.85L\rceil, 5), \ldots, (\lceil 1.90L\rceil, 5)$ in the vertical path. By removing this interval of consecutive vertices, we disconnect the graph into two components where the initial state $|11_{\text{in}}\rangle^{c,\text{m}}$ has one particle in each component. This could be achieved by removing a single vertex, but instead we remove an interval of approximately $0.05L$ vertices to separate the components of $G_A$ by more than the interaction range $C$ (for sufficiently large $L$), simplifying our use of the truncation lemma.

We choose $t_A = 3L/2$. Consider the time evolution of the initial state $|11_{\text{in}}\rangle^{c,\text{m}}$ with the two-particle Hamiltonian $H^{(2)}_{G_A}$ for time $t_A$. The states $|1_{\text{in}}\rangle^{c}$ and $|1_{\text{in}}\rangle^{\text{m}}$ are supported on disconnected components of the graph $G_A$, so we can analyze the time evolution of the state $|11_{\text{in}}\rangle^{c,\text{m}}$ under $H^{(2)}_{G_A}$ by analyzing two single-particle problems, using the results of Section **??** for each particle. During the interval $[0, t_A]$, each particle passes through one switch, ending up a distance $\Theta(L)$ from the switch that it passed through and $\Theta(L)$ from the vertices that have been removed, as shown in Figure **??**(b) (with error at most $\emptyset(L^{-1/4})$). Up to these error terms, the support of each particle remains at least $N_0 = \Theta(L)$ vertices from the endpoints of the graph, so we can apply the truncation lemma using $H = H^{(2)}_{G'}$, $W = \tilde{H} = H^{(2)}_{G_A}$, $T = t_{\text{A}}$, and $\delta = \emptyset(L^{-1/4})$. Here $P$ is the projector onto states where both particles are located at vertices of $G_A$. We have $PH^{(2)}_{G'}P = H^{(2)}_{G_A}$ since the number of vertices in the removed segment is greater than the interaction range $C$. Applying the truncation lemma gives

$$\left\| e^{-iH^{(2)}_{G_A}t_A}|11_{\text{in}}\rangle^{c,\text{m}} - e^{-iH^{(2)}_{G'}t_A}|11_{\text{in}}\rangle^{c,\text{m}} \right\| = \emptyset(L^{-1/4}).$$

We approximate the evolution on the interval $[t_A, t_B]$ using the two-particle Hamiltonian $H^{(2)}_{G_B}$, where $G_B$ is the vertical path $(1, 5), \ldots, (Z, 5)$. Using the result of Section **??**, we know that (up to terms bounded as $\emptyset(L^{-1/4})$) the wave packets move with their respective speeds and acquire a phase of $e^{i\theta}$ as they pass each other. We choose $t_B = 5L/2$ so that during the evolution the wave packets have no support on vertices within a distance $\Theta(L)$ from the endpoints of the vertical segment where the graph has been truncated (again up to terms bounded as $\emptyset(L^{-1/4})$). Using $H^{(2)}_{G_B}$ (rather than $H^{(2)}_{G'}$) to evolve the state on this interval, we incur errors bounded as $\emptyset(L^{-1/4})$ (using the truncation lemma with $N_0 = \Theta(L)$, $W = \tilde{H} = H^{(2)}_{G_B}$, $H = H^{(2)}_{G'}$, and $\delta = \emptyset(L^{-1/4})$).

We choose $G_C = G_A$; in the final interval $[t_B, t_{\text{II}}]$ we evolve using the Hamiltonian $H^{(2)}_{G_A}$ again, and we use the truncation lemma as we did for the first interval. The initial state is approximated by two wave packets supported on disconnected sections of $G_A$ and the evolution of this initial state reduces to two single-particle scattering problems. During the interval $[t_B, t_{\mathrm{II}}]$, each particle passes through a second switch, and at time $t_{\mathrm{II}}$ is a distance $M(k)$ from the end of the appropriate output path.

Our analysis shows that for the input state $|11_{\mathrm{in}}\rangle^{c,\mathrm{m}}$ the only effect of the interaction is to alter the global phase of the final state by a factor of $e^{i\theta}$ relative to the case where no interaction is present, up to error terms bounded as $\emptyset(L^{-1/4})$. This establishes equation (5.25). In Figure **??** we illustrate the movement of the two wave packets through the graph when the initial state is $|11_{\mathrm{in}}\rangle^{c,\mathrm{m}}$.

## 5.3 Universal Computation

### 5.3.1 Two-qubit blocks

### 5.3.2 Combining blocks

## 5.4 Improvements and Modifications

What about long-range interactions, but where the interactions die off? Additionally, what about error correction?

# Chapter 6

# Ground energy of quantum walk

To get some flavor for QMA-completeness results.

Now that we have shown the universality of these Quantum Walk Hamiltonians via time evolution, we might want to ask related computational questions about these systems. In particular, once the computational universality of a system is shown, people often ask about the related ground energy problem. The reason for this is that many of these systems that allow for universal computation via time evolution also allow for the encoding of a computation in the ground space, which along with some energy penalties, allow one to show that the ground energy problem is QMA-hard.

The point of this chapter is to give a decent introduction to the flavor of QMA-hardness proofs, as well as providing a QMA-complete problem that might be more accessible to classical computer scientists.

## 6.1 The ground-energy problem

Essentially, we know that the single-particle quantum walk is governed by the adjacency matrix of the underlying graph. In particular, the Hamiltonian is exactly equal to the adjacency matrix, and thus asking questions about the ground energy of a single-particle quantum walk is simply asking a question about the smallest eigenvalue of a particular adjacency matrix.

However, the Hilbert space on which the quantum walk acts is necessarily exponential in size, with efficiently computable matrix entries. As such, this is a question about very specific types of matrices.

**Problem 1** ($d$-sparse graph eigenvalue problem)**.** Given a $d$-sparse, row-computable graph $G$, and two constants $a < b$, is the smallest eigenvalue of $A(G)$ below $a$ or above $b$, with the guarantee that one of these cases occur.

While this problem is definitely inspired from quantum walks, it actually makes no reference to quantum mechanics.

### 6.1.1 Containment in QMA

The proof that this problem is in QMAfollows many other such Hamiltonian problems. In particular, this proof strategy works for any system in which we can evolve according to a particular Hamiltonian.

The main idea is to be given a particular state, and use phase estimation to determine the energy of the given state, up to some error. In the case that the smallest eigenvalue of the system is below $a$, the prover can provide the corresponding eigenvector encoded in a quantum state. The phase estimation algorithm will then (with high probability) find this eigenvalue, and the system will accept. If the smallest eigenvalue is above $b$, then no matter what state the prover provides, the phase estimation algorithm will project onto one of the eigenstates and determine the corresponding eigenvalue, which will necessarily be above $b$.

More concretely, we have

## 6.2 QMA-hardness

The main way that this works is that we will use the well known Kitaev Hamiltonian, with some particular changes so that we get taken to a Hamiltonian of a particular form. Once we have that form, we can easily see that the result we want.

### 6.2.1 Kitaev Hamiltonian

With the definition of the class QMA, the requirement is that for each input there exists some quantum circuit and some particular input state that the circuit either accepts or rejects. When attempting to prove that a particular Hamiltonian has a similar computational power, we need to construct a "circuit-to-Hamiltionian" map. The predominant (and really only) such map is the so-called Kitaev-Hamiltonian.

In this mapping, we attempt to encode the computation into the ground space of the Hamiltonian, in a similar manner to how the proof that 3-SAT is NP-Hard encodes the entire computation of a nondeterministic Turing Machine. [**TO DO:** *NP-hardness of 3-Sat reference*] However, we run into a problem on how to insure that neighboring time steps are only seperated by a single local unitary. In the classical case we can write down the entire state of the system at each timestep, or else only write down the changes that occur at each time step. In the first case we run into a problem in that information is copied between time steps, which is impossible for a general state by the no-cloning theorem [**TO DO:** *reference no-cloning*] while the second case quickly becomes infeasible as the changes to the quantum state might effect many basis states.

Kitaev worked around this problem by enlarging the Hilbert space on which the circuit acts, by having both a clock and a state register. The computation of the system was then encoded as an entangled state between these two registers. In this way, by having a projection into those states that evolve correctly for a particular time step, we can have a local check for the correctness of evolution.

In particular, if a given circuit $\mathcal{C}$ acts on $\mathbb{C}^{2^m}$ and can be written as $\mathcal{C} = U_T U_{T-1} \cdots U_1$, then the Kitaev Hamiltonian $H_{\mathcal{C}}$ acts on the Hilbert space $\mathbb{C}^{2^m} \otimes \mathbb{C}^{T+1}$, and can be written as

$$H_{\mathcal{C}} = \sum_{t=0}^{T-1} \left(\mathbb{I}_{\mathbb{C}^{2^m}} \otimes |\, t\,\rangle - U_{t+1} \otimes |\, t+1\,\rangle\right)\left(\mathbb{I}_{\mathbb{C}^{2^m}} \otimes \langle\, t\,| - U_{t+1}^{\dagger} \otimes \langle\, t+1\,|\right) = \sum_{t=0}^{T-1} H_t \tag{6.1}$$

Note that each term $H_t$ is a projector off those states of the form

$$|\,\psi\,\rangle \otimes |\,t\,\rangle + U_{t+1}|\,\psi\,\rangle \otimes |\,t+1\,\rangle. \tag{6.2}$$

Hence, we have that the ground state of $H_C$ corresponds to the history states:

$$|\,\psi_{\text{hist}}\,\rangle = \sum_{t=0}^{T} U_t U_{t-1} \cdots U_1 |\,\psi\,\rangle \otimes |\,t\,\rangle. \tag{6.3}$$

These states encode the computation, as for a given initial state $|\,\psi\,\rangle$, the projection onto the time register gives the state of the computation at time $t$. Note that the energy gap for this Hamiltonian is exactly $1 - \cos(\pi/T)$, as the Hamiltonian is unitarily equivalent to a quantum walk on a line of length $T$.

With this mapping corresponding to a particular circuit, we can then force the initial state to have a particular form by adding in projectors tensored with a projection onto the $|\,t = 0\rangle$ state, with a similar projection for the requisite form of the final state. Putting everything together we then have a log-local Hamiltonian that will have a polynomial gap depending on whether the initial circuit accepted or rejected.

One can then show that this Hamiltonian will have a low energy eigenvector if and only if the corresponding circuit $\mathcal{C}$ has an accepting input.

### 6.2.2 Transformation to Adjacency Matrix

While the above prescription works well for the conversion to local-Hamiltonians in the general case, in the situation we are interested in we want all of the non-zero matrix elements to be the same value. As the matrix elements of $H_{\mathcal{C}}$ are related to the matrix values of the unitaries involved in the circuit $\mathcal{C}$, we thus want to force the matrix values of $\mathcal{C}$ to all be of the same form.

To enforce this, we suppose $\mathcal{C}$ implements a unitary

$$U_{\mathcal{C}_x} = U_M \ldots U_2 U_1 \tag{6.4}$$

where each $U_i$ acts as

$$\mathcal{G} = \left\{H, HT, (HT)^{\dagger}, (H \otimes \mathbb{I})\,\text{CNOT}\right\} \tag{6.5}$$

on some qubits, and the identity on the rest.

Note that this gate set is universal, as we can easily simulate the gate set $\{H, T, \text{CNOT}\}$ with gates from $\mathcal{G}$ since $H^2 = \mathbb{I}$ and we can thus cancel the $H$ terms before the interesting portion of the gates. Further, each non-zero matrix element of these unitaries has norm $2^{-1/2}$, as we wanted.

However, when we look at one of the local terms in the Hamiltonian, we find that not all of the matrix elements have the same norm. In particular, we find that

$$H_t = \left(\mathbb{I}_{\mathbb{C}^{2^m}} \otimes |\,t\,\rangle - U_{t+1} \otimes |\,t+1\,\rangle\right)\left(\mathbb{I}_{\mathbb{C}^{2^m}} \otimes \langle\,t\,| - U_{t+1}^{\dagger} \otimes \langle\,t+1\,|\right) \tag{6.6}$$

$$= \mathbb{I}_{\mathbb{C}^{2^m}} \otimes \left(|\,t\,\rangle\langle\,t\,| + |\,t+1\,\rangle\langle\,t+1\,|\right) - \left(U_{t+1} \otimes |\,t+1\,\rangle\langle\,t\,| + U_{t+1}^{\dagger} \otimes |\,t\,\rangle\langle\,t+1\,|\right). \tag{6.7}$$

While each off-diagonal term is either zero or has norm $2^{-1/2}$ in (6.7), the diagonal terms have norm 1. When each term is summed, we almost have that the sum of the diagonal terms are proportional to the identity, but unfortunately the boundary terms (with $t = 0$ or $t = T$) are only involved in one unitary. However, this problem can be avoided by having circular time, in which we both compute and uncompute the comptutation. With this, each timestep is involved in exactly two local terms, and thus the diagonal term is proportional to the identity.

With this, it will be convenient to consider

$$U_{\mathcal{C}}^{\dagger} U_{\mathcal{C}} = W_{2M} \dots W_2 W_1 \tag{6.8}$$

where

$$W_t = \begin{cases} U_t & 1 \le t \le M \\ U_{2M+1-t}^{\dagger} & M+1 \le t \le 2M. \end{cases} \tag{6.9}$$

As in Section 6.2.1 we start with a version of the Feynman-Kitaev Hamiltonian (with a different norm) [?, ?] acting on the Hilbert space $\mathcal{H}_{\text{comp}} \otimes \mathcal{H}_{\text{clock}}$ where $\mathcal{H}_{\text{comp}} = (\mathbb{C}^2)^{\otimes m}$ is an $m$-qubit computational register and $\mathcal{H}_{\text{clock}} = \mathbb{C}^{2M}$ is a $2M$-level register with periodic boundary conditions (i.e., we let $|2M+1\rangle = |1\rangle$). However, we then subtract a term proportional to the identity, which yields the Hamiltonian

$$H_{\mathcal{C}} = -\sqrt{2} \sum_{t=1}^{2M} \left( W_t^{\dagger} \otimes |t\rangle\langle t+1| + W_t \otimes |t+1\rangle\langle t| \right). \tag{6.10}$$

Note that

$$V^{\dagger} H_{\mathcal{C}} V = -\sqrt{2} \sum_{t=1}^{2M} \left( \mathbb{I} \otimes |t\rangle\langle t+1| + \mathbb{I} \otimes |t+1\rangle\langle t| \right) \tag{6.11}$$

where

$$V = \sum_{t=1}^{2M} \left( \prod_{j=t-1}^{1} W_j \right) \otimes |t\rangle\langle t| \tag{6.12}$$

and $W_0 = 1$. Since $V$ is unitary, the eigenvalues of $H_x$ are the same as the eigenvalues of (6.11), namely

$$-2\sqrt{2}\cos\left(\frac{\pi \ell}{M}\right) \tag{6.13}$$

for $\ell = 0, \dots, 2M-1$. The ground energy of (6.11) is $-2\sqrt{2}$ and its ground space is spanned by

$$|\phi\rangle \frac{1}{\sqrt{2M}} \sum_{j=1}^{2M} |t\rangle, \quad |\phi\rangle \in \Lambda \tag{6.14}$$

where $\Lambda$ is any orthonormal basis for $\mathcal{H}_{\text{comp}}$. A basis for the ground space of $H_x$ is therefore

$$V\left(|\phi\rangle\frac{1}{\sqrt{2M}}\sum_{j=1}^{2M}|t\rangle\right)=\frac{1}{\sqrt{2M}}\sum_{t=1}^{2M}W_{t-1}W_{t-2}\dots W_1|\phi\rangle|t\rangle \tag{6.15}$$

where $|\phi\rangle\in\Lambda$. The first excited energy of $H_x$ is

$$\eta=-2\sqrt{2}\cos\left(\frac{\pi}{M}\right) \tag{6.16}$$

and the gap between ground and first excited energies is lower bounded as

$$\eta+2\sqrt{2}\geq\sqrt{2}\frac{\pi^2}{M^2} \tag{6.17}$$

(using the fact that $1-\cos(x)\leq\frac{x^2}{2}$).

The universal set $\mathcal{G}$ is chosen so that each gate has nonzero entries that are integer powers of $\omega=e^{i\frac{\pi}{4}}$. Correspondingly, the nonzero standard basis matrix elements of $H_{\mathcal{C}}$ are also integer powers of $\omega=e^{i\frac{\pi}{4}}$. We consider the $8\times 8$ shift operator

$$S=\sum_{j=0}^{7}|j+1 \bmod 8\rangle\langle j| \tag{6.18}$$

and note that $\omega$ is an eigenvalue of $S$ with eigenvector

$$|\omega\rangle=\frac{1}{\sqrt{8}}\sum_{j=0}^{7}\omega^{-j}|j\rangle. \tag{6.19}$$

We modify $H_{\mathcal{C}}$ as follows. For each operator $-\sqrt{2}H$, $-\sqrt{2}HT$, $-\sqrt{2}(HT)^\dagger$, or $-\sqrt{2}\,(H\otimes\mathbb{I})\,\text{CNOT}$ appearing in equation (6.10), define another operator that acts on $\mathbb{C}^2\otimes\mathbb{C}^8$ or $\mathbb{C}^4\otimes\mathbb{C}^8$ (as appropriate) by replacing nonzero matrix elements with powers of the operator $S$:

$$\omega^k\mapsto S^k.$$

Matrix elements that are zero are mapped to the $8\times 8$ all-zeroes matrix. Write $B(W)$ for the operators obtained by making this replacement, e.g.,

$$-\sqrt{2}HT=\begin{pmatrix}\omega^4 & \omega^5\\ \omega^4 & \omega\end{pmatrix}\mapsto B(HT)=\begin{pmatrix}S^4 & S^5\\ S^4 & S\end{pmatrix}.$$

Adjoining an 8-level ancilla as a third register and making this replacement in equation (**??**) gives

$$H_{\text{prop}}=\sum_{t=1}^{2M}\left(B(W_t)_{13}^\dagger\otimes|t\rangle\langle t+1|_2+B(W_t)_{13}\otimes|t+1\rangle\langle t|_2\right) \tag{6.20}$$

which is a symmetric 0-1 matrix (the subscripts indicate which registers the operators act on). Note that $H_{\text{prop}}$ commutes with $S$ (acting on the 8-level ancilla) and therefore is block diagonal with eight sectors. In the sector where $S$ has eigenvalue $\omega$, $H_{\text{prop}}$ is identical to the Hamiltonian $H_{\mathcal{C}}$ that we started with (see equation (6.10)). There is also a sector (where $S$ has eigenvalue $\omega^*$) where the Hamiltonian is the element-wise complex conjugate of $H_{\mathcal{C}}$. We will add a term to $H_{\text{prop}}$ that introduces an energy penalty for states in any of the other six sectors, ensuring that none of these states lie in the ground space.

To see what kind of energy penalty is needed, we lower bound the eigenvalues of $H_{\text{prop}}$. Note that for each $W \in \mathcal{G}$, $B(W)$ contains at most 2 ones in each row or column. Looking at equation (6.20) and using this fact, we see that each row and each column of $H_{\text{prop}}$ contains at most four ones (with the remaining entries all zero). Therefore $\|H_{\text{prop}}\| \leq 4$, so every eigenvalue of $H_{\text{prop}}$ is at least $-4$.

The matrix $A_x$ associated with the circuit $\mathcal{C}_x$ acts on the Hilbert space

$$\mathcal{H}_{\text{comp}} \otimes \mathcal{H}_{\text{clock}} \otimes \mathcal{H}_{\text{anc}} \tag{6.21}$$

where $\mathcal{H}_{\text{anc}} = \mathbb{C}^8$ holds the 8-level ancilla. We define

$$A_x = H_{\text{prop}} + H_{\text{penalty}} + H_{\text{input}} + H_{\text{output}} \tag{6.22}$$

where

$$H_{\text{penalty}} = \mathbb{I} \otimes \mathbb{I} \otimes \left(S^3 + S^4 + S^5\right) \tag{6.23}$$

is the penalty ensuring that the ancilla register holds either $|\omega\rangle$ or $|\omega^*\rangle$ and the terms

$$H_{\text{input}} = \sum_{j=n_{\text{input}}+1}^{n} |1\rangle\langle 1|_j \otimes |1\rangle\langle 1| \otimes \mathbb{I}$$
$$H_{\text{output}} = |0\rangle\langle 0|_{\text{output}} \otimes |M+1\rangle\langle M+1| \otimes \mathbb{I}$$

ensure that the ancilla qubits are initialized in the state $|0\rangle$ when $t = 1$ and that the output qubit is in the state $|1\rangle\langle 1|$ when the circuit $\mathcal{C}_x$ has been applied (i.e., at time $t = M + 1$). Observe that $A_x$ is a symmetric 0-1 matrix.

Now consider the ground space of the first two terms $H_{\text{prop}} + H_{\text{penalty}}$ in (6.22). Note that $[H_{\text{prop}}, H_{\text{penalty}}] = 0$, so these operators can be simultaneously diagonalized. Furthermore, $H_{\text{penalty}}$ has smallest eigenvalue $-1-\sqrt{2}$, with eigenspace spanned by $|\omega\rangle$ and $|\omega^*\rangle$. One can also easily confirm that the first excited energy of $H_{\text{penalty}}$ is $-1$.

The ground space of $H_{\text{prop}} + H_{\text{penalty}}$ lives in the sector where $H_{\text{penalty}}$ has minimal eigenvalue $-1-\sqrt{2}$. To see this, note that within this sector $H_{\text{prop}}$ has the same eigenvalues as $H_x$, and therefore has lowest eigenvalue $-2\sqrt{2}$. The minimum eigenvalue $e_1$ of $H_{\text{prop}} + H_{\text{penalty}}$ in this sector is

$$e_1 = -2\sqrt{2} + \left(-1 - \sqrt{2}\right) = -1 - 3\sqrt{2} = -5.24\ldots, \tag{6.24}$$

whereas in any other sector $H_{\text{penalty}}$ has eigenvalue at least $-1$ and (using the fact that $H_{\text{prop}} \geq -4$) the minimum eigenvalue of $H_{\text{prop}} + H_{\text{penalty}}$ is at least $-5$. Thus, an orthonormal basis for the ground space of $H_{\text{prop}} + H_{\text{penalty}}$ is furnished by the states

$$\frac{1}{\sqrt{2M}} \sum_{t=1}^{2M} W_{t-1} W_{t-2} \ldots W_1 |\phi\rangle |t\rangle |\omega\rangle \tag{6.25}$$

$$\frac{1}{\sqrt{2M}} \sum_{t=1}^{2M} (W_{t-1} W_{t-2} \ldots W_1)^* |\phi^*\rangle |t\rangle |\omega^*\rangle \tag{6.26}$$

where $|\phi\rangle$ ranges over the basis $\Lambda$ for $\mathcal{H}_{\text{comp}}$ and $*$ denotes (elementwise) complex conjugation.

At this point, we then have a symmetric 0-1 matrix whose ground-space is spanned by history states. While we have not yet shown that determining the ground energy of this matrix is QMA-hard, this graph is the result of our circuit-to-graph mapping.

### 6.2.3 Upper bound on the smallest eigenvalue for yes instances

Suppose $x$ is a yes instance; then there exists some $n_{\text{input}}$-qubit state $|\psi_{\text{input}}\rangle$ satisfying $\text{AP}\left(\mathcal{C}_x, |\psi_{\text{input}}\rangle\right) \geq 1 - \frac{1}{2^{|x|}}$. Let

$$|\text{wit}\rangle = \frac{1}{\sqrt{2M}} \sum_{t=1}^{2M} W_{t-1} W_{t-2} \ldots W_1 \left(|\psi_{\text{input}}\rangle |0\rangle^{\otimes n - n_{\text{input}}}\right) |t\rangle |\omega\rangle \tag{6.27}$$

and note that this state is in the $e_1$-energy ground space of $H_{\text{prop}} + H_{\text{penalty}}$ (since it has the form (6.25)). One can also directly verify that $|\text{wit}\rangle$ has zero energy for $H_{\text{input}}$. Thus

$$\begin{aligned}
\langle \text{wit}|A_x|\text{wit}\rangle &= e_1 + \langle \text{wit}|H_{\text{output}}|\text{wit}\rangle \\
&= e_1 + \frac{1}{2M} \langle \psi_{\text{input}}|\langle 0|^{\otimes n - n_{\text{input}}} U_{\mathcal{C}_x}^{\dagger} |0\rangle\langle 0|_{\text{output}} U_{\mathcal{C}_x} |\psi_{\text{input}}\rangle |0\rangle^{\otimes n - n_{\text{input}}} \\
&= e_1 + \frac{1}{2M} \left(1 - \text{AP}(\mathcal{C}_x, |\psi_{\text{input}}\rangle)\right) \\
&\leq e_1 + \frac{1}{2M} \frac{1}{2^{|x|}}.
\end{aligned}$$

### 6.2.4 Lower bound on the smallest eigenvalue for no instances

Now suppose $x$ is a no instance. Then the verification circuit $\mathcal{C}_x$ has acceptance probability $\text{AP}\left(\mathcal{C}_x, |\psi\rangle\right) \leq \frac{1}{3}$ for all $n_{\text{input}}$-qubit input states $|\psi\rangle$.

We backtrack slightly to obtain bounds on the eigenvalue gaps of the Hamiltonians $H_{\text{prop}}+H_{\text{penalty}}$ and $H_{\text{prop}} + H_{\text{penalty}} + H_{\text{input}}$. We begin by showing that the energy gap of $H_{\text{prop}} + H_{\text{penalty}}$ is at least an inverse polynomial function of $M$. Subtracting a constant equal to the ground energy times the identity matrix sets the smallest eigenvalue to zero, and the smallest nonzero eigenvalue satisfies

$$\gamma(H_{\text{prop}} + H_{\text{penalty}} - e_1 \cdot \mathbb{I}) \geq \min\left\{\sqrt{2}\frac{\pi^2}{M^2}, -5 - e_1\right\} \geq \frac{1}{5M^2}. \tag{6.28}$$

since $-5 - e_1 \approx 0.24\ldots > \frac{1}{5}$. The first inequality above follows from the fact that every eigenvalue of $H_{\text{prop}}$ in the range $[e_1, -5)$ is also an eigenvalue of $H_x$ (as discussed above) and the bound (6.17) on the energy gap of $H_x$.

Now use the Nullspace Projection Lemma (Lemma **??**) with

$$H_A = H_{\text{prop}} + H_{\text{penalty}} - e_1 \cdot \mathbb{I} \qquad H_B = H_{\text{input}}. \tag{6.29}$$

Note that $H_A$ and $H_B$ are positive semidefinite. Let $S_A$ be the ground space of $H_A$ and consider the restriction $H_B|_{S_A}$. Here it is convenient to use the basis for $S_A$ given by (6.25) and (6.26) with $|\phi\rangle$ ranging over the computational basis states of $n$ qubits. In this basis, $H_B|_{S_A}$ is diagonal with all diagonal entries equal to $\frac{1}{2M}$ times an integer, so $\gamma(H_B|_{S_A}) \geq \frac{1}{2M}$. We also have $\gamma(H_A) \geq \frac{1}{5M^2}$ from equation (6.28), and clearly $\|H_B\| \leq n$. Thus Lemma **??** gives

$$\gamma(H_{\text{prop}} + H_{\text{penalty}} + H_{\text{input}} - e_1 \cdot \mathbb{I}) \geq \frac{\left(\frac{1}{5M^2}\right)\left(\frac{1}{2M}\right)}{\frac{1}{5M^2} + \frac{1}{2M} + n} \geq \frac{1}{10M^3\,(1+n)} \geq \frac{1}{20M^3 n}. \tag{6.30}$$

Now consider adding the final term $H_{\text{output}}$. We use Lemma **??** again, now setting

$$H_A = H_{\text{prop}} + H_{\text{penalty}} + H_{\text{input}} - e_1 \cdot \mathbb{I} \qquad H_B = H_{\text{output}}. \tag{6.31}$$

Let $S_A$ be the ground space of $H_A$. Note that it is spanned by states of the form (6.25) and (6.26) where $|\phi\rangle = |\psi\rangle|0\rangle^{\otimes n - n_{\text{input}}}$ and $|\psi\rangle$ ranges over any orthonormal basis of the $n_{\text{input}}$-qubit input register. The restriction $H_B|_{S_A}$ is block diagonal, with one block for states of the form

$$\frac{1}{\sqrt{2M}} \sum_{t=1}^{2M} W_{t-1}W_{t-2}\ldots W_1 \left(|\psi\rangle|0\rangle^{\otimes n-n_{\text{input}}}\right)|t\rangle|\omega\rangle \tag{6.32}$$

and another block for states of the form

$$\frac{1}{\sqrt{2M}} \sum_{t=1}^{2M} (W_{t-1}W_{t-2}\ldots W_1)^* \left(|\psi\rangle^*|0\rangle^{\otimes n-n_{\text{input}}}\right)|t\rangle|\omega^*\rangle. \tag{6.33}$$

We now show that the minimum eigenvalue of $H_B|_{S_A}$ is nonzero, and we lower bound it. We consider the two blocks separately. By linearity, every state in the first block can be written in the form (6.32) for some state $|\psi\rangle$. Thus the minimum eigenvalue within this block is the minimum expectation of $H_{\text{output}}$ in a state (6.32), where the minimum is taken over all $n_{\text{input}}$-qubit states $|\psi\rangle$. This is equal to

$$\min_{|\psi\rangle} \frac{1}{2M}\left(1 - \text{AP}(\mathcal{C}_x, |\psi\rangle)\right) \geq \frac{1}{3M} \tag{6.34}$$

where we used the fact that $\text{AP}\left(\mathcal{C}_x, |\psi\rangle\right) \leq \frac{1}{3}$ for all $|\psi\rangle$. Likewise, every state in the second block can be written as (6.33) for some state $|\psi\rangle$, and the minimum eigenvalue within this block is

$$\min_{|\psi\rangle} \frac{1}{2M}\left(1 - \text{AP}(\mathcal{C}_x, |\psi\rangle)^*\right) \geq \frac{1}{3M} \tag{6.35}$$

(since $\text{AP}(\mathcal{C}_x, |\psi\rangle)^* = \text{AP}(\mathcal{C}_x, |\psi\rangle) \leq \frac{1}{3}$). Thus we see that $H_B|_{S_A}$ has an empty nullspace, so its smallest eigenvalue is equal to its smallest nonzero eigenvalue, namely

$$\gamma(H_B|_{S_A}) \geq \frac{1}{3M}. \tag{6.36}$$

Now applying Lemma **??** using this bound, the fact that $\|H_B\| = 1$, and the fact that $\gamma(H_A) \geq \frac{1}{20M^3 n}$ (from equation (6.30)), we get

$$\gamma(A_x - e_1 \cdot \mathbb{I}) \geq \frac{\frac{1}{60M^4 n}}{\frac{1}{20M^3 n} + \frac{1}{3M} + 1} \geq \frac{1}{120M^4 n}. \tag{6.37}$$

Since $H_B|_{S_A}$ has an empty nullspace, $A_x - e_1 \cdot \mathbb{I}$ has an empty nullspace, and this is a lower bound on its smallest eigenvalue.

## 6.3 Extensions and Discussion

While this result is interesting in its own right, as it shows that finding the ground energy of a sparse, row-computable matrix is QMA-complete, perhaps the most interesting result is that nothing particularly quantum is involved in the definition of the problem. In particular, the only condition we have on the matrix is that it is sparse, and row-computable. This condition might allow for a more natural understanding for more classically-minded computer scientists, as a QMA-complete problem could be stated without having to delve into any quantum computing.

As an additional problem, since the circuit-to-Hamiltonian map creates a 7-regular, simple graph, one might wonder if the removal of these conditions are necessary when the boundary terms are added. This is obviously going to be necessary, as otherwise we would have that determining the lowest eigenvalue of a Laplacian is QMA-complete, but it is a well known fact that the smallest eigenvalue of a Laplacian is zero.

[**TO DO:** *can I use the same techniques as the self-loop removal to remove self-loops from this system?*]

[**TO DO:** *Write more*]

# Chapter 7

# Ground energy of multi-particle quantum walk

With our proof that the ground state problem for a single-particle quantum walk is QMA-complete, we would now like to examine the corresponding problem for the multi-particle quantum walk. The similarities between the two systems make us expect that very similar results will hold for the multi-particle case, but we will again need to examine the problem in a lot of detail.

In particular, the QMA-completeness for the single particle walk was relatively straightforward, in that there is really only one particle to deal with. Because of this, we understand the dynamics and can exactly analyze the system on which things interact, leading to exact solutions for the energies of the resulting Hamiltonian. With the MPQW, a full analysis is currently beyond our knowledge, and our universality construction relied on a reduction to the cases with at most two interacting particles. In order to show that finding the ground energy of a MPQW is QMA-complete using our techniques, we'd need to again reduce to the case of a small number of particles.

To make this reduction, we will show that the problem is QMA-hard when restricted to the problem where the interaction term adds (almost) no energy to the ground state, so that the ground state is contained within the span of single-particle states that don't overlap. With this restriction, we will still have correlations between many particles, but we will be able to analyze the correlations and determine the corresponding ground energy.

## 7.1 MPQW Hamiltonian ground-energy problem

In order to make things precise, we will fix a particular finite-range interaction, and show that with this fixed interaction, the resulting question is QMA-complete to solve. In particular let $\mathcal{U}$ be an interaction with finite support and no negative coefficients. For a particular graph $G$, we can then define a Hamiltonian on such a graph as [**TO DO:** *find a correct way to define* $\mathcal{U}$]

$$H_{f,G} = \sum_{(i,j)\in E(G)} a_i a_j + a_j a_i + \sum_{i,j\in V(G)} U_{d(i,j)}(n_i, n_j) = H_{G,\mathrm{move}} + H_{G,\mathrm{int}}. \qquad (7.1)$$

Note that because of the positivity restrictions placed on $\mathcal{U}$, we have that $H_{G,\text{int}}$ is positive semi-definite, and thus the ground energy of $H_{f,G}$ is at least the ground energy of $H_{G,\text{move}}$.

With this particular interaction, we can then construct the corresponding problem.

Note that these Hamiltonians actually act on an infinite dimensional Hilbert space, in that the number of particles is unbounded. In order to reduce the complexity of these problems to a reasonable amount, we restrict our attention to a particular number of particles. Once again, as each term in the Hamiltonian preserves the number of particles, we have that $H_{\mathcal{U},G}$ decomposes into blocks with a particular particle number, and we represent these blocks as $\overline{H}^N_{\mathcal{U},G}$.

**Problem 2** ($\mathcal{U}$-interaction MPQW Hamiltonion)**.** Given as input a $K$-vertex graph $G$, a number of particles $N$, a real number $c$, and a precision parameter $\epsilon = 1/T$, where the positive integers $N$ and $T$ are given in unary, and the graph $G$ is given as its adjacency matrix (a $K \times K$ symmetric 0-1 matrix), the $\mathcal{U}$-interaction MPQW Hamiltonian problem is to determine whether the smallest eigenvalue of $\overline{H}^N_{\mathcal{U},G}$ is at most $c$ or is at least $c + \epsilon$, with a promise that one of these two cases hold.

### 7.1.1 MPQW Hamiltonian is contained in QMA

To prove that $\mathcal{U}$-interaction MPQW Hamiltonian problem is contained in QMA, we provide a verification algorithm satisfying the requirements of Definition **??**. In the Definition this algorithm is specified by a circuit involving only one measurement of the output qubit at the end of the computation. The procedure we describe below, which contains intermediate measurements in the computational basis, can be converted into a verification circuit of the desired form by standard techniques.

We are given an instance specified by $G$, $N$, $c$, and $\epsilon$. We are also given an input state $|\phi\rangle$ of $n_{\text{input}}$ qubits, where $n_{\text{input}} = \lceil \log_2 D_N \rceil$ and $D_N$ is the dimension of $\mathcal{Z}_N(G)$ as given in equation (**??**). Note, using the inequality $\binom{a}{b} \leq a^b$ in equation (**??**), that $n_{\text{input}} = \mathcal{O}(K \log (N + K))$, where $K = |V|$ is the number of vertices in the graph $G$. We embed $\mathcal{Z}_N(G)$ into the space of $n_{\text{input}}$ qubits straightforwardly as the subspace spanned by the first $D_N$ standard basis vectors (with lexicographic ordering, say). The first step of the verification procedure is to measure the projector onto this space $\mathcal{Z}_N(G)$. If the measurement outcome is 1 then the resulting state $|\phi'\rangle$ is in $\mathcal{Z}_N(G)$ and we continue; otherwise we reject.

In the second step of the verification procedure, the goal is to measure $\bar{H}^N_G$ in the state $|\phi'\rangle$. The Hamiltonian $\bar{H}^N_G$ is sparse and efficiently row-computable, with norm

$$\left\|\bar{H}^N_G\right\| \leq \left\|H^N_G\right\| \leq N \left\|A(G)\right\| + \left\|\sum_{k\in V} \hat{n}_k \left(\hat{n}_k - 1\right)\right\| \leq NK + N^2. \tag{7.2}$$

We use phase estimation (see for example [**?**]) to estimate the energy of $|\phi'\rangle$, using sparse Hamiltonian simulation [**?**] to approximate evolution according to $\bar{H}^N_G$. We choose the parameters of the phase estimation so that, with probability at least $\frac{2}{3}$, it produces an approximation $E$ of the energy with error at most $\frac{\epsilon}{4}$. This can be done in time $\text{poly}(N, K, \frac{1}{\epsilon})$. If $E \leq c + \frac{\epsilon}{2}$ then we accept; otherwise we reject.

We now show that this verification procedure satisfies the completeness and soundness requirements of Definition **??**. For a yes instance, an eigenvector of $\bar{H}_G^N$ with eigenvalue $e \leq c$ is accepted by this procedure as long as the energy $E$ computed in the phase estimation step has the desired precision. To see this, note that we measure $|E - e| \leq \frac{\epsilon}{4}$, and hence $E \leq c+\frac{\epsilon}{4}$, with probability at least $\frac{2}{3}$. For a no instance, write $|\phi'\rangle \in \mathcal{Z}_N(G)$ for a state obtained after passing the first step. The value $E$ computed by the subsequent phase estimation step satisfies $E \geq c + \frac{3\epsilon}{4}$ with probability at least $\frac{2}{3}$, in which case the state is rejected. From this we see that the probability of accepting a no instance is at most $\frac{1}{3}$.

### 7.1.2 Frustration-free

While showing that this problem is contained in QMAis relatively easy, in our proof of QMA-hardness we will want to impose additional structure on the problem. In particular, we will want the problem to have the extra promise that if the particular instance is a yes instance, then the interaction term will essentially add no energy to the ground state. In particular, we will want the ground state of the system to be a ground state for each term in the Hamilonian individually, which is usually a statement that the Hamiltonian is frustration-free.

The reason that this helps us is that it actually allows us to determine the actual ground energies of various Hamiltonians, and lets us convert the problem to one of adding positive semi-definite matrices. This allows us to use our Nullspace Projection Lemma (Lemma **??**), and give strong bounds on the resulting eigenvalue gaps. Additionally, the guarantee that certain Hamilonians are frustration-free will allow us to give some additional results on various spin systems.

[**TO DO:** *does this work for both bosons and fermions?. I think it will, but I'm not sure. It might not be worth it to discuss fermions right now.*]

With all of this, let $G$ be a graph, and let us assume that the interaction is $\mathcal{U}$. If we then restrict to the $N$-particle sector, we have that the Hamiltonian is given by

$$H_{\mathcal{U},G}^N = \sum_{(i,j)\in E(G)} (a_i^\dagger a_j + a_j^\dagger a_i) + \sum_{i,j\in V(G)} \mathcal{U}_{d(i,j)}(n_i, n_j) \tag{7.3}$$

$$= \sum_{w=1}^{N} A(G)^{(w)} + \sum_{i,j\in V(G)} \mathcal{U}_{d(i,j)}(\hat{n}_i, \hat{n}_j) \tag{7.4}$$

where

$$\hat{n}_i = \sum_{w=1}^{N} |\, i\,\rangle\langle\, i\,|^{(w)}. \tag{7.5}$$

Additionally, we will again assume that

$$H_{G,\text{move}}^N = \sum_{w=1}^{N} A(G)^{(w)} \tag{7.6}$$

is the movement term of the Hamiltonian, and that

$$H_{\mathcal{U},G,\text{int}}^N = \sum_{i,j\in V(G)} \mathcal{U}_{d(i,j)}(\hat{n}_i, \hat{n}_j) \tag{7.7}$$

is the interaction term of the Hamiltonian.

While $H^N_{\mathcal{U},G}$ acts on the entire $|V|^N$ dimensional system of distinguishable particles, we want to deal with indistinguishable particles (and in particular bosonic particles). As such, we will want to look at the restriction of $H^N_{\mathcal{U},G}$ to the bosonic subspace:

$$\overline{H}^N_{\mathcal{U},G} := H^N_{\mathcal{U},G}\big|_{\mathcal{Z}_N(G)} \tag{7.8}$$

[**TO DO:** *check boson/fermion*]

At this point, it will be extremely useful to add a term proportional to the identity in order to make a positive semidefinite operator. In particular, if we let $\mu(G)$ be the smallest eigenvalue of $A(G)$, we can consider

$$H_{\mathcal{U}}(G, N) = \overline{H}^n_{\mathcal{U},G} - N\mu(G) \tag{7.9}$$

which is a positive-semidefinite matrix. Additionally, as $\mu(G)$ can be efficiently computed using a classical polynomial-time algorithm, we have that the complexity of approximating the ground energy of $H_{\mathcal{U}}(G, N)$ is equivalent to the complexity of approximating the ground energy of $\overline{H}^N_{\mathcal{U},G}$.

We shall write

$$0 \leq \lambda^1_N(G) \leq \lambda^2_N(G) \leq \cdots \leq \lambda^{D_N}_N(G) \tag{7.10}$$

for the eigenvalues of $H_{\mathcal{U}}(G, N)$ and $\{|\lambda^j_N(G)\rangle\}$ for the associated eigenvectors.

Note that when $\lambda^1_N(G) = 1$, the ground energy of the $N$-particle MPQW Hamiltonian $\overline{H}^N_{\mathcal{U},G}$ is equal to $N$ times the single-particle ground energy $\mu(G)$. In this case, we say that the $N$-particle MPQW Hamiltonian is frustration free, as the ground state minimizes both the movement term and the interaction term. We also define frustration freeness for $N$-particle states.

**Definition 6** (Frustration-free state)**.** If $|\psi\rangle \in \mathcal{Z}_N(G)$ satisfies $H_{\mathcal{U}}(G, N)|\psi\rangle = 0$, then we say that $|\psi\rangle$ is an $N$-particle frustration-free state for $\mathcal{U}$ on $G$.

#### 7.1.2.1 Basic properties

We now give some basic properties of $H_{\mathcal{U}}(G, N)$. In particular we will want to understand how the eigenvalues of the Hamiltonian change when we increase the number of particles, as well as understand such a system when looking at many disconnected copies of graphs.

**Lemma 11.** *For all $N > 1$, $\lambda^1_{N+1}(G) \geq \lambda^1_N(G)$.*

*Proof.* [**TO DO:** *Fix this for an arbitrary interaciton*] Let $\widehat{n}^N_i$ be the number operator (**??**) defined in the $N$-particle space and let $\widehat{n}^{N+1}_i$ be the corresponding operator in the $(N+1)$-particle space. Note that

$$\widehat{n}^{N+1}_i = \widehat{n}^N_i \otimes \mathbb{I} + |i\rangle\langle i|^{(N+1)} \geq \widehat{n}^N_i \otimes \mathbb{I}. \tag{7.11}$$

Using this and the fact that $A(G) \geq \mu(G)$, we get

$$H^{N+1}_G - (N+1)\,\mu(G) \geq \big(H^N_G - N\mu(G)\big) \otimes \mathbb{I}. \tag{7.12}$$

Hence

$$\lambda^1_{N+1}(G) = \min_{|\psi\rangle \in \mathcal{Z}_{N+1}(G)\colon \langle\psi|\psi\rangle=1} \langle\psi|H_G^{N+1} - (N+1)\,\mu(G)|\psi\rangle \tag{7.13}$$

$$\geq \min_{|\psi\rangle \in \mathcal{Z}_N(G)\otimes\mathbb{C}^{|V|}\colon \langle\psi|\psi\rangle=1} \langle\psi|\left(H_G^N - N\mu(G)\right)\otimes\mathbb{I}|\psi\rangle \tag{7.14}$$

$$= \lambda^1_N(G) \tag{7.15}$$

(using the fact that $\mathcal{Z}_{N+1}(G) \subset \mathcal{Z}_N(G)\otimes\mathbb{C}^{|V|}$). $\square$

We will encounter graphs $G$ with more than one component. In the cases of interest, the smallest eigenvalue of the adjacency matrix for each component is the same. The following Lemma shows that the eigenvalues of $H(G,N)$ on such a graph can be written as sums of eigenvalues for the components. In this Lemma (and throughout the paper), we let $[k] = \{1,2,\ldots,k\}$.

**Lemma 12.** *Suppose $G = \bigcup_{i=1}^k G_i$ with $\mu(G_1) = \mu(G_2) = \cdots = \mu(G_k)$. The eigenvalues of $H(G,N)$ are*

$$\sum_{i\in[k]\colon N_i\neq 0} \lambda^{y_i}_{N_i}(G_i) \tag{7.16}$$

*where $N_1,\ldots,N_k \in \{0,1,2,\ldots\}$ with $\sum_i N_i = N$ and $y_i \in [D_{N_i}]$. The corresponding eigenvectors are (up to normalization)*

$$\mathrm{Sym}\left(\prod_{i\in[k]\colon N_i\neq 0} |\lambda^{y_i}_{N_i}(G_i)\rangle\right). \tag{7.17}$$

*Proof.* Recall that the action of $H_G - N\mu(G)$ on the Hilbert space (**??**) is the same as the action of $H(G,N)$ on the Hilbert space $\mathcal{Z}_N(G)$. States in these Hilbert spaces are identified via the mapping described in equation (**??**). It is convenient to prove the Lemma by working with the second-quantized Hamiltonian $H_G$. We then translate our results into the first-quantized picture to obtain the stated claims.

For a graph with $k$ components, equation (**??**) gives

$$H_G = \sum_{i=1}^k H_{G_i} \tag{7.18}$$

where $[H_{G_i}, H_{G_j}] = 0$. Label each vertex of $G$ by $(a,b)$ where $b \in [k]$ and $a \in [|V_b|]$, where $V_b$ is the vertex set of the component $G_b$. An occupation number basis state (**??**) can be written

$$|l_{1,1},\ldots,l_{|V_1|,1}\rangle|l_{1,2},\ldots,l_{|V_2|,2}\rangle\ldots|l_{1,k},\ldots,l_{|V_k|,k}\rangle. \tag{7.19}$$

The Hamiltonian $H_G - N\mu(G)$ conserves the number of particles $N_b$ in each component $b$. Within the sector corresponding to a given set $N_1,\ldots,N_k$ with $\sum_{i\in[k]} N_i = N$, we have

$$(H_G - N\mu(G))\,|l_{1,1},\ldots,l_{|V_1|,1}\rangle|l_{1,2},\ldots,l_{|V_2|,2}\rangle\ldots|l_{1,k},\ldots,l_{|V_k|,k}\rangle \tag{7.20}$$

$$= \left(H_{G_1} - N_1\mu(G_1)|l_{1,1},\ldots,l_{|V_1|,1}\rangle\right)|l_{1,2},\ldots,l_{|V_2|,2}\rangle\ldots|l_{1,k},\ldots,l_{|V_k|,k}\rangle \tag{7.21}$$

$$+ |l_{1,1},\ldots,l_{|V_1|,1}\rangle\left(H_{G_2} - N_2\mu(G_2)|l_{1,2},\ldots,l_{|V_2|,2}\rangle\right)\ldots|l_{1,k},\ldots,l_{|V_k|,k}\rangle + \cdots \tag{7.22}$$

$$+ |l_{1,1},\ldots,l_{|V_1|,1}\rangle|l_{1,2},\ldots,l_{|V_2|,2}\rangle\ldots\left(H_{G_k} - N_k\mu(G_k)|l_{1,k},\ldots,l_{|V_k|,k}\rangle\right), \tag{7.23}$$

where we used the fact that $\mu(G_i) = \mu(G)$ for $i \in [k]$. From this equation we see that the eigenstates of $H_G$ can be obtained as product states with $k$ factors in the basis (7.19). In each such product state, the $i$th factor is an eigenstate of $H_{G_i} - N_i\mu(G_i) = H_{G_i} - N_i\mu(G)$ in the $N_i$-particle sector, with eigenvalue $\lambda^{j_i}_{N_i}(G_i)$. Rewriting this result in the "first-quantized" language, we obtain the Lemma. □

#### 7.1.2.2 QMA-hard problem

With all of these definitions floating around, it will then be useful to actually define the basic problem that we will show is QMA-hard. In particular, we have that for any positive integer $\alpha$, the following problem:

**Problem 3** ($\alpha$-frustration-free$\mathcal{U}$-interaction MPQW Hamiltonian)**.** We are given as input a $K$-vertex simple graph $G$, a number of particles $N \leq K$, and a precision parameter $\epsilon = 1/T$, where the positive integers $N$ and $T \geq 4K$ are given in unary, and the graph $G$ is given as its adjacency matrix (a $K \times K$ symmetric 0-1 matrix). We arp promised that either $\lambda^1_N(G) \leq \epsilon^\alpha$ (a yes instance), or else that $\lambda^1_N(G) \geq \epsilon + \epsilon^\alpha$ (a no instance) and we are asked to decide which is the case.

Note that for each interaction type, this is an infinite family of problems. The positive integer $\alpha$ parameterizes how much the yes cases can deviate from a true frustration-free case. The reason that we define the problem in such a way is that it will facilitate the reduction found in Chapter 8.

Note that this is a special case of the $\mathcal{U}$-interaction MPQW Hamiltonian, with $c = N\mu(G) + \epsilon^\alpha$. As such, if we show that the $\alpha$-frustration free $\mathcal{U}$-interaction MPQW Hamiltonian problem is QMA-hard, we will also show that the non-frustration-free problem is QMA-complete.

## 7.2 Useful graph primitives

At this point, we will want to construct a graph for which our QMA-hardness result will hold. As such, we will at this point restrict our attention to a particular interaction, $\mathcal{U}$. While the idea behind the construction of these graphs will not change, the exact graph will depend on both the largest distance for which there is a non-zero interaction. We will want to construct a foundational graph that does not have a two-particle ground state, and also we will want to ensure that our connections between these building blocks will not have multiple particles interacting except on specially chosen building blocks.

As such, let us assume that the minimum distance that the interaction $\mathcal{U}$ has non-zero interactions is $d_{\min}$, while the maximum distance is $d_{\max}$. Our graph will only depend on $d_{\max}$, but it will be useful to also know $d_{\min}$. We will also assume that $\mathcal{U}^{(1,1)}_{d_{\min}} > 0$, so that there is some energy penalty if two particles are at a distance $d_{\min}$ (assuming that $d_{\min} > 0$ — otherwise we will assume that $\mathcal{U}^2_0 > 0$).

Additionally, we will want the eventual graph to be a simple graph, so that there is always at most a single edge between two vertices and no self-loops. Unfortunately, our proof strategy will involve adding many positive semi-definite terms to the adjacency matrix, which correspond to adding in edges and self-loops. As such, we will instead force every vertex in the graph to contain a self-loop, so that by removing all of the self loops we only shift the energy levels by a constant amount. Keep this in mind, as the eventual graph is defined.

With all of this said, however, this section will only define some useful foundational graphs that will be used in the final construction of the graph. All of these graphs will be constant sized, and we will show a spanning set for their single-particle and two-particle ground states. By construction, they will not have any three-particle frustration-free states.

### 7.2.1 Gate graphs

[**TO DO:** *make each node a distance at least $2d_{max}$ apart*]

In this subsection we define a class of graphs (*gate graphs*) and a diagrammatic notation for them (*gate diagrams*) that will allow us to construct the overall graph. We will also discuss the MPQW Hamiltonian acting on these graphs, with a particular emphasis on the low-energy states.

Every gate graph is constructed using a specific, finite-sized graph $g_0$ as a building block. This graph is shown in Figure 7.1 (for graphs with $d_{\min} <= 3$ and discussed in Section **??**. In Section **??** we define gate graphs and gate diagrams. A gate graph is obtained by adding edges and self-loops (in a prescribed way) to a collection of disjoint copies of $g_0$.

In Section **??** we discuss the ground states of the Bose-Hubbard model on gate graphs. For any gate graph $G$, the smallest eigenvalue $\mu(G)$ of the adjacency matrix $A(G)$ satisfies $\mu(G) \geq -1 - 3\sqrt{2}$. It is convenient to define the constant

$$e_1 = -1 - 3\sqrt{2}. \tag{7.24}$$

When $\mu(G) = e_1$ we say $G$ is an $e_1$-gate graph. We focus on the frustration-free states of $e_1$-gate graphs (recall from Definition **??** that $|\phi\rangle \in \mathcal{Z}_N(G)$ is frustration free iff $H(G, N)|\phi\rangle = 0$). We show that all such states live in a convenient subspace (called $\mathcal{I}(G, N)$) of the $N$-particle Hilbert space. This subspace has the property that no two (or more) particles ever occupy vertices of the same copy of $g_0$. The restriction to this subspace makes it easier to analyze the ground space.

In Section **??** we consider a class of subspaces that, like $\mathcal{I}(G, N)$, are defined by a set of constraints on the locations of $N$ particles in an $e_1$-gate graph $G$. We state an "Occupancy Constraints Lemma" (proven in Appendix **??**) that relates a subspace of this form to the ground space of the Bose-Hubbard model on a graph derived from $G$.

#### 7.2.1.1 The graph $g_0$

The graph $g_0$ shown in Figure 7.1 is constructed using the method of Chapter 6, with the single qubit circuit corresponding to a sequence of $H$ and $HT$ gates. The idea is to force the ground state of the resulting graph to correspond to these computations while also spreading the wave-function over most of the vertices. In this way, we can use the ground state to compute these single-particle unitaries while also forcing the graph to only have single-particle frustration free states.

[**TO DO:** *run through to check whether the change of $k$ to $d_{max}$ actually causes problems*]

In particular, let $k = \max\{2d_{\max} + 2, 4\}$, and then let us look at the single-qubit circuit $\mathcal{C}_0$ with $k$ gates $U_j$, for $j \in [k]$, where

$$U_1 = HT \qquad U_2 = (HT)^{\dagger} \tag{7.25}$$

and the rest of the $U_j = H$. We can then use the circuit to graph construction from Chapter 6 to construct a simple graph with the ground space spanned by the history states of this circuit. Note that this transformation includes an uncomputation as well, so that there will be a total of $2k$ time-steps, and that the time is cyclic (so that $2k+1 = 0$).

In particular, remembering that $B(U)$ is the operator that takes $\omega \mapsto S$, where $S$ is the shift operator acting on $\mathbb{C}^8$, we will have that the portion of the adjacency matrix corresponding to the computation acts on the Hilbert space $\mathbb{C}^2 \otimes \mathbb{C}^{2k} \otimes \mathbb{C}^8$, and is equal to

$$H_{\text{prop}} = -\sqrt{2} \sum_{t=0}^{2k} B(W_{t+1})_{13} \otimes |t+1\rangle\langle t| + B(W_{t+1}^{\dagger})_{13} \otimes |t\rangle\langle t+1|. \tag{7.26}$$

With this, term, along a penalty to the $\mathbb{C}^8$ Hilbert space given by

$$H_{\text{pen}} = \mathbb{I}_{\mathbb{C}^2} \otimes \mathbb{I}_{\mathbb{C}^{2k}} \otimes \left(S^3 + S^4 + S^3\right) \tag{7.27}$$

will allow us to construct the adjacency matrix of $g(0)$, namely

$$A(g_0) = H_{\text{prop}} + H_{\text{pen}} \tag{7.28}$$

[**TO DO:** *fix the $g_0$ graph*]

Now we can define the graph $g_0$. Each vertex in $g_0$ corresponds to a standard basis vector in the Hilbert space $\mathbb{C}^2 \otimes \mathbb{C}^{2K} \otimes \mathbb{C}^8$. We label the vertices $(z, t, j)$ with $z \in \mathbb{F}_2$ describing the state of the computational qubit, $t \in [2k]$ giving the state of the clock, and $j \in [8]$ describing the state of the ancilla. The adjacency matrix is

$$A(g_0) = H_{\text{prop}} + H_{\text{penalty}} \tag{7.29}$$

where the penalty term

$$H_{\text{penalty}} = \mathbb{I} \otimes \mathbb{I} \otimes \left(S^3 + S^4 + S^5\right) \tag{7.30}$$

acts nontrivially on the third register. The graph $g_0$ is shown in Figure 7.1.

Now consider the ground space of $A(g_0)$. Note that $H_{\text{prop}}$ and $H_{\text{penalty}}$ commute, so they can be simultaneously diagonalized. Furthermore, $H_{\text{penalty}}$ has smallest eigenvalue $-1-\sqrt{2}$ (with eigenspace spanned by $|\omega\rangle$ and $|\omega^*\rangle$) and first excited energy $-1$. The norm of $H_{\text{prop}}$ satisfies $\|H_{\text{prop}}\| \leq 4$, which follows from the fact that $H_{\text{prop}}$ has four ones in each row and column (with the remaining entries all zero).

The smallest eigenvalue of $A(g_0)$ lives in the sector where $H_{\text{penalty}}$ has eigenvalue $-1-\sqrt{2}$ and is equal to

$$-2\sqrt{2} + (-1-\sqrt{2}) = -1 - 3\sqrt{2} = -5.24\ldots. \tag{7.31}$$

This is the constant $e_1$ from equation (7.24). To see this, note that in any other sector $H_{\text{penalty}}$ has eigenvalue at least $-1$ and every eigenvalue of $A(g_0)$ is at least $-5$ (using the

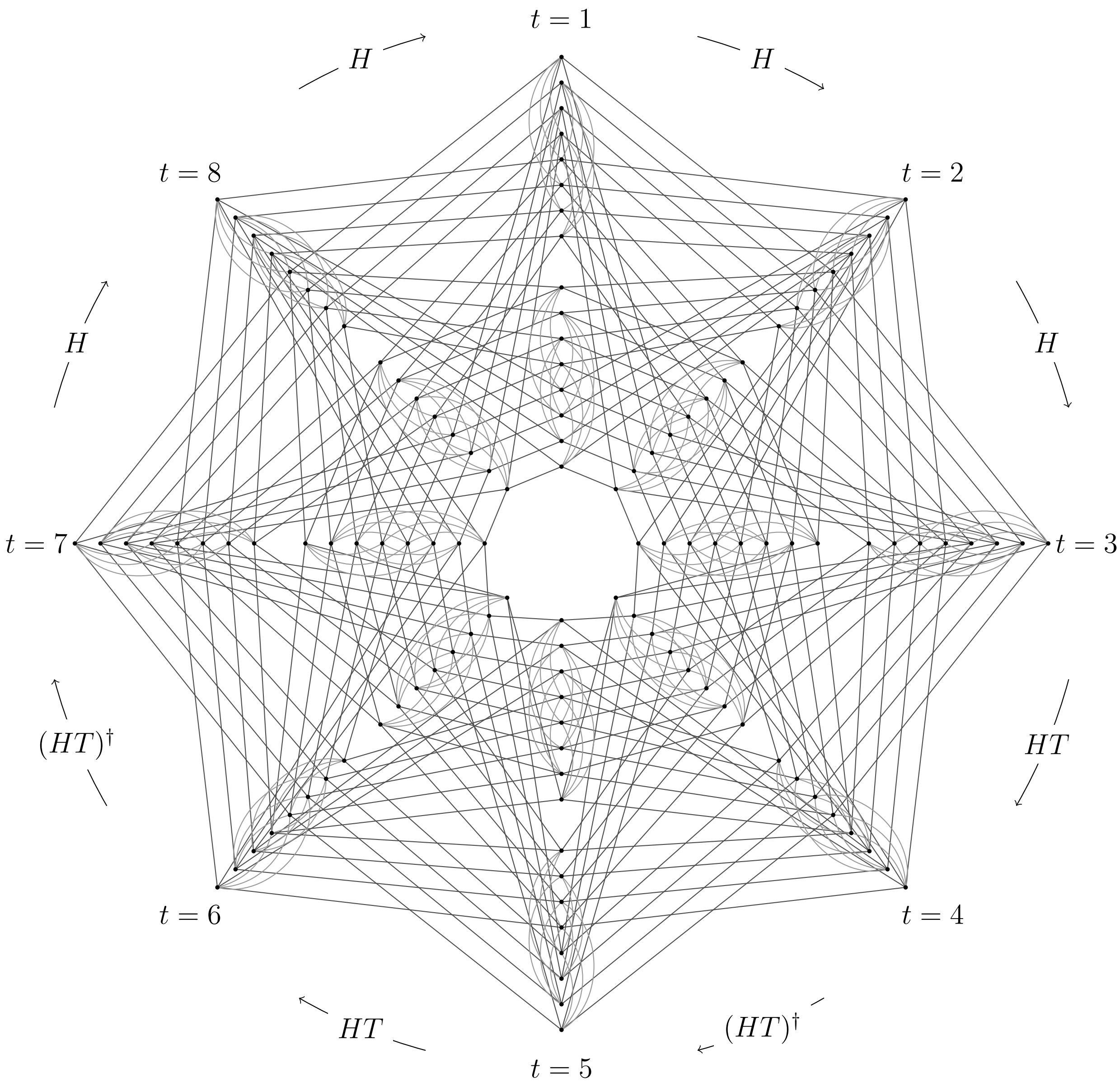


Figure 7.1: The graph $g_0$ for the case $d_{\min} < 3$.

fact that $H_{\text{prop}} \geq -4$). An orthonormal basis for the ground space of $A(g_0)$ is furnished by the states

$$|\psi_{z,0}\rangle = \frac{1}{\sqrt{8}}\big(|z\rangle(|1\rangle + |3\rangle + |5\rangle + |7\rangle) + H|z\rangle(|2\rangle + |8\rangle) + HT|z\rangle(|4\rangle + |6\rangle)\big)|\omega\rangle \tag{7.32}$$

$$|\psi_{z,1}\rangle = |\psi_{z,0}\rangle^* \tag{7.33}$$

where $z \in \{0, 1\}$.

Note that the amplitudes of $|\psi_{z,0}\rangle$ in the above basis contain the result of computing either the identity, Hadamard, or $HT$ gate acting on the "input" state $|z\rangle$.

We prove that the graph $g_0$ has no two-particle frustration-free states. By Lemma **??**, it follows that $g_0$ has no $N$-particle frustration-free states for $N \geq 2$.

**Lemma 13.** $\lambda_2^1(g_0) > 0$.

*Proof.* Suppose (for a contradiction) that $|Q\rangle \in \mathcal{Z}_2(g_0)$ is a nonzero vector in the nullspace of $H(g_0, 2)$, so

$$H_{g_0}^2|Q\rangle = \Big(A(g_0) \otimes \mathbb{I} + \mathbb{I} \otimes A(g_0) + \sum_{i,j \in g_0} \mathcal{U}_{d(i,j)}(\hat{n}_i, \hat{n}_j)\Big)|Q\rangle = 2e_1|Q\rangle. \tag{7.34}$$

This implies

$$A(g_0) \otimes \mathbb{I}|Q\rangle = \mathbb{I} \otimes A(g_0)|Q\rangle = e_1|Q\rangle \tag{7.35}$$

since $A(g_0)$ has smallest eigenvalue $e_1$ and the interaction term is positive semidefinite. We can therefore write

$$|Q\rangle = \sum_{z,a,x,y \in \{0,1\}} Q_{za,xy}|\psi_{z,a}\rangle|\psi_{x,y}\rangle \tag{7.36}$$

with $Q_{za,xy} = Q_{xy,za}$ (since $|Q\rangle \in \mathcal{Z}_2(g_0)$) and

$$\mathcal{U}_{d(u,v)}(\hat{n}_u, \hat{n}_v)|Q\rangle = 0 \tag{7.37}$$

for all vertices $u, v \in g_0$. If we then assume that $\mathcal{U}_{d_{\min}}^{(1,1)} \geq 0$ if $d_{\min} > 0$ or $\mathcal{U}_0^2 > 0$ if $d_{\min} = 0$, we have that for all vertices $u, v$ of distance $d_{\min}$,

$$\big(|u\rangle\langle u| \otimes |v\rangle\langle v|\big)|Q\rangle = 0. \tag{7.38}$$

Let us first look at the case where $d_{\min}$ is even. In this case, we know that the combination of unitaries applied over a time $d_{\min}$ is the identity, so that vertices $(0, 0, j)$ and $(0, d_{\min}, j)$ are at a distance $d_{\min}$. In particular, if we examine (7.38) with $|u\rangle = |0, 0, j\rangle$ and $|v\rangle = |0, d_{\min}, j\rangle$ we find that

$$Q_{00,00}\langle 0, 0, j|\psi_{0,0}\rangle\langle 0, d_{\min}, j|\psi_{0,0}\rangle + Q_{01,01}\langle 0, 0, j|\psi_{0,1}\rangle\langle 0, d_{\min}, j|\psi_{0,1}\rangle \tag{7.39}$$

$$+ Q_{01,00}\big(\langle 0, 0, j|\psi_{0,1}\rangle\langle 0, d_{\min}, j|\psi_{0,0}\rangle + \langle 0, 0, j|\psi_{0,0}\rangle\langle 0, d_{\min}, j|\psi_{0,1}\rangle\big) \tag{7.40}$$

$$= \frac{1}{64}\left(Q_{00,00}i^{-j} + 2Q_{01,00} + Q_{01,01}i^j\right) \tag{7.41}$$

$$= 0 \tag{7.42}$$

for each $j \in \{0,\ldots,7\}$. The only solution to this set of equations is $Q_{00,00} = Q_{01,00} = Q_{01,01} = 0$. The same analysis, now using $|v\rangle = |1,0,j\rangle$ and $|\,u\,\rangle = |\,1,0,j\,\rangle$, gives $Q_{10,10} = Q_{11,10} = Q_{11,11} = 0$.

If we then examine what happens starting on a state corresponding to a Hadamard being applied to the initial state, using equation (7.38) with $|v\rangle = |0,3,j\rangle$ and $|\,u\,\rangle = |\,0,3{+}d_{\min},j\,\rangle$ gives

$$\frac{1}{16k}\langle 0|H|1\rangle\langle 0|H|0\rangle\left(2Q_{10,00}i^{-j} + 2Q_{10,01} + 2Q_{11,00} + 2Q_{11,01}i^{j}\right) \tag{7.43}$$

$$= \frac{1}{16k}\left(Q_{10,00}i^{-j} + Q_{10,01} + Q_{11,00} + Q_{11,01}i^{j}\right) \tag{7.44}$$

$$= 0 \tag{7.45}$$

for all $j \in \{0,\ldots,7\}$, which implies that $Q_{10,00} = Q_{11,01} = 0$ and $Q_{11,00} = -Q_{10,01}$. Thus, up to normalization,

$$|Q\rangle = |\psi_{1,0}\rangle|\psi_{0,1}\rangle + |\psi_{0,1}\rangle|\psi_{1,0}\rangle - |\psi_{11}\rangle|\psi_{00}\rangle - |\psi_{00}\rangle|\psi_{11}\rangle. \tag{7.46}$$

Finally, we can apply equation (7.38) with $|v\rangle = |0,1,j\rangle$ and $|\,u\,\rangle = |\,0,1+d_{\min},j\,\rangle$, we see that the quantity

$$\frac{1}{16k}\Big(\langle 0|HT|1\rangle\langle 0|H|0\rangle + \langle\,0\,|\,(HT)^*\,|\,0\,\rangle\langle\,0\,|\,H\,|\,1\,\rangle \tag{7.47}$$

$$- \langle 0|(HT)^*|1\rangle\langle 0|H|0\rangle - \langle\,0\,|\,(HT)^*\,|\,0\,\rangle\langle\,0\,|\,H\,|\,1\,\rangle\Big) = \frac{1}{32k}\left(e^{i\frac{\pi}{4}} - e^{-i\frac{\pi}{4}}\right) \tag{7.48}$$

must be zero, which is a contradiction. Hence we conclude that the nullspace of $H(g_0,2)$ is empty if $d_{\min}$ is even.

In the case that $d_{\min}$ is odd, we have a little more difficulty in that the unitaries corresponding to odd lengths of time do not multiply to the identity, and thus we the above proof strategy is a little more involved. In particular, we no longer have that vertices $(0,0,j)$ and $(0,d_{\min},j)$ need to be at a distance $d_{\min}$. However, we can get around this by being careful how we connect the $j$ registers. Letting $t = 2$ if $d_{\min} = 1$ or $t = 0$ otherwise, we have that the unitary computed between $t$ and $t + d_{\min}$ is a negative Hadamard, so that vertices $(0,t,j)$ and $(0,t+d_{\min},j+4)$ are connected. Thus we have

$$\sum_{x,z,a,b} Q_{xa,zb}\langle\,0,t,j\,|\,\psi_{x,a}\,\rangle\langle\,0,t+d_{\min},j+4\,|\,\psi_{z,b}\,\rangle \tag{7.49}$$

$$= -\frac{1}{16k}\sum_{z,a,b} Q_{0a,zb}\,\omega^{(-1)^a j + (-1)^b j}\langle\,0\,|\,H\,|\,z\,\rangle \tag{7.50}$$

$$= -\frac{1}{32k}\left[(Q_{00,00} + Q_{00,10})\omega^{2j} + (Q_{01,01} + Q_{01,11})\omega^{-2j} + (Q_{00,11} + Q_{01,10} + 2Q_{00,01})\right]. \tag{7.51}$$

A similar approach with $(0,t,j)$ and $(1,t+d_{\min},j+4)$ yeilds

$$\sum_{x,z,a,b} Q_{xa,zb}\langle 0,t,j\,|\,\psi_{x,a}\rangle\langle 1,t+d_{\min},j+4\,|\,\psi_{z,b}\rangle \tag{7.52}$$

$$= -\frac{1}{32k}\big[(Q_{00,00}-Q_{00,10})\omega^{2j}+(Q_{01,01}-Q_{01,11})\omega^{-2j}+(-Q_{00,11}-Q_{01,10}+2Q_{00,01})\big]. \tag{7.53}$$

Putting these two together, we find that $Q_{00,00}=Q_{00,10}=Q_{01,01}=Q_{01,11}=Q_{00,01}=0$ and that $Q_{00,11}=-Q_{01,10}$. A similar result between $(1,t,j)$ and $(0,t+d_{\min},j)$ and between $(1,t,j)$ and $(t,t+d_{\min},j+4)$ also shows that $Q_{10,10}=Q_{11,11}=Q_{10,11}=0$, so that we are at the same form of $|Q\rangle$, namely (7.46).

At this point we must then examine something corresponding to the $HT$ computation. Thus, we will examine the interaction between $(0,1,j)$ and $(0,1+d_{\min},j+4)$ so that

$$\big(\langle 0,1,j\,|\otimes\langle 0,1+d_{\min},j+4\,|\big)|\,Q\,\rangle \tag{7.54}$$

$$= \frac{1}{16k}\big[\langle 0\,|\,HT\,|\,1\rangle\langle 0\,|\,0\rangle\omega^{j-j-4}+\langle 0\,|\,(HT)^*\,|\,0\rangle\langle 0\,|\,1\rangle\omega^{-j+j+4} \tag{7.55}$$

$$-\langle 0\,|\,HT\,|\,0\rangle\langle 0\,|\,1\rangle\omega^{j-j-4}-\langle 0\,|\,(HT)^*\,|\,1\rangle\langle 0\,|\,0\rangle\omega^{-j+j+4}\big] \tag{7.56}$$

$$= -\frac{1}{16k}\big[\langle 0\,|\,HT\,|\,1\rangle-\langle 0\,|\,(HT)^*\,|\,1\rangle\big] \tag{7.57}$$

$$= -\frac{1}{16k\sqrt{2}}(e^{i\pi/4}-e^{-i\pi/4}). \tag{7.58}$$

We again have that this must be equal to zero, and thus we have reached a contradiction, so that the nullspace of $H(g_0,2)$ is empty if $d_{\min}$ is odd.

Since we have shown that $H(g_0,2)$ is empty when $d_{\min}$ is both even and odd, we have that it is empty for all $d_{\min}$. □

#### 7.2.1.2 Diagram elements

We use several different graphs closely related to the graph $g_0$, with some depicted in Figure 7.2. We call these figures *diagram elements*, which are also the simplest examples of *gate diagram*, which we will define shortly.

[**TO DO:** *fix diagram element graphs*] [**TO DO:** *make simple labelling scheme for diagram element nodes*]

Each diagram element actually corresponds to two copies of the graph $g_0$, along with self-loops and edges between the two copies to force the ground space into a particular form while also ensuring that almost all of the vertices of the two copies will have self-loops. We need these additional self-loops and edges to ensure that the final graph that we construct has self-loops on all vertices.

In particular, each diagram element will be labeled by a unitary it computes, along with four numbers between 0 and two, corresponding to the number of inputs "nodes" and output "nodes" of the diagram. Each such node will correspond to 16 vertices of the underlying graph representing one logical state and time of the two $g_0$ graphs. In particular, the nodes in the diagram element $U\in\{\mathbb{I},H,HT\}$ correspond to values of $t\in[2k]$ where the first

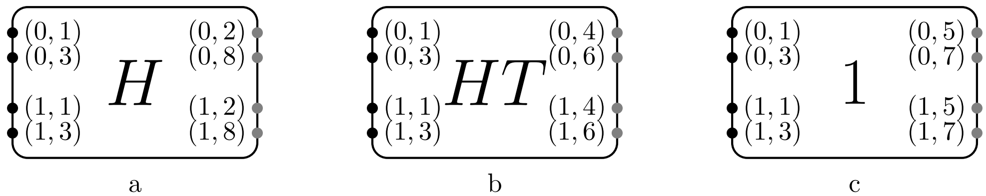


Figure 7.2: Diagram elements from which a gate diagram is constructed. Each diagram element is a schematic representation of the graph $g_0$ shown in Figure 7.1.

register in equation (7.32) is either $|z\rangle$ or $U|z\rangle$. For example, the nodes for the $H$ diagram element with four nodes have labels with $t \in \{1, k\}$ (where $|\psi_{z,0}\rangle$ contains the "input" $|z\rangle$) or $t = \{4, 2k-4\}$ (where $|\psi_{z,0}\rangle$ contains the "output" $H|z\rangle$). We draw the input nodes in black and the output nodes in grey.

Explicitly, for a diagram element implementing a unitary $U$ with $n_{0,in}$ inputs for 0, $n_{1,\text{in}}$ inputs for 1, $n_{0,\text{out}}$ outputs for 0, and $n_{1,\text{out}}$ outputs for 1, we shall call such a diagram element a $U^{(n_{0,\text{in}},n_{1,\text{in}})}_{(n_{0,\text{out}},n_{1,\text{out}})}$ element. The vertex set for the corresponding diagram element corresponds to two copies of $g_0$ (namely, $2 \times 2k \times 8 \times 2$ vertices, labeled as $(z, t, j, d)$ for $z, d \in \mathbb{F}_2$, $t \in [2k]$, and $j \in [8]$). Let $t_1$ and $t_2$ be two times for which the ground state relative to $t = 1$ has computed the unitary $U$ (other than $t = 1$ and $t = k$ if $U = \mathbb{I}$). Now, these times will be important as they will correspond to the only vertices of the graph corresponding to the diagram element that do not have self loops. In particular, let $S \subset \mathbb{F}_2 \times [2k]$ denote the required state and times that are required for the element, such as $S = \{(0, 1), (0, 4)\}$ for an $H^{(1,0)}_{(1,0)}$ element. Then the adjacency matrix for the diagram element $U^{(a,b)}_{(c,d)}$ will be

$$A(G_U^{(a,b),(c,d)}) = A(g_0) \otimes \mathbb{I}_2 + \sum_{(z,t)\notin S, j\in[8]} |\, z, t, j\,\rangle\langle\, z, t, j\,| \otimes \sum_{a,b\in\mathbb{F}_2} |\, a\,\rangle\langle\, b\,| \tag{7.59}$$

$$= A(g_0) \otimes \mathbb{I}_2 + 2\Pi_{\neg S} \otimes \mathbb{I}_8 \otimes |+\rangle\langle+| \tag{7.60}$$

In particular, the graph for $G_U^{(a,b),(c,d)}$ will simply correspond to two copies of $g_0$, along with a projector onto the equal superposition between the two graphs for each vertex not used as a node.

Because of the very similar form between $G_U^{(a,b),(c,d)}$ and $g_0$, there ground spaces and ground energies are closely related. As the second term in (7.60) is positive semi-definite, we have that the ground energy of $A(G_U^{(a,b),(c,d)})$ is at least that of $A(g_0)$. With more exact results, we have the following lemma:

**Lemma 14.** *Let $G_U^{(a,b),(c,d)}$ be the graph corresponding to a diagram element. The ground space of $A(G_U^{(a,b),(c,d)})$ is*

$$S = \text{span}\{|\,\psi_{z,a}, -\,\rangle : z, a \in \mathbb{F}_2\}. \tag{7.61}$$

*Proof.* Note that $A(G_U^{(a,b),(c,d)})$ commutes with $\mathbb{I}_2 \otimes \mathbb{I}_{2k} \otimes \mathbb{I}_8 \otimes |+\rangle\langle+|$, and thus there exists an eigenbasis for the adjacency matrix in which each vector is of the form $|\,\phi\,\rangle|+\rangle$ or $|\,\phi\,\rangle|-\rangle$.

For states of this latter form, the second term in (7.60) vanishes, so $|\psi, -\rangle$ is in the ground space of $A(g_U^{(a,b),(c,d)})$ if and only if $|\psi\rangle$ is in the ground space of $A(g_0)$.

Now let us examine $|\alpha, +\rangle$ for any state $|\alpha\rangle$. Since the first term of (7.60) has no dependence on the state $|+\rangle$, we have that the ground energy of $A(G_U^{(a,b),(c,d)}$ is at least $e_1$. Hence, if $|\alpha, +\rangle$ is in the ground space, then

$$\langle \alpha, + | A(G_U^{(a,b),(c,d)}) | \alpha, + \rangle = e_1 = \langle \alpha | A(g_0) | \alpha \rangle \tag{7.62}$$

and thus

$$\langle \alpha | \Pi_{\neg S} \otimes \mathbb{I}_8 | \alpha \rangle = 0. \tag{7.63}$$

However, let $t^*$ be a time not used as a node for the diagram element (i.e, anything time other than 1, 3, $t_1$, and $t_3$). We then have that

$$\Pi_{\neg S} \geq \mathbb{I}_2 \otimes | t^* \rangle\langle t^* | \otimes \mathbb{I}_8. \tag{7.64}$$

Note that this latter operator is strictly positive when restricted to the ground space of $A(g_0)$:

$$| \psi_{x,\gamma} \rangle \mathbb{I}_2 \otimes | t^* \rangle\langle t^* | \otimes \mathbb{I}_8 \langle \psi_{z,\delta} | = \frac{1}{2k} \delta_{\gamma,\delta} \delta_{x,z}. \tag{7.65}$$

Hence, $\Pi_{\neg S}$ is also strictly positive when restricted to the ground space of $A(g_0)$, and thus $|\alpha, +\rangle$ is not in the ground space of $A(G_U^{(a,b),(c,d)}$.

Putting this together, we have that the ground space of $A(G_U^{(a,b),(c,d)})$ is $S$. Further, as this is a finite sized system, there exists a constant eigenvalue gap. □

Additionally, because of this relationship between the single-particle ground spaces of $A(g_0)$ and $A(g_U)$, we can use the result that there are no two-particle frustration-free states on $g_0$ to show a similar result for $g_U$. In particular, we have that $\lambda_2^1(g_U) > 0$:

**Lemma 15.** $\lambda_2^1(g_U^{(a,b),(c,d)}) > 0$.

*Proof.* Note that using Lemma 14, the ground space of $A(G_U^{(a,b),(c,d)})$ is in one-to-one correspondence with the ground space of $A(g_0)$, by the transformation

$$| \phi_{x,a}, - \rangle \leftrightarrow | \phi_{x,a} \rangle. \tag{7.66}$$

Namely, by attaching (or removing) a second register in the $|-\rangle$ state, corresponding to having equal and opposite amplitudes between the two copies of $g_0$ present in $g_U^{(a,b),(c,d)}$, we can transform between these two ground spaces.

We will use this relation, along with the fact that $\lambda_2^1(g_0) > 0$, to show that $\lambda_2^1(g_U^{(a,b),(c,d)}) > 0$.

Let us then look at any two-particle state that minimizes the movement term. In particular, it takes the form

$$| \overline{\phi} \rangle = \sum_{\alpha,\beta,x,z \in \mathbb{F}_2} q_{\alpha,\beta}^{x,z} | \psi_{x,\alpha}, - \rangle | \psi_{z,\beta}, - \rangle. \tag{7.67}$$

Additionally, let us define the related two-particle state on $g_0$ as

$$|\phi\rangle = \sum_{\alpha,\beta,x,z\in\mathbb{F}_2} q^{x,z}_{\alpha,\beta}|\psi_{x,\alpha}\rangle|\psi_{z,\beta}\rangle. \tag{7.68}$$

We can then see what the expectation of the interaction term of the Hamiltonian is under the state $|\overline{\phi}\rangle$:

$$\begin{aligned}
\langle\overline{\phi}|H_{\text{int}}\langle\overline{\phi}| &= \sum_{u,v\in V(G_U^{(a,b),(c,d)})} \langle\overline{\phi}|U_{d(u,v)}(\hat{n}_u,\hat{n}_v)|\overline{\phi}\rangle &(7.69)\\
&= \sum_{u,v\in V(g_0),d_1,d_2\in\mathbb{F}_2} \langle\overline{\phi}|U_{d((u,d_1),(v,d_2))}(\hat{n}_{(u,d_1)},\hat{n}_{(v,d_2)})|\overline{\phi}\rangle &(7.70)\\
&\geq \sum_{u,v\in V(g_0),d_1\in\mathbb{F}_2} \langle\overline{\phi}|U_{d(u,v)}(\hat{n}_{(u,d_1)},\hat{n}_{(v,d_2)})|\overline{\phi}\rangle &(7.71)
\end{aligned}$$

where in the third line we only count the contributions to the interaction when both particles are in the same copy of $g_0$. As the interaction is positive-semidefinite, this can only decrease the expectation.

Now, from the form of $|\overline{\phi}\rangle$, we have that for any two $u,v\in V(g_0)$ and either copy of $g_0$,

$$\begin{aligned}
&\langle\overline{\phi}|U_{d(u,v)}(\hat{n}_{(u,d_1)},\hat{n}_{(v,d_1)})|\overline{\phi}\rangle &(7.72)\\
&= \sum_{x_1,x_2,z_1,z_2,\alpha_1,\alpha_2,\beta_1,\beta_2} (q^{x_1,z_1}_{\alpha_1,\beta_1})^* q^{x_2,z_2}_{\alpha_2,\beta_2}\langle\phi_{x_1,\alpha_1},-|\langle\phi_{z_1,\beta_2},-|U_{d(u,v)}(\hat{n}_{(u,d_1)},\hat{n}_{(v,d_1)})|\phi_{x_2,\alpha_2},-\rangle|\phi_{z_2,\beta_2},-\rangle &(7.73)\\
&\geq (\langle d|-\rangle\langle -|d\rangle)^2 \sum_{x_1,x_2,z_1,z_2,\alpha_1,\alpha_2,\beta_1,\beta_2} (q^{x_1,z_1}_{\alpha_1,\beta_1})^* q^{x_2,z_2}_{\alpha_2,\beta_2}\langle\phi_{x_1,\alpha_1}|\langle\phi_{z_1,\beta_2}|U_{d(u,v)}(\hat{n}_u,\hat{n}_v)|\phi_{x_2,\alpha_2}\rangle|\phi_{z_2,\beta_2}\rangle &(7.74)\\
&= \frac{1}{4}\langle\phi|U_{d(u,v)}(\hat{n}_u,\hat{n}_v)|\phi\rangle. &(7.75)
\end{aligned}$$

Hence, we have that

$$\begin{aligned}
\langle\overline{\phi}|H_{\text{int}}|\overline{\phi}\rangle &\geq \sum_{u,v\in V(g_0),d_1\in\mathbb{F}_2} \langle\overline{\phi}|U_{d(u,v)}(\hat{n}_{(u,d_1)},\hat{n}_{(v,d_2)})|\overline{\phi}\rangle &(7.76)\\
&\geq \frac{1}{4}\sum_{u,v\in V(g_0),d\in\mathbb{F}_2} \langle\phi|U_{d(u,v)}(\hat{n}_u,\hat{n}_v)|\phi\rangle &(7.77)\\
&= \frac{1}{4}\sum_{d\in\mathbb{F}_2}\langle\phi|H_{\text{int}}|\phi\rangle &(7.78)\\
&= \frac{1}{2}\langle\phi|H_{\text{int}}|\phi\rangle. &(7.79)
\end{aligned}$$

Using Lemma 13, we have that (7.79) is larger than zero for all states $|\phi\rangle$, and thus $\langle\overline{\phi}|H_{\text{int}}|\overline{\phi}\rangle > 0$. As such, there does not exist a two-particle frustration free state on the graph $g_U^{(a,b),(c,d)}$. [**TO DO:** *check this result; it works for BH, but does it hold for others?*]

□

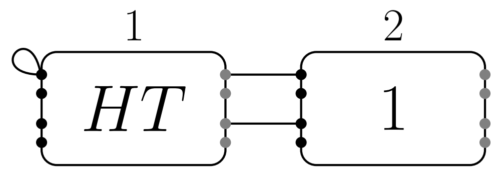


Figure 7.3: A gate diagram with two diagram elements labeled $q = 1$ (left) and $q = 2$ (right).

At this point, we now have several simple diagram elements, each of which has a well defined ground space, and that suffer an energy penalty when multiple particles occupy the same element (relative to the frustration-free case). We will be able to then combine these basic structures in such a way so that more complex interactions occur.

#### 7.2.1.3 Gate diagrams

While these simple diagram elements are useful, we will eventually want to construct much larger graphs. As such, it will be useful to have a diagramatic construction for these graphs. These shall be the gate diagrams.

The rules for constructing gate diagrams are simple. A gate diagram consists of some number $R \in \{1, 2, \ldots\}$ of diagram elements, with self-loops attached to a subset $\mathcal{S}$ of the nodes and edges connecting a set $\mathcal{E}$ of pairs of nodes. A node may have a single edge or a single self-loop attached to it, but never more than one edge or self-loop and never both an edge and a self-loop. Each node in a gate diagram has a label $(q, z, t)$ where $q \in [R]$ indicates the diagram element it belongs to. An example is shown in Figure 7.3.

Sometimes it is convenient to draw the input nodes on the right-hand side of a diagram element; e.g., in Figure 7.4 the node closest to the top left corner is labeled $(q, z, t) = (3, 0, 2)$.

To every gate diagram we associate a *gate graph* $G$ with vertex set

$$\{(q, z, t, j) \colon q \in [R],\ z \in \{0, 1\},\ t \in [8],\ j \in \{0, \ldots, 7\}\} \tag{7.80}$$

and adjacency matrix

$$A(G) = \sum_{q \in [R]} |\, q \,\rangle\langle\, q \,| \otimes A(G_q) + h_{\mathcal{S}} + h_{\mathcal{E}} \tag{7.81}$$

$$A(G_q) = A(G_{U_q}^{(a_q, b_q), (c_q, d_q)}) \tag{7.82}$$

$$h_{\mathcal{S}} = \sum_{\mathcal{S}} |q, z, t\rangle\langle q, z, t| \otimes \mathbb{I}_j \tag{7.83}$$

$$h_{\mathcal{E}} = \sum_{\mathcal{E}} \left(|q, z, t\rangle + |q', z', t'\rangle\right)\left(\langle q, z, t| + \langle q', z', t'|\right) \otimes \mathbb{I}_j. \tag{7.84}$$

The sums in equations (7.83) and (7.84) run over the set of nodes with self-loops $(q, z, t) \in \mathcal{S}$ and the set of pairs of nodes connected by edges $\{(q, z, t), (q', z', t')\} \in \mathcal{E}$, respectively. We write $\mathbb{I}_q$ and $\mathbb{I}_j$ for the identity operator on the registers with variables $q$ and $j$, respectively. We see from the above expression that each self-loop in the gate diagram corresponds to 16 self-loops in the graph $G$, and an edge in the gate diagram corresponds to 16 edges and 32 self-loops in $G$.

Since a node in a gate graph never has more than one edge or self-loop attached to it, equations (7.83) and (7.84) are sums of orthogonal Hermitian operators. Therefore

$$\|h_{\mathcal{S}}\| = \max_{\mathcal{S}} \||q,z,t\rangle\langle q,z,t| \otimes \mathbb{I}_j\| = 1 \quad \text{if } \mathcal{S} \neq \emptyset \tag{7.85}$$

$$\|h_{\mathcal{E}}\| = \max_{\mathcal{E}} \|(|q,z,t\rangle + |q',z',t'\rangle)(\langle q,z,t| + \langle q',z',t'|) \otimes \mathbb{I}_j\| = 2 \quad \text{if } \mathcal{E} \neq \emptyset \tag{7.86}$$

for any gate graph. (Of course, this also shows that $\|h_{\mathcal{S}'}\| = 1$ and $\|h_{\mathcal{E}'}\| = 2$ for any nonempty subsets $\mathcal{S}' \subseteq \mathcal{S}$ and $\mathcal{E}' \subseteq \mathcal{E}$.)

[**TO DO:** *fix frustration free stuff*]

### 7.2.2 Gadgets

In Example **??** we saw how a single-particle ground state can encode a single-qubit computation. In this Section we see how a two-particle frustration-free state on a suitably designed $e_1$-gate graph can encode a two-qubit computation. We design specific $e_1$-gate graphs (called *gadgets*) that we use in Section **??** to prove that these ground state problems for the MPQW are QMA-hard. For each gate graph we discuss, we show that the smallest eigenvalue of its adjacency matrix is $e_1$ and we solve for all of the frustration-free states.

We first design a gate graph where, in any two-particle frustration-free state, the locations of the particles are synchronized. This "move-together" gadget is presented in Section **??**. In Section **??**, we design gadgets for two-qubit gates using four move-together gadgets, one for each two-qubit computational basis state. Finally, in Section **??** we describe a small modification of a two-qubit gate gadget called the "boundary gadget."

The circuit-to-gate graph mapping described in Section **??** uses a two-qubit gate gadget for each gate in the circuit, together with boundary gadgets in parts of the graph corresponding to the beginning and end of the computation.

In important piece of these gadgets will be the inclusion of $\mathbb{I}_{(1,0)}^{(1,1)}$ diagram elements to separate the locations of particles, so as to ensure that certain states are in the ground space.

#### 7.2.2.1 The move-together gadget

The gate diagram for the *move-together gadget* is shown in Figure 7.4. Using equation (7.81), we write the adjacency matrix of the corresponding gate graph $G_W$ as

$$A(G_W) = \sum_{q=1}^{14} |q\rangle\langle q| \otimes A(G_q) + h_{\mathcal{E}} \tag{7.87}$$

where

$$G_q = \begin{cases} G_H^{(2,2),(1,1)} & q \in \{1,2\} \\ G_{\mathbb{I}}^{(1,1),(0,0)} & q \in \{3,4,5,6\} \\ G_{\mathbb{I}}^{(1,1),(1,0)} & q > 6, \end{cases} \tag{7.88}$$

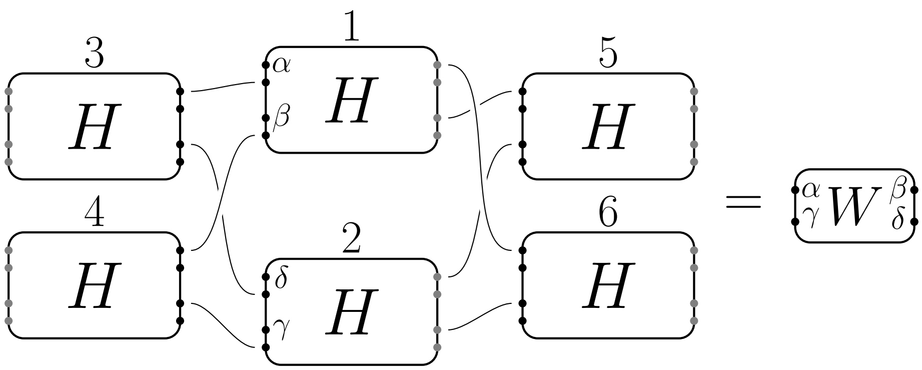


Figure 7.4: The gate diagram for the move-together gadget, assuming that $d_{\max} = 0$.

$h_{\mathcal{E}}$ is given by (7.84), $h_{\mathcal{S}}$ is given by (**??**), $\mathcal{E}$ is the set of edges in the gate diagram, and $\mathcal{S}$ is the set of self-loops in the diagram.

We begin by solving for the single-particle ground states, i.e., the eigenvectors of (7.87) with eigenvalue $e_1 = -1 - 3\sqrt{2}$. As in Example **??**, we can solve for the states with $a = 0$ and $a = 1$ separately, since

$$\langle \psi^{j}_{x,1} | h_{\mathcal{E}} | \psi^{i}_{z,0} \rangle = 0 \tag{7.89}$$

for all $i, j \in [14]$ and $x, z \in \mathbb{F}_2$. We write a single-particle ground state as

$$\sum_{i=1}^{14} \left( \tau_i |\psi^{i}_{0,a}\rangle + \nu_i |\psi^{i}_{1,a}\rangle \right) \tag{7.90}$$

and solve for the coefficients $\tau_i$ and $\nu_i$ using equation (**??**) (in this case equation (**??**) is automatically satisfied since $h_{\mathcal{S}} = 0$). Enforcing (**??**) gives sixteen equations, one for each edge in the gate diagram:

$$\tau_3 = -\tau_7 \qquad \tau_7 = -\tau_1 \qquad \frac{1}{\sqrt{2}}(\tau_1 + \nu_1) = -\tau_{11} \qquad \tau_{11} = -\tau_6 \tag{7.91}$$

$$\nu_3 = -\tau_9 \qquad \tau_9 = -\tau_2 \qquad \frac{1}{\sqrt{2}}(\tau_2 + \nu_2) = -\tau_{13} \qquad \tau_{13} = -\nu_5 \tag{7.92}$$

$$\tau_4 = -\tau_8 \qquad \tau_8 = -\nu_1 \qquad \frac{1}{\sqrt{2}}(\tau_1 - \nu_1) = -\tau_{12} \qquad \tau_{12} = -\tau_5 \tag{7.93}$$

$$\nu_3 = -\tau_{10} \qquad \tau_{10} = -\nu_2 \qquad \frac{1}{\sqrt{2}}(\tau_2 - \nu_2) = -\tau_{14} \qquad \tau_{14} = -\nu_6. \tag{7.94}$$

Similarly, enforcing (**??**) gives eight equations, namely that $\nu_q = 0$ for $q > 6$. There are four linearly independent solutions to this set of equations, given by

$$\textit{Solution 1:}\quad \tau_1 = \tau_3 = -\tau_7 = 1 \quad \tau_5 = \tau_6 = -\tau_{11} = -\tau_{12} = \frac{1}{\sqrt{2}} \quad \text{all other coefficients 0} \tag{7.95}$$

$$\textit{Solution 2:}\quad \nu_1 = \tau_4 = -\tau_8 = 1 \quad -\tau_5 = \tau_6 = -\tau_{11} = \tau_{12} = \frac{1}{\sqrt{2}} \quad \text{all other coefficients 0} \tag{7.96}$$

$$\textit{Solution 3:}\quad \nu_2 = \nu_4 = -\tau_{10} = 1 \quad \nu_5 = -\nu_6 = -\tau_{13} = \tau_{14} = \frac{1}{\sqrt{2}} \quad \text{all other coefficients 0} \tag{7.97}$$

$$\textit{Solution 4:}\quad \tau_2 = \nu_3 = -\tau_9 = 1 \quad \nu_5 = \nu_6 = -\tau_{13} = -\tau_{14} = \frac{1}{\sqrt{2}} \quad \text{all other coefficients 0.} \tag{7.98}$$

For each of these solutions, and for each $a \in \{0, 1\}$, we find a single-particle state with energy $e_1$. This result is summarized in the following Lemma.

**Lemma 16.** *$G_W$ is an $e_1$-gate graph. A basis for the eigenspace of $A(G_W)$ with eigenvalue $e_1$ is*

$$|\chi_{1,a}\rangle = \frac{1}{\sqrt{5}}\big(|\psi^1_{0,a}\rangle + |\psi^3_{0,a}\rangle - |\psi^7_{0,a}\rangle\big) + \frac{1}{\sqrt{10}}\big(|\psi^5_{0,a}\rangle + |\psi^6_{0,a}\rangle - |\psi^{11}_{0,a}\rangle - |\psi^{12}_{0,a}\rangle\big) \tag{7.99}$$

$$|\chi_{2,a}\rangle = \frac{1}{\sqrt{5}}\big(|\psi^1_{1,a}\rangle + |\psi^4_{0,a}\rangle - |\psi^8_{0,a}\rangle\big) + \frac{1}{\sqrt{10}}\big(-|\psi^5_{0,a}\rangle + |\psi^6_{0,a}\rangle - |\psi^{11}_{0,a}\rangle + |\psi^{12}_{0,a}\rangle\big) \tag{7.100}$$

$$|\chi_{3,a}\rangle = \frac{1}{\sqrt{5}}\big(|\psi^2_{1,a}\rangle + |\psi^4_{1,a}\rangle - |\psi^{10}_{0,a}\rangle\big) + \frac{1}{\sqrt{10}}\big(|\psi^5_{1,a}\rangle - |\psi^6_{1,a}\rangle - |\psi^{13}_{0,a}\rangle + |\psi^{14}_{0,a}\rangle\big) \tag{7.101}$$

$$|\chi_{4,a}\rangle = \frac{1}{\sqrt{5}}\big(|\psi^2_{0,a}\rangle + |\psi^3_{1,a}\rangle - |\psi^9_{0,a}\rangle\big) + \frac{1}{\sqrt{10}}\big(|\psi^5_{1,a}\rangle + |\psi^6_{1,a}\rangle - |\psi^{13}_{0,a}\rangle - |\psi^{14}_{0,a}\rangle\big) \tag{7.102}$$

*where $a \in \mathbb{F}_2$.*

In Figure 7.4 we have used a shorthand $\alpha, \beta, \gamma, \delta$ to identify four nodes of the move-together gadget; these are the nodes with labels $(q, z, t) = (1, 0, 1), (1, 1, 1), (2, 1, 1), (2, 0, 1)$, respectively. We view $\alpha$ and $\gamma$ as "input" nodes and $\beta$ and $\delta$ as "output" nodes for this gate diagram. It is natural to associate each single-particle state $|\chi_{i,a}\rangle$ with one of these four nodes. We also associate the set of 8 vertices represented by the node with the corresponding node, e.g.,

$$S_\alpha = \{(1, 0, 1, j) \colon j \in \{0, \ldots, 7\}\}\,. \tag{7.103}$$

Looking at equation (7.99) (and perhaps referring back to equation (7.32)) we see that $|\chi_{1,a}\rangle$ has support on vertices in $S_\alpha$ but not on vertices in $S_\beta$, $S_\gamma$, or $S_\delta$. Looking at the picture on the right-hand side of the equality sign in Figure 7.4, we think of $|\chi_{1,a}\rangle$ as localized at the node $\alpha$, with no support on the other three nodes. The states $|\chi_{2,a}\rangle, |\chi_{3,a}\rangle, |\chi_{4,a}\rangle$ are similarly localized at nodes $\beta, \gamma, \delta$. We view $|\chi_{1,a}\rangle$ and $|\chi_{3,a}\rangle$ as input states and $|\chi_{2,a}\rangle$ and $|\chi_{4,a}\rangle$ as output states.

Now we turn our attention to the two-particle frustration-free states of the move-together gadget, i.e., the states $|\Phi\rangle \in \mathcal{Z}_2(G_W)$ in the nullspace of $H(G_W, 2)$. As $\lambda_2^1(G_U) > 0$ for all $U$, we have that any such state must take the form

$$|\Phi\rangle = \sum_{a,b\in\{0,1\},\, I,J\in[4]} C_{(I,a),(J,b)}|\chi_{I,a}\rangle|\chi_{J,b}\rangle \tag{7.104}$$

where the coefficients are symmetric, i.e.,

$$C_{(I,a),(J,b)} = C_{(J,b),(I,a)}, \tag{7.105}$$

and where

$$\langle\psi^q_{z,a}|\langle\psi^q_{x,b}|\Phi\rangle = 0 \tag{7.106}$$

for all $z, a, x, b \in \{0, 1\}$ and $q \in [14]$. Note that this does not guarantee that the state is frustration-free, merely that these are necessary conditions for the state to be frustration free.

However, in the construction of the $G_W$ gadget, we placed the $H^{(1,1)}_{(1,0)}$ elements specifically to ensure that the two-particle states were separated by a distance of at least $k > d_{\min}$. If we can ensure that the state $|\,\Phi\,\rangle$ has no support on pairs of diagram elements that are closer than $k > d_{\max}$, then we can guarantee that $|\,\Phi\,\rangle$ is frustration-free.

The move-together gadget is designed so that each solution $|\Phi\rangle$ to these equations is a superposition of a term where both particles are in input states and a term where both particles are in output states. The particles move from input nodes to output nodes together. We now solve equations (7.104)–(7.106) and prove the following.

**Lemma 17.** *A basis for the nullspace of $H(G_W, 2)$ is*

$$|\Phi_{a,b}\rangle = \mathrm{Sym}\left(\frac{1}{\sqrt{2}}|\chi_{1,a}\rangle|\chi_{3,b}\rangle + \frac{1}{\sqrt{2}}|\chi_{2,a}\rangle|\chi_{4,b}\rangle\right), \quad a, b \in \{0, 1\}. \tag{7.107}$$

*There are no $N$-particle frustration-free states on $G_W$ for $N \geq 3$, i.e.,*

$$\lambda^1_N(G_W) > 0 \quad \textit{for } N \geq 3. \tag{7.108}$$

*Proof.* The states $|\Phi_{a,b}\rangle$ manifestly satisfy equations (7.104) and (7.105), and one can directly verify that they also satisfy (7.106) (the nontrivial cases to check are for $q = 5$, $q = 6$, and $q > 10$). Additionally, one can also directly verify that $|\,\Phi_{a,b}\,\rangle$ has no support on states for which the two particles are located on diagram elements closer than $k$, and thus the state is in the ground space of the interaction Hamiltonian, and thus is frustration-free.

To complete the proof that (7.107) is a basis for the nullspace of $H(G_W, 2)$, we verify that any state satisfying these conditions must be a linear combination of these four states. Applying equation (7.106) to the first 4 diagram elements gives

$$\langle\psi^1_{0,a}|\langle\psi^1_{0,b}|\Phi\rangle = \frac{1}{5}C_{(1,a),(1,b)} = 0 \qquad \langle\psi^1_{1,a}|\langle\psi^1_{1,b}|\Phi\rangle = \frac{1}{5}C_{(2,a),(2,b)} = 0 \tag{7.109}$$

$$\langle\psi^2_{1,a}|\langle\psi^2_{1,b}|\Phi\rangle = \frac{1}{5}C_{(3,a),(3,b)} = 0 \qquad \langle\psi^2_{0,a}|\langle\psi^2_{0,b}|\Phi\rangle = \frac{1}{5}C_{(4,a),(4,b)} = 0 \tag{7.110}$$

$$\langle\psi^1_{0,a}|\langle\psi^1_{1,b}|\Phi\rangle = \frac{1}{5}C_{(1,a),(2,b)} = 0 \qquad \langle\psi^2_{0,a}|\langle\psi^2_{1,b}|\Phi\rangle = \frac{1}{5}C_{(4,a),(3,b)} = 0 \tag{7.111}$$

$$\langle\psi^3_{0,a}|\langle\psi^3_{1,b}|\Phi\rangle = \frac{1}{5}C_{(1,a),(4,b)} = 0 \qquad \langle\psi^4_{0,a}|\langle\psi^4_{1,b}|\Phi\rangle = \frac{1}{5}C_{(2,a),(3,b)} = 0 \tag{7.112}$$

for all $a, b \in \{0, 1\}$. Using the fact that all of these coefficients are zero, and using equation (7.105), we get

$$|\Phi\rangle = \sum_{a,b\in\{0,1\}} \left(C_{(1,a),(3,b)} \left(|\chi_{1,a}\rangle|\chi_{3,b}\rangle + |\chi_{3,b}\rangle|\chi_{1,a}\rangle\right) + C_{(2,a),(4,b)} \left(|\chi_{2,a}\rangle|\chi_{4,b}\rangle + |\chi_{4,b}\rangle|\chi_{2,a}\rangle\right)\right). \tag{7.113}$$

Finally, applying equation (7.106) again gives

$$\langle\psi^6_{0,a}|\langle\psi^6_{1,b}|\Phi\rangle = \frac{1}{6}C_{(2,a),(4,b)} - \frac{1}{6}C_{(1,a),(3,b)} = 0. \tag{7.114}$$

Hence

$$|\Phi\rangle = \sum_{a,b\in\{0,1\}} C_{(1,a),(3,b)} \left(|\chi_{1,a}\rangle|\chi_{3,b}\rangle + |\chi_{3,b}\rangle|\chi_{1,a}\rangle + |\chi_{2,a}\rangle|\chi_{4,b}\rangle + |\chi_{4,b}\rangle|\chi_{2,a}\rangle\right), \tag{7.115}$$

which is a superposition of the states $|\Phi_{a,b}\rangle$.

Finally, we prove that there are no frustration-free ground states of the Bose-Hubbard model on $G_W$ with more than two particles. By Lemma **??**, it suffices to prove that there are no frustration-free three-particle states.

Suppose (for a contradiction) that $|\Gamma\rangle \in \mathcal{Z}_3(G_W)$ is a normalized three-particle frustration-free state. Write

$$|\Gamma\rangle = \sum D_{(i,a),(j,b),(k,c)}|\chi_{i,a}\rangle|\chi_{j,b}\rangle|\chi_{k,c}\rangle. \tag{7.116}$$

Note that each reduced density matrix of $|\Gamma\rangle$ on two of the three subsystems must have all of its support on two-particle frustration-free states (see the remark following Lemma **??**), i.e., on the states $|\Phi_{a,b}\rangle$. Using this fact for the subsystem consisting of the first two particles, we see in particular that

$$(i, j) \notin \{(1, 3), (3, 1), (2, 4), (4, 2)\} \quad \Longrightarrow \quad D_{(i,a),(j,b),(k,c)} = 0 \tag{7.117}$$

(since $|\Phi_{a_1,a_2}\rangle$ only has support on vectors $|\chi_{i,a}\rangle|\chi_{j,b}\rangle$ with $i, j \in \{(1, 3), (3, 1), (2, 4), (4, 2)\}$).

Using this fact for subsystems consisting of particles $2, 3$ and $1, 3$, respectively, gives

$$(j, k) \notin \{(1, 3), (3, 1), (2, 4), (4, 2)\} \quad \Longrightarrow \quad D_{(i,a),(j,b),(k,c)} = 0 \tag{7.118}$$

$$(i, k) \notin \{(1, 3), (3, 1), (2, 4), (4, 2)\} \quad \Longrightarrow \quad D_{(i,a),(j,b),(k,c)} = 0. \tag{7.119}$$

Putting together equations (7.117), (7.118), and (7.119), we see that $|\Gamma\rangle = 0$. This is a contradiction, so no three-particle frustration-free states exist. □

With this gadget allowing us to entangle the locations of particles, we will be able to create a pseudo history state, in which time is encoded in the location of particles. This is the large workhorse of the construction, as this allows us to understand the multi-particle ground space by understanding the simple two-particle ground states.

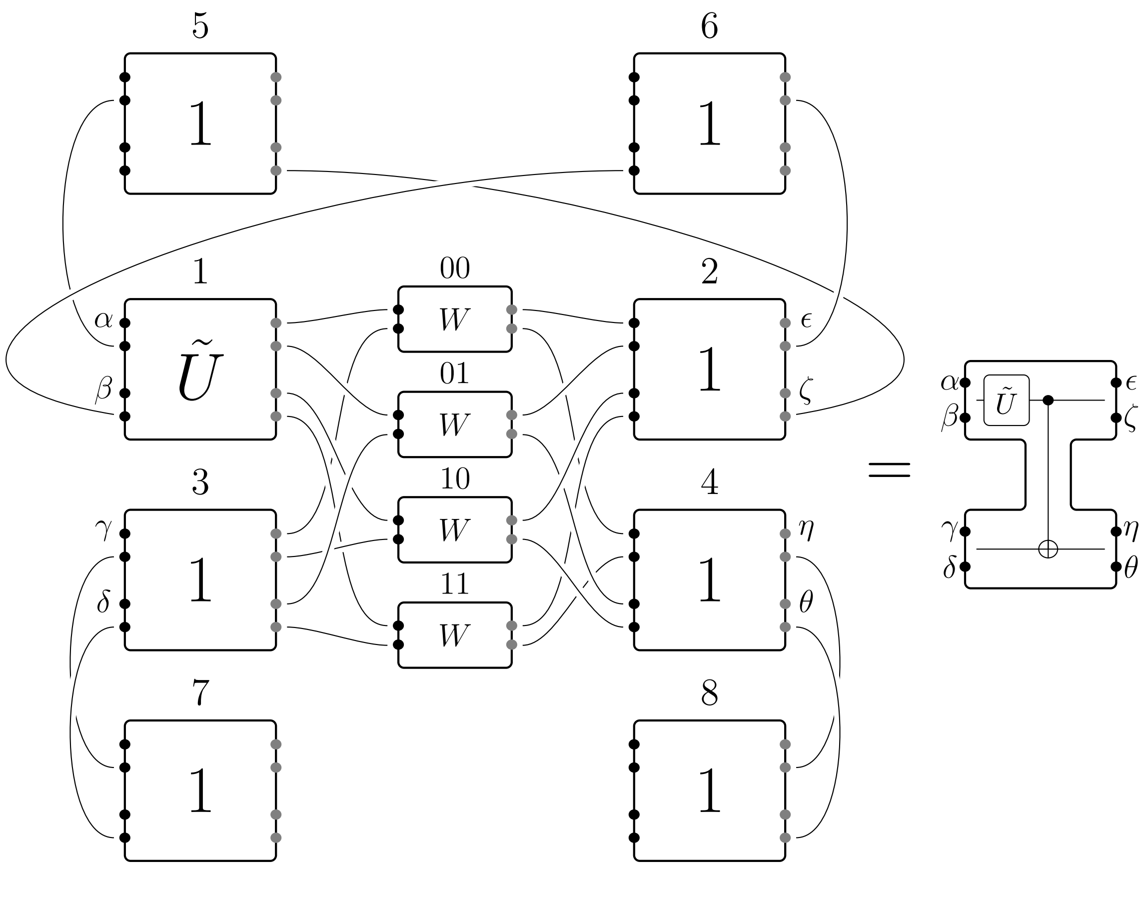


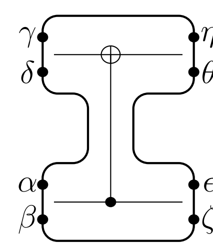


Figure 7.5: (a) Gadget for the two-qubit unitary $U = (\tilde{U} \otimes \mathbb{I})\mathrm{CNOT}_{12}$ with $\tilde{U} \in \{1, H, HT\}$. (b) For the $U = \mathrm{CNOT}_{21}$ gate (first qubit is the target), we use the same gate graph as in (a) with $\tilde{U} = 1$; we represent it schematically as shown.

#### 7.2.2.2 Two-qubit gate gadget

With the previous construction of a gadget that has a well defined, and entangled, two-qubit ground state, we will be to define a gate graph for each of the two-qubit unitaries

$$\{\mathrm{CNOT}_{12}, \mathrm{CNOT}_{21}, \mathrm{CNOT}_{12}\left(H \otimes \mathbb{I}\right), \mathrm{CNOT}_{12}\left(HT \otimes \mathbb{I}\right)\}. \tag{7.120}$$

Here $\mathrm{CNOT}_{12}$ is the standard controlled-not gate with the second qubit as a target, whereas $\mathrm{CNOT}_{21}$ has the first qubit as target.

We define the gate graphs by exhibiting their gate diagrams. For the three cases

$$U = \mathrm{CNOT}_{12}(\tilde{U} \otimes \mathbb{I}) \tag{7.121}$$

with $\tilde{U} \in \{\mathbb{I}, H, HT\}$, we associate $U$ with the gate diagram shown in Figure 7.5a. In the Figure we also indicate a shorthand used to represent this gate diagram. As one might expect, for the case $U = \text{CNOT}_{21}$, we use the same gate diagram as for $U = \text{CNOT}_{12}$; however, we use the slightly different shorthand shown in Figure 7.5b.

Roughly speaking, the two-qubit gate gadgets work as follows. In Figure 7.5a there are four move-together gadgets, one for each two-qubit basis state $|00\rangle, |01\rangle, |10\rangle, |11\rangle$. These enforce the constraint that two particles must move through the graph together. The connections between the four diagram elements labeled $1, 2, 3, 4$ and the move-together gadgets ensure that certain frustration-free two-particle states encode two-qubit computations, while the connections between diagram elements $1, 2, 3, 4$ and $5, 6, 7, 8$ ensure that there are no additional frustration-free two-particle states (i.e., states that do not encode computations).

To describe the frustration-free states of the gate graph depicted in Figure 7.5a, first recall the definition of the states $|\chi_{1,a}\rangle, |\chi_{2,a}\rangle, |\chi_{3,a}\rangle, |\chi_{4,a}\rangle$ from equations (7.99)–(7.102). For each of the move-together gadgets $xy \in \{00, 01, 10, 11\}$ in Figure 7.5a, write

$$|\chi_{L,a}^{xy}\rangle \tag{7.122}$$

for the state $|\chi_{L,a}\rangle$ with support (only) on the gadget labeled $xy$. Write

$$U(a) = \begin{cases} U & \text{if } a = 0 \\ U^* & \text{if } a = 1 \end{cases} \tag{7.123}$$

and similarly for $\tilde{U}$ (we use this notation throughout the paper to indicate a unitary or its elementwise complex conjugate).

We now prove the following Lemma, which shows that $G_U$ is an $e_1$-gate graph and solves for its frustration-free states.

**Lemma 18.** *Let $U = \text{CNOT}_{12}(\tilde{U} \otimes \mathbb{I})$ where $\tilde{U} \in \{\mathbb{I}, H, HT\}$. The corresponding gate graph $G_U$ is defined by its gate diagram shown in Figure 7.5a. The adjacency matrix $A(G_U)$ has ground energy $e_1$; a basis for the corresponding eigenspace is*

$$|\rho_{z,a}^{1,U}\rangle = \frac{1}{\sqrt{12}}|\psi_{z,a}^{1}\rangle - \frac{1}{\sqrt{12}}|\psi_{z,a}^{5+z}\rangle - \sqrt{\frac{5}{12}}\sum_{x,y=0}^{1} \tilde{U}(a)_{yz}|\chi_{1,a}^{yx}\rangle \tag{7.124}$$

$$|\rho_{z,a}^{2,U}\rangle = \frac{1}{\sqrt{12}}|\psi_{z,a}^{2}\rangle - \frac{1}{\sqrt{12}}|\psi_{z,a}^{6-z}\rangle - \sqrt{\frac{5}{12}}\sum_{x=0}^{1} |\chi_{2,a}^{zx}\rangle \tag{7.125}$$

$$|\rho_{z,a}^{3,U}\rangle = \frac{1}{\sqrt{12}}|\psi_{z,a}^{3}\rangle - \frac{1}{\sqrt{12}}|\psi_{z,a}^{7}\rangle - \sqrt{\frac{5}{12}}\sum_{x=0}^{1} |\chi_{3,a}^{xz}\rangle \tag{7.126}$$

$$|\rho_{z,a}^{4,U}\rangle = \frac{1}{\sqrt{12}}|\psi_{z,a}^{4}\rangle - \frac{1}{\sqrt{12}}|\psi_{z,a}^{8}\rangle - \sqrt{\frac{5}{12}}\sum_{x=0}^{1} |\chi_{4,a}^{x(z\oplus x)}\rangle \tag{7.127}$$

*where $z, a \in \{0, 1\}$.*

*Proof.* As the gate graph $G_U$ is specified by its gate diagram, shown in Figure 7.5a, the adjacency matrix of the gate graph $G_U$ is of the form in equation (7.81). There are 14 diagram elements for each of the move-together gadgets, so there are 64 diagram elements in total. We will need to refer to those diagram elements labeled $q \in [8]$ in Figure 7.5a (i.e., those not contained in the move-together gadgets).

Write

$$A(G_U) = A(G'_U) + h_{\mathcal{E}'} \tag{7.128}$$

where $G'_U$ is the gate graph obtained from $G_U$ by removing all 24 edges shown in Figure 7.5a ($G'_U$ does include the edges within each of the move-together gadgets). Here $h_{\mathcal{E}'}$ is given by equation (7.84) with $\mathcal{E}'$ the set of 24 edges shown in Figure 7.5a.

One basis for the $e_1$-energy ground space of $A(G'_U)$ is given by the 64 states

$$|\psi^q_{z,a}\rangle, \quad q \in [8],\ z, a \in \{0,1\} \tag{7.129}$$

$$|\chi^{xy}_{L,a}\rangle, \quad x, y, a \in \{0,1\},\ L \in [4]. \tag{7.130}$$

However, it is convenient to work with the following slightly different basis for this space:

$$|\psi^q_{z,a}\rangle, \quad q \in [8],\ z, a \in \{0,1\} \tag{7.131}$$

$$\sum_{x\in\{0,1\}} \tilde{U}(a)_{xz} |\chi^{xy}_{1,a}\rangle, \quad y, z, a \in \{0,1\} \tag{7.132}$$

$$|\chi^{xy}_{L,a}\rangle, \quad x, y, a \in \{0,1\},\ L \in \{2,3,4\}. \tag{7.133}$$

Here some of the states are in a superposition corresponding to the output of the single-qubit unitary $\tilde{U}$.

We are interested in the intersection of the ground space of $A(G'_U)$ with the nullspace of $h_{\mathcal{E}'}$, so we compute the matrix elements of $h_{\mathcal{E}'}$ in the above basis. The resulting $64 \times 64$ matrix is block diagonal with sixteen $4 \times 4$ blocks. Each block is identical, with entries

$$\begin{pmatrix} \frac{3}{2k} & \frac{1}{2k} & \frac{1}{2k\sqrt{5}} & \frac{1}{2k\sqrt{5}} \\ \frac{1}{2k} & \frac{1}{2k} & 0 & 0 \\ \frac{1}{2k\sqrt{5}} & 0 & \frac{1}{10k} & 0 \\ \frac{1}{2k\sqrt{5}} & 0 & 0 & \frac{1}{10k} \end{pmatrix}. \tag{7.134}$$

The four states involved in each block are given by (in order from left to right as in the matrix above):

$$|\psi^1_{z,a}\rangle, |\psi^{5+z}_{z,a}\rangle, \sum_{x\in\{0,1\}} \tilde{U}(a)_{xz} |\chi^{x0}_{1,a}\rangle, \sum_{x\in\{0,1\}} \tilde{U}(a)_{xz} |\chi^{x1}_{1,a}\rangle \tag{7.135}$$

$$|\psi^2_{z,a}\rangle, |\psi^{6-z}_{z,a}\rangle, |\chi^{z0}_{2,a}\rangle, |\chi^{z1}_{2,a}\rangle \tag{7.136}$$

$$|\psi^3_{z,a}\rangle, |\psi^7_{z,a}\rangle, |\chi^{0z}_{3,a}\rangle, |\chi^{1z}_{3,a}\rangle \tag{7.137}$$

$$|\psi^4_{z,a}\rangle, |\psi^8_{z,a}\rangle, |\chi^{0z}_{4,a}\rangle, |\chi^{1(z\oplus 1)}_{4,a}\rangle. \tag{7.138}$$

The unique zero eigenvector of the matrix (7.134) is

$$\frac{1}{\sqrt{12}} \begin{pmatrix} 1 \\ -1 \\ -\sqrt{5} \\ -\sqrt{5} \end{pmatrix}. \tag{7.139}$$

Constructing this vector within each of the 16 blocks, we get the states found in the lemma. ☐

We view the nodes labeled $\alpha, \beta, \gamma, \delta$ in Figure 7.5a as "input" nodes and those labeled $\epsilon, \zeta, \eta, \theta$ as "output nodes". Each of the states $|\rho_{x,y}^{i,U}\rangle$ is associated with one of the nodes, depending on the values of $i \in \{1,2,3,4\}$ and $x \in \{0,1\}$. For example, the states $|\rho_{0,0}^{1,U}\rangle$ and $|\rho_{0,1}^{1,U}\rangle$ are associated with input node $\alpha$ since they both have nonzero amplitude on vertices of the gate graph that are associated with $\alpha$ (and zero amplitude on vertices associated with other labeled nodes).

With the single particle states found, we now turn our attention to the two-particle states. It will turn out that the two particle eigenstates of the W-gadget found in Lemma 17 will play a critical part in our construction.

**Lemma 19.** *A basis for the nullspace of $H(G_U, 2)$ is*

$$\mathrm{Sym}(|T_{z_1,a,z_2,b}^{U}\rangle), \quad z_1, z_2, a, b \in \{0,1\} \tag{7.140}$$

*where*

$$|T_{z_1,a,z_2,b}^{U}\rangle = \frac{1}{\sqrt{2}}|\rho_{z_1,a}^{1,U}\rangle|\rho_{z_2,b}^{3,U}\rangle + \frac{1}{\sqrt{2}}\sum_{x_1,x_2=0}^{1} U(a)_{x_1x_2,z_1z_2}|\rho_{x_1,a}^{2,U}\rangle|\rho_{x_2,b}^{4,U}\rangle \tag{7.141}$$

*for $z_1, z_2, a, b \in \{0,1\}$. There are no $N$-particle frustration-free states on $G_U$ for $N \geq 3$, i.e.,*

$$\lambda_N^1(G_U) > 0 \quad \textit{for } N \geq 3. \tag{7.142}$$

*Proof.* Let us first show that the states $|T_{z_1,a,z_2,b}^{U}\rangle$ are contained within the nullspace of $H(G_U, 2)$. By definition, they satisfy equations (7.104) and (7.105). If we then expand these states in terms of the $|\psi_{z,a}^{q}\rangle$ for $q \in [8]$ and $|\chi_{j,a}^{xy}\rangle$, we can then simply check to see that the states $|T_{z_1,a,z_2,b}^{U}\rangle$ have no support on states for which particles are located closer than $k > d_{\max}$. In particular, note that whenever at least one particle is in state $|\psi_{z,a}^{q}\rangle$, the other particle is located either on a diagram element that is only connected to the first through nodes of the W-gadgets that have a distance of much more than $k$, or else the other particle is supported on states in the W-gadget that have support only on vertices at a distance of more than $k$ from the closest input node to the original particle. The only difficult case to check is when both particles are in the W-gadget, but the structure of the states $|T_{z_1,a,z_2,b}^{U}\rangle$ are such that either both particle are in different W-gadgets (and further on states with support at a distance much larger than $k$), or the two particles are in a state within the span of $|\Phi_{a,b}\rangle$. Using this, we have that the states $|T_{z_1,a,z_2,b}^{U}\rangle$ are in the nullspace of the interaction Hamiltonian, and thus are frustration-free.

Now let us show that any state in the nullspace of $H(G_U, 2)$ are within the span of the states $|T_{z_1,a,z_2,b}^{U}\rangle$. Using Lemma **??** we can write any two-particle frustration-free state as

$$|\Theta\rangle = \sum_{z,a,x,b \in \{0,1\}} \sum_{I,J \in [4]} B_{(z,a,I),(x,b,J)}|\rho_{z,a}^{I,U}\rangle|\rho_{x,b}^{J,U}\rangle \tag{7.143}$$

where

$$B_{(z,a,I),(x,b,J)} = B_{(x,b,J),(z,a,I)} \tag{7.144}$$

and

$$\langle\psi^q_{x,a}|\langle\psi^q_{z,b}|\Theta\rangle = 0 \tag{7.145}$$

for all $x, z, a, b \in \{0,1\}$ and $q \in [64]$. To enforce equation (7.145) we consider the diagram elements $q \in [8]$ (as labeled in Figure 7.5a) separately from the other 24 diagram elements (those inside the move-together gadgets).

Using equation (7.145) with $q \in \{1,2,3,4,7,8\}$ and $x, z, a, b \in \{0,1\}$ gives

$$B_{(x,a,I),(z,b,I)} = 0 \quad I \in [4],\ x, z, a, b \in \{0,1\}. \tag{7.146}$$

Using $q = 5$, $x = 0$, and $z = 1$ in equation (7.145) gives

$$\langle\psi^5_{0,a}|\langle\psi^5_{1,b}|\Theta\rangle = \frac{1}{8}B_{(0,a,1),(1,b,2)} = 0, \tag{7.147}$$

for $a, b \in \{0,1\}$, while $q = 6$, $x = 0$, and $z = 1$ gives

$$\langle\psi^6_{0,a}|\langle\psi^6_{1,b}|\Theta\rangle = \frac{1}{8}B_{(0,a,2),(1,b,1)} = 0. \tag{7.148}$$

Applying equation (7.145) with $q = 5$ or $q = 6$ and other choices for $x$ and $z$ does not lead to any additional independent constraints on the state $|\Theta\rangle$.

Now consider the constraint (7.145) for diagram elements inside the move-together gadgets in Figure 7.5a. Let $\Pi_{xy}$ be the projector onto two-particle states where both particles are located at vertices contained within the move-together gadget labeled $xy \in \{00, 01, 10, 11\}$. Using the results of Lemma 17, we see that for diagram elements inside the move-together gadgets, (7.145) is satisfied if and only if

$$\Pi_{xy}|\Theta\rangle \in \operatorname{span}\big\{\mathrm{Sym}\left(|\chi^{xy}_{1,a}\rangle|\chi^{xy}_{3,b}\rangle + |\chi^{xy}_{2,a}\rangle|\chi^{xy}_{4,b}\rangle\right),\ a, b \in \{0,1\}\big\}. \tag{7.149}$$

Since we already know

$$\Pi_{xy}|\Theta\rangle \in \operatorname{span}\big\{\mathrm{Sym}\left(|\chi^{xy}_{i,a}\rangle|\chi^{xy}_{j,b}\rangle\right),\ i, j \in [4], a, b \in \{0,1\}\big\} \tag{7.150}$$

we get

$$\langle\chi^{xy}_{K,a}|\langle\chi^{xy}_{K,b}|\Theta\rangle = 0 \quad K \in [4] \tag{7.151}$$

$$\langle\chi^{xy}_{K,a}|\langle\chi^{xy}_{L,b}|\Theta\rangle = 0 \quad (K, L) \in \{(1,2), (2,3), (3,4), (1,4)\} \tag{7.152}$$

$$\big(\langle\chi^{xy}_{1,a}|\langle\chi^{xy}_{3,b}| - \langle\chi^{xy}_{2,a}|\langle\chi^{xy}_{4,b}|\big)|\Theta\rangle = 0 \tag{7.153}$$

for all $a, b \in \{0,1\}$. Note that (7.151) is automatically satisfied whenever (7.146) holds.

Applying equation (7.152) with $(K, L) = (1,2)$ and $a, b, x, y \in \{0,1\}$, we get

$$\langle\chi^{xy}_{1,a}|\langle\chi^{xy}_{2,b}|\Theta\rangle = \frac{3}{8}\sum_{z\in\{0,1\}}\tilde{U}(a)_{xz}B_{(z,a,1),(x,b,2)} = \frac{3}{8}\tilde{U}(a)_{xx}B_{(x,a,1),(x,b,2)} = 0. \tag{7.154}$$

In the second equality we used the fact that $B_{(z,a,1),(x,b,2)}$ is zero whenever $z \neq x$ (from equations (7.144), (7.147), and (7.148)). Since $\tilde{U} \in \{1, H, HT\}$ we have $\tilde{U}(a)_{xx} \neq 0$, and it follows that

$$B_{(x,a,1),(x,b,2)} = 0 \tag{7.155}$$

for all $x, a, b \in \{0,1\}$.

Applying equation (7.152) with $(K, L) = (1, 4)$ gives

$$\langle \chi^{xy}_{1,a} | \langle \chi^{xy}_{4,b} | \Theta \rangle = \frac{3}{8} \sum_{z \in \{0,1\}} \tilde{U}(a)_{xz} B_{(z,a,1),(x \oplus y,b,4)} = 0 \qquad x, y, a, b \in \{0,1\}. \tag{7.156}$$

By taking appropriate combinations of these equations, we have

$$\sum_{x \in \{0,1\}} \tilde{U}(a)^{\dagger}_{wx} \langle \chi^{x(y\oplus x)}_{1,a} | \langle \chi^{x(y \oplus x)}_{4,b} | \Theta \rangle = B_{(w,a,1),(y,b,4)} = 0 \qquad w, y, a, b \in \{0,1\}. \tag{7.157}$$

Applying equation (7.152) with $(K, L) = (2, 3)$ and $(K, L) = (3, 4)$ gives

$$\langle \chi^{xy}_{2,a} | \langle \chi^{xy}_{3,b} | \Theta \rangle = \frac{3}{8} B_{(x,a,2),(y,b,3)} = 0 \tag{7.158}$$

$$\langle \chi^{xy}_{3,a} | \langle \chi^{xy}_{4,b} | \Theta \rangle = \frac{3}{8} B_{(x,a,3),(x \oplus y,b,4)} = 0 \tag{7.159}$$

for all $x, y, a, b \in \{0,1\}$.

Now putting together equations (7.146), (7.147), (7.148), (7.155), (7.157), (7.158), and (7.159) (and using the symmetrization (7.144)), we get

$$B_{(x,a,I),(z,b,J)} = 0 \quad \text{for all } x, z, a, b \in \{0,1\}, \text{ where } I = J \text{ or } \{I, J\} \in \big\{\{1,2\}, \{1,4\}, \{2,3\}, \{3,4\}\big\}, \tag{7.160}$$

so

$$|\Theta\rangle = \sum_{z,c,w,d \in \{0,1\}} B_{(z,c,1),(w,d,3)} \left( |\rho^{1,U}_{z,c}\rangle |\rho^{3,U}_{w,d}\rangle + |\rho^{3,U}_{w,d}\rangle |\rho^{1,U}_{z,c}\rangle \right) + B_{(z,c,2),(w,d,4)} \left( |\rho^{2,U}_{z,c}\rangle |\rho^{4,U}_{w,d}\rangle + |\rho^{4,U}_{w,d}\rangle |\rho^{2,U}_{z,c}\rangle \right). \tag{7.161}$$

Now

$$\langle \chi^{xy}_{1,a} | \langle \chi^{xy}_{3,b} | \rho^{1,U}_{z,c}\rangle |\rho^{3,U}_{w,d}\rangle = \frac{3}{8} \delta_{a,c} \delta_{b,d} \tilde{U}(a)_{xz} \delta_{y,w} \tag{7.162}$$

$$\langle \chi^{xy}_{2,a} | \langle \chi^{xy}_{4,b} | \rho^{2,U}_{z,c}\rangle |\rho^{4,U}_{w,d}\rangle = \frac{3}{8} \delta_{a,c} \delta_{b,d} \delta_{x,z} \delta_{y,w \oplus x}, \tag{7.163}$$

so enforcing equation (7.153) gives

$$\sum_{z \in \{0,1\}} \tilde{U}(a)_{xz} B_{(z,a,1),(y,b,3)} = B_{(x,a,2),(x \oplus y,b,4)} \tag{7.164}$$

for each $x, y, a, b \in \{0,1\}$. In other words

$$B_{(z,c,2),(w,d,4)} = \sum_{x \in \{0,1\}} \tilde{U}(c)_{zx} B_{(x,c,1),(z \oplus w,d,3)} = \sum_{x,y \in \{0,1\}} U(c)_{zw,xy} B_{(x,c,1),(y,d,3)} \tag{7.165}$$

where we used $U(a) = \mathrm{CNOT}_{12}(\tilde{U}(a) \otimes 1)$. Plugging this into (7.161) gives

$$|\Theta\rangle = \sum_{z,c,w,d\in\{0,1\}} \Bigg( B_{(z,c,1),(w,d,3)} \left( |\rho^{1,U}_{z,c}\rangle|\rho^{3,U}_{w,d}\rangle + |\rho^{3,U}_{w,d}\rangle|\rho^{1,U}_{z,c}\rangle \right) \tag{7.166}$$

$$+ \sum_{x,y\in\{0,1\}} U(c)_{zw,xy} B_{(x,c,1),(y,d,3)} \left( |\rho^{2,U}_{z,c}\rangle|\rho^{4,U}_{w,d}\rangle + |\rho^{4,U}_{w,d}\rangle|\rho^{2,U}_{z,c}\rangle \right) \Bigg) \tag{7.167}$$

$$= \sum_{z,c,w,d\in\{0,1\}} B_{(z,c,1),(w,d,3)} \Bigg[ |\rho^{1,U}_{z,c}\rangle|\rho^{3,U}_{w,d}\rangle + |\rho^{3,U}_{w,d}\rangle|\rho^{1,U}_{z,c}\rangle \tag{7.168}$$

$$+ \sum_{x,y\in\{0,1\}} U(c)_{xy,zw} \left( |\rho^{2,U}_{x,c}\rangle|\rho^{4,U}_{y,d}\rangle + |\rho^{4,U}_{y,d}\rangle|\rho^{2,U}_{x,c}\rangle \right) \Bigg] \tag{7.169}$$

$$= \sum_{z,c,w,d\in\{0,1\}} 2B_{(z,c,1),(w,d,3)} \,\mathrm{Sym}(|T_{z,c,w,d}\rangle). \tag{7.170}$$

This is the general solution to equations (7.143)–(7.145), so the space of two-particle frustration-free states for $G_U$ is spanned by the 16 orthonormal states (7.140).

Finally, we show that there are no three-particle frustration-free states. By Lemma **??**, this implies that there are no frustration-free states for more than two particles. Suppose (to reach a contradiction) that $|\Gamma\rangle$ is a normalized three-particle frustration-free state. Write

$$|\Gamma\rangle = \sum E_{(x,a,q),(y,b,r),(z,c,s)} |\rho^q_{x,a}\rangle|\rho^r_{y,b}\rangle|\rho^s_{z,c}\rangle \tag{7.171}$$

and note that each reduced density matrix of $|\Gamma\rangle$ on two of the three subsystems must have all of its support on two-particle frustration-free states (see the remark following Lemma **??**). Using this fact for each two-particle subsystem we get

$$(q,r) \notin \{(1,3),(3,1),(2,4),(4,2)\} \quad \Longrightarrow \quad E_{(x,a,q),(y,b,r),(z,c,s)} = 0 \tag{7.172}$$

$$(q,s) \notin \{(1,3),(3,1),(2,4),(4,2)\} \quad \Longrightarrow \quad E_{(x,a,q),(y,b,r),(z,c,s)} = 0 \tag{7.173}$$

$$(r,s) \notin \{(1,3),(3,1),(2,4),(4,2)\} \quad \Longrightarrow \quad E_{(x,a,q),(y,b,r),(z,c,s)} = 0 \tag{7.174}$$

which together imply that $|\Gamma\rangle = 0$ (a contradiction). Hence no three-particle frustration-free state exists. □

The two-particle state $\mathrm{Sym}(|T^U_{z_1,a,z_2,b}\rangle)$ is a superposition of a term

$$\mathrm{Sym}\left( \frac{1}{\sqrt{2}} |\rho^{1,U}_{z_1,a}\rangle|\rho^{3,U}_{z_2,b}\rangle \right) \tag{7.175}$$

with both particles located on vertices corresponding to input nodes and a term

$$\mathrm{Sym}\left( \frac{1}{\sqrt{2}} \sum_{x_1,x_2\in\{0,1\}} U(a)_{x_1x_2,z_1z_2} |\rho^{2,U}_{x_1,a}\rangle|\rho^{4,U}_{x_2,b}\rangle \right) \tag{7.176}$$

with both particles on vertices corresponding to output nodes. The two-qubit gate $U(a)$ is applied as the particles move from input nodes to output nodes. Note that we have essentially constructed a graph such that the ground states correspond to the history states. Assuming that we can guarantee that particles will have the correct locations, we will be able to combine these gadgets together to construct a history state.

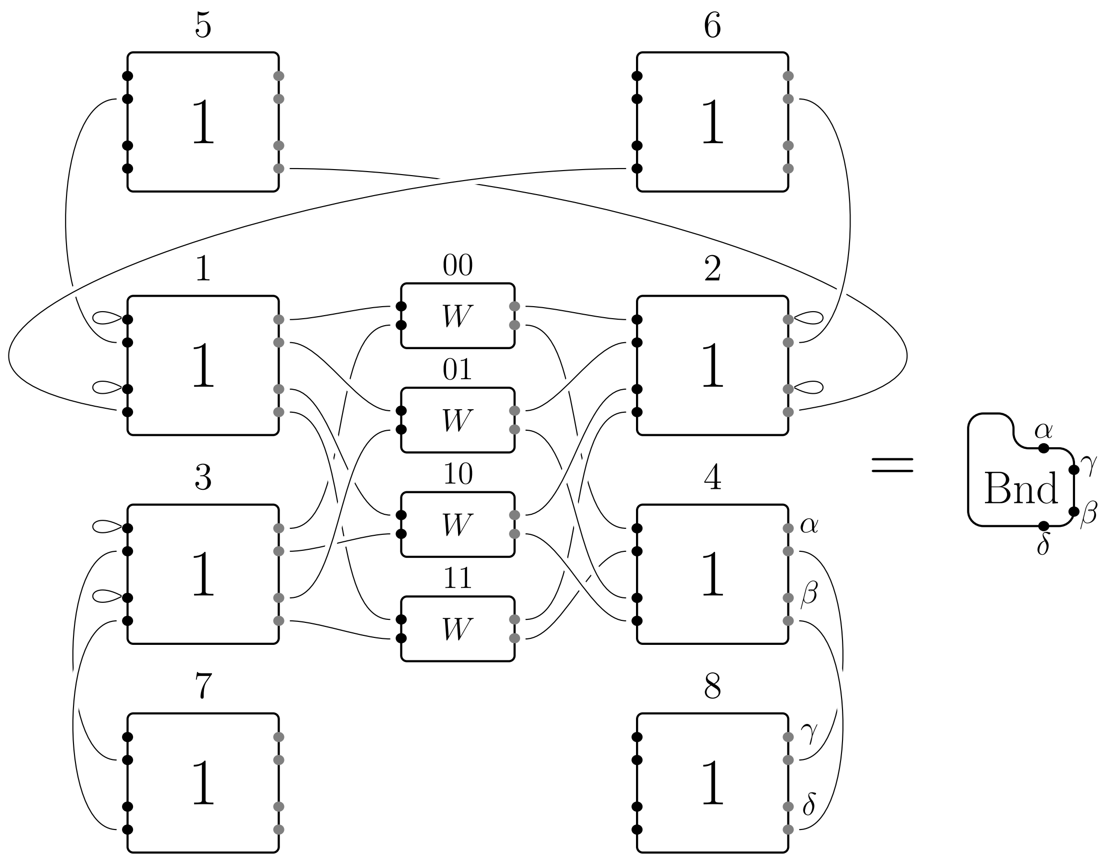


Figure 7.6: The gate diagram for the boundary gadget is obtained from Figure 7.5a by setting $\tilde{U} = 1$ and adding 6 self-loops.

#### 7.2.2.3 Boundary gadget

The *boundary gadget* is shown in Figure 7.6. This gate diagram is obtained from Figure 7.5a (with $\tilde{U} = \mathbb{I}$) by adding self-loops. The adjacency matrix is

$$A(G_{\text{bnd}}) = A(G_{\text{CNOT}_{12}}) + h_{\mathcal{S}} \tag{7.177}$$

where

$$h_{\mathcal{S}} = \sum_{z=0}^{1} (|1,z,1\rangle\langle 1,z,1| \otimes \mathbb{I}_j + |2,z,5\rangle\langle 2,z,5| \otimes \mathbb{I}_j + |3,z,1\rangle\langle 3,z,1| \otimes \mathbb{I}_j). \tag{7.178}$$

The single-particle ground states (with energy $e_1$) are superpositions of the states $|\rho_{z,a}^{i,U}\rangle$ from Lemma 18 that are in the nullspace of $h_{\mathcal{S}}$. Note that

$$\langle \rho_{x,b}^{j,U} | h_{\mathcal{S}} | \rho_{z,a}^{i,U} \rangle = \delta_{a,b}\delta_{x,z}\left(\delta_{i,1}\delta_{j,1} + \delta_{i,2}\delta_{j,2} + \delta_{i,3}\delta_{j,3}\right)\frac{1}{12} \cdot \frac{1}{2k} \tag{7.179}$$

(the factor of $\frac{1}{12}$ comes from the normalization in equations (7.125)–(7.127) and the other factor comes from the normalization in equation (7.32)), so the only single-particle ground states are

$$|\rho^{\mathrm{bnd}}_{z,a}\rangle = |\rho^{4,U}_{z,a}\rangle \tag{7.180}$$

with $z, a \in \{0,1\}$. Thus there are no two- (or more) particle frustration-free states, because no superposition of the states (7.140) lies in the subspace

$$\mathrm{span}\{\mathrm{Sym}(|\rho^{4,U}_{z,a}\rangle|\rho^{4,U}_{x,b}\rangle)\colon z,a,x,b \in \{0,1\}\} \tag{7.181}$$

of states with single-particle reduced density matrices in the ground space of $A(G_{\mathrm{bnd}})$. We summarize these results as follows.

**Lemma 20.** *The smallest eigenvalue of $A(G_{bnd})$ is $e_1$, with corresponding eigenvectors*

$$|\rho^{bnd}_{z,a}\rangle = \frac{1}{\sqrt{12}}|\psi^4_{z,a}\rangle - \frac{1}{\sqrt{12}}|\psi^8_{z,a}\rangle - \sqrt{\frac{5}{12}}\sum_{x=0,1}|\chi^{x(z\oplus x)}_{4,a}\rangle. \tag{7.182}$$

*There are no frustration-free states with two or more particles, i.e., $\lambda^1_N(G_{bnd}) > 0$ for $N \geq 2$.*

## 7.3 The occupancy constraints lemma

While the graphs defined in Section 7.2 have many useful features, such as simple single- and two-particle states and a constant energy gap, they do require that the particles are located in very particular locations. In particular, in order for the two-particle gadgets to encode a computation we require that two-particles have non-zero amplitude on the particle. While this is simple to achieve if the number of particles is larger than the number of gadgets, the final gate graph that we construct will have many more gate graphs than particles, which will result in the existence of many unwanted states remaining in the $n$-particle ground space.

To get around this problem, we will need to ensure that certain two-particle states are removed from the ground space. In particular, if we want to encode each logical qubit via a single particle, we will want to ensure that only one particle corresponds to a specific qubit. If we encode time in a spatial manner, this will require that two particles don't correspond to the same qubit at different times.

We will get around this problem via a lemma that we call the *occupancy constraints lemma*. The basic idea is that it will take in a gate graph, and a set of two-particle states that we don't want to occur, and then construct a larger graph that has related $n$-particle ground states but without the unwanted states.

### 7.3.1 Occupancy constraints

With the idea of excluding certain two-particle states from the ground space of the quantum walk on a gate graph, we will somehow need to encode these constraints. To do so, let us assume that $G$ is a gate graph with $R$ diagram elements (of some type). We will then define $G^{\mathrm{occ}}$ to be a graph with $R$ vertices, where the vertices of $G^{\mathrm{occ}}$ correspond to the diagram elements of $G$. The edge set of $G^{\mathrm{occ}}$ is then defined to encode the occupancy constraints of $G$, namely there exists an edge between two vertices of $G^{\mathrm{occ}}$ if and only if we want to exclude those states from the ground-space of $G$ where two particles are located on the corresponding diagram elements of $G$. In this way, we can easily encode our requisite occupancy constraints: simply add an edge in the graph $G^{\text{occ}}$.

[**TO DO:** *find whatever section we defined frustration-free stuff, and reference*]

With these occupancy constraints well defined, it will also be useful to define the frustration-free ground space that also respects these constraints. In particular, remember that for a particular gate graph $G$, we defined the $N$-particle frustration-free ground space of the gate graph without edges between the diagram elements and without self-loops as

$$\mathcal{I}(G,N) = \operatorname{span}\left\{ \operatorname{Sym}\left(|\,\psi^{q_1}_{z_1,a_1}\rangle \cdots |\,\psi^{q_N}_{z_N,a_N}\rangle\right) : \forall i,j \in [N], z_i, a_i \in \mathbb{F}_2, q_i \in [R], i \neq j \Rightarrow q_i \neq q_j \right\}. \tag{7.183}$$

In particular, this subspace guarantees that each individual particle is in the ground state of a diagram element, and further that no two particles are located on the same element. To also ensure that the particles satisfy a particular pair of occupancy constraints, we can restrict this subspace even farther. Once again, if $G$ is a gate graph, and if $G^{\text{occ}}$ is a set of occupancy constraints for $G$, then we can define

$$\mathcal{I}(G,G^{\text{occ}},N) := \operatorname{span}\left\{ \operatorname{Sym}\left(|\,\psi^{q_1}_{z_1,a_1}\rangle \cdots |\,\psi^{q_N}_{z_N,a_N}\rangle\right) : \forall i,j \in [N], z_i, a_i \in \mathbb{F}_2, q_i \in [R], i \neq j \Rightarrow q_i \neq q_j \text{ and } (i, \tag{7.184}$$

This subspace explicitly excludes those states that violate the occupancy constraints of $G^{\text{occ}}$, and thus will be useful for when we want to assume that the occupancy constraints are satisfied.

Now that we have a subspace that satisfy our occupancy constraints, we will want to understand how the eigenvalues change when we add in the various edges and self-loops of the original gate graph. In particular, we will define

$$H(G,G^{\text{occ}},N) = H(G,N)\big|_{\mathcal{I}(G,G^{\text{occ}},N)} \tag{7.185}$$

to be the MPQW Hamiltonian when restricted to the subspace that satisfies the occupancy constraints. We then define $\lambda^1_N(G,G^{\text{occ}})$ for the smallest eigenvalue of this Hamiltonian. Note that if the system is exactly frustration-free, $\lambda^1_N(G,G^{\text{occ}}) = 0$.

### 7.3.2 Occupancy Constraints Lemma statement

Now that we can easily encode our occupancy constraints, we would like to have the technical results that our transformation allows us to perform. Specifically, while our transform might raise certain states out of the ground space, it might also drastically reduce the energy gap of the Hamiltonian as well. As our eventual goal is to show that the MPQW-ground state problem is QMA-complete, we need to bound this reduction in the gap.

[**TO DO:** *correct occupancy constraints bounds*]

With this in mind, we can state the explicit bounds for our lemma:

**Lemma 21** (**Occupancy Constraints Lemma**). *Let $G$ be an $e_1$-gate graph specified as a gate diagram with $R \geq 2$ diagram elements. Let $N \in [R]$, let $G^{occ}$ specify a set of occupancy constraints on $G$, and suppose the subspace $\mathcal{I}(G,G^{occ},N)$ is nonempty. Then there exists an efficiently computable $e_1$-gate graph $G^{\square}$ with at most $7R^2$ diagram elements such that*

1. *If $\lambda^1_N(G,G^{occ}) \leq a$ then $\lambda^1_N(G^{\square}) \leq \frac{a}{R}$.*

2. *If $\lambda_N^1(G, G^{occ}) \geq b$ with $b \in [0,1]$, then $\lambda_N^1(G^{\square}) \geq \frac{\gamma_{\square} b}{R^{9+\nu}}$, where $\gamma_{\square}$ is a constant that depends only on the interaction $\mathcal{U}$, and $\nu$ is the bound on the maximum strength of the interaction potential.*

Note that this implies that there exists some transformation to the graph $G$ that enforces the constraints. While the actual transformation itself is not particularly complicated, in order to show how the energy gap transforms we will need to define several intermediate graphs in which not all of the edges are added. Thus our proof of the occupancy constraints lemma will also be rather iterative, and will be done later in this section.

In order to ease the definition of $G^{\square}$, let us first fix notation for the gate graph $G$ and the occupancy constraints graph $G^{\text{occ}}$. Write the adjacency matrix of $G$ as (see equation (7.81))

$$A(G) = \sum_{q=1}^{R} |q\rangle\langle q| \otimes A(g_q) + h_{\mathcal{E}^G} + h_{\mathcal{S}^G} \tag{7.186}$$

where $h_{\mathcal{E}^G}$ and $h_{\mathcal{S}^G}$ are determined (through equations (7.84) and (7.83)) by the sets $\mathcal{E}^G$ and $\mathcal{S}^G$ of edges and self-loops in the gate diagram for $G$, and where $g_q$ is the $64k$-vertex graph corresponding to each diagram element.

#### 7.3.2.1 Definition of $G^{\square}$

To ensure that the ground space has the appropriate form, the construction of $G^{\square}$ is slightly different depending on whether $R$ is even or odd. The following description handles both cases.

1. Replace each diagram element $q \in [R]$ in the gate diagram for $G$ as shown in Figure 7.7, with diagram elements labeled $q_{\text{in}}, q_{\text{out}}$ and $d(q,s)$ where $q, s \in [R]$ and $q \neq s$ if $R$ is even. In particular, if the diagram element labeled $q$ is a $U_{(c,d)}^{(a,b)}$ diagram element, then $q_{\text{in}}$ is a $\mathbb{I}_{(1,1)}^{(a,b)}$ diagram element, $q_{\text{out}}$ is a $U_{(c,d)}^{(1,1)}$ diagram element, and each $d(q,s)$ is a $\mathbb{I}_{(2,2)}^{(2,2)}$ diagram element. Each node $(q,z,t)$ in the gate diagram for $G$ is mapped to a new node $\text{new}(q,z,t)$ as shown by the black and grey arrows, i.e.,

$$\text{new}(q,z,t) = \begin{cases} (q_{\text{in}}, z, t) & \text{if } (q,z,t) \text{ is an input node} \\ (q_{\text{out}}, z, t) & \text{if } (q,z,t) \text{ is an output node.} \end{cases} \tag{7.187}$$

   Edges and self-loops in the gate diagram for $G$ are replaced by edges and self-loops between the corresponding nodes in the modified diagram.

2. For each edge $\{q_1, q_2\} \in E(G^{\text{occ}})$ in the occupancy constraints graph we add four $\mathbb{I}_{(0,1)}^{(1,0)}$ diagram elements, as shown in Figure 7.2c. We refer to these diagram elements by labels $e_{ij}(q_1, q_2)$ with $i, j \in \{0, 1\}$. For these diagram elements the labeling function is symmetric, i.e., $e_{ij}(q_1, q_2) = e_{ji}(q_2, q_1)$ whenever $\{q_1, q_2\} \in E(G^{\text{occ}})$.

3. For each non-edge $\{q_1, q_2\} \notin E(G^{\text{occ}})$ with $q_1, q_2 \in [R]$ and $q_1 \neq q_2$ we add 8 $\mathbb{I}_{(0,0)}^{(1,1)}$ diagram elements, as shown in Figure 7.2c. We refer to these diagram elements as

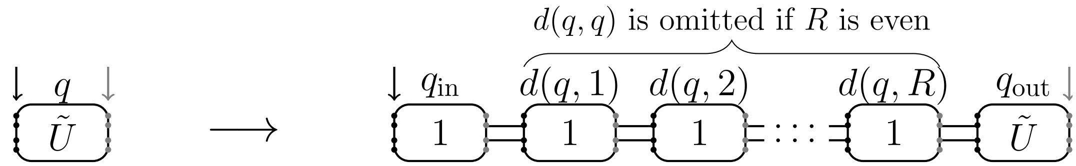


Figure 7.7: The first step in constructing the gate diagram of $G^{\square}$ from that of $G$ is to replace each diagram element as shown. The four input nodes (black arrow) and four output nodes (grey arrow) on the left-hand side are identified with nodes on the right-hand side as shown.

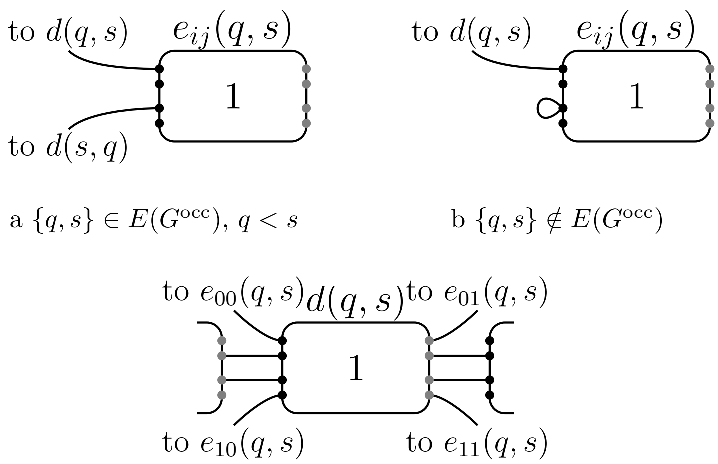


a $\{q,s\} \in E(G^{\text{occ}})$, $q < s$

b $\{q,s\} \notin E(G^{\text{occ}})$

c

Figure 7.8: Edges and self-loops added in step 4 of the construction of the gate diagram of $G^{\square}$. When $\{q,s\} \in E(G^{\text{occ}})$ with $q < s$, we add two outgoing edges to $e_{ij}(q,s)$ as shown in (a). Note that if $q > s$ and $\{q,s\} \in E(G^{\text{occ}})$ then $e_{ij}(q,s) = e_{ji}(s,q)$. When $\{q,s\} \notin E(G^{\text{occ}})$ we add a self-loop and a single outgoing edge from $e_{ij}(q,s)$ as shown in (b). Each diagram element $d(q,s)$ has eight outgoing edges (four of which are added in step 4), as shown in (c).

$e_{ij}(q_1,q_2)$ and $e_{ij}(q_2,q_1)$ with $i,j \in \{0,1\}$; when $\{q_1,q_2\} \notin E(G^{\text{occ}})$ the labeling function is not symmetric, i.e., $e_{ij}(q_1,q_2) \neq e_{ji}(q_2,q_1)$. If $R$ is odd we also add $4R\ \mathbb{I}_{(0,0)}^{(1,1)}$ diagram elements labeled $e_{ij}(q,q)$ with $i,j \in \{0,1\}$ and $q \in [R]$.

4. Finally, we add edges and self-loops to the gate diagram as shown in Figure 7.8. This gives the gate diagram for $G^{\square}$.

[**TO DO:** *fix this graph. I want to make sure that we can guarantee a distance separation between particles. I don't think we actually need it, but it will be useful none-the-less*]

[**TO DO:** *fix these graphs*]

The set of diagram elements in the gate graph for $G^{\square}$ is indexed by

$$L^{\square} = Q_{\text{in}} \cup D \cup E_{\text{edges}} \cup E_{\text{non-edges}} \cup Q_{\text{out}} \tag{7.188}$$

where

$$\begin{aligned} Q_{\text{in}} &= \{q_{\text{in}} : q \in [R]\} && (7.189)\\ D &= \{d(q,s) :\ q, s \in [R] \text{ and } q \neq s \text{ if } R \text{ is even}\} && (7.190)\\ E_{\text{edges}} &= \{e_{ij}(q,s) :\ i,j \in \{0,1\},\ \{q,s\} \in E(G^{\text{occ}}) \text{ and } q < s\} \\ E_{\text{non-edges}} &= \{e_{ij}(q,s) :\ i,j \in \{0,1\},\ \{q,s\} \notin E(G^{\text{occ}}) \text{ and } q \neq s \text{ if } R \text{ is even}\} \\ Q_{\text{out}} &= \{q_{\text{out}} : q \in [R]\}\,. && (7.191) \end{aligned}$$

The total number of diagram elements in $G^{\square}$ is

$$\begin{aligned} |L^{\square}| &= |Q_{\text{in}}| + |D| + |E_{\text{edges}}| + |E_{\text{non-edges}}| + |Q_{\text{out}}| && (7.192)\\ &= \begin{cases} R + R^2 + 4|E(G^{\text{occ}})| + 4\left(R^2 - 2|E(G^{\text{occ}})|\right) + R & R \text{ odd} \\ R + R\,(R-1) + 4|E(G^{\text{occ}})| + 4\left(R(R-1) - 2|E(G^{\text{occ}})|\right) + R & R \text{ even} \end{cases} && (7.193)\\ &= \begin{cases} 5R^2 + 2R - 4|E(G^{\text{occ}})| & R \text{ odd} \\ 5R^2 - 3R - 4|E(G^{\text{occ}})| & R \text{ even.} \end{cases} && (7.194) \end{aligned}$$

In both cases this is upper bounded by $7R^2$ as claimed in the statement of the Lemma. Write

$$A(G^{\square}) = \sum_{l \in L^{\square}} |l\rangle\langle l| \otimes A(g_l) + h_{\mathcal{S}^{\square}} + h_{\mathcal{E}^{\square}} \tag{7.195}$$

where $g_l$ corresponds to the diagram element labeled $l \in L^{\square}$, $\mathcal{S}^{\square}$ and $\mathcal{E}^{\square}$ are the sets of self-loops and edges in the gate diagram for $G^{\square}$.

We now focus on the input nodes of diagram elements in $Q_{\text{in}}$ and the output nodes of the diagram elements in $Q_{\text{out}}$. These are the nodes indicated by the black and grey arrows in Figure 7.7. Write $\mathcal{E}^0 \subset \mathcal{E}^{\square}$ and $\mathcal{S}^0 \subset \mathcal{S}^{\square}$ for the sets of edges and self-loops that are incident on these nodes in the gate diagram for $G^{\square}$. Note that the sets $\mathcal{E}^0$ and $\mathcal{S}^0$ are in one-to-one correspondence with (respectively) the sets $\mathcal{E}^G$ and $\mathcal{S}^G$ of edges and self-loops in the gate diagram for $G$. The other edges and self-loops in $G^{\square}$ do not depend on the sets of edges and self-loops in $G$, as they are created in our effort to enforce the occupancy constraints. Writing

$$\mathcal{S}^{\triangle} = \mathcal{S}^{\square} \setminus S^0 \qquad \mathcal{E}^{\triangle} = \mathcal{E}^{\square} \setminus \mathcal{E}^0, \tag{7.196}$$

we have

$$h_{\mathcal{S}^{\square}} = h_{\mathcal{S}^0} + h_{\mathcal{S}^{\triangle}} \qquad h_{\mathcal{E}^{\square}} = h_{\mathcal{E}^0} + h_{\mathcal{E}^{\triangle}}. \tag{7.197}$$

### Definition of $G^{\triangle}$

The gate diagram for $G^{\triangle}$ is obtained from that of $G^{\square}$ by removing all edges and self-loops attached to the input nodes of the diagram elements in $Q_{\text{in}}$ and the output nodes of the diagram elements in $Q_{\text{out}}$. Its adjacency matrix is

$$A(G^{\triangle}) = \sum_{l \in L^{\square}} |l\rangle\langle l| \otimes A(g_l) + h_{\mathcal{S}^{\triangle}} + h_{\mathcal{E}^{\triangle}}. \tag{7.198}$$

Note that $G^{\triangle} = G^{\square}$ whenever the gate diagram for $G$ contains no edges or self-loops.

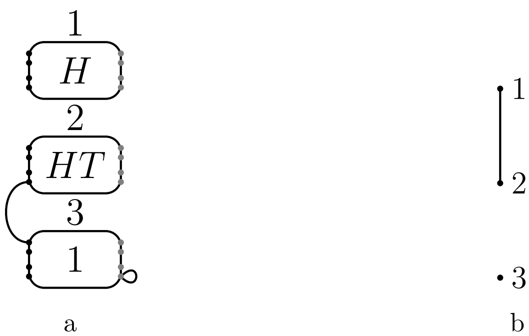


Figure 7.9: An example (a) Gate diagram for a gate graph $G$ and (b) Occupancy constraints graph $G^{\mathrm{occ}}$. In the text we describe how these two ingredients are mapped to a gate graph $G^{\square}$; the gate diagram for $G^{\square}$ is shown in Figure 7.10.

**Definition of $G^{\diamondsuit}$**

We also define a gate graph $G^{\diamondsuit}$ with gate diagram obtained from that of $G^{\triangle}$ by removing all edges (but leaving the self-loops). Note that $G^{\diamondsuit}$ has a component for each diagram element $l \in L^{\square}$. The components corresponding to diagram elements without a self-loop (those with $l \in L^{\square} \setminus E_{\text{non-edges}}$) have adjacency matrix $A(g_0)$; those with a self-loop ($l \in E_{\text{non-edges}}$) have adjacency matrix $A(g_l) + |1,1\rangle\langle 1,1| \otimes \mathbb{I}$, so

$$A(G^{\diamondsuit}) = \sum_{l\in L^{\square}} |l\rangle\langle l| \otimes A(g_l) + h_{\mathcal{S}^{\triangle}} \tag{7.199}$$

$$= \sum_{l\in L^{\square}\setminus E_{\text{non-edges}}} |l\rangle\langle l| \otimes A(g_l) + \sum_{l\in E_{\text{non-edges}}} |l\rangle\langle l| \otimes \left(A(g_l) + |1,1\rangle\langle 1,1| \otimes \mathbb{I}\right). \tag{7.200}$$

**Example**

We provide an example of this construction in Figure 7.9 (which shows a gate graph and an occupancy constraints graph) and Figure 7.10 (which describes the derived gate graphs $G^{\square}$, $G^{\triangle}$, and $G^{\diamondsuit}$).

[**TO DO:** *completely fix these example graphs*]

### 7.3.3 The gate graph $G^{\diamondsuit}$

We now solve for the $e_1$-energy ground states of the adjacency matrix $A(G^{\diamondsuit})$. We can recall from (7.200) that each component of $G^{\diamondsuit}$ is a copy of a diagram element, possibly with a self-loop on one of the input nodes. We can then use Lemma 14 to remember that each diagram element has four orthonormal $e_1$-energy ground states, while those diagram elements with a self-loop only have two states that remain in the ground space.

More concretely, for each diagram element in $A(G^{\diamondsuit})$, we can write $g'_l$ for the graph with adjacency matrix

$$A(g'_l) = A(g_l) + |1,1\rangle\langle 1,1| \otimes \mathbb{I} \tag{7.201}$$

(i.e., $g_l$ with 16 self-loops added), so (recalling equation (7.200)) each component of $G^{\diamondsuit}$ is either $g_l$ or $g_1$. We then use Lemma 14 to show that $A(g_0)$ has four orthonormal $e_1$-energy

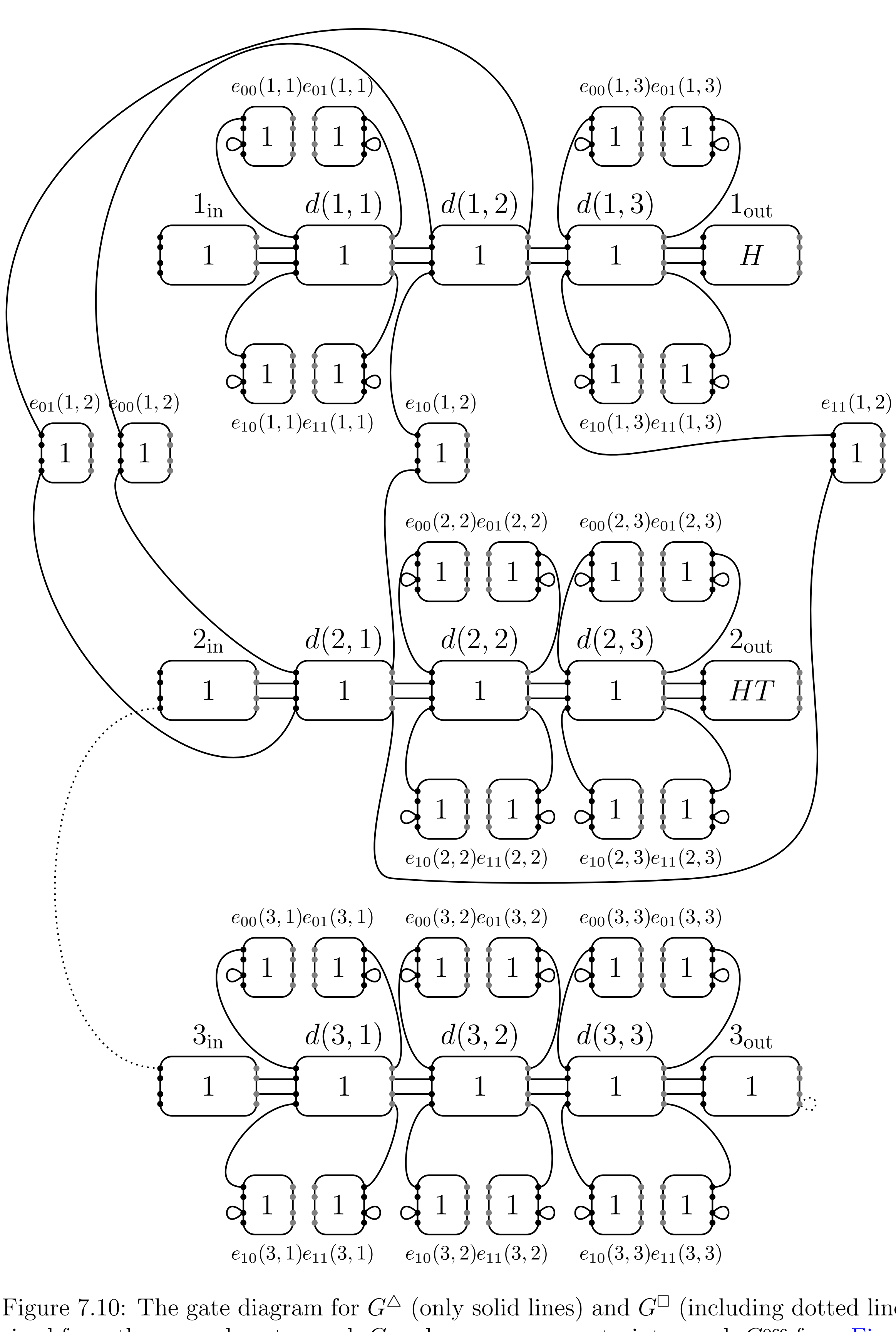


Figure 7.10: The gate diagram for $G^{\triangle}$ (only solid lines) and $G^{\square}$ (including dotted lines) derived from the example gate graph $G$ and occupancy constraints graph $G^{\text{occ}}$ from Figure 7.9. The gate diagram for $G^{\diamond}$ is obtained from that of $G^{\triangle}$ by removing all edges (but leaving the self-loops).

ground states $|\psi_{z,a}\rangle$ with $z, a \in \{0,1\}$. It is also easily seen that the $e_1$-energy ground space of $A(g_l')$ is spanned by two of these states $|\psi_{0,a}\rangle$ for $a \in \{0,1\}$, as these states are in the nullspace of $|1,1\rangle\langle 1,1| \otimes \mathbb{I}$, while the operator is strictly positive for the states $|\psi_{1,a}\rangle$ . Now letting $|\psi^l_{z,a}\rangle = |l\rangle|\psi_{z,a}\rangle$, we choose a basis $\mathcal{W}$ for the $e_1$-energy ground space of $A(G^\diamondsuit)$ where each basis vector is supported on one of the components:

$$\mathcal{W} = \left\{|\psi^l_{z,a}\rangle \,:\, z, a \in \mathbb{F}_2,\, l \in L^\square \setminus E_{\text{non-edges}}\right\} \cup \left\{|\psi^l_{0,a}\rangle \,:\, a \in \mathbb{F}_2,\, l \in E_{\text{non-edges}}\right\}. \tag{7.202}$$

The eigenvalue gap of $A(G^\diamondsuit)$ is equal to that of either $A(g_l)$ or $A(g_l')$ for some $l$. Since $g_l$ and $g_l'$ are constant-sized $64k$-vertex graphs, there exists a constant sized gap for each; let $c_\diamondsuit$ be the minimum value of this gap for all possible diagram elements, both with and without the added self-loops. We then have that

$$\gamma(A(G^\diamondsuit) - e_1) \geq c_\diamondsuit \tag{7.203}$$

The ground space of $A(G^\diamondsuit)$ has dimension

$$|\mathcal{W}| = 4\left|L^\square\right| - 2\left|E_{\text{non-edges}}\right| \tag{7.204}$$

$$= \begin{cases} 4\left(5R^2 + 2R - 4|E(G^{\text{occ}})|\right) - 2\left(4R^2 - 8|E(G^{\text{occ}})|\right) & R \text{ odd} \\ 4\left(5R^2 - 3R - 4|E(G^{\text{occ}})|\right) - 2\left(4R(R-1) - 8|E(G^{\text{occ}})|\right) & R \text{ even} \end{cases} \tag{7.205}$$

$$= \begin{cases} 12R^2 + 8R & R \text{ odd} \\ 12R^2 - 4R & R \text{ even.} \end{cases} \tag{7.206}$$

We now consider the $N$-particle Hamiltonian $H(G^\diamondsuit, N)$ and characterize its nullspace.

**Lemma 22.** *The nullspace of $H(G^\diamondsuit, N)$ is*

$$\mathcal{I}_\diamondsuit = \operatorname{span}\{\operatorname{Sym}(|\psi^{q_1}_{z_1,a_1}\rangle|\psi^{q_2}_{z_2,a_2}\rangle \ldots |\psi^{q_N}_{z_N,a_N}\rangle) : |\psi^{q_i}_{z_i,a_i}\rangle \in \mathcal{W} \text{ and } \forall i,j \in [N], i \neq j \Rightarrow q_i \neq q_j\} \tag{7.207}$$

*where $\mathcal{W}$ is given in equation (7.202). The smallest nonzero eigenvalue satisfies*

$$\gamma(H(G^\diamondsuit, N)) > \gamma_\diamondsuit, \tag{7.208}$$

*where $\gamma_\diamondsuit$ is a constant that only depends on the interaction $\mathcal{U}$.*

*Proof.* For the first part of the proof we use the fact that the basis vectors $|\psi^l_{z,a}\rangle \in \mathcal{W}$ span the $e_1$-eigenspace of the component $G^\diamondsuit_l$ of $G^\diamondsuit$ corresponding to the diagram element $l \in L^\square$, i.e., the nullspace of $H(G^\diamondsuit_l, 1)$. Furthermore, no component of $G^\diamondsuit$ supports a two-particle frustration-free state, i.e., $\lambda^1_2(g_l) > 0$ and $\lambda^1_2(g_l') > 0$ (by Lemma 13). Now applying Lemma 12 we see that $\mathcal{I}_\diamondsuit$ is the nullspace of $H(G^\diamondsuit, N)$. We also see that the smallest nonzero eigenvalue $\gamma(H(G^\diamondsuit, N))$ is either $\lambda^1_2(g_l)$, $\lambda^1_2(g_l')$, $\gamma(H(g_l, 1))$, or $\gamma(H(g_l', 1))$. Note that the second two only depend on the graph $g_l$, and thus are constants that only depend on $d_{\max}$, while the first two are similarly constants that depend only on $\mathcal{U}$. Letting $\gamma_\diamondsuit$ be this minimum value for all diagram elements, we have that

$$\gamma(H(G^\diamondsuit, N)) \geq \min_{l \in L^\square}\{\lambda^1_2(g_l), \lambda^1_2(g_l'), \gamma(H(g_l, 1)), \gamma(H(g_l', 1))\} > \gamma_\diamondsuit. \tag{7.209}$$

□

At this point, we have a basic graph that we can guarantee has a constant gap.

### 7.3.4 The adjacency matrix of the gate graph $G^{\triangle}$

With the foundational graph $G^{\diamond}$ defined and its ground-states and energy gaps well bounded, we now want to examine the graph with the edges that enforce the occupancy constraints. In particular, we now examine $G^{\triangle}$.

We begin by solving for the $e_1$-energy ground space of the adjacency matrix $A(G^{\triangle})$. From equations (7.198) and (7.199) we have

$$A(G^{\triangle}) = A(G^{\diamond}) + h_{\mathcal{E}^{\triangle}}. \tag{7.210}$$

Recall the $e_1$-energy ground space of $A(G^{\diamond})$ is spanned by $\mathcal{W}$ from equation (7.202). Since $h_{\mathcal{E}^{\triangle}} \geq 0$ it follows that $A(G^{\triangle}) \geq e_1$. To solve for the $e_1$-energy groundspace of $A(G^{\triangle})$ we construct superpositions of vectors from $\mathcal{W}$ that are in the nullspace of $h_{\mathcal{E}^{\triangle}}$. To this end we consider the restriction

$$h_{\mathcal{E}^{\triangle}}\big|_{\mathrm{span}(\mathcal{W})}. \tag{7.211}$$

We now show that it is block diagonal in the basis $\mathcal{W}$ and we compute its matrix elements.

First recall from equation (7.84) that

$$h_{\mathcal{E}^{\triangle}} = \sum_{\{(l,z,t),(l',z',t')\}\in\mathcal{E}^{\triangle}} \left(|l,z,t\rangle + |l',z',t'\rangle\right)\left(\langle l,z,t| + \langle l',z',t'|\right) \otimes \mathbb{I}. \tag{7.212}$$

The edges $\{(l,z,t),(l',z',t')\} \in \mathcal{E}^{\triangle}$ can be read off from Figure 7.7 and Figure 7.8, respectively (referring back to Figure 7.2 for our convention regarding the labeling of nodes on a diagram element). The edges from Figure 7.7 are

$$\{(q_{\mathrm{in}}, z, k+1), (d(q,), z, 1)\}, \{(d(q,i), z, 3), (d(q,i+1), z, 1)\}, \{(d(q,R), z, 3), (q_{\mathrm{out}}, z, 1)\} \tag{7.213}$$

with $q \in [R]$, $i \in [R-1]$ and $z \in \mathbb{F}_2$, and where $d(q,q)$ does not appear if $R$ is even (i.e., $d(q,q-1)$ is followed by $d(q,q+1)$. The edges from Figure 7.8 take the form

$$\{(d(q,s), z, k+1), (e_{za}(q,s), \alpha(q,s), 1 + k * \alpha(q,s))\}, \tag{7.214}$$

with $q, s \in [R]$, $q \neq s$ if $R$ is even, $a \in \mathbb{F}_2$, and where

$$\alpha(q,s) = \begin{cases} 1 & q > s \text{ and } \{q,s\} \in E(G^{\mathrm{occ}}) \\ 0 & \text{otherwise.} \end{cases} \tag{7.215}$$

The set $\mathcal{E}^{\triangle}$ consists of all edges (7.213) and (7.214).

We claim that (7.211) is block diagonal with a block $\mathcal{W}_{(z,a,q)} \subseteq \mathcal{W}$ of size

$$\left|\mathcal{W}_{(z,a,q)}\right| = \begin{cases} 3R+2 & R \text{ odd} \\ 3R-1 & R \text{ even} \end{cases} \tag{7.216}$$

for each for each triple $(z,a,q)$ with $z, a \in \mathbb{F}_2$ and $q \in [R]$. Using equation (7.206) we confirm that $|\mathcal{W}| = 4R\left|\mathcal{W}_{(z,a,q)}\right|$, so this accounts for all basis vectors in $\mathcal{W}$. The subset of basis vectors for a given block is

$$\begin{aligned} \mathcal{W}_{(z,a,q)} = &\left\{|\psi^{q_{\mathrm{in}}}_{z,a}\rangle, |\psi^{q_{\mathrm{out}}}_{z,a}\rangle\right\} \cup \left\{|\psi^{d(q,s)}_{z,a}\rangle \colon s \in [R],\, s \neq q \text{ if } R \text{ even}\right\} \\ &\cup \left\{|\psi^{e_{zx}(q,s)}_{\alpha(q,s),a}\rangle \colon x \in \{0,1\},\, s \in [R],\, s \neq q \text{ if } R \text{ even}\right\}. \end{aligned} \tag{7.217}$$

Using equation (7.212) and the description of $\mathcal{E}^{\triangle}$ from (7.213) and (7.214), one can check by direct inspection that (7.211) only has nonzero matrix elements between basis vectors in $\mathcal{W}$ from the same block (by construction). We also compute the matrix elements between vectors from the same block. For example, if $R$ is odd, there are edges $\{(q_{\text{in}},0,k+1),(d(q,1),0,1)\}$, $\{(q_{\text{in}},1,k+1),($ $\mathcal{E}^{\triangle}$. Using the fact that $|\psi^{l}_{z,a}\rangle = |l\rangle|\psi_{z,a}\rangle$ where $|\psi_{z,a}\rangle$ is given by (7.32) and (7.33), we compute the relevant matrix elements:

$$\langle\, \psi^{q_{\text{in}}}_{z,a}\,|h_{\mathcal{E}^{\triangle}}|\,\psi^{d(q,1)}_{z,a}\,\rangle \tag{7.218}$$

$$= \langle\, \psi^{q_{\text{in}}}_{z,a}\,|\left(\sum_{x\in\mathbb{F}_2}\big(|q_{\text{in}},x,k+1\rangle + |d(q,1),x,1\rangle\big)\big(\langle q_{\text{in}},x,k+1| + \langle d(q,1),x,1|\big)\otimes \mathbb{I}\right)|\psi^{d(q,1)}_{z,a}\rangle \tag{7.219}$$

$$= \sum_{x\in\mathbb{F}_2}\langle\psi_{z,a}|\left(|x,k+1\rangle\langle x,1|\otimes\mathbb{I}\right)|\psi_{z,a}\rangle = \frac{1}{2k}. \tag{7.220}$$

Continuing in this manner, we can compute the principal submatrix of (7.211) corresponding to the set $\mathcal{W}_{(z,a,q)}$. This matrix is shown in Figure 7.11a. In the Figure each vertex is associated with a state in the block and the weight on a given edge is the matrix element between the two states associated with vertices joined by that edge. The diagonal matrix elements are described by the weights on the self-loops. The matrix described by Figure 7.11a is the same for each block. [**TO DO:** *fix this for the correct values* $1/2k$]

For each triple $(z,a,q)$ with $z,a\in\mathbb{F}_2$ and $q\in[R]$, define

$$|\phi^{q}_{z,a}\rangle = \begin{cases} \frac{1}{\sqrt{3R+2}}\left(|\psi^{q_{\text{in}}}_{z,a}\rangle + \sum_{j\in[R]}(-1)^j\left(|\psi^{d(q,j)}_{z,a}\rangle - |\psi^{e_{z0}(q,j)}_{\alpha(q,j),a}\rangle - |\psi^{e_{z1}(q,j)}_{\alpha(q,j),a}\rangle\right) + |\psi^{q_{\text{out}}}_{z,a}\rangle\right) & R \text{ odd}\\ \frac{1}{\sqrt{3R-1}}\left(|\psi^{q_{\text{in}}}_{z,a}\rangle + \left(\sum_{j<q} - \sum_{j>q}\right)(-1)^j\left(|\psi^{d(q,j)}_{z,a}\rangle - |\psi^{e_{z0}(q,j)}_{\alpha(q,j),a}\rangle - |\psi^{e_{z1}(q,j)}_{\alpha(q,j),a}\rangle\right) + |\psi^{q_{\text{out}}}_{z,a}\rangle\right) & R \text{ even.}\end{cases} \tag{7.221}$$

The choice to omit $d(q,q)$ for $R$ even ensures that $|\psi^{q_{\text{in}}}_{z,a}\rangle$ and $|\psi^{q_{\text{out}}}_{z,a}\rangle$ have the same sign in these ground states, similar to the original gate diagram this gate graph replaced. We now show that these states span the ground space of $A(G^{\triangle})$.

**Lemma 23.** *An orthonormal basis for the $e_1$-energy ground space of $A(G^{\triangle})$ is given by the states*

$$\left\{|\phi^{q}_{z,a}\rangle : \ z,a\in\{0,1\},\ q\in[R]\right\} \tag{7.222}$$

*defined by equation (7.221). The eigenvalue gap is bounded as*

$$\gamma(A(G^{\triangle}) - e_1) > \frac{c_{\triangle}}{R^2}, \tag{7.223}$$

*where $c_{\triangle}$ is a constant that only depends on the interaction $\mathcal{U}$.*

*Proof.* The $e_1$-energy ground space of $A(G^{\triangle})$ is equal to the nullspace of (7.211). Since this operator is block diagonal in the basis $\mathcal{W}$, we can solve for the eigenvectors in the nullspace of each block. Thus, to prove the first part of the Lemma, we analyze the $|\mathcal{W}_{(z,a,q)}|\times|\mathcal{W}_{(z,a,q)}|$ matrix described by Figure 7.11a and show that (7.221) is the unique vector in its nullspace.

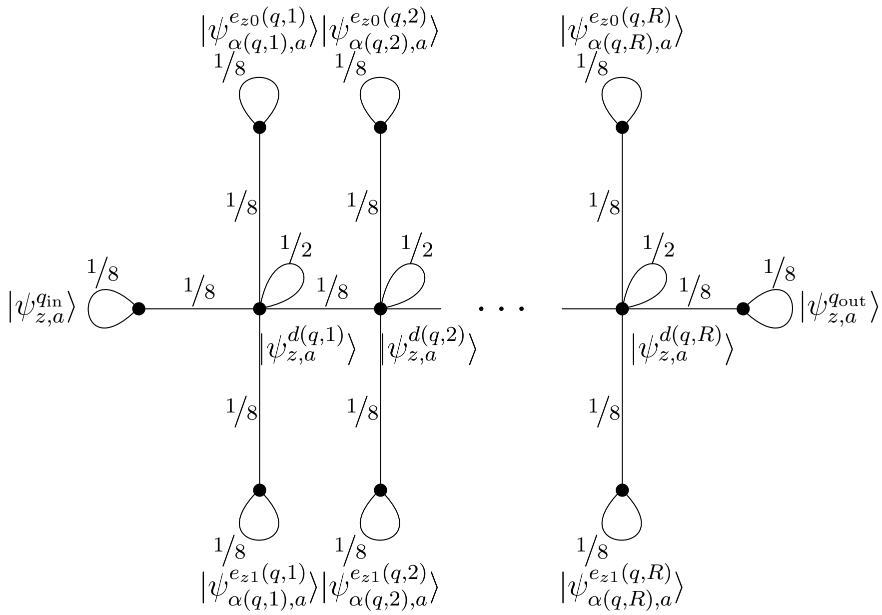


a The matrix $h^{\triangle}_{\mathcal{E}}|_{\text{span}(\mathcal{W})}$ is block diagonal in the basis $\mathcal{W}$, with a block $\mathcal{W}_{(z,a,q)}$ for each $z, a \in \{0,1\}$ and $q \in \{1,\ldots,R\}$. The states involved in a given block and the matrix elements between them are depicted.

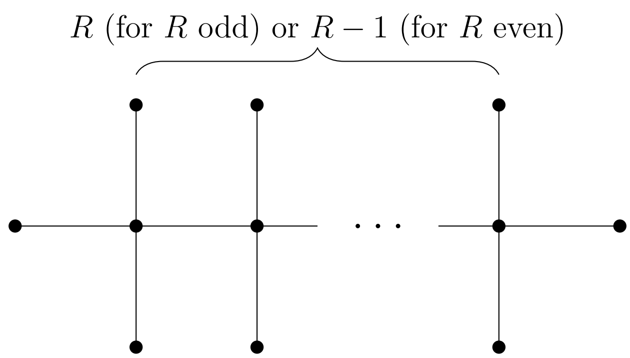


b After multiplying some of the basis vectors by $-1$, the matrix depicted in (a) is transformed into $1/8$ times the Laplacian matrix of this graph.

Figure 7.11

We first rewrite it in a slightly different basis obtained by multiplying some of the basis vectors by a phase of $-1$. Specifically, we use the basis

$$\left\{|\psi^{q_{\mathrm{in}}}_{z,a}\rangle, -|\psi^{d(q,1)}_{z,a}\rangle, |\psi^{e_{z0}(q,1)}_{\alpha(q,1),a}\rangle, |\psi^{e_{z1}(q,1)}_{\alpha(q,1),a}\rangle, |\psi^{d(q,2)}_{z,a}\rangle, -|\psi^{e_{z0}(q,2)}_{\alpha(q,2),a}\rangle, -|\psi^{e_{z1}(q,2)}_{\alpha(q,2),a}\rangle, \ldots, |\psi^{q_{\mathrm{out}}}_{z,a}\rangle\right\} \tag{7.224}$$

where the state associated with each vertex on one side of a bipartition of the graph is multiplied by $-1$; these are the phases appearing in equation (7.221). Changing to this basis replaces the weight $\frac{1}{2k}$ on each edge in Figure 7.11a by $-\frac{1}{2k}$ and does not change the weights on the self-loops. The resulting matrix is $\frac{1}{2k}L_0$, where $L_0$ is the Laplacian matrix of the graph shown in Figure 7.11b. Now we use the fact that the Laplacian of any connected graph has smallest eigenvalue zero, with a unique eigenvector equal to the all-ones vector. Hence for each block we get an eigenvector in the nullspace of (7.211)) given by (7.221). Ranging over all $z, a \in \mathbb{F}_2$ and $q \in [R]$ gives the claimed basis for the $e_1$-energy ground space of $A(G^{\triangle})$.

To prove the lower bound, we use the Nullspace Projection Lemma (Lemma ??) with

$$H_A = A(G^{\diamondsuit}) - e_1 \qquad H_B = h_{\mathcal{E}^{\triangle}} \tag{7.225}$$

and where $S = \mathrm{span}(\mathcal{W})$ is the nullspace of $H_A$ as shown in Section 7.3.3. Since it is block diagonal in the basis $\mathcal{W}$, the smallest nonzero eigenvalue of (7.211) is equal to the smallest nonzero eigenvalue of one of its blocks. The matrix for each block is $\frac{1}{2k}L_0$. Thus we can lower bound the smallest nonzero eigenvalue of $H_B|_S$ using standard bounds on the smallest nonzero eigenvalue of the Laplacian $L$ of a graph $G$. In particular, Theorem 4.2 of reference [?] shows that

$$\gamma(L) \geq \frac{4}{|V(G)|\,\mathrm{diam}(G)} \geq \frac{4}{|V(G)|^2}$$

(where $\mathrm{diam}(G)$ is the diameter of $G$). Since the size of the graph in Figure 7.11b is either $3R-1$ or $3R+2$, we have

$$\gamma(H_B|_S) = \frac{1}{2k}\gamma(L_0) \geq \frac{1}{2k}\frac{4}{(3R+2)^2} \geq \frac{1}{8kR^2}$$

since $R \geq 2$. Using this bound and the fact that $\gamma(H_A) > c_{\diamondsuit}$ (from equation (7.203)) and $\|H_B\| = 2$ (from equation (7.86)) and plugging into Lemma ?? gives

$$\gamma(A(G^{\triangle}) - e_1) \geq \frac{c_{\diamondsuit} \cdot \frac{1}{8kR^2}}{c_{\diamondsuit} + 2} \geq \frac{c_{\diamondsuit}}{24kR^2} > \frac{c_{\triangle}}{R^2}. \tag{7.226}$$

where we used the fact that $c_{\diamondsuit} \leq 1$, and we define $c_{\triangle} = c_{\diamondsuit}/(24k)$. □

### 7.3.5 The Hamiltonian $H(G^{\triangle}, N)$

With our analysis of the graph $G^{\triangle}$, and in particular its adjacency matrix's eigenvalue gap, we can now analyze the multi-particle energy gap. We will now consider the $N$-particle Hamiltonian $H(G^{\triangle}, N)$ and solve for its nullspace. We use the following fact about the subsets $\mathcal{W}_{(z,a,q)} \subset \mathcal{W}$ defined in equation (7.217).

**Definition 7.** We say $\mathcal{W}_{(z_1,a_1,q_1)}$ and $\mathcal{W}_{(z_2,a_2,q_2)}$ *overlap on a diagram element* if there exists $l \in L^{\square}$ such that $|\psi^l_{x_1,b_1}\rangle \in \mathcal{W}_{(z_1,a_1,q_1)}$ and $|\psi^l_{x_2,b_2}\rangle \in \mathcal{W}_{(z_2,a_2,q_2)}$ for some $x_1, x_2, b_1, b_2 \in \{0,1\}$.

**Fact 2** (Key property of $\mathcal{W}_{(z,a,q)}$)**.** *Sets $\mathcal{W}_{(z_1,a_1,q_1)}$ and $\mathcal{W}_{(z_2,a_2,q_2)}$ overlap on a diagram element if and only if $q_1 = q_2$ or $\{q_1, q_2\} \in E(G^{\mathrm{occ}})$.*

This fact can be confirmed by direct inspection of the sets $\mathcal{W}_{(z,a,q)}$. If $q_1 = q_2 = q$ the diagram element $l$ on which they overlap can be chosen to be $l = q_{\mathrm{in}}$; if $q_1 \neq q_2$ and $\{q_1, q_2\} \in E(G^{\mathrm{occ}})$ then $l = e_{z_1 z_2}(q_1, q_2) = e_{z_2 z_1}(q_2, q_1)$. Conversely, if $\{q_1, q_2\} \notin E(G^{\mathrm{occ}})$ with $q_1 \neq q_2$, then there is no overlap.

We show that the nullspace $\mathcal{I}_{\triangle}$ of $H(G^{\triangle}, N)$ is

$$\begin{aligned}\mathcal{I}_{\triangle} = \mathrm{span}\{&\mathrm{Sym}(|\phi^{q_1}_{z_1,a_1}\rangle|\phi^{q_2}_{z_2,a_2}\rangle \ldots |\phi^{q_N}_{z_N,a_N}\rangle)\colon \\ &z_i, a_i \in \mathbb{F}_2,\ q_i \in [R],\ q_i \neq q_j, \text{ and } \{q_i, q_j\} \notin E(G^{\mathrm{occ}})\}.\end{aligned} \tag{7.227}$$

Note that $\mathcal{I}_{\triangle}$ is very similar to $\mathcal{I}(G, G^{\mathrm{occ}}, N)$ (from equation (**??**)) but with each single-particle state $|\psi^q_{z,a}\rangle \in \mathcal{Z}_N(G)$ replaced by $|\phi^q_{z,a}\rangle \in \mathcal{Z}_N(G^{\triangle})$.

**Lemma 24.** *The nullspace of $H(G^{\triangle}, N)$ is $\mathcal{I}_{\triangle}$ as defined in equation (7.227). Its smallest nonzero eigenvalue is*

$$\gamma(H(G^{\triangle}, N)) > \frac{\gamma_{\triangle}}{R^7}, \tag{7.228}$$

*where $\gamma_{\triangle}$ is a constant that only depends on $\mathcal{U}$.*

In addition to Fact 2, we use the following simple fact in the proof of the Lemma.

**Fact 3.** *Let $|p\rangle = c|\alpha_0\rangle + \sqrt{1-c^2}|\alpha_1\rangle$ with $\langle \alpha_i|\alpha_j\rangle = \delta_{ij}$ and $c \in [0,1]$. Then*

$$|p\rangle\langle p| = c^2|\alpha_0\rangle\langle\alpha_0| + M \tag{7.229}$$

*where $\|M\| \leq 1 - \frac{3}{4}c^4$.*

To prove this Fact, one can calculate $\|M\| = \frac{1}{2}(1-c^2) + \frac{1}{2}\sqrt{1+2c^2-3c^4}$ and use the inequality $\sqrt{1+x} \leq 1 + \frac{x}{2}$ for $x \geq -1$.

*Proof of Lemma 24.* Using equation (7.210), the fact that the smallest eigenvalues of $A(G^{\diamondsuit})$ and $A(G^{\triangle})$ are the same (equal to $e_1$, from Section 7.3.3 and Lemma 23), and the fact that for any two vertices in $G^{\triangle}$, if their distance in $G^{\diamondsuit}$ is at most $d_{\max}$ then their distance in $G^{\triangle}$ remains the same, we can break the MPQW-Hamiltonian on $G^{\triangle}$ into three terms. Namely, we have

$$H(G^{\triangle}, N) = H(G^{\diamondsuit}, N) + \sum_{w=1}^{N} h^{(w)}_{\mathcal{E}^{\triangle}}\Big|_{\mathcal{Z}_N(G^{\triangle})} + B, \tag{7.230}$$

where $B$ is the positive semi-definite term corresponding to the added interactions resulting from vertices that were originally disconnected now becoming connected. Recall from Lemma 22 that the nullspace of $H(G^{\diamondsuit}, N)$ is $\mathcal{I}_{\diamondsuit}$. We consider

$$\sum_{w=1}^{N} h^{(w)}_{\mathcal{E}^{\triangle}}\Big|_{\mathcal{I}_{\diamondsuit}}. \tag{7.231}$$

We show that its nullspace is equal to $\mathcal{I}_\triangle$, and we lower bound its smallest nonzero eigenvalue. Specifically, we prove

$$\gamma\left(\sum_{w=1}^{N} h_{\mathcal{E}^\triangle}^{(w)}\bigg|_{\mathcal{I}_\diamondsuit}\right) > \frac{12c_\triangle}{(4R)^6}. \tag{7.232}$$

Additionally, we will show that $B$ annihilates those states in $\mathcal{I}_\triangle$, so that $\mathcal{I}_\triangle$ is the nullspace of $H(G^\triangle, N)$ as claimed.

We will first prove equation (7.228) using this bound on the added movement terms (equation (7.232)) and the fact that $B$ annihilates $\mathcal{I}_\triangle$. We apply the Nullspace Projection Lemma (Lemma **??**) with $H_A$ and $H_B$ given by the first and second terms in equation (7.230); in this case the nullspace of $H_A$ is $S = \mathcal{I}_\diamondsuit$ (from Lemma 22). Now applying Lemma **??** and using the bounds $\gamma(H_A) > \frac{1}{300}$ (from Lemma 22), $\|H_B\| \leq N\|h_{\mathcal{E}^\triangle}\| = 2N \leq 2R$ (from equation (7.86) and the fact that $N \leq R$), and the bound (7.232) on $\gamma(H_B|_S)$, we find

$$\gamma(H(G^\triangle, N) - M) \geq \frac{\frac{12c_\triangle\gamma_\diamondsuit}{(4R)^6}}{\gamma_\diamondsuit + 2R} \geq \frac{16\gamma_\diamondsuit c_\triangle}{(4R)^7} = \frac{\gamma_\triangle}{R^7}. \tag{7.233}$$

If we then remember the fact that $M$ annihilates all states in $\mathcal{I}_\triangle$, we can use a variational argument to show that the same bound holds for the entire MPQW Hamiltonian (i.e., adding $M$ to the Hamiltonian does not reduce the gap):

$$\gamma(H(G^\triangle, N)) \geq \frac{\gamma_\triangle}{R^7}. \tag{7.234}$$

With the final reductions for the proof completed, we must now establish that $B$ annihilates all terms in $\mathcal{I}_\triangle$, the nullspace of (7.231) is $\mathcal{I}_\triangle$, and prove the lower bound (7.232). Let us first show that each state in $\mathcal{I}_\triangle$ has no energy penalty due to new interactions arising from the addition of edges in the graph $G^\triangle$. By definition, note that the only vertices in $G^\triangle$ that have vertices at a distance closer than $d_{\max}$ either belong to the same diagram element, belong to diagram elements corresponding to $\{q_{\text{in}}, q_{\text{out}}, d(q,s)\}$ for some $q \in [R]$, or else belong to diagram elements labeled $\{d(q,s), e_{z_1,z_2}(q,s)\}$ for some $q, s \in [R]$, and $z_1, z_2 \in \mathbb{F}_2$. As such, if any state has energy penalties resulting from the added edges (i.e., is not annihilated by the operator $B$,), then it must have at least two particles located on one of these pairs of diagram elements. However, each state $|\Phi\rangle \in \mathcal{I}_\triangle$ is guaranteed to only have a single particle on each such pair of diagram elements, by construction. Hence, $B|\Phi\rangle = 0$.

To analyze (7.231) we use the fact (established in Section 7.3.4) that (7.211) is block diagonal with a block $\mathcal{W}_{(z,a,q)} \subset \mathcal{W}$ for each triple $(z,a,q)$ with $z, a \in \mathbb{F}_2$ and $q \in [R]$, as the operator (7.231) inherits a block structure from this fact. For any basis vector

$$\mathrm{Sym}(|\psi_{z_1,a_1}^{q_1}\rangle|\psi_{z_2,a_2}^{q_2}\rangle \ldots |\psi_{z_N,a_N}^{q_N}\rangle) \in \mathcal{I}_\diamondsuit, \tag{7.235}$$

we define a set of occupation numbers that correspond to the number of particles in each block. Namely, we will define

$$\mathcal{N} = \left\{N_{(x,b,r)} \colon x, b \in \{0,1\},\ r \in [R]\right\} \tag{7.236}$$

where

$$N_{(x,b,r)} = |\{j \colon |\psi_{z_j,a_j}^{q_j}\rangle \in \mathcal{W}_{(x,b,r)}\}|. \tag{7.237}$$

Observe that (7.231) conserves the set of occupation numbers (due to the inherited block structure) and is therefore block diagonal with a block for each possible set $\mathcal{N}$.

For a given block corresponding to a set of occupation numbers $\mathcal{N}$, we write $\mathcal{I}_{\diamondsuit}(\mathcal{N}) \subset \mathcal{I}_{\diamondsuit}$ for the subspace spanned by basis vectors (7.235) in the block. We classify the blocks into three categories depending on $\mathcal{N}$.

**Classification of the blocks of (7.231) according to $\mathcal{N}$**

Consider the following two conditions on a set $\mathcal{N} = \{N_{(x,b,r)} \colon x, b \in \{0,1\},\ r \in [R]\}$ of occupation numbers:

(a) $N_{(x,b,r)} \in \{0,1\}$ for all $x, b \in \{0,1\}$ and $r \in [R]$. If this holds, write $(y_i, c_i, s_i)$ for the nonzero occupation numbers (with some arbitrary ordering), i.e., $N_{(y_i,c_i,s_i)} = 1$ for $i \in [N]$.

(b) The sets $\mathcal{W}_{(y_i,c_i,s_i)}$ and $\mathcal{W}_{(y_j,c_j,s_j)}$ do not overlap on a diagram element for all distinct $i, j \in [N]$.

We say a block is of type 1 if $\mathcal{N}$ satisfies (a) and (b). We say it is of type 2 if $\mathcal{N}$ does not satisfy (a). We say it is of type 3 if $\mathcal{N}$ satisfies (a) but does not satisfy (b).

Note that every block must be of type 1, 2, or 3. We will show that each block of type 1 contains one state in the nullspace of (7.231) and, ranging over all blocks of this type, we will obtain a basis for $\mathcal{I}_{\triangle}$. We will also show that the smallest nonzero eigenvalue within a block of type 1 is at least $\frac{\gamma_{\diamondsuit}}{R^2}$. We will then show that blocks of type 2 and 3 do not contain any states in the nullspace of (7.231) and that the smallest eigenvalue within any block of type 2 or 3 is greater than [**TO DO:** *get correct bound*] $\frac{12c_{\triangle}}{(4R)^6}$. Hence, the nullspace of (7.231) is $\mathcal{I}_{\triangle}$ and its smallest nonzero eigenvalue is lower bounded as in equation (7.232).

**Type 1**

Let us first investigate those blocks of type 1. Note (from Definition 7) that requirement (b) implies $q \neq r$ whenever

$$|\psi^{q}_{x,b}\rangle \in \mathcal{W}_{(y_i,c_i,s_i)} \text{ and } |\psi^{r}_{z,a}\rangle \in \mathcal{W}_{(y_j,c_j,s_j)} \tag{7.238}$$

for distinct $i, j \in [N]$. Hence, we can remove the requirement that $q_i \neq q_j$:

$$\begin{aligned}\mathcal{I}_{\diamondsuit}(\mathcal{N}) &= \operatorname{span}\{\operatorname{Sym}(|\psi^{q_1}_{z_1,a_1}\rangle|\psi^{q_2}_{z_2,a_2}\rangle \ldots |\psi^{q_N}_{z_N,a_N}\rangle) \colon q_i \neq q_j \text{ and } |\psi^{q_j}_{z_j,a_j}\rangle \in \mathcal{W}_{(y_j,c_j,s_j)}\} &(7.239)\\ &= \operatorname{span}\{\operatorname{Sym}(|\psi^{q_1}_{z_1,a_1}\rangle|\psi^{q_2}_{z_2,a_2}\rangle \ldots |\psi^{q_N}_{z_N,a_N}\rangle) \colon |\psi^{q_j}_{z_j,a_j}\rangle \in \mathcal{W}_{(y_j,c_j,s_j)}\}. &(7.240)\end{aligned}$$

From this we see that

$$\dim(\mathcal{I}_{\diamondsuit}(\mathcal{N})) = \prod_{j=1}^{N} \left|\mathcal{W}_{(y_j,c_j,s_j)}\right| = \begin{cases} (3R+2)^N & R \text{ odd} \\ (3R-1)^N & R \text{ even.} \end{cases} \tag{7.241}$$

We now solve for all the eigenstates of (7.231) within the block.

As we need only understand the eigenvectors of each individual block, it will be useful to remember Lemma 23 as we have already determined all of the single-particle eigenstates.

It will convenient to write an orthonormal basis of eigenvectors of the $|\mathcal{W}_{(z,a,q)}| \times |\mathcal{W}_{(z,a,q)}|$ matrix described by Figure 7.11a as

$$|\phi^q_{z,a}(u)\rangle, \quad u \in [|\mathcal{W}_{(z,a,q)}|] \tag{7.242}$$

and their ordered eigenvalues as

$$\theta_1 \leq \theta_2 \leq \ldots \leq \theta_{|\mathcal{W}_{(z,a,q)}|}. \tag{7.243}$$

From the proof of Lemma 23, the eigenvector with smallest eigenvalue $\theta_1 = 0$ is $|\phi^q_{z,a}\rangle = |\phi^q_{z,a}(1)\rangle$ and $\theta_2 \geq \frac{c_\diamond}{R^2}$. For any $u_1, u_2, \ldots, u_N \in [|\mathcal{W}_{(z,a,q)}|]$, the state

$$\mathrm{Sym}(|\phi^{s_1}_{y_1,c_1}(u_1)\rangle|\phi^{s_2}_{y_2,c_2}(u_2)\rangle \ldots |\phi^{s_N}_{y_N,c_N}(u_N)\rangle) \tag{7.244}$$

is an eigenvector of (7.231) with eigenvalue $\sum_{j=1}^N \theta_{u_j}$. Furthermore, states corresponding to different choices of $u_1, \ldots, u_N$ are orthogonal, and ranging over all $\dim(\mathcal{I}_\diamond(\mathcal{N}))$ choices we get every eigenvector in the block. The smallest eigenvalue within the block is $N\theta_1 = 0$ and there is a unique vector in the nullspace, given by

$$|\,\Phi_{\mathcal{N}}\,\rangle := \mathrm{Sym}(|\phi^{s_1}_{y_1,c_1}\rangle|\phi^{s_2}_{y_2,c_2}\rangle \ldots |\phi^{s_N}_{y_N,c_N}\rangle) \tag{7.245}$$

(recall $|\phi^q_{z,a}\rangle = |\phi^q_{z,a}(1)\rangle$). The smallest nonzero eigenvalue of (7.231) within the block is $(N-1)\theta_1 + \theta_2 = \theta_2 \geq \frac{c_\diamond}{R^2}$.

With the knowledge that each state of the form (7.245) minimizes the energy of (7.231), and is in fact the unique ground state within a particular type 1 block, we will now show that the collection of all such states span the space $\mathcal{I}_\triangle$. As the second requirement on type 1 blocks requires that the sets $\mathcal{W}_{(y_i,c_i,s_i)}$ no not pairwise overlap, we can use Fact 2 to see that this is equivalent to the sets satisfying $s_i \neq s_j$ and $\{s_i, s_j\} \notin E(G^{\mathrm{occ}})$ for distinct $i, j \in [N]$ (as well as arbitrary $y_i$ and $c_i$). Hence the set of states (7.245) obtained from of all blocks of type 1 is

$$\begin{aligned}&\big\{|\,\Phi_{\mathcal{N}}\,\rangle : \mathcal{N} \text{ is a type 1 block}\big\}\\ &\quad = \big\{\,\mathrm{Sym}(|\phi^{s_1}_{y_1,c_1}\rangle|\phi^{s_2}_{y_2,c_2}\rangle \ldots |\phi^{s_N}_{y_N,c_N}\rangle) :\\ &\qquad\qquad \forall i,j \in [N], y_i, c_i \in \mathbb{F}_2,\ s_i \in [R],\ i \neq j \Rightarrow s_i \neq s_j \text{ and } \{s_i, s_j\} \notin E(G^{\mathrm{occ}})\big\}\end{aligned} \tag{7.246}$$

which by definition spans $\mathcal{I}_\triangle$.

### Type 2

Now let $\mathcal{N}$ be of type 2. We then have that there exist $x, b \in \mathbb{F}_2$ and $r \in [R]$ such that $N_{(x,b,r)} \geq 2$. We will show there are no eigenvectors in the nullspace of (7.231) within a block of this type and we lower bound the smallest eigenvalue within the block. Specifically, we show

$$\min_{|\kappa\rangle \in \mathcal{I}_\diamond(\mathcal{N})} \langle\kappa| \sum_{w=1}^N h^{(w)}_{\mathcal{E}^\triangle} |\kappa\rangle > \frac{12 c_\triangle}{(4R)^6}. \tag{7.247}$$

First note that all $|\kappa\rangle \in \mathcal{I}_\diamondsuit$ satisfy $(A(G^\diamondsuit) - e_1)^{(w)}|\kappa\rangle = 0$ for each $w \in [N]$, which can be seen using the definition of $\mathcal{I}_\diamondsuit$ and the fact that $\mathcal{W}$ spans the nullspace of $A(G^\diamondsuit) - e_1$. We can then add these terms to equation (7.210), so that

$$\min_{|\kappa\rangle \in \mathcal{I}_\diamondsuit(\mathcal{N})} \langle\kappa| \sum_{w=1}^{N} h^{(w)}_{\mathcal{E}^\triangle} |\kappa\rangle = \min_{|\kappa\rangle \in \mathcal{I}_\diamondsuit(\mathcal{N})} \langle\kappa| \sum_{w=1}^{N} \left(A(G^\triangle) - e_1\right)^{(w)} |\kappa\rangle. \tag{7.248}$$

If we then examine only the ground space of this operator, we can see that

$$\begin{aligned} \sum_{w=1}^{N} \left(A(G^\triangle) - e_1\right)^{(w)} &\geq \gamma \left( \sum_{w=1}^{N} \left(A(G^\triangle) - e_1\right)^{(w)} \right) \cdot \left(1 - \Pi^\triangle\right) \\ &= \gamma(A(G^\triangle) - e_1) \cdot \left(1 - \Pi^\triangle\right) > \frac{c_\triangle}{R^2} \left(1 - \Pi^\triangle\right), \end{aligned} \tag{7.249}$$

where $\Pi^\triangle$ is the projector onto the nullspace of $\sum_{w=1}^{N} \left(A(G^\triangle) - e_1\right)^{(w)}$, and where in the last step we used Lemma 23. Plugging equation (7.249) into equation (7.248) gives

$$\min_{|\kappa\rangle \in \mathcal{I}_\diamondsuit(\mathcal{N})} \langle\kappa| \sum_{w=1}^{N} h^{(w)}_{\mathcal{E}^\triangle} |\kappa\rangle > \frac{c_\triangle}{R^2} \Big(1 - \max_{|\kappa\rangle \in \mathcal{I}_\diamondsuit(\mathcal{N})} \langle\kappa|\Pi^\triangle|\kappa\rangle\Big). \tag{7.250}$$

Using Lemma 23 we can write $\Pi^\triangle$ explicitly as

$$\Pi^\triangle = \sum_{(\vec{z},\vec{a},\vec{q}) \in \mathcal{Q}} \mathcal{P}_{(\vec{z},\vec{a},\vec{q})} \tag{7.251}$$

where

$$\mathcal{P}_{(\vec{z},\vec{a},\vec{q})} = |\phi^{q_1}_{z_1,a_1}\rangle\langle\phi^{q_1}_{z_1,a_1}| \otimes |\phi^{q_2}_{z_2,a_2}\rangle\langle\phi^{q_2}_{z_2,a_2}| \otimes \cdots \otimes |\phi^{q_N}_{z_N,a_N}\rangle\langle\phi^{q_N}_{z_N,a_N}| \tag{7.252}$$

$$\mathcal{Q} = \{(z_1, \ldots z_N, a_1, \ldots, a_N, q_1, \ldots, q_N) : \; z_i, a_i \in \mathbb{F}_2 \text{ and } q_i \in [R]\}. \tag{7.253}$$

Essentially, each particle is projected onto the ground state of a block, where the blocks are labeled by the elements of $\mathcal{Q}$ and there are no correlations between the particles. For each $(\vec{z}, \vec{a}, \vec{q}) \in \mathcal{Q}$ we also define a space

$$S_{(\vec{z},\vec{a},\vec{q})} = \mathrm{span}(\mathcal{W}_{(z_1,a_1,q_1)}) \otimes \mathrm{span}(\mathcal{W}_{(z_2,a_2,q_2)}) \otimes \cdots \otimes \mathrm{span}(\mathcal{W}_{(z_N,a_N,q_N)}). \tag{7.254}$$

Note that $\mathcal{P}_{(\vec{z},\vec{a},\vec{q})}$ has all of its support in $S_{(\vec{z},\vec{a},\vec{q})}$, and that

$$S_{(\vec{z},\vec{a},\vec{q})} \perp S_{(\vec{z}',\vec{a}',\vec{q}')} \text{ for distinct } (\vec{z}, \vec{a}, \vec{q}), (\vec{z}', \vec{a}', \vec{q}') \in \mathcal{Q}. \tag{7.255}$$

Therefore $\mathcal{P}_{(\vec{z},\vec{a},\vec{q})}\mathcal{P}_{(\vec{z}',\vec{a}',\vec{q}')} = 0$ for distinct $(\vec{z}, \vec{a}, \vec{q}), (\vec{z}', \vec{a}', \vec{q}') \in \mathcal{Q}$. (Below we use similar reasoning to obtain a less obvious result.) Note that $\mathcal{P}_{(\vec{z},\vec{a},\vec{q})}$ is orthogonal to $\mathcal{I}_\diamondsuit(\mathcal{N})$ unless

$$|\{j : (z_j, a_j, q_j) = (w, u, v)\}| = N_{(w,u,v)} \text{ for all } w, u \in \{0, 1\}, \; v \in [R]. \tag{7.256}$$

We restrict our attention to the projectors that are not orthogonal to $\mathcal{I}_\diamondsuit(\mathcal{N})$. Letting $\mathcal{Q}(\mathcal{N}) \subset \mathcal{Q}$ be the set of $(\vec{z}, \vec{a}, \vec{q})$ satisfying equation (7.256), we have

$$\langle\kappa| \sum_{(\vec{z},\vec{a},\vec{q}) \in \mathcal{Q}} \mathcal{P}_{(\vec{z},\vec{a},\vec{q})} |\kappa\rangle = \langle\kappa| \sum_{(\vec{z},\vec{a},\vec{q}) \in \mathcal{Q}(\mathcal{N})} \mathcal{P}_{(\vec{z},\vec{a},\vec{q})} |\kappa\rangle \quad \text{for all } |\kappa\rangle \in \mathcal{I}_\diamondsuit(\mathcal{N}). \tag{7.257}$$

Since $N_{(x,b,r)} \geq 2$, note that in each term $\mathcal{P}_{(\vec{z},\vec{a},\vec{q})}$ with $(\vec{z},\vec{a},\vec{q}) \in \mathcal{Q}(\mathcal{N})$, the operator

$$|\phi^r_{x,b}\rangle\langle\phi^r_{x,b}| \otimes |\phi^r_{x,b}\rangle\langle\phi^r_{x,b}| \tag{7.258}$$

appears between two of the $N$ registers (tensored with rank-1 projectors on the other $N-2$ registers). Using equation (7.221) we may expand $|\phi^r_{x,b}\rangle$ as a sum of states from $\mathcal{W}_{(x,b,r)}$. This gives

$$|\phi^r_{x,b}\rangle|\phi^r_{x,b}\rangle = c_0|\psi^{r_{\text{in}}}_{x,b}\rangle|\psi^{r_{\text{in}}}_{x,b}\rangle + \left(1-c_0^2\right)^{\frac{1}{2}}|\Phi^r_{x,b}\rangle \tag{7.259}$$

where $c_0$ is either $\frac{1}{3R+2}$ (if $R$ is odd) or $\frac{1}{3R-1}$ (if $R$ is even), and where $|\psi^{r_{\text{in}}}_{x,b}\rangle|\psi^{r_{\text{in}}}_{x,b}\rangle$ is orthogonal to $|\Phi^r_{x,b}\rangle$. Note that each of the states $|\phi^r_{x,b}\rangle|\phi^r_{x,b}\rangle$, $|\psi^{r_{\text{in}}}_{x,b}\rangle|\psi^{r_{\text{in}}}_{x,b}\rangle$, and $|\Phi^r_{x,b}\rangle$ lie in the space

$$\operatorname{span}(\mathcal{W}_{(x,b,r)}) \otimes \operatorname{span}(\mathcal{W}_{(x,b,r)}). \tag{7.260}$$

Now applying Fact 3 gives

$$|\phi^r_{x,b}\rangle\langle\phi^r_{x,b}| \otimes |\phi^r_{x,b}\rangle\langle\phi^r_{x,b}| = c_0^2|\psi^{r_{\text{in}}}_{x,b}\rangle\langle\psi^{r_{\text{in}}}_{x,b}| \otimes |\psi^{r_{\text{in}}}_{x,b}\rangle\langle\psi^{r_{\text{in}}}_{x,b}| + M^r_{x,b} \tag{7.261}$$

where $M^r_{x,b}$ is a Hermitian operator with all of its support on the space (7.260) and

$$\left\|M^r_{x,b}\right\| \leq 1 - \frac{3}{4}c_0^4 \leq 1 - \frac{3}{4}\left(\frac{1}{3R+2}\right)^4 \leq 1 - \frac{3}{4}\frac{1}{(4R)^4} \tag{7.262}$$

since $R \geq 2$. For each $(\vec{z},\vec{a},\vec{q}) \in \mathcal{Q}(\mathcal{N})$ we define $\mathcal{P}^M_{(\vec{z},\vec{a},\vec{q})}$ to be the operator obtained from $\mathcal{P}_{(\vec{z},\vec{a},\vec{q})}$ by replacing

$$|\phi^r_{x,b}\rangle\langle\phi^r_{x,b}| \otimes |\phi^r_{x,b}\rangle\langle\phi^r_{x,b}| \mapsto M^r_{x,b} \tag{7.263}$$

on two of the registers (if $N_{(x,b,r)} > 2$ there is more than one way to do this; we fix one choice for each $(\vec{z},\vec{a},\vec{q}) \in \mathcal{Q}(\mathcal{N})$). Note that $\mathcal{P}^M_{(\vec{z},\vec{a},\vec{q})}$ has all of its support in the space $S_{(\vec{z},\vec{a},\vec{q})}$. Using (7.255) gives

$$\mathcal{P}^M_{(\vec{z},\vec{a},\vec{q})}\mathcal{P}^M_{(\vec{z}',\vec{a}',\vec{q}')} = 0 \text{ for distinct } (\vec{z},\vec{a},\vec{q}),(\vec{z}',\vec{a}',\vec{q}') \in \mathcal{Q}(\mathcal{N}). \tag{7.264}$$

Using equation (7.261) and the fact that

$$\langle\kappa|\left(|\psi^{r_{\text{in}}}_{x,b}\rangle\langle\psi^{r_{\text{in}}}_{x,b}|^{(w_1)}\right)\left(|\psi^{r_{\text{in}}}_{x,b}\rangle\langle\psi^{r_{\text{in}}}_{x,b}|^{(w_2)}\right)|\kappa\rangle = 0 \quad \text{for all } |\kappa\rangle \in \mathcal{I}_{\diamondsuit}(\mathcal{N}) \text{ and distinct } w_1, w_2 \in [N] \tag{7.265}$$

(which can be seen from the definition of $\mathcal{I}_{\diamondsuit}$), we have

$$\langle\kappa|\mathcal{P}_{(\vec{z},\vec{a},\vec{q})}|\kappa\rangle = \langle\kappa|\mathcal{P}^M_{(\vec{z},\vec{a},\vec{q})}|\kappa\rangle \quad \text{for all } |\kappa\rangle \in \mathcal{I}_{\diamondsuit}(\mathcal{N}). \tag{7.266}$$

Hence, letting

$$\Pi^{\triangle}_{\mathcal{N}} = \sum_{(\vec{z},\vec{a},\vec{q})\in\mathcal{Q}(\mathcal{N})} \mathcal{P}^M_{(\vec{z},\vec{a},\vec{q})}, \tag{7.267}$$

we have $\langle\kappa|\Pi^{\triangle}|\kappa\rangle = \langle\kappa|\Pi^{\triangle}_{\mathcal{N}}|\kappa\rangle$ for all $|\kappa\rangle \in \mathcal{I}_{\diamondsuit}(\mathcal{N})$. To obtain the desired bound (**??**) on the norm of $\Pi^{\triangle}_{\mathcal{N}}$, we use the fact that the norm of a sum of pairwise orthogonal Hermitian operators is upper bounded by the maximum norm of an operator in the sum, so

$$\left\|\Pi^{\triangle}_{\mathcal{N}}\right\| = \left\|\sum_{(\vec{z},\vec{a},\vec{q})\in\mathcal{Q}(\mathcal{N})} \mathcal{P}^M_{(\vec{z},\vec{a},\vec{q})}\right\| = \max_{(\vec{z},\vec{a},\vec{q})\in\mathcal{Q}(\mathcal{N})}\left\|\mathcal{P}^M_{(\vec{z},\vec{a},\vec{q})}\right\| = \left\|M^r_{x,b}\right\| \leq 1 - \frac{3}{4}\frac{1}{(4R)^4}. \tag{7.268}$$

Putting this together, we then have that

$$\max_{|\kappa\rangle\in\mathcal{I}_\diamondsuit(\mathcal{N})}\langle\kappa|\Pi^{\triangle}|\kappa\rangle=\max_{|\kappa\rangle\in\mathcal{I}_\diamondsuit(\mathcal{N})}\langle\kappa|\Pi^{\triangle}_{\mathcal{N}}|\kappa\rangle\leq\|\Pi^{\triangle}_{\mathcal{N}}\|\leq 1-\frac{3}{4(4R)^4}. \tag{7.269}$$

If we then use (7.250), we have that

$$\min_{|\kappa\rangle\in\mathcal{I}_\diamondsuit(\mathcal{N})}\langle\kappa|\sum_{w=1}^{N}h^{(w)}_{\mathcal{E}^{\triangle}}|\kappa\rangle>\frac{c_\triangle}{R^2}\Big(1-\max_{|\kappa\rangle\in\mathcal{I}_\diamondsuit(\mathcal{N})}\langle\kappa|\Pi^{\triangle}|\kappa\rangle\Big)\geq\frac{12c_\triangle}{(4R)^6}. \tag{7.270}$$

**Type 3**

Let us finally examine the case where $\mathcal{N}$ is of type 3 then $N_{(x,b,r)}\in\{0,1\}$ for all $x,b\in\mathbb{F}_2$ and $r\in[R]$, and

$$N_{(y,c,s)}=N_{(t,d,u)}=1 \tag{7.271}$$

for some $(y,c,s)\neq(t,d,u)$ with either $u=s$ or $\{u,s\}\in E(G^{\mathrm{occ}})$ (using property (b) and Fact 2). We show there are no eigenvectors in the nullspace of (7.231) within a block of this type and we lower bound the smallest eigenvalue within the block. We establish the same bound (7.247) as for blocks of Type 2.

The proof is very similar to that given above for blocks of Type 2. In fact, the first part of proof is identical, from equation (7.248) up to and including equation (7.257). That is to say, as in the previous case we have

$$\langle\kappa|\sum_{(\vec{z},\vec{a},\vec{q})\in\mathcal{Q}}\mathcal{P}_{(\vec{z},\vec{a},\vec{q})}|\kappa\rangle=\langle\kappa|\sum_{(\vec{z},\vec{a},\vec{q})\in\mathcal{Q}(\mathcal{N})}\mathcal{P}_{(\vec{z},\vec{a},\vec{q})}|\kappa\rangle\quad\text{for all }|\kappa\rangle\in\mathcal{I}_\diamondsuit(\mathcal{N}). \tag{7.272}$$

In this case, since $N_{(y,c,s)}=N_{(t,d,u)}=1$, in each term $\mathcal{P}_{(\vec{z},\vec{a},\vec{q})}$ with $(\vec{z},\vec{a},\vec{q})\in\mathcal{Q}(\mathcal{N})$, the operator

$$|\phi^s_{y,c}\rangle\langle\phi^s_{y,c}|\otimes|\phi^u_{t,d}\rangle\langle\phi^u_{t,d}| \tag{7.273}$$

appears between two of the $N$ registers (tensored with rank 1 projectors on the other $N-2$ registers). Using equation (7.221) we may expand $|\phi^s_{y,c}\rangle$ and $|\phi^u_{t,d}\rangle$ as superpositions (with amplitudes $\pm\frac{1}{\sqrt{3R+2}}$ if $R$ is odd or $\pm\frac{1}{\sqrt{3R-1}}$ if $R$ is even) of the basis states from $\mathcal{W}_{(y,c,s)}$ and $\mathcal{W}_{(t,d,u)}$ respectively. Since $\mathcal{W}_{(y,c,s)}$ and $\mathcal{W}_{(t,d,u)}$ overlap on some diagram element, there exists $l\in L^{\square}$ such that $|\psi^l_{x_1,b_1}\rangle\in\mathcal{W}_{(y,c,s)}$ and $|\psi^l_{x_2,b_2}\rangle\in\mathcal{W}_{(t,d,u)}$ for some $x_1,x_2,b_1,b_2\in\{0,1\}$. Hence

$$|\phi^s_{y,c}\rangle|\phi^u_{t,d}\rangle=c_0\left(\pm|\psi^l_{x_1,b_1}\rangle|\psi^l_{x_2,b_2}\rangle\right)+\left(1-c_0^2\right)^{\frac{1}{2}}|\Phi^{s,u}_{y,c,t,d}\rangle \tag{7.274}$$

where $c_0$ is either $\frac{1}{3R+2}$ (if $R$ is odd) or $\frac{1}{3R-1}$ (if $R$ is even). Now applying Fact 3 we get

$$|\phi^s_{y,c}\rangle\langle\phi^s_{y,c}|\otimes|\phi^u_{t,d}\rangle\langle\phi^u_{t,d}|=c_0^2|\psi^l_{x_1,b_1}\rangle\langle\psi^l_{x_1,b_1}|\otimes|\psi^l_{x_2,b_2}\rangle\langle\psi^l_{x_2,b_2}|+M^{s,u}_{y,c,t,d} \tag{7.275}$$

where $\|M^{s,u}_{y,c,t,d}\|\leq 1-\frac{3}{4}\left(\frac{1}{4R}\right)^4$. For each $(\vec{z},\vec{a},\vec{q})\in\mathcal{Q}(\mathcal{N})$ we define $\mathcal{P}^M_{(\vec{z},\vec{a},\vec{q})}$ to be the operator obtained from $\mathcal{P}_{(\vec{z},\vec{a},\vec{q})}$ by replacing

$$|\phi^s_{y,c}\rangle\langle\phi^s_{y,c}|\otimes|\phi^u_{t,d}\rangle\langle\phi^u_{t,d}|\mapsto M^{s,u}_{y,c,t,d} \tag{7.276}$$

on two of the registers and we let $\Pi^{\triangle}_{\mathcal{N}}$ be given by (7.267). Then, as in the previous case, $\langle\kappa|\Pi^{\triangle}|\kappa\rangle = \langle\kappa|\Pi^{\triangle}_{\mathcal{N}}|\kappa\rangle$ for all $|\kappa\rangle \in \mathcal{I}_{\diamond}(\mathcal{N})$ and using the same reasoning as before, we get the bound (7.268) on $\|\Pi^{\triangle}_{\mathcal{N}}\|$. Using these two facts we get the same bound on the smallest eigenvalue within a block of type 3 as the bound we obtained for blocks of type 2:

$$\min_{|\kappa\rangle\in\mathcal{I}_{\diamond}(\mathcal{N})} \langle\kappa|\sum_{w=1}^{N} h^{(w)}_{\mathcal{E}^{\triangle}}|\kappa\rangle > \frac{c_{\triangle}}{R^2}\Big(1 - \max_{|\kappa\rangle\in\mathcal{I}_{\diamond}(\mathcal{N})}\langle\kappa|\Pi^{\triangle}|\kappa\rangle\Big) \geq \frac{12c_{\triangle}}{(4R)^6}. \qquad \square$$

### 7.3.6 The gate graph $G^{\square}$

With all of the intermediate graphs characterized, we now consider the gate graph $G^{\square}$ and prove Lemma 21. We first show that $G^{\square}$ is an $e_1$-gate graph. From equations (7.195), (7.197), and (7.198) we have

$$A(G^{\square}) = A(G^{\triangle}) + h_{\mathcal{E}^0} + h_{\mathcal{S}^0}. \tag{7.277}$$

Lemma 23 characterizes the $e_1$-energy ground space of $G^{\triangle}$ and gives an orthonormal basis $\{|\phi^q_{z,a}\rangle\colon z, a \in \{0,1\},\, q \in [R]\}$ for it. To solve for the $e_1$-energy ground space of $A(G^{\square})$, we solve for superpositions of the states $\{|\phi^q_{z,a}\rangle\}$ in the nullspace of $h_{\mathcal{E}^0} + h_{\mathcal{S}^0}$.

Recall the definition of the sets $\mathcal{E}^0$ and $\mathcal{S}^0$, as these are the edges and self-loops that are inherited from the graph $G$. From Section 7.3.2.1, each node $(q, z, t)$ in the gate diagram for $G$ is associated with a node $\mathrm{new}(q, z, t)$ in the gate diagram for $G^{\square}$ as described by (7.187). This mapping is depicted in Figure 7.7 by the black and grey arrows. Applying this mapping to each pair of nodes in the edge set $\mathcal{E}^G$ and each node in the self-loop set $\mathcal{S}^G$ of the gate diagram for $G$, we get the sets $\mathcal{E}^0$ and $\mathcal{S}^0$. Hence, using equations (7.83) and (7.84),

$$h_{\mathcal{S}^0} = \sum_{(q,z,t)\in\mathcal{S}^G} |\mathrm{new}(q,z,t)\rangle\langle\mathrm{new}(q,z,t)| \otimes \mathbb{I} \tag{7.278}$$

$$h_{\mathcal{E}^0} = \sum_{\{(q,z,t),(q',z',t')\}\in\mathcal{E}^G} \left(|\mathrm{new}(q,z,t)\rangle + |\mathrm{new}(q',z',t')\rangle\right)\left(\langle\mathrm{new}(q,z,t)| + \langle\mathrm{new}(q',z',t')|\right) \otimes \mathbb{I}. \tag{7.279}$$

Using equation (7.221), we see that for all nodes $(q, z, t)$ in the gate diagram for $G$ and for all $j \in [8]$, $x, b, d \in \mathbb{F}_2$, and $r \in [R]$,

$$\begin{aligned}\langle\mathrm{new}(q,z,t), j, d|\phi^r_{x,b}\rangle &= \sqrt{c_0}\begin{cases}\langle q_{\mathrm{in}}, z, t, j, d|\psi^{r_{\mathrm{in}}}_{x,b}\rangle & \text{if } (q,z,t) \text{ is an input node}\\ \langle q_{\mathrm{out}}, z, t, j, d|\psi^{r_{\mathrm{out}}}_{x,b}\rangle & \text{if } (q,z,t) \text{ is an output node}\end{cases}\\ &= \sqrt{c_0}\,\delta_{r,q}\langle z, t, j, d|\psi_{x,b}\rangle\end{aligned} \tag{7.280}$$

where $c_0$ is $\frac{1}{3R+2}$ if $R$ is odd or $\frac{1}{3R-1}$ if $R$ is even, and where $|\psi_{x,b}\rangle$ is defined by equations (7.32) and (7.33). The matrix element on the left-hand side of this equation is evaluated in the Hilbert space $\mathcal{Z}_1(G^{\square})$ where each basis vector corresponds to a vertex of the graph $G^{\square}$; these vertices are labeled $(l, z, t, j, d)$ with $l \in L^{\square}$, $z, d \in \mathbb{F}_2$, $t \in [2k]$, and $j \in [8]$. However, from (7.280) we see that

$$\underbrace{\langle\mathrm{new}(q,z,t), j, d|\phi^r_{x,b}\rangle}_{\text{in } \mathcal{Z}_1(G^{\square})} = \sqrt{c_0}\,\underbrace{\langle q, z, t, j, d|\psi^r_{x,b}\rangle}_{\text{in } \mathcal{Z}_1(G)} \tag{7.281}$$

where the right-hand side is evaluated in the Hilbert space $\mathcal{Z}_1(G)$.

Putting together equations (7.278), (7.279), and (7.281) gives

$$\langle\phi^q_{z,a}|h_{\mathcal{E}^0}+h_{\mathcal{S}^0}|\phi^r_{x,b}\rangle=\langle\psi^q_{z,a}|h_{\mathcal{E}^G}+h_{\mathcal{S}^G}|\psi^r_{x,b}\rangle\cdot\begin{cases}\frac{1}{3R+2} & R\text{ odd}\\ \frac{1}{3R-1} & R\text{ even}\end{cases}\tag{7.282}$$

for all $z,a,x,b\in\mathbb{F}_2$ and $q,r\in[R]$. On the left-hand side of this equation, the Hilbert space is $\mathcal{Z}_1(G^\square)$; on the right-hand side it is $\mathcal{Z}_1(G)$.

We use equation (7.282) to relate the $e_1$-energy ground states of $A(G)$ to those of $A(G^\square)$. Since $G$ is an $e_1$-gate graph, there is a state

$$|\Gamma\rangle=\sum_{z,a,q}\alpha_{z,a,q}|\psi^q_{z,a}\rangle\in\mathcal{Z}_1(G)\tag{7.283}$$

that satisfies $A(G)|\Gamma\rangle=e_1|\Gamma\rangle$ and hence $h_{\mathcal{E}^G}|\Gamma\rangle=h_{\mathcal{S}^G}|\Gamma\rangle=0$. Letting

$$|\Gamma'\rangle=\sum_{z,a,q}\alpha_{z,a,q}|\phi^q_{z,a}\rangle\in\mathcal{Z}_1(G^\square)\tag{7.284}$$

and using equation (7.282), we see that $\langle\Gamma'|h_{\mathcal{E}^0}+h_{\mathcal{S}^0}|\Gamma'\rangle=0$ and therefore $\langle\Gamma'|A(G^\square)|\Gamma'\rangle=e_1$. Hence $G^\square$ is an $e_1$-gate graph. Moreover, the linear mapping from $\mathcal{Z}_1(G)$ to $\mathcal{Z}_1(G^\square)$ defined by

$$|\psi^q_{z,a}\rangle\mapsto|\phi^q_{z,a}\rangle\tag{7.285}$$

maps each $e_1$-energy eigenstate of $A(G)$ to an $e_1$-energy eigenstate of $A(G^\square)$.

Now consider the $N$-particle Hamiltonian $H(G^\square,N)$. Using equation (7.277) and the fact that both $A(G^\square)$ and $A(G^\triangle)$ have smallest eigenvalue $e_1$, we have

$$H(G^\square,N)=H(G^\triangle,N)+\sum_{w=1}^{N}\left(h_{\mathcal{E}^0}+h_{\mathcal{S}^0}\right)^{(w)}\Big|_{\mathcal{Z}_N(G^\square)}+C',\tag{7.286}$$

where $C$ corresponds to the added interactions resulting from the additional edges. IRecall from Lemma 23 that the nullspace of the first term is $\mathcal{I}_\triangle$. The $N$-fold tensor product of the mapping (7.285) acts on basis vectors of $\mathcal{I}(G,G^{\text{occ}},N)$ as

$$\text{Sym}(|\psi^{q_1}_{z_1,a_1}\rangle|\psi^{q_2}_{z_2,a_2}\rangle\ldots|\psi^{q_N}_{z_N,a_N}\rangle)\mapsto\text{Sym}(|\phi^{q_1}_{z_1,a_1}\rangle|\phi^{q_2}_{z_2,a_2}\rangle\ldots|\phi^{q_N}_{z_N,a_N}\rangle),\tag{7.287}$$

where $z_i,a_i\in\mathbb{F}_2$, $q_i\neq q_j$, and $\{q_i,q_j\}\notin E(G^{\text{occ}})$. Clearly this defines an invertible linear map between the two spaces $\mathcal{I}(G,G^{\text{occ}},N)$ and $\mathcal{I}_\triangle$. Let $|\Theta\rangle\in\mathcal{I}(G,G^{\text{occ}},N)$ and write $|\Theta'\rangle\in\mathcal{I}_\triangle$ for its image under the map (7.287). Then

$$\langle\Theta'|H(G^\square,N)-C'|\Theta'\rangle=\langle\Theta'|\sum_{w=1}^{N}\left(h_{\mathcal{E}^0}+h_{\mathcal{S}^0}\right)^{(w)}|\Theta'\rangle\tag{7.288}$$

$$=\langle\Theta|\sum_{w=1}^{N}\left(h_{\mathcal{E}^G}+h_{\mathcal{S}^G}\right)^{(w)}|\Theta\rangle\cdot\begin{cases}\frac{1}{3R+2} & R\text{ odd}\\ \frac{1}{3R-1} & R\text{ even}\end{cases}\tag{7.289}$$

where in the first equality we used the fact that $|\Theta'\rangle$ is in the nullspace $\mathcal{I}_\triangle$ of $H(G^\triangle, N)$ and in the second equality we used equation (7.282) and the fact that $\langle \phi^q_{z,a}|\phi^r_{x,b}\rangle = \langle \psi^q_{z,a}|\psi^r_{x,b}\rangle$.

Understanding how $C'$ relates to the added interactions in the original gate-graph $G$ is slightly more tricksome, as an arbitrary state we might have $N$-particle interactions which under our transformation would require a factor of $(3R)^{-N}$ to the energy. However, the fact that each state in $\mathcal{I}_\triangle$ and each state in $\mathcal{I}(G, G^{\text{occ}}, N)$ satisfy the occupancy constraints implies that at most a single particle ever occupies a single vertex (and thus $C' = 0$ if $d_{\max} = 0$). Using this, we have that when restricted to those states in $\mathcal{I}_\triangle$, $C'$ only affects two-particles at a time and the requisite change to the energy penalty will only be $(3R)^{-2}$.

[**TO DO:** *probably I should make this more coherent*] As such, let $\mathcal{V}^\square \subset V(G^\square) \times V(G^\square)$ consist of those pairs of vertices that could be affected by the new interactions caused by the added edges. Since each node of every diagram element is separated by a distance at least $d_{\max}$, we have that each pair of vertices must come from diagram elements labeled $q_{\text{in}}$ or $q_{\text{out}}$. Further, if we let $\mathcal{V} \subset V(G) \times V(G)$ be the similar set of vertices that can have interactions caused by the added edges in $G$, we have that $\mathcal{V}^\square$ is in one-to-one correspondence to those of $\mathcal{V}$, since we have added the same number of edges. In particular, we have that the vertices on [**TO DO:** *actually figure out this mapping*]

With this in mind, along with the fact that we have at most a single particle located on each vertex and the relation between $|\phi^q_{z,a}\rangle$ and $|\psi^q_{z,a}\rangle$, we have that

$$\langle\Theta'|C'|\Theta'\rangle = \sum_{(u',v')\in\mathcal{V}^\square} \sum_{w_1\neq w_2\in[N]} \langle\Theta'|\big(|u'\rangle\langle u'|^{(w_1)} \otimes |v'\rangle\langle v'|^{(w_2)}\big)|\Theta'\rangle \tag{7.290}$$

$$= \sum_{(u,v)\in\mathcal{V}} \sum_{w_1\neq w_2\in[N]} \langle\Theta|\big(|u\rangle\langle u|^{(w_1)} \otimes |v\rangle\langle v|^{(w_2)}\big)|\Theta\rangle \begin{cases} \frac{1}{(3R+2)^2} & R \text{ odd} \\ \frac{1}{(3R-1)^2} & R \text{ even} \end{cases} \tag{7.291}$$

$$= \langle\Theta|C|\Theta\rangle \begin{cases} \frac{1}{(3R+2)^2} & R \text{ odd} \\ \frac{1}{(3R-1)^2} & R \text{ even} \end{cases} \tag{7.292}$$

We now complete the proof of Lemma 21 using equation (7.289) and (7.292).

**Case 1:** $\lambda_N(G, G^{\mathbf{occ}}) \leq a$

In this case there exists a state $|\Theta\rangle \in \mathcal{I}(G, G^{\text{occ}}, N)$ satisfying

$$\langle\Theta|\sum_{w=1}^{N}(h_{\mathcal{E}^G} + h_{\mathcal{S}^G})^{(w)} + C|\Theta\rangle = a_{\text{adj}} + a_{\text{int}} \leq a, \tag{7.293}$$

From equation (7.289) we see that the state $|\Theta'\rangle \in \mathcal{I}_\triangle$ satisfies $\langle\Theta'||\Theta'\rangle \leq \frac{a_{\text{adj}}}{3R-1}$, and from (7.292) that it also satisfies $\langle\Theta'|C'|\Theta\rangle' \leq \frac{a_{\text{int}}}{(3R-1)^2}$.

Putting this together, (along with the fact that $|\Theta'\rangle \in \mathcal{I}_\triangle$ and thus is in the nullspace of $H(G^\triangle, N)$),

$$\langle\Theta'|H(G^\square, N)|\Theta'\rangle \leq \frac{a_{\text{adj}}}{3R-1} + \frac{a_{\text{int}}}{(3R-1)^2} < \frac{a_{\text{adj}}}{R} + \frac{a_{\text{int}}}{R} = \frac{a}{R}. \tag{7.294}$$

**Case 2:** $\lambda_N(G, G^{\mathbf{occ}}) \geq b$

In this case

$$\lambda_N(G, G^{\text{occ}}) = \min_{|\Theta\rangle \in \mathcal{I}(G, G^{\text{occ}}, N)} \langle \Theta | H(G, G^{\text{occ}}, N) | \Theta \rangle \tag{7.295}$$

$$= \min_{|\Theta\rangle \in \mathcal{I}(G, G^{\text{occ}}, N)} \langle \Theta | \sum_{w=1}^{N} (h_{\mathcal{E}^G} + h_{\mathcal{S}^G})^{(w)} |\Theta\rangle + \langle \Theta | C | \Theta \rangle \tag{7.296}$$

$$= b_{\text{adj}} + b_{\text{int}} \geq b. \tag{7.297}$$

Now applying equation (7.289) and (7.292) gives

$$\min_{|\Theta'\rangle \in \mathcal{I}_{\triangle}} \langle \Theta' | H(G^{\square}, N) | \Theta' \rangle = \min_{|\Theta'\rangle \in \mathcal{I}_{\triangle}} \langle \Theta' | \sum_{w=1}^{N} (h_{\mathcal{E}^0} + h_{\mathcal{S}^0})^{(w)} |\Theta'\rangle + \langle \Theta' | C' | \Theta' \rangle \tag{7.298}$$

$$\geq \frac{b_{\text{adj}}}{3R+2} + \frac{b_{\text{int}}}{(3R+2)^2} \tag{7.299}$$

$$\geq \frac{1}{(3R+2)^2} b, \tag{7.300}$$

This establishes that the nullspace of $H(G^{\square}, N)$ is empty, i.e., $\lambda_N^1(G^{\square}) > 0$, so $\lambda_N^1(G^{\square}) = \gamma(H(G^{\square}, N))$. We lower bound $\lambda_N^1(G^{\square})$ using the Nullspace Projection Lemma (Lemma **??**) with

$$H_A = H(G^{\triangle}, N) \qquad H_B = \sum_{w=1}^{N} (h_{\mathcal{E}^0} + h_{\mathcal{S}^0})^{(w)} \Big|_{\mathcal{Z}_N(G^{\square})} + C' \tag{7.301}$$

and where the nullspace of $H_A$ is $S = \mathcal{I}_{\triangle}$. We apply Lemma **??** and use the bounds $\gamma(H_A) > \frac{\gamma_{\triangle}}{R^7}$ (from Lemma 24), $\gamma(H_B|_S) \geq \frac{b}{(3R+2)^2}$ (from equation (7.300)), and

$$\|H_B\| \leq N \|h_{\mathcal{E}^0} + h_{\mathcal{S}^0}\| + \|H_{\text{int}}\| \leq 3N + d_{\mathcal{U}} N^{\nu} \leq d_{\mathcal{U}} R^{\nu_{\mathcal{U}}} \tag{7.302}$$

(using equations (7.86) and (7.85), the bounds on $H_{\text{int}}$, and the fact that $N \leq R$) to find

$$\lambda_N^1(G^{\square}) = \gamma(H(G^{\square}, N)) \tag{7.303}$$

$$\geq \frac{\gamma_{\triangle} b}{(3R+2)^2 R^7} \frac{1}{\frac{\gamma_{\triangle}}{R^7} + d_{\mathcal{U}} R^{\nu_{\mathcal{U}}}} \tag{7.304}$$

$$> \frac{\gamma_{\square} b}{R^{9+\nu}} \tag{7.305}$$

where $\gamma_{\square}$ depends only on the interaction $\mathcal{U}$.

## 7.4 Constructing the graph for QMA-completeness

With the graphs defined in Section 7.2 and the ability to ensure that certain states are excluded from the ground space via the occupancy constraints lemma Section 7.3.1, we will now be able to construct the graph that will be used in our QMA-completeness proof. In particular, we will show how to transform a given circuit into a graph, such that the $n$-particle ground-energy will correspond to whether the circuit has an accepting state when certain states are excluded from the ground space.

The main idea will be to use the graph primitives of Section 7.2 to construct a gate graph replacing circuits of a particular form. We will use a single particle for each qubit, and use the location of a single qubit to encode the current "time" of the occupation. Using our two-particle graph gadgets, we can then ensure that the particles move together through the entire computation (assuming that they start in the correct possitions).

### 7.4.1 Verification circuits

[**TO DO:** *Show that the circuit can be written in the requisite form.*]

### 7.4.2 Gate graph for a given circuit

For any $n$-qubit, $M$-gate verification circuit $\mathcal{C}_X$ of the form described above, we associate a gate graph $G_X$. The gate diagram for $G_X$ is built using the gadgets described in Section **??**; specifically, we use $M$ two-qubit gadgets and $2(n-1)$ boundary gadgets. Since each two-qubit gadget and each boundary gadget contains 32 diagram elements, the total number of diagram elements in $G_X$ is $R = 32(M + 2n - 2)$.

We now present the construction of the gate diagram for $G_X$. We also describe some gate graphs obtained as intermediate steps that are used in our analysis in Section **??**. The reader may find this description easier to follow by looking ahead to Figure 7.12, which illustrates this construction for a specific 3-qubit circuit.

1. **Draw a grid** with columns labeled $j = 0, 1, \ldots, M + 1$ and rows labeled $i = 1, \ldots, n$ (this grid is only used to help describe the diagram).

2. **Place gadgets in the grid to mimic the quantum circuit.** For each $j = 1, \ldots, M$, place a gadget for the two-qubit gate $U_j$ between rows 1 and $s(j)$ in the $j$th column. Place boundary gadgets in rows $i = 2, \ldots, n$ of column 0 and in the same rows of column $M + 1$. Write $G_1$ for the gate graph associated with the resulting diagram.

3. **Connect the nodes within each row.** First add edges connecting the nodes in rows $i = 2, \ldots, n$; call the resulting gate graph $G_2$. Then add edges connecting the nodes in row 1; call the resulting gate graph $G_3$.

4. **Add self-loops to the boundary gadgets.** In this step we add self-loops to enforce initialization of ancillas (at the beginning) and the proper output of the circuit (at the end). For each row $k = n_{\text{in}}+1, \ldots, n$, add a self-loop to node $\delta$ (as shown in Figure 7.6) of the corresponding boundary gadget in column $r = 0$, giving the gate diagram for $G_4$. Finally, add a self-loop to node $\alpha$ of the boundary gadget (as in Figure 7.6) in row 2 and column $M + 1$, giving the gate diagram for $G_X$.

Figure 7.12 illustrates the step-by-step construction of $G_X$ using a simple 3-qubit circuit with four gates

$$\mathrm{CNOT}_{12}\,(\mathrm{CNOT}_{13} HT \otimes \mathbb{I})\,\mathrm{CNOT}_{21}\mathrm{CNOT}_{13}. \tag{7.306}$$

In this example, two of the qubits are input qubits (so $n_{\text{in}} = 2$), while the third qubit is an ancilla initialized to $|0\rangle$. Following the convention described in Section **??**, we take qubit 2 to be the output qubit. (In this example the circuit is not meant to compute anything interesting; its only purpose is to illustrate our method of constructing a gate graph).

We made some choices in designing this circuit-to-gate graph mapping that may seem arbitrary (e.g., we chose to place boundary gadgets in each row except the first). We have tried to achieve a balance between simplicity of description and ease of analysis, but we expect that other choices could be made to work.

#### 7.4.2.1 Notation for $G_X$

We now introduce some notation that allows us to easily refer to a subset $\mathcal{L}$ of the diagram elements in the gate diagram for $G_X$.

Recall from Section **??** that each two-qubit gate gadget and each boundary gadget is composed of 64 diagram elements. This can be seen by looking at Figure 7.5a and noting (from Figure 7.4) that each move-together gadget comprises 14 diagram elements.

For each of the two-qubit gate gadgets in the gate diagram for $G_X$, we focus our attention on the four diagram elements labeled 1–4 in Figure 7.5a. In total there are $4M$ such diagram elements in the gate diagram for $G_X$: in each column $j \in \{1, \ldots, M\}$ there are two in row 1 and two in row $s(j)$. When $U_j \in \{\mathrm{CNOT}_{1s(j)}, \mathrm{CNOT}_{1s(j)}\,(H \otimes \mathbb{I})\,, \mathrm{CNOT}_{1s(j)}\,(HT \otimes \mathbb{I})\}$ the diagram elements labeled $1, 2$ are in row 1 and those labeled $3, 4$ are in row $s(j)$; when $U_j = \mathrm{CNOT}_{s(j)1}$ those labeled $1, 2$ are in row $s(j)$ and those labeled $3, 4$ are in row 1. We denote these diagram elements by triples $(i, j, d)$. Here $i$ and $j$ indicate (respectively) the row and column of the grid in which the diagram element is found, and $d$ indicates whether it is the leftmost ($d = 0$) or rightmost ($d = 1$) diagram element in this row and column. We define

$$\mathcal{L}_{\text{gates}} = \{(i, j, d) : i \in \{1, s(j)\},\ j \in [M],\ d \in \{0, 1\}\} \tag{7.307}$$

to be the set of all such diagram elements.

For example, in Figure 7.12 the first gate is

$$U_1 = \mathrm{CNOT}_{13}, \tag{7.308}$$

so the gadget from Figure 7.5a (with $\tilde{U} = 1$) appears between rows 1 and 3 in the first column. The diagram elements labeled $1, 2, 3, 4$ from Figure 7.5a are denoted by $(1, 1, 0), (1, 1, 1), (3, 1, 0), (3, 1, 1)$, respectively. The second gate in Figure 7.12 is $U_2 = \mathrm{CNOT}_{21}$, so the gadget from Figure 7.5b (with $\tilde{U} = 1$) appears between rows 2 and 1; in this case the diagram elements labeled $1, 2, 3, 4$ in Figure 7.5a are denoted by $(2, 2, 0), (2, 2, 1), (1, 2, 0), (1, 2, 1)$, respectively.

We also define notation for the boundary gadgets in $G_X$. For each boundary gadget. we focus on a single diagram element, labeled 4 in Figure 7.6. For the left hand-side and right-hand side boundary gadgets, respectively, we denote these diagram elements as

$$\mathcal{L}_{\text{in}} = \{(i, 0, 1) \colon i \in \{2, \ldots, n\}\} \tag{7.309}$$

$$\mathcal{L}_{\text{out}} = \{(i, M+1, 0) \colon i \in \{2, \ldots, n\}\}\,. \tag{7.310}$$

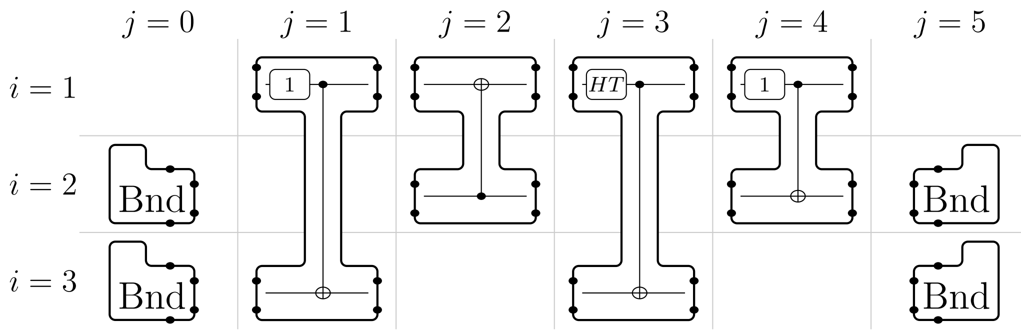


a

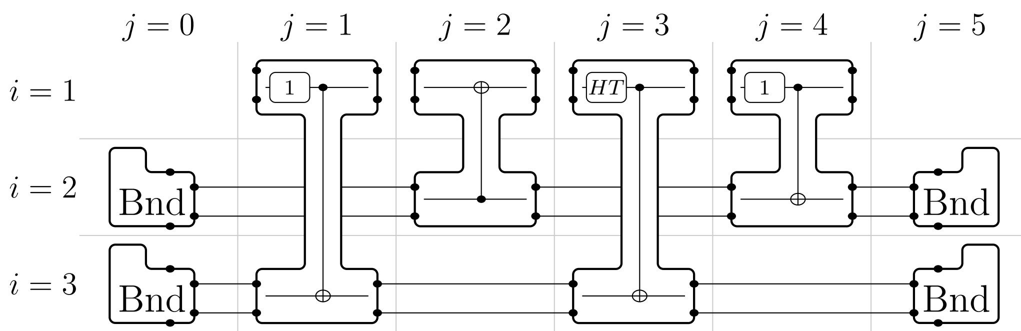


b

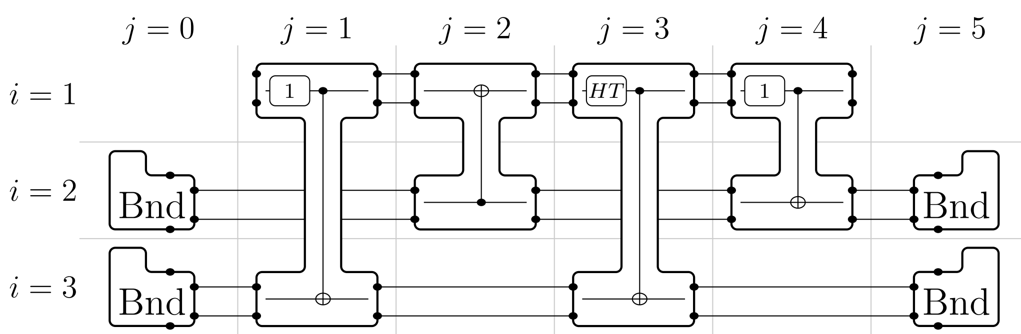


c

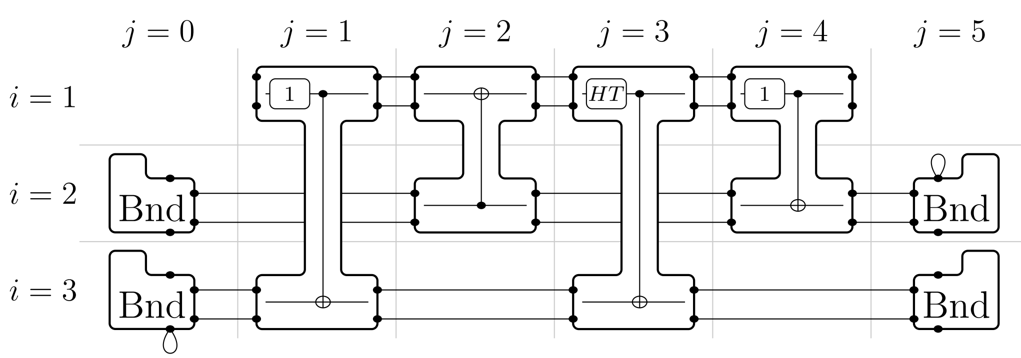


d

Figure 7.12: Step-by-step construction of the gate diagram for $G_X$ for the three-qubit example circuit described in the text. (a) The gate diagram for $G_1$. (b) Add edges in all rows except the first to obtain the gate diagram for $G_2$. (c) Add edges in the first row to obtain the gate diagram for $G_3$. (d) Add self-loops to the boundary gadgets to obtain the gate diagram for $G_X$ (the diagram for $G_4$ in this case differs from (d) by removing the self-loop in column 5; this diagram is not shown).

**Definition 8.** Let $\mathcal{L}$ be the set of diagram elements

$$\mathcal{L} = \mathcal{L}_{\text{in}} \cup \mathcal{L}_{\text{gates}} \cup \mathcal{L}_{\text{out}} \tag{7.311}$$

where $\mathcal{L}_{\text{in}}$, $\mathcal{L}_{\text{gates}}$, and $\mathcal{L}_{\text{out}}$ are given by equations (7.309), (7.307), and (7.310), respectively.

Finally, it is convenient to define a function $F$ that describes horizontal movement within the rows of the gate diagram for $G_X$. The function $F$ takes as input a two-qubit gate $j \in [M]$, a qubit $i \in \{2, \ldots, n\}$, and a single bit and outputs a diagram element from the set $\mathcal{L}$. If the bit is 0 then $F$ outputs the diagram element in row $i$ that appears in a column $0 \le k < j$ with $k$ maximal (i.e., the closest diagram element in row $i$ to the left of column $j$):

$$F(i, j, 0) = \begin{cases} (i, k, 1) & \text{where } 1 \le k < j \text{ is the largest } k \text{ such that } s(k) = i \text{, if it exists} \\ (i, 0, 1) & \text{otherwise.} \end{cases} \tag{7.312}$$

On the other hand, if the bit is 1, then $F$ outputs the diagram element in row $i$ that appears in a column $j < k \le M + 1$ with $k$ minimal (i.e., the closest diagram element in row $i$ to the right of column $j$).

$$F(i, j, 1) = \begin{cases} (i, k, 0) & \text{where } j < k \le M \text{ is the smallest } k \text{ such that } s(k) = j \text{, if it exists} \\ (i, M+1, 0) & \text{otherwise.} \end{cases} \tag{7.313}$$

#### 7.4.2.2 Occupancy constraints graph

In this Section we define an occupancy constraints graph $G_X oc$. Along with $G_X$ and the number of particles $n$, this determines a subspace $\mathcal{I}(G_X, G_X oc, n) \subset \mathcal{Z}_n(G_X)$ through equation (**??**). We will see in Section **??** how low-energy states of the Bose-Hubbard model that live entirely within this subspace encode computations corresponding to the quantum circuit $\mathcal{C}_X$. This fact is used in the proof of Theorem **??**, which shows that the smallest eigenvalue $\lambda_n^1(G_X, G_X oc)$ of

$$H(G_X, G_X oc, n) = H(G_X, n)\big|_{\mathcal{I}(G_X, G_X oc, n)} \tag{7.314}$$

is related to the maximum acceptance probability of the circuit.

We encode quantum data in the locations of $n$ particles in the graph $G_X$ as follows. Each particle encodes one qubit and is located in one row of the graph $G_X$. Since all two-qubit gates in $\mathcal{C}_X$ involve the first qubit, the location of the particle in the first row determines how far along the computation has proceeded. We design the occupancy constraints graph to ensure that low-energy states of $H(G_X, G_X oc, n)$ have exactly one particle in each row (since there are $n$ particles and $n$ rows), and so that the particles in rows $2, \ldots, n$ are not too far behind or ahead of the particle in the first row. To avoid confusion, we emphasize that not *all* states in the subspace $\mathcal{I}(G_X, G_X oc, n)$ have the desired properties—for example, there are states in this subspace with more than one particle in a given row. We see in the next Section that states with low energy for $H(G_X, n)$ that also satisfy the occupancy constraints (i.e., low-energy states of $H(G_X, G_X oc, n)$) have the desired properties.

We now define $G_X oc$, which is a simple graph with a vertex for each diagram element in $G_X$. Each edge in $G_X oc$ places a constraint on the locations of particles in $G_X$. The graph $G_X oc$ only has edges between diagram elements in the set $\mathcal{L}$ from Definition 8; we define the edge set $E(G_X oc)$ by specifying pairs of diagram elements $L_1, L_2 \in \mathcal{L}$. We also indicate (in bold) the reason for choosing the constraints, which will become clearer in Section **??**.

1. **No two particles in the same row.** For each $i \in [n]$ we add constraints between diagram elements $(i, j, c) \in \mathcal{L}$ and $(i, k, d) \in \mathcal{L}$ in row $i$ but in different columns, i.e.,

$$\{(i, j, c), (i, k, d)\} \in E(G_X oc) \text{ whenever } j \neq k. \tag{7.315}$$

2. **Synchronization with the particle in the first row.** For each $j \in [M]$ we add constraints between row 1 and row $s(j)$:

$$\{(1, j, c), (s(j), k, d)\} \in E(G_X oc) \text{ whenever } k \neq j \text{ and } (s(j), k, d) \neq F(s(j), j, c). \tag{7.316}$$

   For each $j \in [M]$ we also add constraints between row 1 and rows $i \in [n] \setminus \{1, s(j)\}$:

$$\{(1, j, c), (i, k, d)\} \in E(G_X oc) \text{ whenever } (i, k, d) \notin \{F(i, j, 0), F(i, j, 1)\}. \tag{7.317}$$

## 7.5 Proof of QMA-hardness for MPQW ground energy

Theorem **??** bounds the smallest eigenvalue $\lambda_n^1(G_X, G_X oc)$ of $H(G_X, G_X oc, n)$. To prove the Theorem, we investigate a sequence of Hamiltonians starting with $H(G_1, n)$ and $H(G_1, G_X oc, n)$ and then work our way up to the Hamiltonian $H(G_X, G_X oc, n)$ by adding positive semidefinite terms.

For each Hamiltonian we consider, we solve for the nullspace and the smallest nonzero eigenvalue. To go from one Hamiltonian to the next, we use the following "Nullspace Projection Lemma," which was used (implicitly) in reference [**?**]. The Lemma bounds the smallest nonzero eigenvalue $\gamma(H_A + H_B)$ of a sum of positive semidefinite Hamiltonians $H_A$ and $H_B$ using knowledge of the smallest nonzero eigenvalue $\gamma(H_A)$ of $H_A$ and the smallest nonzero eigenvalue $\gamma(H_B|_S)$ of the restriction of $H_B$ to the nullspace $S$ of $H_A$.

We prove the Lemma in Section **??**. When we apply this Lemma, we are usually interested in an asymptotic limit where $c, d \ll \|H_B\|$ and the right-hand side of (**??**) is $\Omega(\frac{cd}{\|H_B\|})$.

Our proof strategy, using repeated applications of the Nullspace Projection Lemma, is analogous to that of reference [**?**], where the so-called Projection Lemma was used similarly. Our technique has the advantage of not requiring the terms we add to our Hamiltonian to have "unphysical" problem-size dependent coefficients (it also has this advantage over the method of perturbative gadgets [**?**, **?**]). This allows us to prove results about the "physically realistic" Bose-Hubbard Hamiltonian. A similar technique based on Kitaev's Geometric Lemma was used recently in reference [**?**] (however, that method is slightly more computation intensive, requiring a lower bound on $\gamma(H_B)$ as well as bounds on $\gamma(H_A)$ and $\gamma(H_B|_S)$).

### 7.5.1 Single-particle ground-states

We begin by discussing the graphs

$$G_1, G_2, G_3, G_4, G_X \tag{7.318}$$

(as defined in Section **??**; see Figure 7.12) in more detail and deriving some properties of their adjacency matrices.

The graph $G_1$ has a component for each of the two-qubit gates $j \in [M]$, for each of the boundary gadgets $i = 2, \ldots, n$ in column 0, and for each of the boundary gadgets $i = 2, \ldots, n$ in column $M + 1$. In other words

$$G_1 = \underbrace{\left(\bigcup_{i=2}^{n} G_{\mathrm{bnd}}\right)}_{\text{left boundary}} \cup \underbrace{\left(\bigcup_{j=1}^{M} G_{U_j}\right)}_{\text{two-qubit gates}} \cup \underbrace{\left(\bigcup_{i=2}^{n} G_{\mathrm{bnd}}\right)}_{\text{right boundary}}. \tag{7.319}$$

We use our knowledge of the adjacency matrices of the components $G_{\mathrm{bnd}}$ and $G_{U_j}$ to understand the ground space of $A(G_1)$. Recall (from Section **??**) that the smallest eigenvalue of $A(G_{U_j})$ is

$$e_1 = -1 - 3\sqrt{2} \tag{7.320}$$

(with degeneracy 16) which is also the smallest eigenvalue of $A(G_{\mathrm{bnd}})$ (with degeneracy 4). For each diagram element $L \in \mathcal{L}$ and pair of bits $z, a \in \{0, 1\}$ there is an eigenstate $|\rho_{z,a}^{L}\rangle$ of $A(G_1)$ with this minimal eigenvalue $e_1$. In total we get sixteen eigenstates

$$|\rho_{z,a}^{(1,j,0)}\rangle, |\rho_{z,a}^{(1,j,1)}\rangle, |\rho_{z,a}^{(s(j),j,0)}\rangle, |\rho_{z,a}^{(s(j),j,1)}\rangle, \quad z, a \in \{0, 1\} \tag{7.321}$$

for each two-qubit gate $j \in [M]$, four eigenstates

$$|\rho_{z,a}^{(i,0,1)}\rangle, \quad z, a \in \{0, 1\} \tag{7.322}$$

for each boundary gadget $i \in \{2, \ldots, n\}$ in column 0, and four eigenstates

$$|\rho_{z,a}^{(i,M+1,0)}\rangle, \quad z, a \in \{0, 1\} \tag{7.323}$$

for each boundary gadget $i \in \{2, \ldots, n\}$ in column $M + 1$. The set

$$\left\{|\rho_{z,a}^{L}\rangle \colon z, a \in \{0, 1\},\ L \in \mathcal{L}\right\} \tag{7.324}$$

is an orthonormal basis for the ground space of $A(G_1)$.

We write the adjacency matrices of $G_2$, $G_3$, $G_4$, and $G_X$ as

$$A(G_2) = A(G_1) + h_1 \qquad A(G_4) = A(G_3) + \sum_{i=n_{\mathrm{in}}+1}^{n} h_{\mathrm{in},i} \tag{7.325}$$

$$A(G_3) = A(G_2) + h_2 \qquad A(G_X) = A(G_4) + h_{\mathrm{out}}. \tag{7.326}$$

From step 3 of the construction of the gate diagram in Section **??**, we see that $h_1$ and $h_2$ are both sums of terms of the form

$$\left(|q, z, t\rangle + |q', z, t'\rangle\right)\left(\langle q, z, t| + \langle q', z, t'|\right) \otimes \mathbb{I}_j, \tag{7.327}$$

where $h_1$ contains a term for each edge in rows $2, \ldots, n$ and $h_2$ contains a term for each of the $2(M-1)$ edges in the first row. The operators

$$h_{\text{in},i} = |(i,0,1),1,7\rangle\langle(i,0,1),1,7| \otimes \mathbb{I} \quad h_{\text{out}} = |(2,M+1,0),0,5\rangle\langle(2,M+1,0),0,5| \otimes \mathbb{I} \tag{7.328}$$

correspond to the self-loops added in the gate diagram in step 4 of Section **??**.

We prove that $G_1$, $G_2$, $G_3$, $G_4$, and $G_X$ are $e_1$-gate graphs.

**Lemma 25.** *The smallest eigenvalues of $G_1, G_2, G_3, G_4$ and $G_X$ are*

$$\mu(G_1) = \mu(G_2) = \mu(G_3) = \mu(G_4) = \mu(G_X) = e_1. \tag{7.329}$$

*Proof.* We showed in the above discussion that $\mu(G_1) = e_1$. The adjacency matrices of $G_2$, $G_3$, $G_4$, and $G_X$ are obtained from that of $G_1$ by adding positive semidefinite terms ($h_1$, $h_2$, $h_{\text{in},i}$, and $h_{\text{out}}$ are all positive semidefinite). It therefore suffices to exhibit an eigenstate $|\varrho\rangle$ of $A(G_1)$ with

$$h_1|\varrho\rangle = h_2|\varrho\rangle = h_{\text{in},i}|\varrho\rangle = h_{\text{out}}|\varrho\rangle = 0 \tag{7.330}$$

(for each $i \in \{n_{\text{in}}+1, \ldots, n\}$). There are many states $|\varrho\rangle$ satisfying these conditions; one example is

$$|\varrho\rangle = |\rho_{0,0}^{(1,1,0)}\rangle \tag{7.331}$$

which is supported on vertices where $h_1$, $h_2$, $h_{\text{in},i}$, and $h_{\text{out}}$ have no support. □

#### 7.5.1.1 Multi-particle Hamiltonian

We now outline the sequence of Hamiltonians considered in the following Sections and describe the relationships between them. As a first step, in Section **??** we exhibit a basis $\mathcal{B}_n$ for the nullspace of $H(G_1, n)$ and we prove that its smallest nonzero eigenvalue is lower bounded by a positive constant. We then discuss the restriction

$$H(G_1, G_X oc, n) = H(G_1, n)\big|_{\mathcal{I}(G_1, G_X oc, n)} \tag{7.332}$$

in Section **??**, where we prove that a subset $\mathcal{B}_{\text{legal}} \subset \mathcal{B}_n$ is a basis for the nullspace of (7.332), and that its smallest nonzero eigenvalue is also lower bounded by a positive constant.

For the remainder of the proof we use the Nullspace Projection Lemma (Lemma **??**) four times, using the decompositions

$$H(G_2, G_X oc, n) = H(G_1, G_X oc, n) + H_1\big|_{\mathcal{I}(G_2, G_X oc, n)} \tag{7.333}$$

$$H(G_3, G_X oc, n) = H(G_2, G_X oc, n) + H_2\big|_{\mathcal{I}(G_3, G_X oc, n)} \tag{7.334}$$

$$H(G_4, G_X oc, n) = H(G_3, G_X oc, n) + \sum_{i=n_{\text{in}}+1}^{n} H_{\text{in},i}\big|_{\mathcal{I}(G_4, G_X oc, n)} \tag{7.335}$$

$$H(G_X, G_X oc, n) = H(G_4, G_X oc, n) + H_{\text{out}}\big|_{\mathcal{I}(G_X, G_X oc, n)} \tag{7.336}$$

where

$$H_1 = \sum_{w=1}^{n} h_1^{(w)} \qquad H_{\text{in},i} = \sum_{w=1}^{n} h_{\text{in},i}^{(w)} \qquad H_2 = \sum_{w=1}^{n} h_2^{(w)} \qquad H_{\text{out}} = \sum_{w=1}^{n} h_{\text{out}}^{(w)}$$

are all positive semidefinite, with $h_1, h_2, h_{\text{in},i}, h_{\text{out}}$ as defined in Section **??**. Note that in writing equations (7.333), (7.334), (7.335), and (7.336), we have used the fact (from Lemma 25) that the adjacency matrices of the graphs we consider all have the same smallest eigenvalue $e_1$. Also note that

$$\mathcal{I}\left(G_i, G_X oc, n\right) = \mathcal{I}\left(G_X, G_X oc, n\right) \tag{7.337}$$

for $i \in [4]$ since the gate diagrams for each of the graphs $G_1, G_2, G_3, G_4$ and $G_X$ have the same set of diagram elements.

Let $S_k$ be the nullspace of $H(G_k, G_X oc, n)$ for $k = 1, 2, 3, 4$. Since these positive semidefinite Hamiltonians are related by adding positive semidefinite terms, their nullspaces satisfy

$$S_4 \subseteq S_3 \subseteq S_2 \subseteq S_1 \subseteq \mathcal{I}\left(G_X, G_X oc, n\right). \tag{7.338}$$

We solve for $S_1 = \text{span}(\mathcal{B}_{\text{legal}})$ in Section **??** and we characterize the spaces $S_2, S_3$, and $S_4$ in Section **??** in the course of applying our strategy.

For example, to use the Nullspace Projection Lemma to lower bound the smallest nonzero eigenvalue of $H(G_2, G_X oc, n)$, we consider the restriction

$$\left(H_1\big|_{\mathcal{I}(G_2, G_X oc, n)}\right)\Big|_{S_1} = H_1\big|_{S_1}. \tag{7.339}$$

We also solve for $S_2$, which is equal to the nullspace of (7.339). To obtain the corresponding lower bounds on the smallest nonzero eigenvalues of $H(G_k, G_X oc, n)$ for $k = 2, 3, 4$ and $H(G_X, G_X oc, n)$, we consider restrictions

$$H_2\big|_{S_2}, \sum_{i=n_{\text{in}}+1}^{n} H_{\text{in},i}\big|_{S_3}, \quad \text{and} \quad H_{\text{out}}\big|_{S_4}. \tag{7.340}$$

Analyzing these restrictions involves extensive computation of matrix elements. To simplify and organize these computations, we first compute the restrictions of each of these operators to the space $S_1$. We present the results of this computation in Section **??**; details of the calculation can be found in Section **??**. In Section **??** we proceed with the remaining computations and apply the Nullspace Projection Lemma three times using equations (7.333), (7.334), and (7.335). Finally, in Section **??** we apply the Lemma again using equation (7.336) and we prove Theorem **??**.

### 7.5.2 Configurations

In this Section we use Lemma 12 to solve for the nullspace of $H(G_1, n)$, i.e., the $n$-particle frustration-free states on $G_1$. Lemma 12 describes how frustration-free states for $G_1$ are built out of frustration-free states for its components.

To see how this works, consider the example from Figure 7.12a. In this example, with $n = 3$, we construct a basis for the nullspace of $H(G_1, 3)$ by considering two types of eigenstates. First, there are frustration-free states

$$\text{Sym}(|\rho^{L_1}_{z_1,a_1}\rangle|\rho^{L_2}_{z_2,a_2}\rangle|\rho^{L_3}_{z_3,a_3}\rangle) \tag{7.341}$$

where $L_k = (i_k, j_k, d_k) \in \mathcal{L}$ belong to different components of $G_1$. That is to say, $j_w \neq j_t$ unless $j_w = j_t \in \{0, 5\}$, in which case $i_w \neq i_t$ (in this case the particles are located either at the left or right boundary, in different rows of $G_1$). There are also frustration-free states where two of the three particles are located in the same two-qubit gadget $J \in [M]$ and one of the particles is located in a diagram element $L_1$ from a different component of the graph. These states have the form

$$\mathrm{Sym}(|T^J_{z_1,a_1,z_2,a_2}\rangle|\rho^{L_1}_{z_3,a_3}\rangle) \tag{7.342}$$

where

$$|T^J_{z_1,a_1,z_2,a_2}\rangle = \frac{1}{\sqrt{2}}|\rho^{(1,J,0)}_{z_1,a_1}\rangle|\rho^{(s(J),J,0)}_{z_2,a_2}\rangle + \frac{1}{\sqrt{2}}\sum_{x_1,x_2\in\{0,1\}} U_J(a_1)_{x_1x_2,z_1z_2}|\rho^{(1,J,1)}_{x_1,a_1}\rangle|\rho^{(s(J),J,1)}_{x_2,a_2}\rangle \tag{7.343}$$

and $L_1 = (i, j, k) \in \mathcal{L}$ satisfies $j \neq J$. Each of the states (7.341) and (7.342) is specified by 6 "data" bits $z_1, z_2, z_3, a_1, a_2, a_3 \in \{0, 1\}$ and a "configuration" indicating where the particles are located in the graph. The configuration is specified either by three diagram elements $L_1, L_2, L_3 \in \mathcal{L}$ from different components of $G_1$ or by a two-qubit gate $J \in [M]$ along with a diagram element $L_1 \in \mathcal{L}$ from a different component of the graph.

We now define the notion of a configuration for general $n$. Informally, we can think of an $n$-particle configuration as a way of placing $n$ particles in the graph $G_1$ subject to the following restrictions. We first place each of the $n$ particles in a component of the graph, with the restriction that no boundary gadget may contain more than one particle and no two-qubit gadget may contain more than two particles. For each particle on its own in a component (i.e., in a component with no other particles), we assign one of the diagram elements $L \in \mathcal{L}$ associated to that component. We therefore specify a configuration by a set of two-qubit gadgets $J_1, \ldots, J_Y$ that contain two particles, along with a set of diagram elements $L_k \in \mathcal{L}$ that give the locations of the remaining $n - 2Y$ particles. We choose to order the $J$s and the $L$s so that each configuration is specified by a unique tuple $(J_1, \ldots, J_Y, L_1, \ldots, L_{n-2Y})$. For concreteness, we use the lexicographic order on diagram elements in the set $\mathcal{L}$: $L_A = (i_A, j_A, d_A)$ and $L_B = (i_B, j_B, d_B)$ satisfy $L_A < L_B$ iff either $i_A < i_B$, or $i_A = i_B$ and $j_A < j_B$, or $(i_A, j_A) = (i_B, j_B)$ and $d_A < d_B$.

**Definition 9** (**Configuration**)**.** An $n$-particle configuration on the gate graph $G_1$ is a tuple

$$(J_1, \ldots, J_Y, L_1, \ldots, L_{n-2Y}) \tag{7.344}$$

with $Y \in \{0, \ldots, \lfloor \frac{n}{2} \rfloor\}$, ordered integers

$$1 \leq J_1 < J_2 < \cdots < J_Y \leq M, \tag{7.345}$$

and lexicographically ordered diagram elements

$$L_1 < L_2 < \cdots < L_{n-2Y}, \qquad L_k = (i_k, j_k, d_k) \in \mathcal{L}. \tag{7.346}$$

We further require that each $L_k$ is from a different component of $G_1$, i.e.,

$$j_w = j_t \quad \implies \quad j_w \in \{0, M+1\} \text{ and } i_w \neq i_t, \tag{7.347}$$

and we require that $j_u \neq J_v$ for all $u \in [n - 2Y]$ and $v \in [Y]$.

In Figure **??** we give some examples of configurations (for the example from Figure 7.12a with $n = 3$) and we introduce a diagrammatic notation for them.

For any configuration and $n$-bit strings $\vec{z}$ and $\vec{a}$, there is a state in the nullspace of $H(G_1, n)$, given by

$$\mathrm{Sym}(|T^{J_1}_{z_1,a_1,z_2,a_2}\rangle \dots |T^{J_Y}_{z_{2Y-1},a_{2Y-1},z_{2Y},a_{2Y}}\rangle |\rho^{L_1}_{z_{2Y+1},a_{2Y+1}}\rangle \dots |\rho^{L_{n-2Y}}_{z_n,a_n}\rangle). \tag{7.348}$$

The ordering in the definition of a configuration ensures that each distinct choice of configuration and $n$-bit strings $\vec{z}, \vec{a}$ gives a different state.

**Definition 10.** Let $\mathcal{B}_n$ be the set of all states of the form (7.348), where $(J_1, \dots, J_Y, L_1, \dots, L_{n-2Y})$ is a configuration and $\vec{z}, \vec{a} \in \{0,1\}^n$.

**Lemma 26.** *The set $\mathcal{B}_n$ is an orthonormal basis for the nullspace of $H(G_1, n)$. Furthermore,*

$$\gamma(H(G_1, n)) \geq \mathcal{K}_0 \tag{7.349}$$

*where $\mathcal{K}_0 \in (0, 1]$ is an absolute constant.*

*Proof.* Each component of $G_1$ is either a two-qubit gadget or a boundary gadget (see equation (7.319)). The single-particle states of $A(G_1)$ with energy $e_1$ are the states $|\rho^L_{z,a}\rangle$ for $L \in \mathcal{L}$ and $z, a \in \{0, 1\}$, as discussed in Section **??**. Each of these states has support on only one component of $G_1$. In addition, $G_1$ has a two-particle frustration-free state for each two-qubit gadget $J \in [M]$ and bits $z, a, x, b$, namely $\mathrm{Sym}(|T^J_{z,a,x,b}\rangle)$. Furthermore, no component of $G_1$ has any three- (or more) particle frustration-free states. Using these facts and applying Lemma 12, we see that $\mathcal{B}_n$ spans the nullspace of $H(G_1, n)$.

Lemma 12 also expresses each eigenvalue of $H(G_1, n)$ as a sum of eigenvalues for its components. We use this fact to obtain the desired lower bound on the smallest nonzero eigenvalue. Our analysis proceeds on a case-by-case basis, depending on the occupation numbers for each component of $G_1$ (the values $N_1, \dots, N_k$ in Lemma 12).

First consider any set of occupation numbers where some two-qubit gate gadget $J \in [M]$ contains 3 or more particles. By Lemma **??** and Lemma 12, any such eigenvalue is at least $\lambda^1_3(G_{U_J})$, which is a positive constant by Lemma 18. Next consider a case where some boundary gadget contains more than one particle. The corresponding eigenvalues are similarly lower bounded by $\lambda^1_2(G_{\mathrm{bnd}})$, which is also a positive constant by Lemma 20. Finally, consider a set of occupation numbers where each two-qubit gadget contains at most two particles and each boundary gadget contains at most one particle. The smallest eigenvalue with such a set of occupation numbers is zero. The smallest nonzero eigenvalue is either

$$\gamma(H(G_{U_J}, 1)),\ \gamma(H(G_{U_J}, 2)) \text{ for some } J \in [M], \text{ or } \gamma(H(G_{\mathrm{bnd}}, 1)). \tag{7.350}$$

However, these quantities are at least some positive constant since $H(G_{U_J}, 1)$, $H(G_{U_J}, 2)$, and $H(G_{\mathrm{bnd}}, 1)$ are nonzero constant-sized positive semidefinite matrices.

Now combining the lower bounds discussed above and using the fact that, for each $J \in [M]$, the two-qubit gate $U_J$ is chosen from a fixed finite gate set (given in (**??**)), we see that $\gamma(H(G_1, n))$ is lower bounded by the positive constant

$$\min\{\lambda^1_3(G_U), \lambda^1_2(G_{\mathrm{bnd}}), \gamma(H(G_U, 1)), \gamma(H(G_U, 2)), \gamma(H(G_{\mathrm{bnd}}, 1))\colon U \text{ is from the gate set } (\textbf{??})\}. \tag{7.351}$$

The condition $\mathcal{K}_0 \leq 1$ can be ensured by setting $\mathcal{K}_0$ to be the minimum of 1 and (7.351). $\square$

Note that the constant $\mathcal{K}_0$ can in principle be computed using (7.351): each quantity on the right-hand side can be evaluated by diagonalizing a specific finite-dimensional matrix.

#### 7.5.2.1 Legal configurations

In this section we define a subset of the $n$-particle configurations that we call legal configurations, and we prove that the subset of the basis vectors in $\mathcal{B}_n$ that have legal configurations spans the nullspace of $H(G_1, G_X oc, n)$.

We begin by specifying the set of legal configurations. Every legal configuration

$$(J_1, \ldots, J_Y, L_1, \ldots, L_{n-2Y}) \tag{7.352}$$

has $Y \in \{0, 1\}$. The legal configurations with $Y = 0$ are

$$((1, j, d_1), F(2, j, d_2), F(3, j, d_3), \ldots, F(n, j, d_n)) \tag{7.353}$$

where $j \in [M]$ and where $\vec{d} = (d_1, \ldots, d_n)$ satisfies $d_i \in \{0, 1\}$ and $d_1 = d_{s(j)}$. (Recall that the function $F$, defined in equations (7.312) and (7.313), describes horizontal movement of particles.) The legal configurations with $Y = 1$ are

$$(j, F(2, j, d_2), \ldots, F(s(j) - 1, j, d_{s(j)-1}), F(s(j) + 1, j, d_{s(j)+1}), \ldots, F(n, j, d_n)) \tag{7.354}$$

where $j \in \{1, \ldots, M\}$ and $d_i \in \{0, 1\}$ for $i \in [n] \setminus \{1, s(j)\}$. Although the values $d_1$ and $d_{s(j)}$ are not used in equation (7.354), we choose to set them to

$$d_1 = d_{s(j)} = 2 \tag{7.355}$$

for any legal configuration with $Y = 1$. In this way we identify the set of legal configurations with the set of pairs $j, \vec{d}$ with $j \in [M]$ and

$$\vec{d} = (d_1, d_2, d_3, \ldots, d_n) \tag{7.356}$$

satisfying

$$d_1 = d_{s(j)} \in \{0, 1, 2\} \quad \text{and} \quad d_i \in \{0, 1\} \text{ for } i \notin \{1, s(j)\}. \tag{7.357}$$

The legal configuration is given by equation (7.353) if $d_1 = d_{s(j)} \in \{0, 1\}$ and equation (7.354) if $d_1 = d_{s(j)} = 2$.

The examples in Figures **??**, **??**, and **??** show legal configurations whereas the examples in Figures **??**, **??**, and **??** are illegal. The legal examples correspond to $j = 1$, $\vec{d} = (1, 1, 1)$; $j = 2$, $\vec{d} = (2, 2, 0)$; and $j = 1$, $\vec{d} = (1, 0, 1)$, respectively. We now explain why the other examples are illegal. Looking at (7.354), we see that the configuration $(3, (2, 0, 1))$ depicted in Figure **??** is illegal since $F(2, 3, 0) = (2, 2, 1) \neq (2, 0, 1)$ and $F(2, 3, 1) = (2, 4, 0) \neq (2, 0, 1)$. The configuration in Figure **??** is illegal since there are two particles in the same row. Looking at equation (7.353), we see that the configuration $((1, 1, 1), (2, 2, 0), (3, 5, 0))$ in Figure **??** is illegal since $(3, 5, 0) \notin \{F(3, 1, 0), F(3, 1, 1)\} = \{(3, 0, 1), (3, 3, 0)\}$.

We now identify the subset of basis vectors $\mathcal{B}_{\text{legal}} \subset \mathcal{B}_n$ that have legal configurations. We write each such basis vector as

$$|j, \vec{d}, \vec{z}, \vec{a}\rangle = \begin{cases} \text{Sym}\left(|\rho_{z_1,a_1}^{(1,j,d_1)}\rangle \bigotimes_{i=2}^{n} |\rho_{z_i,a_i}^{F(i,j,d_i)}\rangle\right) & d_1 = d_{s(j)} \in \{0,1\} \\ \text{Sym}\left(|T_{z_1,a_1,z_{s(j)},a_{s(j)}}^{j}\rangle \bigotimes_{\substack{i=2 \\ i\neq s(j)}}^{n} |\rho_{z_i,a_i}^{F(i,j,d_i)}\rangle\right) & d_1 = d_{s(j)} = 2 \end{cases} \tag{7.358}$$

where $j, \vec{d}$ specifies the legal configuration and $\vec{z}$,$\vec{a} \in \{0,1\}^n$. (Note that the bits in $\vec{z}$ and $\vec{a}$ are ordered slightly differently than in equation (7.348); here the labeling reflects the indices of the encoded qubits).

**Definition 11.** Let

$$\mathcal{B}_{\text{legal}} = \left\{|j, \vec{d}, \vec{z}, \vec{a}\rangle \colon j \in [M],\ d_1 = d_{s(j)} \in \{0,1,2\} \text{ and } \ d_i \in \{0,1\} \text{ for } i \notin \{1, s(j)\},\ \vec{z}, \vec{a} \in \{0,1\}^n\right\} \tag{7.359}$$

and $\mathcal{B}_{\text{illegal}} = \mathcal{B}_n \setminus \mathcal{B}_{\text{illegal}}$.

The basis $\mathcal{B}_n = \mathcal{B}_{\text{legal}} \cup \mathcal{B}_{\text{illegal}}$ is convenient when considering the restriction to the subspace $\mathcal{I}(G_1, G_X oc, n)$. Letting $\Pi_0$ be the projector onto $\mathcal{I}(G_1, G_X oc, n)$, the following Lemma (proven in Section **??**) shows that the restriction

$$\Pi_0\Big|_{\text{span}(\mathcal{B}_n)} \tag{7.360}$$

is diagonal in the basis $\mathcal{B}_n$. The Lemma also bounds the diagonal entries.

**Lemma 27.** *Let $\Pi_0$ be the projector onto $\mathcal{I}(G_1, G_X oc, n)$. For any $|j, \vec{d}, \vec{z}, \vec{a}\rangle \in \mathcal{B}_{legal}$, we have*

$$\Pi_0|j, \vec{d}, \vec{z}, \vec{a}\rangle = |j, \vec{d}, \vec{z}, \vec{a}\rangle. \tag{7.361}$$

*Furthermore, for any two distinct basis vectors $|\phi\rangle, |\psi\rangle \in \mathcal{B}_{illegal}$, we have*

$$\langle\phi|\Pi_0|\phi\rangle \leq \frac{255}{256} \tag{7.362}$$

$$\langle\phi|\Pi_0|\psi\rangle = 0. \tag{7.363}$$

We use this Lemma to characterize the nullspace of $H(G_1, G_X oc, n)$ and bound its smallest nonzero eigenvalue.

**Lemma 28.** *The nullspace $S_1$ of $H(G_1, G_X oc, n)$ is spanned by the orthonormal basis $\mathcal{B}_{legal}$. Its smallest nonzero eigenvalue is*

$$\gamma(H(G_1, G_X oc, n)) \geq \frac{\mathcal{K}_0}{256} \tag{7.364}$$

*where $\mathcal{K}_0 \in (0, 1]$ is the absolute constant from Lemma 26.*

*Proof.* Recall from Section **??** that

$$H(G_1, G_X oc, n) = H(G_1, n)|_{\mathcal{I}(G_1, G_X oc, n)}. \tag{7.365}$$

Its nullspace is the space of states $|\kappa\rangle$ satisfying

$$\Pi_0|\kappa\rangle = |\kappa\rangle \quad \text{and} \quad H(G_1, n)|\kappa\rangle = 0 \tag{7.366}$$

(recall that $\Pi_0$ is the projector onto $\mathcal{I}(G_1, G_X oc, n)$, the states satisfying the occupancy constraints). Since $\mathcal{B}_n$ is a basis for the nullspace of $H(G_1, n)$, to solve for the nullspace of $H(G_1, G_X oc, n)$ we consider the restriction (7.360) and solve for the eigenspace with eigenvalue 1. This calculation is simple because (7.360) is diagonal in the basis $\mathcal{B}_n$, according to Lemma 27. We see immediately from the Lemma that $\mathcal{B}_{\text{legal}}$ spans the nullspace of $H(G_1, G_X oc, n)$; we now show that Lemma 27 also implies the lower bound (7.364). Note that

$$\gamma(H(G_1, G_X oc, n)) = \gamma(\Pi_0 H(G_1, n)\Pi_0). \tag{7.367}$$

Let $\Pi_{\text{legal}}$ and $\Pi_{\text{illegal}}$ project onto the spaces spanned by $\mathcal{B}_{\text{legal}}$ and $\mathcal{B}_{\text{illegal}}$ respectively, so $\Pi_{\text{legal}} + \Pi_{\text{illegal}}$ projects onto the nullspace of $H(G_1, n)$. The operator inequality

$$H(G_1, n) \geq \gamma(H(G_1, n)) \cdot (1 - \Pi_{\text{legal}} - \Pi_{\text{illegal}}) \tag{7.368}$$

implies

$$\Pi_0 H(G_1, n)\Pi_0 \geq \gamma(H(G_1, n)) \cdot \Pi_0(1 - \Pi_{\text{legal}} - \Pi_{\text{illegal}})\Pi_0. \tag{7.369}$$

Since the operators on both sides of this inequality are positive semidefinite and have the same nullspace, their smallest nonzero eigenvalues are bounded as

$$\gamma(\Pi_0 H(G_1, n)\Pi_0) \geq \gamma(H(G_1, n)) \cdot \gamma(\Pi_0(1 - \Pi_{\text{legal}} - \Pi_{\text{illegal}})\Pi_0). \tag{7.370}$$

Hence

$$\gamma(H(G_1, G_X oc, n)) = \gamma(\Pi_0 H(G_1, n)\Pi_0) \geq \mathcal{K}_0 \cdot \gamma(\Pi_0(1 - \Pi_{\text{legal}} - \Pi_{\text{illegal}})\Pi_0) \tag{7.371}$$

where we used Lemma 26. From equations (7.362) and (7.363) we see that

$$\Pi_0|g\rangle = |g\rangle \quad \text{and} \quad \Pi_{\text{illegal}}|f\rangle = |f\rangle \qquad \Longrightarrow \qquad \langle f|g\rangle\langle g|f\rangle \leq \frac{255}{256}. \tag{7.372}$$

The nullspace of

$$\Pi_0\left(1 - \Pi_{\text{legal}} - \Pi_{\text{illegal}}\right)\Pi_0 \tag{7.373}$$

is spanned by

$$\mathcal{B}_{\text{legal}} \cup \left\{|\tau\rangle : \Pi_0|\tau\rangle = 0\right\}. \tag{7.374}$$

To see this, note that (7.373) commutes with $\Pi_0$, and the space of $+1$ eigenvectors of $\Pi_0$ that are annihilated by (7.373) is spanned by $\mathcal{B}_{\text{legal}}$ (by Lemma 27). Any eigenvector $|g_1\rangle$ corresponding to the smallest nonzero eigenvalue of this operator therefore satisfies $\Pi_0|g_1\rangle = |g_1\rangle$ and $\Pi_{\text{legal}}|g_1\rangle = 0$, so

$$\gamma(\Pi_0(1 - \Pi_{\text{legal}} - \Pi_{\text{illegal}})\Pi_0) = 1 - \langle g_1|\Pi_{\text{illegal}}|g_1\rangle \geq \frac{1}{256} \tag{7.375}$$

using equation (7.372). Plugging this into equation (7.371) gives the lower bound (7.364). □

We now consider

$$H_1|_{S_1}, H_2|_{S_1}, H_{\text{in},i}|_{S_1}, H_{\text{out}}|_{S_1} \tag{7.376}$$

where these operators are defined in Section 7.5.1.1 and

$$S_1 = \text{span}(\mathcal{B}_{\text{legal}}) \tag{7.377}$$

is the nullspace of $H(G_1, G_X oc, n)$.

We specify the operators (7.376) by their matrix elements in an orthonormal basis for $S_1$. Although the basis $\mathcal{B}_{\text{legal}}$ was convenient in Section **??**, here we use a different basis in which the matrix elements of $H_1$ and $H_2$ are simpler. We define

$$|j, \vec{d}, \text{In}(\vec{z}), \vec{a}\rangle = \sum_{\vec{x}\in\{0,1\}^n} \left(\langle \vec{x}|\bar{U}_{j,d_1}(a_1)|\vec{z}\rangle\right)|j, \vec{d}, \vec{x}, \vec{a}\rangle \tag{7.378}$$

where

$$\bar{U}_{j,d_1}(a_1) = \begin{cases} U_{j-1}(a_1)U_{j-2}(a_1)\ldots U_1(a_1) & \text{if } d_1 \in \{0,2\} \\ U_j(a_1)U_{j-1}(a_1)\ldots U_1(a_1) & \text{if } d_1 = 1. \end{cases} \tag{7.379}$$

In each of these states the quantum data (represented by the $\vec{x}$ register on the right-hand side) encodes the computation in which the unitary $\bar{U}_{j,d_1}(a_1)$ is applied to the initial $n$-qubit state $|\vec{z}\rangle$ (the notation $\text{In}(\vec{z})$ indicates that $\vec{z}$ is the input). The vector $\vec{a}$ is only relevant insofar as its first bit $a_1$ determines whether or not each two-qubit unitary is complex conjugated; the other bits of $\vec{a}$ go along for the ride. Letting $\vec{z}, \vec{a} \in \{0,1\}^n$ , $j \in [M]$, and

$$\vec{d} = (d_1, \ldots, d_n) \quad \text{with} \quad d_1 = d_{s(j)} \in \{0,1,2\} \quad \text{and} \quad d_i \in \{0,1\},\ i \notin \{1, s(j)\}, \tag{7.380}$$

we see that the states (7.378) form an orthonormal basis for $S_1$. In Section **??** we compute the matrix elements of the operators (7.376) in this basis, which are reproduced below.

Roughly speaking, the nonzero off-diagonal matrix elements of the operator $H_1$ in the basis (7.378) occur between states $|j, \vec{d}, \text{In}(\vec{z}), \vec{a}\rangle$ and $|j, \vec{c}, \text{In}(\vec{z}), \vec{a}\rangle$ where the legal configurations $j, \vec{d}$ and $j, \vec{c}$ are related by horizontal motion of a particle in one of the rows $i \in \{2, \ldots, n\}$.

**Matrix elements of $H_1$**

$$\langle k, \vec{c}, \text{In}(\vec{x}), \vec{b}|H_1|j, \vec{d}, \text{In}(\vec{z}), \vec{a}\rangle = \delta_{k,j}\delta_{\vec{a},\vec{b}}\delta_{\vec{z},\vec{x}} \cdot \begin{cases} \frac{n-1}{64} & \vec{c} = \vec{d} \\ \frac{1}{64}\prod_{\substack{r=1\\ r\neq i}}^{n} \delta_{d_r,c_r} & d_i \neq c_i \text{ for some } i \in [n] \setminus \{1, s(j)\} \\ \frac{1}{64\sqrt{2}} \prod_{\substack{r=2\\ r\neq s(j)}}^{n} \delta_{d_r,c_r} & (c_1, d_1) \in \{(2,0),(0,2),(1,2),(2,1)\} \\ 0 & \text{otherwise.} \end{cases} \tag{7.381}$$

From this expression we see that $H_1|_{S_1}$ is block diagonal in the basis (7.378), with a block for each $\vec{z}, \vec{a} \in \{0,1\}^n$ and $j \in [M]$. Moreover, the submatrix for each block is the same. In Figure ?? we illustrate some of the off-diagonal matrix elements of $H_1|_{S_1}$ for the example from Figure 7.12.

Next, we present the matrix elements of $H_2$.

**Matrix elements of $H_2$**

$$\langle k, \vec{c}, \mathrm{In}(\vec{x}), \vec{b}|H_2|j, \vec{d}, \mathrm{In}(\vec{z}), \vec{a}\rangle = f_{\mathrm{diag}(\vec{d},j)\cdot\delta_{j,k}\delta_{\vec{a},\vec{b}}\delta_{\vec{z},\vec{x}}\delta_{\vec{c},\vec{d}}} + \left(f_{\text{off-diag}}(\vec{c}, \vec{d}, j)\cdot\delta_{k,j-1} + f_{\text{off-diag}}(\vec{d}, \vec{c}, k)\cdot\delta_{k-1,j}\right)\delta_{\vec{a},\vec{b}}\delta_{\vec{z},\vec{x}} \tag{7.382}$$

where

$$f_{\mathrm{diag}}(\vec{d}, j) = \begin{cases} 0 & d_1 = 0 \text{ and } j = 1, \text{ or } d_1 = 1 \text{ and } j = M \\ \frac{1}{128} & d_1 = 2 \text{ and } j \in \{1, M\} \\ \frac{1}{64} & \text{otherwise} \end{cases} \tag{7.383}$$

and

$$f_{\text{off-diag}}(\vec{c}, \vec{d}, j) = \left(\prod_{\substack{r=2 \\ r\notin\{s(j-1),s(j)\}}}^{n} \delta_{d_r,c_r}\right) \cdot \begin{cases} \frac{1}{64\sqrt{2}} & (c_1, c_{s(j)}, d_1, d_{s(j-1)}) \in \{(2,0,0,0),(1,1,2,1)\} \\ \frac{1}{64} & (c_1, c_{s(j)}, d_1, d_{s(j-1)}) = (1,0,0,1) \\ \frac{1}{128} & (c_1, c_{s(j)}, d_1, d_{s(j-1)}) = (2,1,2,0) \\ 0 & \text{otherwise.} \end{cases} \tag{7.384}$$

This shows that $H_2|_{S_1}$ is block diagonal in the basis (7.378), with a block for each $\vec{z}, \vec{a} \in \{0,1\}^n$. Also note that (in contrast with $H_1$) $H_2$ connects states with different values of $j$. In Figure ?? we illustrate some of the off-diagonal matrix elements of $H_2|_{S_1}$, for the example from Figure 7.12.

Finally, we present the matrix elements of $H_{\mathrm{in},i}$ (for $i \in \{n_{\mathrm{in}}+1, \ldots, n\}$) and $H_{\mathrm{out}}$:

**Matrix elements of $H_{\mathrm{in},i}$**

For each ancilla qubit $i \in \{n_{\mathrm{in}}+1, \ldots, n\}$, define $j_{\min,i} = \min\{j \in [M] \colon s(j) = i\}$ to be the index of the first gate in the circuit that involves this qubit (recall from Section ?? that we consider circuits where each ancilla qubit is involved in at least one gate). The operator $H_{\mathrm{in},i}$ is diagonal in the basis (7.378), with entries

$$\langle j, \vec{d}, \mathrm{In}(\vec{z}), \vec{a}|H_{\mathrm{in},i}|j, \vec{d}, \mathrm{In}(\vec{z}), \vec{a}\rangle = \begin{cases} \frac{1}{64} & j \le j_{\min,i},\ z_i = 1, \text{ and } d_i = 0 \\ 0 & \text{otherwise.} \end{cases} \tag{7.385}$$

**Matrix elements of $H_{\mathrm{out}}$**

Let $j_{\max} = \max\{j \in [M] \colon s(j) = 2\}$ be the index of the last gate $U_{j_{\max}}$ in the circuit that acts between qubits 1 and 2 (the output qubit). Then

$$\langle k, \vec{c}, \mathrm{In}(\vec{x}), \vec{b}|H_{\mathrm{out}}|j, \vec{d}, \mathrm{In}(\vec{z}), \vec{a}\rangle = \delta_{j,k}\delta_{\vec{c},\vec{d}}\delta_{\vec{a},\vec{b}} \begin{cases} \langle \vec{x}|U^{\dagger}_{\mathcal{C}_X}(a_1)|0\rangle\langle 0|_2 U_{\mathcal{C}_X}(a_1)|\vec{z}\rangle \frac{1}{64} & j \geq j_{\max} \text{ and } d_2 = 1 \\ 0 & \text{otherwise.} \end{cases} \tag{7.386}$$

### 7.5.3 Frustration-Free states

Define the $(n-2)$-dimensional hypercubes

$$\mathcal{D}^j_k = \left\{(d_1, \ldots, d_n) \colon d_1 = d_{s(j)} = k,\ d_i \in \{0,1\} \text{ for } i \in [n] \setminus \{1, s(j)\}\right\} \tag{7.387}$$

for $j \in \{1, \ldots, M\}$ and $k \in \{0, 1, 2\}$, and the superpositions

$$|\mathrm{Cube}_k(j, \vec{z}, \vec{a})\rangle = \frac{1}{\sqrt{2^{n-2}}} \sum_{\vec{d} \in \mathcal{D}^j_k} (-1)^{\sum_{i=1}^n d_i} |j, \vec{d}, \mathrm{In}(\vec{z}), \vec{a}\rangle \tag{7.388}$$

for $k \in \{0, 1, 2\}$, $j \in [M]$, and $\vec{z}, \vec{a} \in \{0,1\}^n$. For each $j \in [M]$ and $\vec{z}, \vec{a} \in \{0,1\}^n$, let

$$|C(j, \vec{z}, \vec{a})\rangle = \frac{1}{2}|\mathrm{Cube}_0(j, \vec{z}, \vec{a})\rangle + \frac{1}{2}|\mathrm{Cube}_1(j, \vec{z}, \vec{a})\rangle - \frac{1}{\sqrt{2}}|\mathrm{Cube}_2(j, \vec{z}, \vec{a})\rangle. \tag{7.389}$$

We prove

**Lemma 29.** *The Hamiltonian $H(G_2, G_X oc, n)$ has nullspace $S_2$ spanned by the states*

$$|C(j, \vec{z}, \vec{a})\rangle \tag{7.390}$$

*for $j \in [M]$ and $\vec{z}, \vec{a} \in \{0,1\}^n$. Its smallest nonzero eigenvalue is*

$$\gamma(H(G_2, G_X oc, n)) \geq \frac{\mathcal{K}_0}{35000n} \tag{7.391}$$

*where $\mathcal{K}_0 \in (0, 1]$ is the absolute constant from Lemma 26.*

*Proof.* Recall from the previous section that $H_1|_{S_1}$ is block diagonal in the basis (7.378), with a block for each $j \in [M]$ and $\vec{z}, \vec{a} \in \{0,1\}^n$. That is to say, $\langle k, \vec{c}, \mathrm{In}(\vec{x}), \vec{b}|H_1|j, \vec{d}, \mathrm{In}(\vec{z}), \vec{a}\rangle$ is zero unless $\vec{a} = \vec{b}$, $k = j$, and $\vec{z} = \vec{x}$. Equation (7.381) gives the nonzero matrix elements within a given block, which we use to compute the frustration-free ground states of $H_1|_{S_1}$.

Looking at equation (7.381), we see that the matrix for each block can be written as a sum of $n$ commuting matrices: $\frac{n-1}{64}$ times the identity matrix (case 1 in equation (7.381)), $n-2$ terms that each flip a single bit $i \notin \{1, s(j)\}$ of $\vec{d}$ (case 2), and a term that changes the value of the "special" components $d_1 = d_{s(j)} \in \{0, 1, 2\}$ (case 3). Thus

$$\langle j, \vec{c}, \mathrm{In}(\vec{z}), \vec{a}|H_1|j, \vec{d}, \mathrm{In}(\vec{z}), \vec{a}\rangle = \langle j, \vec{c}, \mathrm{In}(\vec{z}), \vec{a}|\frac{1}{64}(n-1) + \frac{1}{64}\sum_{i \in [n] \setminus \{1, s(j)\}} H_{\mathrm{flip},i} + \frac{1}{64}H_{\mathrm{special},j}|j, \vec{d}, \mathrm{In}(\vec{z}), \vec{a}\rangle \tag{7.392}$$

where

$$\langle j, \vec{c}, \mathrm{In}(\vec{z}), \vec{a}|H_{\mathrm{flip},i}|j, \vec{d}, \mathrm{In}(\vec{z}), \vec{a}\rangle = \delta_{c_i, d_i \oplus 1} \prod_{r\in[n]\setminus\{i\}} \delta_{c_r, d_r} \tag{7.393}$$

and

$$\langle j, \vec{c}, \mathrm{In}(\vec{z}), \vec{a}|H_{\mathrm{special},j}|j, \vec{d}, \mathrm{In}(\vec{z}), \vec{a}\rangle = \begin{cases} \frac{1}{\sqrt{2}} & (c_1, d_1) \in \{(2,0),(0,2),(1,2),(2,1)\} \\ & \text{and } d_r = c_r \text{ for } r \in [n]\setminus\{1, s(j)\} \\ 0 & \text{otherwise.} \end{cases} \tag{7.394}$$

Note that these $n$ matrices are mutually commuting, each eigenvalue of $H_{\mathrm{flip},i}$ is $\pm 1$, and each eigenvalue of $H_{\mathrm{special},j}$ is equal to one of the eigenvalues of the matrix

$$\frac{1}{\sqrt{2}}\begin{pmatrix} 0 & 0 & 1 \\ 0 & 0 & 1 \\ 1 & 1 & 0 \end{pmatrix}, \tag{7.395}$$

which are $\{-1, 0, 1\}$. Thus we see that the eigenvalues of $H_1|_{S_1}$ within a block for some $j \in [M]$ and $\vec{z}, \vec{a} \in \{0,1\}^n$ are

$$\frac{1}{64}\left(n - 1 + \sum_{i\notin\{1,s(j)\}} y_i + w\right) \tag{7.396}$$

where $y_i \in \pm 1$ for each $i \in [n]\setminus\{1, s(j)\}$ and $w \in \{-1, 0, 1\}$. In particular, the smallest eigenvalue within the block is zero (corresponding to $y_i = w = -1$). The corresponding eigenspace is spanned by the simultaneous $-1$ eigenvectors of each $H_{\mathrm{flip},i}$ for $i \in [n]\setminus\{1, s(j)\}$ and $H_{\mathrm{special},j}$. The space of simultaneous $-1$ eigenvectors of $H_{\mathrm{flip},i}$ for $i \in [n]\setminus\{1, s(j)\}$ within the block is spanned by $\{|\mathrm{Cube}_0(j, \vec{z}, \vec{a})\rangle, |\mathrm{Cube}_1(j, \vec{z}, \vec{a})\rangle, |\mathrm{Cube}_2(j, \vec{z}, \vec{a})\rangle\}$. The state $|C(j, \vec{z}, \vec{a})\rangle$ is the unique superposition of these states that is a $-1$ eigenvector of $H_{\mathrm{special},j}$. Hence, for each block we obtain a unique state $|C(j, \vec{z}, \vec{a})\rangle$ in the space $S_2$. Ranging over all blocks $j \in [M]$ and $\vec{z}, \vec{a} \in \{0,1\}^n$, we get the basis described in the Lemma.

The smallest nonzero eigenvalue within each block is $\frac{1}{64}$ (corresponding to $y_i = -1$ and $w = 0$ in equation (7.396)), so

$$\gamma(H_1|_{S_1}) = \frac{1}{64}. \tag{7.397}$$

To get the stated lower bound, we use Lemma **??** with $H(G_2, G_X oc, n) = H_A + H_B$ where

$$H_A = H(G_1, G_X oc, n) \qquad H_B = H_1|_{\mathcal{I}(G_2, G_X oc, n)} \tag{7.398}$$

(as in equation (7.333)), along with the bounds

$$\gamma(H_A) \geq \frac{\mathcal{K}_0}{256} \qquad \gamma(H_B|_{S_1}) = \gamma(H_1|_{S_1}) = \frac{1}{64} \qquad \|H_B\| \leq \|H_1\| \leq n\,\|h_1\| = 2n \tag{7.399}$$

from Lemma 28, equations (7.339) and (7.397), and the fact that $\|h_1\| = 2$ from (7.86). This gives

$$\gamma(H(G_2, G_X oc, n)) \geq \frac{\mathcal{K}_0}{64\mathcal{K}_0 + 256 + 2n \cdot 64 \cdot 256} \geq \frac{\mathcal{K}_0}{35000n} \tag{7.400}$$

where we used the facts that $\mathcal{K}_0 \leq 1$ and $n \geq 1$. □

For each $\vec{z}, \vec{a} \in \{0,1\}^n$ define the uniform superposition

$$|\mathcal{H}(\vec{z},\vec{a})\rangle = \frac{1}{\sqrt{M}} \sum_{j=1}^{M} |C\,(j, \vec{z}, \vec{a})\rangle. \tag{7.401}$$

that encodes (somewhat elaborately) the history of the computation that consists of applying either $U_{\mathcal{C}_X}$ or $U^*_{\mathcal{C}_X}$ to the state $|\vec{z}\rangle$. The first bit of $\vec{a}$ determines whether the circuit $\mathcal{C}_X$ or its complex conjugate is applied.

**Lemma 30.** *The Hamiltonian $H(G_3, G_X oc, n)$ has nullspace $S_3$ spanned by the states*

$$|\mathcal{H}(\vec{z},\vec{a})\rangle \tag{7.402}$$

*for $\vec{z}, \vec{a} \in \{0,1\}^n$. Its smallest nonzero eigenvalue is*

$$\gamma(H(G_3, G_X oc, n)) \geq \frac{\mathcal{K}_0}{10^7 n^2 M^2} \tag{7.403}$$

*where $\mathcal{K}_0 \in (0,1]$ is the absolute constant from Lemma 26.*

*Proof.* Recall that

$$H(G_3, G_X oc, n) = H(G_2, G_X oc, n) + H_2|_{\mathcal{I}(G_3, G_X oc, n)} \tag{7.404}$$

with both terms on the right-hand side positive semidefinite. To solve for the nullspace of $H(G_3, G_X oc, n)$, it suffices to restrict our attention to the space

$$S_2 = \operatorname{span}\{|C(j,\vec{z},\vec{a})\rangle \colon j \in [M],\ \vec{z},\vec{a} \in \{0,1\}^n\} \tag{7.405}$$

of states in the nullspace of $H(G_2, G_X oc, n)$. We begin by computing the matrix elements of $H_2$ in the basis for $S_2$ given above. We use equations (7.382) and (7.389) to compute the diagonal matrix elements:

$$\langle C\,(j,\vec{z},\vec{a})\,|H_2|C\,(j,\vec{z},\vec{a})\rangle = \frac{1}{4}\langle \mathrm{Cube}_0(j,\vec{z},\vec{a})|H_2|\mathrm{Cube}_0(j,\vec{z},\vec{a})\rangle + \frac{1}{4}\langle \mathrm{Cube}_1(j,\vec{z},\vec{a})\rangle|H_2|\mathrm{Cube}_1(j,\vec{z},\vec{a})\rangle \tag{7.406}$$

$$+\frac{1}{2}\langle \mathrm{Cube}_2(j,\vec{z},\vec{a})|H_2|\mathrm{Cube}_2(j,\vec{z},\vec{a})\rangle \tag{7.407}$$

$$= \begin{cases} 0 + \frac{1}{256} + \frac{1}{256} & j = 1 \\ \frac{1}{256} + \frac{1}{256} + \frac{1}{128} & j \in \{2,\ldots,M-1\} \\ \frac{1}{256} + 0 + \frac{1}{256} & j = M \end{cases} \tag{7.408}$$

$$= \begin{cases} \frac{1}{128} & j \in \{1, M\} \\ \frac{1}{64} & j \in \{2,\ldots,M-1\}. \end{cases} \tag{7.409}$$

In the second line we used equation (7.383). Looking at equation (7.382), we see that the only nonzero off-diagonal matrix elements of $H_2$ in this basis are of the form

$$\langle C(j-1,\vec{z},\vec{a})|H_2|C(j,\vec{z},\vec{a})\rangle \quad \text{or} \quad \langle C(j,\vec{z},\vec{a})|H_2|C(j-1,\vec{z},\vec{a})\rangle = \langle C(j-1,\vec{z},\vec{a})|H_2|C(j,\vec{z},\vec{a})\rangle^* \tag{7.410}$$

for $j \in \{2, \ldots, M\}$, $\vec{z}, \vec{a} \in \{0,1\}^n$. To compute these matrix elements we first use equation (7.384) to evaluate

$$\langle \mathrm{Cube}_w(j-1, \vec{z}, \vec{a}) | H_2 | \mathrm{Cube}_v(j, \vec{z}, \vec{a}) \rangle \tag{7.411}$$

for $v, w \in \{0,1,2\}$ and $j \in \{2, \ldots, M\}$. For example, using the second case of equation (7.384), we get

$$\langle \mathrm{Cube}_1 (j-1, \vec{z}, \vec{a}) | H_2 | \mathrm{Cube}_0 (j, \vec{z}, \vec{a}) \rangle = \frac{1}{2^{n-2}} \sum_{\vec{d} \in \mathcal{D}_0^j} \sum_{\vec{c} \in \mathcal{D}_1^{j-1}} (-1)^{\sum_{i \in [n]} (c_i + d_i)} \langle j-1, \vec{c}, \mathrm{In}(\vec{z}), \vec{a} | H_2 | j, \vec{d}, \mathrm{In}(\vec{z}), \vec{a} \rangle \tag{7.412}$$

$$= \frac{1}{2^{n-2}} \sum_{\vec{d} \in \mathcal{D}_0^j : d_{s(j-1)} = 1} (-1) \cdot \frac{1}{64} = -\frac{1}{128}. \tag{7.413}$$

To go from the first to the second line we used the fact that, for each $\vec{d} \in \mathcal{D}_0^j$ with $d_{s(j-1)} = 1$, there is one $\vec{c} \in \mathcal{D}_1^{j-1}$ for which $\langle j-1, \vec{c}, \mathrm{In}(\vec{z}), \vec{a} | H_2 | j, \vec{d}, \mathrm{In}(\vec{z}), \vec{a} \rangle = \frac{1}{64}$ (with all other such matrix elements equal to zero). This $\vec{c}$ satisfies $c_1 = c_{s(j-1)} = 1$ and $c_{s(j)} = 0$, with all other bits equal to those of $\vec{d}$, so

$$(-1)^{\sum_{i=1}^{n} (c_i + d_i)} = (-1)^{c_1 + c_{s(j)} + c_{s(j-1)} + d_1 + d_{s(j)} + d_{s(j-1)}} = -1 \tag{7.414}$$

for each nonzero term in the sum.

We perform a similar calculation using cases 1, 3, and 4 in equation (7.384) to obtain

$$\langle \mathrm{Cube}_w(j-1, \vec{z}, \vec{a}) | H_2 | \mathrm{Cube}_v(j, \vec{z}, \vec{a}) \rangle = \begin{cases} -\frac{1}{128} & (w,v) = (1,0) \\ \frac{1}{128\sqrt{2}} & (w,v) \in \{(2,0),(1,2)\} \\ -\frac{1}{256} & (w,v) = (2,2) \\ 0 & \text{otherwise.} \end{cases} \tag{7.415}$$

Hence

$$\langle C\,(j-1, \vec{z}, \vec{a})\,| H_2 | C\,(j, \vec{z}, \vec{a}) \rangle \tag{7.416}$$

$$= \frac{1}{4} \langle \mathrm{Cube}_1 (j-1, \vec{z}, \vec{a}) | H_2 | \mathrm{Cube}_0 (j, \vec{z}, \vec{a}) \rangle - \frac{1}{2\sqrt{2}} \langle \mathrm{Cube}_2 (j-1, \vec{z}, \vec{a}) | H_2 | \mathrm{Cube}_0 (j, \vec{z}, \vec{a}) \rangle \tag{7.417}$$

$$+ \frac{1}{2} \langle \mathrm{Cube}_2 (j-1, \vec{z}, \vec{a}) | H_2 | \mathrm{Cube}_2 (j, \vec{z}, \vec{a}) \rangle - \frac{1}{2\sqrt{2}} \langle \mathrm{Cube}_1 (j-1, \vec{z}, \vec{a}) | H_2 | \mathrm{Cube}_2 (j, \vec{z}, \vec{a}) \rangle \tag{7.418}$$

$$= -\frac{1}{128}. \tag{7.419}$$

Combining this with equation (7.409), we see that $H_2|_{S_2}$ is block diagonal in the basis (7.405), with a block for each pair of $n$-bit strings $\vec{z}, \vec{a} \in \{0,1\}^n$. Each of the $2^{2n}$ blocks is equal to the $M \times M$ matrix

$$\frac{1}{128}\begin{pmatrix} 1 & -1 & 0 & 0 & \cdots & 0 \\ -1 & 2 & -1 & 0 & \cdots & 0 \\ 0 & -1 & 2 & -1 & \ddots & \vdots \\ 0 & 0 & -1 & \ddots & \ddots & 0 \\ \vdots & \vdots & \ddots & \ddots & 2 & -1 \\ 0 & 0 & \cdots & 0 & -1 & 1 \end{pmatrix}. \tag{7.420}$$

This matrix is just $\frac{1}{128}$ times the Laplacian of a path of length $M$, whose spectrum is well known. In particular, it has a unique eigenvector with eigenvalue zero (the all-ones vector) and its eigenvalue gap is $2(1-\cos(\frac{\pi}{M})) \geq \frac{4}{M^2}$. Thus for each of the $2^{2n}$ blocks there is an eigenvector of $H_2|_{S_2}$ with eigenvalue 0, equal to the uniform superposition $|\mathcal{H}(\vec{z},\vec{a})\rangle$ over the $M$ states in the block. Furthermore, the smallest nonzero eigenvalue within each block is at least $\frac{1}{32M^2}$. Hence

$$\gamma(H_2|_{S_2}) \geq \frac{1}{32M^2}. \tag{7.421}$$

To get the stated lower bound on $\gamma(H(G_3, G_X oc, n))$, we apply Lemma **??** with

$$H_A = H(G_2, G_X oc, n) \qquad H_B = H_2|_{\mathcal{I}(G_3, G_X oc, n)} \tag{7.422}$$

and

$$\gamma(H_A) \geq \frac{\mathcal{K}_0}{35000n} \qquad \gamma(H_B|_{S_2}) = \gamma(H_2|_{S_2}) \geq \frac{1}{32M^2} \qquad \|H_B\| \leq \|H_2\| \leq n\|h_2\| = 2n \tag{7.423}$$

from Lemma 29, equation (7.421), and the fact that $\|h_2\| = 2$ from (7.86). This gives

$$\begin{aligned} \gamma(H(G_3, G_X oc, n)) &\geq \frac{\mathcal{K}_0}{32M^2\mathcal{K}_0 + 35000n + 2n(35000n)(32M^2)} \qquad (7.424) \\ &\geq \frac{\mathcal{K}_0}{M^2n^2(32 + 35000 + 70000 \cdot 32)} \geq \frac{\mathcal{K}_0}{10^7 M^2 n^2}. \end{aligned}$$

□

**Lemma 31.** *The nullspace $S_4$ of $H(G_4, G_X oc, n)$ is spanned by the states*

$$|\mathcal{H}(\vec{z},\vec{a})\rangle \quad \text{where} \quad \vec{z} = z_1 z_2 \ldots z_{n_{in}} \underbrace{00\ldots0}_{n-n_{in}} \tag{7.425}$$

*for $\vec{a} \in \{0,1\}^n$ and $z_1, \ldots, z_{n_{in}} \in \{0,1\}$. Its smallest nonzero eigenvalue satisfies*

$$\gamma(H(G_4, G_X oc, n)) \geq \frac{\mathcal{K}_0}{10^{10} M^3 n^3} \tag{7.426}$$

*where $\mathcal{K}_0 \in (0,1]$ is the absolute constant from Lemma 26.*

*Proof.* Using equation (7.385), we find

$$\langle C(k,\vec{x},\vec{b})|H_{\text{in},i}|C(j,\vec{z},\vec{a})\rangle = \delta_{k,j}\delta_{\vec{x},\vec{z}}\delta_{\vec{a},\vec{b}}\Bigg(\frac{1}{4}\langle \text{Cube}_0(j,\vec{z},\vec{a})|H_{\text{in},i}|\text{Cube}_0(j,\vec{z},\vec{a})\rangle \tag{7.427}$$

$$+\frac{1}{4}\langle \text{Cube}_1(j,\vec{z},\vec{a})|H_{\text{in},i}|\text{Cube}_1(j,\vec{z},\vec{a})\rangle \tag{7.428}$$

$$+\frac{1}{2}\langle \text{Cube}_2(j,\vec{z},\vec{a})|H_{\text{in},i}|\text{Cube}_2(j,\vec{z},\vec{a})\rangle\Bigg) \tag{7.429}$$

$$= \delta_{k,j}\delta_{\vec{x},\vec{z}}\delta_{\vec{a},\vec{b}}\left(\frac{1}{64}\delta_{z_i,1}\right)\begin{cases}\frac{1}{4}\cdot\frac{1}{2}+\frac{1}{4}\cdot\frac{1}{2}+\frac{1}{2}\cdot\frac{1}{2} & j<j_{\text{min},i}\\ \frac{1}{4}+0+0 & j=j_{\text{min},i}\\ 0+0+0 & j>j_{\text{min},i}\end{cases} \tag{7.430}$$

for each $i\in\{n_{\text{in}}+1,\ldots,n\}$. Hence

$$\langle\mathcal{H}(\vec{x},\vec{b})|\sum_{i=n_{\text{in}}+1}^{n}H_{\text{in},i}|\mathcal{H}(\vec{z},\vec{a})\rangle = \frac{1}{M}\delta_{\vec{x},\vec{z}}\delta_{\vec{a},\vec{b}}\sum_{i=n_{\text{in}}+1}^{n}\frac{1}{64}\left(\frac{j_{\text{min},i}-1}{2}+\frac{1}{4}\right)\delta_{z_i,1}. \tag{7.431}$$

Therefore

$$\sum_{i=n_{\text{in}}+1}^{n}H_{\text{in},i}\big|_{S_3} \tag{7.432}$$

is diagonal in the basis $\{|\mathcal{H}(\vec{z},\vec{a})\rangle\colon \vec{z},\vec{a}\in\{0,1\}^n\}$. The zero eigenvectors are given by equation (7.425), and the smallest nonzero eigenvalue is

$$\gamma\left(\sum_{i=n_{\text{in}}+1}^{n}H_{\text{in},i}\big|_{S_3}\right)\geq\frac{1}{256M}. \tag{7.433}$$

since $j_{\text{min},i}\geq 1$. To get the stated lower bound we now apply Lemma **??** with

$$H_A = H(G_3,G_Xoc,n) \qquad H_B=\sum_{i=n_{\text{in}}+1}^{n}H_{\text{in},i}\big|_{\mathcal{I}(G_4,G_Xoc,n)} \tag{7.434}$$

and

$$\gamma(H_A)\geq\frac{\mathcal{K}_0}{10^7M^2n^2} \qquad \gamma(H_B|_{S_3})\geq\frac{1}{256M} \qquad \|H_B\|\leq n\left\|\sum_{i=n_{\text{in}}+1}^{n}h_{\text{in},i}\right\|=n \tag{7.435}$$

where we used Lemma 30, equation (7.433), and the fact that $\left\|\sum_{i=n_{\text{in}}+1}^{n}h_{\text{in},i}\right\|=1$ (from equation (7.85). This gives

$$\gamma\left(H(G_4,G_Xoc,n)\right)\geq\frac{\mathcal{K}_0}{256M\mathcal{K}_0+10^7n^2M^2+n(256M)(10^7n^2M^2)} \tag{7.436}$$

$$\geq\frac{\mathcal{K}_0}{(M^3n^3)(256+10^7+256\cdot 10^7)}\geq\frac{\mathcal{K}_0}{10^{10}M^3n^3}. \qquad \square$$

### 7.5.4 Completeness and Soundness

Well fuck.

## 7.6 Discussion and open problems

While these results generalized the problem of the Bose-Hubbard model to arbitrary interactions between bosons, it leaves open the related question of fermions. I would expect that our proof would naturally extend to fermions as well, but the extensions where too extensive to finish in time for this thesis.

Making the eventual graph regular.

Remove the restriction to fixed particle number. Currently, this corresponds to

# Chapter 8

# Ground energy of spin systems

We reduce Frustration-Free Bose-Hubbard Hamiltonian to an eigenvalue problem for a class of 2-local Hamiltonians defined by graphs. The reduction is based on a well-known mapping between hard-core bosons and spin systems, which we now review.

We define the subspace $\mathcal{W}_N(G) \subset \mathcal{Z}_N(G)$ of $N$ hard-core bosons on a graph $G$ to consist of the states where each vertex of $G$ is occupied by either 0 or 1 particle, i.e.,

$$\mathcal{W}_N(G) = \mathrm{span}\{\mathrm{Sym}(|i_1, i_2, \ldots, i_N\rangle) \colon i_1, \ldots, i_N \in V,\ i_j \neq i_k \text{ for distinct } j, k \in [N]\}.$$

A basis for $\mathcal{W}_N(G)$ is the subset of occupation-number states (**??**) labeled by bit strings $l_1 \ldots l_{|V|} \in \{0,1\}^{|V|}$ with Hamming weight $\sum_{j \in V} l_j = N$. The space $\mathcal{W}_N(G)$ can thus be identified with the weight-$N$ subspace

$$\mathrm{Wt}_N(G) = \mathrm{span}\{|z_1, \ldots, z_{|V|}\rangle :\ z_i \in \{0,1\},\ \sum_{i=1}^{|V|} z_i = N\}$$

of a $|V|$-qubit Hilbert space. We consider the restriction of $H_G^N$ to the space $\mathcal{W}_N(G)$, which can equivalently be written as a $|V|$-qubit Hamiltonian $O_G$ restricted to the space $\mathrm{Wt}_N(G)$. In particular,

$$H_G^N\big|_{\mathcal{W}_N(G)} = O_G\big|_{\mathrm{Wt}_N(G)} \tag{8.1}$$

where

$$\begin{aligned} O_G &= \sum_{\substack{A(G)_{ij}=1 \\ i \neq j}} \big(|01\rangle\langle 10| + |10\rangle\langle 01|\big)_{ij} + \sum_{A(G)_{ii}=1} |1\rangle\langle 1|_i \\ &= \sum_{\substack{A(G)_{ij}=1 \\ i \neq j}} \frac{\sigma_x^i \sigma_x^j + \sigma_y^i \sigma_y^j}{2} + \sum_{A(G)_{ii}=1} \frac{1 - \sigma_z^i}{2}. \end{aligned}$$

Note that the Hamiltonian $O_G$ conserves the total magnetization $M_z = \sum_{1=1}^{|V|} \frac{1-\sigma_z^i}{2}$ along the $z$ axis.

We define $\theta_N(G)$ to be the smallest eigenvalue of (8.1), i.e., the ground energy of $O_G$ in the sector with magnetization $N$. We show that approximating this quantity is QMA-complete.

**Problem 4** (**XY Hamiltonian**). We are given a $K$-vertex graph $G$, an integer $N \leq K$, a real number $c$, and a precision parameter $\epsilon = \frac{1}{T}$. The positive integer $T$ is provided in unary; the graph is specified by its adjacency matrix, which can be any $K \times K$ symmetric 0-1 matrix. We are promised that either $\theta_N(G) \leq c$ (yes instance) or else $\theta_N(G) \geq c + \epsilon$ (no instance) and we are asked to decide which is the case.

## 8.1 Relation between spins and particles

### 8.1.1 The transform

## 8.2 Hardness reduction from frustration-free BH model

**Theorem 3.** *XY Hamiltonian is QMA-complete.*

*Proof.* An instance of XY Hamiltonian can be verified by the standard QMA verification protocol for the Local Hamiltonian problem [**?**] with one slight modification: before running the protocol Arthur measures the magnetization of the witness and rejects unless it is equal to $N$. Thus the problem is contained in QMA.

To prove QMA-hardness, we show that the solution (yes or no) of an instance of Frustration-Free Bose-Hubbard Hamiltonian with input $G$, $N$, $\epsilon$ is equal to the solution of the instance of XY Hamiltonian with the same graph $G$ and integer $N$, with precision parameter $\frac{\epsilon}{4}$ and $c = N\mu(G) + \frac{\epsilon}{4}$.

We separately consider yes instances and no instances of Frustration-Free Bose-Hubbard Hamiltonian and show that the corresponding instance of XY Hamiltonian has the same solution in both cases.

#### Case 1: no instances

First consider a no instance of Frustration-Free Bose-Hubbard Hamiltonian, for which $\lambda_N^1(G) \geq \epsilon + \epsilon^3$. We have

$$\begin{aligned}
\lambda_N^1(G) &= \min_{\substack{|\phi\rangle \in \mathcal{Z}_N(G) \\ \langle\phi|\phi\rangle = 1}} \langle\phi|H_G^N - N\mu(G)|\phi\rangle && (8.2)\\
&\leq \min_{\substack{|\phi\rangle \in \mathcal{W}_N(G) \\ \langle\phi|\phi\rangle = 1}} \langle\phi|H_G^N - N\mu(G)|\phi\rangle && (8.3)\\
&= \min_{\substack{|\phi\rangle \in \mathrm{Wt}_N(G) \\ \langle\phi|\phi\rangle = 1}} \langle\phi|O_G - N\mu(G)|\phi\rangle && (8.4)\\
&= \theta_N(G) - N\mu(G) && (8.5)
\end{aligned}$$

where in the inequality we used the fact that $\mathcal{W}_N(G) \subset \mathcal{Z}_N(G)$. Hence

$$\theta_N(G) \geq N\mu(G) + \lambda_N^1(G) \geq N\mu(G) + \epsilon + \epsilon^3 \geq N\mu(G) + \frac{\epsilon}{2},$$

so the corresponding instance of XY Hamiltonian is a no instance.

**Case 2: yes instances**

Now consider a yes instance of Frustration-Free Bose-Hubbard Hamiltonian, so $0 \leq \lambda_N^1(G) \leq \epsilon^3$.

We consider the case $\lambda_N^1(G) = 0$ separately from the case where it is strictly positive. If $\lambda_N^1(G) = 0$ then any state $|\psi\rangle$ in the ground space of $H_G^N$ satisfies

$$\langle\phi|\sum_{w=1}^{N}(A(G)-\mu(G))^{(w)} + \sum_{k\in V}\widehat{n}_k(\widehat{n}_k - 1)|\phi\rangle = 0.$$

Since both terms are positive semidefinite, the state $|\phi\rangle$ has zero energy for each of them. In particular, it has zero energy for the second term, or equivalently, $|\phi\rangle \in \mathcal{W}_N(G)$. Therefore

$$\lambda_N^1(G) = \min_{\substack{|\phi\rangle\in\mathcal{W}_N(G)\\ \langle\phi|\phi\rangle=1}}\langle\phi|H_G^N - N\mu(G)|\phi\rangle = \min_{\substack{|\phi\rangle\in\mathrm{Wt}_N(G)\\ \langle\phi|\phi\rangle=1}}\langle\phi|O_G - N\mu(G)|\phi\rangle = \theta_N(G) - N\mu(G),$$

so $\theta_N(G) = N\mu(G)$, and the corresponding instance of XY Hamiltonian is a yes instance.

Finally, suppose $0 < \lambda_N^1(G) \leq \epsilon^3$. Then $\lambda_N^1(G)$ is also the smallest *nonzero* eigenvalue of $H(G,N)$, which we denote by $\gamma(H(G,N))$. (Here and throughout this paper we write $\gamma(M)$ for the smallest nonzero eigenvalue of a positive semidefinite matrix $M$.) Note that $\lambda_N^1(G) > 0$ also implies (by the inequalities (8.2)–(8.5)) that $\theta_N(G) - N\mu(G) > 0$, so

$$\theta_N(G) - N\mu(G) = \gamma\left(\left(O_G - N\mu(G)\right)\big|_{\mathrm{Wt}_N(G)}\right).$$

To upper bound $\theta_N(G)$ we use the Nullspace Projection Lemma (Lemma **??**). We apply this Lemma using the decomposition $H(G,N) = H_A + H_B$ where

$$H_A = \sum_{k\in V}\widehat{n}_k(\widehat{n}_k-1)\big|_{\mathcal{Z}_N(G)} \qquad H_B = \sum_{w=1}^{N}(A(G)-\mu(G))^{(w)}\big|_{\mathcal{Z}_N(G)}.$$

Note that $H_A$ and $H_B$ are both positive semidefinite, and that the nullspace $S$ of $H_A$ is equal the space $\mathcal{W}_N(G)$ of hard-core bosons. To apply the Lemma we compute bounds on $\gamma(H_A)$, $\|H_B\|$, and $\gamma(H_B|_S)$. We use the bounds $\gamma(H_A) = 2$ (since the operators $\{\widehat{n}_k \colon k \in V\}$ commute and have nonnegative integer eigenvalues),

$$\|H_B\| \leq N\|A(G) - \mu(G)\| \leq N(\|A(G)\| + \mu(G)) \leq 2N\|A(G)\| \leq 2KN \leq 2K^2$$

(where we used the fact that $\|A(G)\|$ is at most the maximum degree of $G$, which is at most the number of vertices $K$), and

$$\begin{aligned}\gamma(H_B|_S) &= \gamma\left(\sum_{w=1}^{N}(A(G)-\mu(G))^{(w)}\big|_{\mathcal{W}_N(G)}\right)\\ &= \gamma\left(\left(O_G - N\mu(G)\right)\big|_{\mathrm{Wt}_N(G)}\right)\\ &= \theta_N(G) - N\mu(G).\end{aligned}$$

Now applying the Lemma, we get

$$\lambda_N^1(G) = \gamma(H(G,N)) \geq \frac{2(\theta_N(G) - N\mu(G))}{2 + (\theta_N(G) - N\mu(G)) + 2K^2}.$$

Rearranging this inequality gives

$$\theta_N(G) - N\mu(G) \leq \lambda_N^1(G)\frac{2(K^2+1)}{2 - \lambda_N^1(G)} \leq 4K^2\lambda_N^1(G) \leq 4K^2\epsilon^3$$

where in going from the second to the third inequality we used the fact that $1 \leq K^2$ in the numerator and $\lambda_N^1(G) \leq \epsilon^3 < 1$ in the denominator. Now using the fact (from the definition of Frustration-Free Bose-Hubbard Hamiltonian) that $\epsilon \leq \frac{1}{4K}$, we get

$$\theta_N(G) \leq N\mu(G) + \frac{\epsilon}{4},$$

i.e., the corresponding instance of XY Hamiltonian is a yes instance. □

# Chapter 9

# Conclusions

Many-body systems have, in general, been found to be extremely difficult to understand.

## 9.1 Open Problems

While we have shown several interesting results, many interesting avenues remain open for investigation.

# References

[1] Andrew M. Childs and David Gosset. Levinson's theorem for graphs ii. *Journal of Mathematical Physics*, 53(10), 2012.

[2] Andrew M. Childs, David Gosset, and Zak Webb. Universal computation by multiparticle quantum walk. *Science*, 339(6121):791–794, 2013.

[3] Christophe Texier and Gilles Montambaux. Scattering theory on graphs. *Journal of Physics A: Mathematical and General*, 34(47):10307, 2001.